



THE UNIVERSITY *of* EDINBURGH

This thesis has been submitted in fulfilment of the requirements for a postgraduate degree (e.g. PhD, MPhil, DClinPsychol) at the University of Edinburgh. Please note the following terms and conditions of use:

- This work is protected by copyright and other intellectual property rights, which are retained by the thesis author, unless otherwise stated.
- A copy can be downloaded for personal non-commercial research or study, without prior permission or charge.
- This thesis cannot be reproduced or quoted extensively from without first obtaining permission in writing from the author.
- The content must not be changed in any way or sold commercially in any format or medium without the formal permission of the author.
- When referring to this work, full bibliographic details including the author, title, awarding institution and date of the thesis must be given.



Investigation into the Pathogenesis of
Spinocerebellar Ataxia Type 5

Yvonne Louise Clarkson

A thesis submitted for the degree of Doctor of
Philosophy

The University of Edinburgh

2010

ABSTRACT

Mutations in SPTBN2, the gene encoding β -III spectrin, give rise to spinocerebellar ataxia type 5 (SCA5), an autosomal dominant neurodegenerative disease characterized by motor incoordination and cerebellar degeneration. The work reported in this thesis addressed possible mechanisms of disease pathogenesis using genetically modified mice lacking β -III spectrin (β -III^{-/-}) and also investigated the normal function of β -III spectrin through identification of proteins that interact with its amino-terminus.

Targeted recombination was successful in eliminating expression of full-length β -III spectrin but β -III spectrin lacking exons 2-6 (Δ 2-6 β -III spectrin) was found to be present at a low level in β -III^{-/-} spectrin mice. To ascertain whether the novel truncated protein had any obvious gain-of-function or adverse property that would complicate analysis of β -III^{-/-} spectrin mice the aberrant transcript Δ 2-6 β -III spectrin was cloned and a number of *in vitro* experiments carried out. Protein stability, solubility, cellular localization, and functional assays indicated Δ 2-6 β -III spectrin was less functional than full-length β -III spectrin, confirming the β -III^{-/-} spectrin mouse could be considered a functional knockout.

Analysis of β -III^{-/-} spectrin mice revealed that from 18-weeks of age hind limb gait became progressively wider than age-matched wild-type (WT) controls and three

behavioural tests (stationary rod, rotarod, and elevated beam) demonstrated a progressive impairment in motor performance and coordination. 3-week old β -III^{-/-} spectrin mice performed worse on the rotating rod than age-matched controls but their performance at 3- and 5-rpm improved with consecutive days of testing. Only at 10-rpm did young β -III^{-/-} spectrin mice fail to improve, whereas 6-month old β -III^{-/-} spectrin mice were unable to stay on the rod even at 3-rpm. The ability to balance on a stationary rod was also worse at 6-months of age and the number of hindlimb slips made by β -III^{-/-} spectrin mice on the elevated beam increased from 12-weeks of age. This progressive motor phenotype mirrors symptoms seen in SCA5 patients. In contrast heterozygous mice (β -III^{+/-}) were shown not to develop an ataxic phenotype or display cerebellar degeneration, even at 2-years of age. Cell culture studies using one mutation (L253P) associated with SCA5 revealed that it interfered with protein trafficking from the Golgi apparatus and had a dominant-negative effect on WT function. Incubation at a lower temperature resulted in L253P β -III spectrin reaching the plasma membrane suggesting an altered protein conformation was responsible for the protein trafficking defect. The intracellular accumulation of proteins at the Golgi did not initiate the unfolded protein response. From this work it was concluded that the β -III^{-/-} spectrin mouse is a new model of cerebellar ataxia and loss of β -III spectrin function underlies SCA5 pathogenesis. The results argued against haploinsufficiency and instead suggested disease-causing mutations have dominant-negative effects on WT function and indicate a deficit of cell membrane proteins could participate in SCA5 pathogenesis.

Finally, using a yeast two-hybrid screen the amino terminus of β -III spectrin was found to interact with the carboxy-terminus of prosaposin (a neurotrophic factor) and clathrin light chain. The interactions were confirmed in mammalian cells suggesting neurite outgrowth and movement of membrane vesicles may be normal functions of β -III spectrin.

Declaration

I declare that this thesis was composed entirely by myself and the work on which it is based is my own, unless clearly stated in the text.

Yvonne Louise Clarkson

CONTENTS

Abstract	i
Declaration	iv
Contents	v
Figure List	x
Table List	xiv
Abbreviations	xv
Acknowledgements	xix

CHAPTER 1 INTRODUCTION

1.1 Definition of ataxia	1
1.2 The cerebellum	2
1.2.1 Motor coordination	2
1.2.2 Neurons in the cerebellar cortex	6
1.2.3 Purkinje cell innervation and modulation	7
1.2.4 Motor learning	9
1.2.5 The cerebellar nuclei	10
1.3 Genetic causes of SCA	11
1.3.1 CAG repeat expansions	11
1.3.2 Repeat expansions outwith the protein coding region	12
1.3.3 Conventional mutations	12
1.4 Spinocerebellar ataxia type 5	13
1.4.1 Clinical symptoms	13
1.4.2 Genetic mutations that underlie SCA5	15
1.5 Spectrin	17
1.5.1 Structure of spectrin	17
1.5.2 Erythrocyte spectrin	19
1.5.3 Neuronal spectrin	20
1.5.4 β -III spectrin	22
1.6 Mouse models of ataxia	23
1.6.1 Naturally occurring cerebellar mutants	24
1.6.1.1 <i>Purkinje cell degeneration</i> mutant	24
1.6.1.2 <i>Staggerer</i> mouse	26
1.6.1.3 <i>Lurcher</i> mouse	27
1.6.1.4 <i>Weaver</i> mouse	29
1.6.2 Mouse models generated by genetic manipulation	29
1.6.2.1 CAG repeat expansion models	30
1.6.2.2 Non-coding repeat expansion models	34

1.6.2.3 Conventional mutation models	35
1.7 Aims and approaches	37

CHAPTER 2 MATERIALS AND EXPERIMENTAL METHODS

2.1 Mammalian cell culture	38
2.1.1 Cell maintenance	38
2.1.2 DNA transfection	39
2.1.3 Immunostaining of transfected mammalian cells	39
2.1.4 Solubilisation assay	41
2.1.5 Stability assay	41
2.1.6 Biotinylation	42
2.1.7 Glutamate uptake assay	42
2.2 Polymerase chain (PCR)-based techniques	43
2.2.1 Primer design for PCR	43
2.2.2 PCR	44
2.2.3 Purification of PCR products	44
2.2.4 Site-directed mutagenesis	45
2.3 Methods to subclone DNA fragments	45
2.3.1 Preparation of DNA	45
2.3.2 DNA ligations and bacterial transformations	45
2.3.3 Isolation of plasmid DNA	46
2.3.4 Mammalian expression vectors	47
2.3.5 DNA sequencing	47
2.3.6 Glycerol stocks	48
2.4 SDS-PAGE and Western blotting	48
2.5 Animal procedures	49
2.5.1 Husbandry	49
2.5.2 Genotyping	49
2.5.3 Behaviour tests	50
2.5.3.1 Footprint analysis	50
2.5.3.2 Rotarod	50
2.5.3.3 Elevated beam	51
2.5.3.4 Inverted grid	51
2.5.3.5 Novel Object Recognition	51
2.6 Analysis of mouse tissue	52
2.6.1 Protein homogenates	52
2.6.2 Freezing tissue	52
2.6.3 Transcardial perfusions	53
2.6.4 Frozen sections	53
2.6.5 Paraffin sections	53
2.6.6 Histological techniques	54
2.6.6.1 Haematoxylin and eosin staining	54
2.6.6.2 Cresyl violet staining	55
2.6.6.3 Immunostaining	55
2.6.6.4 Quantification of cerebellar morphology	56
2.7 Co-immunoprecipitations	56

2.8 Methods used in yeast two-hybrid assay	57
2.8.1 Yeast two-hybrid assay	57
2.8.2 Library screen	57
2.8.3 Preparation of yeast protein extracts	58
2.8.4 β -galactosidase activity assays	58
2.8.5 Recovery of plasmid DNA from yeast	59
2.8.6 Yeast Expression Vectors	59
2.9 Statistics	60

CHAPTER 3 ANALYSIS OF $\Delta 2-6$ β -III SPECTRIN

3.1 Background	61
3.2 Results	63
3.2.1 Cloning and expression of $\Delta 2-6$ β -III spectrin	63
3.2.2 Characterisation of $\Delta 2-6$ β -III spectrin protein	64
3.3 Discussion	72
3.3.1 $Spnb3^{-/-}$ mouse	73
3.3.2 Deleterious effects of β spectrin fragments	74
3.3.3 Expression of truncated proteins in other mouse models	75
3.3.4 Conclusions	77

CHAPTER 4 CHARACTERISING THE β -III^{-/-} SPECTRIN MOUSE

4.1 Background	79
4.2 Results	79
4.2.1 Behavioural Analyses	79
4.3 Discussion	88
4.3.1 Loss-of-function in disease pathogenesis	90
4.3.2 Disease pathogenesis in other SCA5 models	93
4.3.3 Conclusions	94

CHAPTER 5 ANALYSIS OF THE HETEROZYGOUS β -III SPECTRIN DEFICIENT ANIMALS

5.1 Background	96
5.2 Results	97
5.2.1 Behavioural Analyses	97
5.2.2 Histological Analysis	103
5.2.3 Analysis of glutamate transporter levels	104
5.3 Discussion	106
5.3.1 Haploinsufficiency as a disease mechanism	107
5.3.2 Lack of glutamate transporter loss in β -III ^{+/-} spectrin mice	110
5.3.3 Conclusions	111

CHAPTER 6 HUMAN MUTATIONS ASSOCIATED WITH SCA5

6.1 Background	113
6.2 Results	114
6.2.1 Generation, expression and cellular localisation of β -III spectrin mutant constructs	114
6.2.2 Dominant negative effect of L253P on WT β -III spectrin	122
6.2.3 Trafficking of membrane proteins disrupted by L253P β -III spectrin	123
6.2.3.1 Membrane trafficking and interaction with Arp1 rescued by temperature shift	126
6.2.4 L253P β -III spectrin does not induce the unfolded protein Response	128
6.3 Discussion	131
6.3.1 Loss of transmembrane proteins in SCA5 pathogenesis	132
6.3.1.1 Mutant β -III spectrin proteins disrupt vesicular trafficking of membrane proteins	132
6.3.1.2 Failure of mutant β -III spectrin proteins to stabilise transmembrane proteins	135
6.3.4 Conclusions	136

CHAPTER 7 IDENTIFYING PROTEINS THAT INTERACT WITH THE AMINO TERMINUS OF β -III SPECTRIN

7.1 Background	137
7.2 Results	138
7.2.1 Yeast-two Hybrid Screen	138
7.2.1.1 Carboxy-terminus of prosaposin/saposin D interacts with β -III spectrin in yeast	141
7.2.1.2 Region of β -III spectrin required for interaction narrowed down to exon 7	142
7.2.2 Bimolecular fluorescence complementation (BiFC) assay	144
7.2.2.1 Prosaposin/saposin D and the amino-terminus of β -III spectrin interact in mammalian cells	144
7.2.2.2 β -III spectrin exon 7 required for protein trafficking From Golgi apparatus	149
7.2.2.3 Interaction between amino terminus β -III spectrin and Arp1 in mammalian cells	149
7.2.3 Interaction of β -III spectrin and prosaposin/saposin D <i>in vivo</i>	153
7.2.4 Expression of prosaposin/saposin D reduced in Purkinje cells of β -III ^{-/-} spectrin mice	154
7.2.5 Normal kidney morphology in β -III ^{-/-} spectrin mice	158

7.2.6 Confirmation that clathrin light chain 1 interacts with β -III spectrin	161
7.2.6.1 Quantification of β -galactosidase activity in retransformed yeast	161
7.2.6.2 Interaction between clathrin light chain and the amino-terminus β -III spectrin in mammalian cells	163
7.3 Discussion	167
7.3.1 Role of saposin D loss in Purkinje cell degeneration	169
7.3.2 Role of prosaposin in Purkinje cell survival	173
7.3.3 Role of clathrin light chain 1 in neurodegeneration	175
7.3.4 Conclusions	177

CHAPTER 8 GENERAL DISCUSSION

8.1 Summary of findings	178
8.2 Outstanding questions	181
8.2.1 How are β -III spectrin mutations associated with SCA5 pathogenesis?	181
8.2.2 What role do glutamate transporters play in Purkinje cell survival?	182
8.2.3 Is a subpopulation of Purkinje cells more vulnerable to cell death?	183
8.2.4 What sodium channel subunit is involved in SCA5 Pathogenesis?	184
8.3 Common mechanisms in neurodegeneration	185
8.4 Conclusions	186

REFERENCES

References	188
-------------------	------------

APPENDICES

Appendix 1 Primer Sequence and PCR Conditions	247
Appendix 2 Predicted Molecular Weights of Fusion Proteins	254
Appendix 3 DVD	256
Appendix 4 List of publications	257

PUBLICATIONS

FIGURE LIST

Figure 1.1	Basic structure of the cerebellar cortex	7
Figure 1.2	MRI scans shows cerebellar atrophy in SCA5 patient	14
Figure 1.3	The formation of spectrin	18
Figure 3.1	Low level of smaller molecular weight protein expressed in β -III ^{+/-} and β -III ^{-/-} spectrin mice	62
Figure 3.2	Cloning and expression of Δ 2-6 β -III spectrin	66
Figure 3.3	Δ 2-6 β -III spectrin is located at the cell membrane	67
Figure 3.4	No difference in solubility between full length and Δ 2-6 β -III spectrin	68
Figure 3.5	Δ 2-6 β -III spectrin is less stable than WT	69
Figure 3.6	Δ 2-6 β -III spectrin fails to increase EAAT4 cell surface expression	71
Figure 4.1	No difference in body weight between β -III ^{-/-} spectrin and WT mice.	80
Figure 4.2	Abnormal Gait in β -III ^{-/-} spectrin Mice	81
Figure 4.3	Progressive loss of balance in β -III ^{-/-} spectrin mice	82
Figure 4.4	Progressive motor deficits in β -III ^{-/-} Spectrin Mice	85
Figure 4.5	Loss of balance in β -III ^{-/-} spectrin mice	86
Figure 4.6	No muscle weakness in β -III ^{-/-} spectrin mice	87
Figure 4.7	β -III ^{-/-} spectrin mice display no deficit in object recognition learning deficit	88
Figure 5.1	No difference in body weight between WT and β -III ^{+/-} spectrin mice	97
Figure 5.2	β -III ^{+/-} spectrin mice have normal gait	98

Figure 5.3	Progressive loss of balance not seen in β -III ^{+/-} spectrin mice	99
Figure 5.4	No progressive motor deficits in β -III ^{+/-} spectrin mice	101
Figure 5.5	No loss of balance in β -III ^{+/-} spectrin mice	102
Figure 5.6	No muscle weakness in β -III ^{+/-} spectrin mice	102
Figure 5.7	β -III ^{+/-} spectrin mice display no deficit in object recognition	103
Figure 5.8	No cerebellar pathology in β -III ^{+/-} spectrin mice	105
Figure 5.9	No loss of neuronal or astroglial transporters in β -III ^{+/-} spectrin mice	106
Figure 6.1	Human mutations associated with SCA5	113
Figure 6.2	Expression of full length β -III spectrin with mutations associated with SCA5	114
Figure 6.3	Lack of expression of L253P β -III spectrin at plasma membrane	115
Figure 6.4	L253P β -III spectrin associates with a Golgi marker	116
Figure 6.5	Δ 39 bp and Δ 15 bp + R634W β -III spectrin associate with the plasma membrane	117
Figure 6.6	Other SCA5 missense mutations associate with the cell membrane	118
Figure 6.7	Full length L253P β -III spectrin associated with Golgi	120
Figure 6.8	Increased protein levels or longer time for protein expression does not result in normal cellular distribution of L253P β -III spectrin	121
Figure 6.9	L253P β -III spectrin has a dominant negative effect on WT β -III spectrin	122
Figure 6.10	L253P β -III spectrin reduces EAAT4 cell surface expression	123
Figure 6.11	Trafficking of proteins from the Golgi disrupted when L253P β -III spectrin expressed	125

Figure 6.12 Membrane localisation rescued by temperature shift	127
Figure 6.13 Interaction with Arp1 rescued by temperature shift	128
Figure 6.14 L253P β -III spectrin does not induce unfolded protein response	130
Figure 7.1 Expression of amino-terminus β -III spectrin fusion protein used as bait in yeast two-hybrid screen	138
Figure 7.2 Carboxy terminus of prosaposin/saposin D	141
Figure 7.3 Carboxy-terminus of prosaposin/saposin D interacts with amino-terminus β -III spectrin in yeast	142
Figure 7.4 Interaction with carboxy-terminus prosaposin/saposin D requires β -III spectrin exon 7	143
Figure 7.5 Bimolecular fluorescence complementation assay	145
Figure 7.6 BiFC assay shows amino-terminus of β -III spectrin and prosaposin interact in mammalian cells	147
Figure 7.7 No interaction seen between full-length β -III spectrin and prosaposin in BiFC assay	148
Figure 7.8 Golgi associated fluorescence when β -III spectrin exon 7 is missing or mutated	151
Figure 7.9 Interaction of Arp1 with amino-terminus of β -III spectrin in mammalian cells using BiFC assay	152
Figure 7.10 Loss of exon 7 results in Golgi associated fluorescence with Arp1 and β -III spectrin	153
Figure 7.11 β -III spectrin interacts with carboxy-terminus prosaposin/saposin D <i>in vivo</i>	154
Figure 7.12 Expression pattern of saposin D/prosaposin in cerebellum	156
Figure 7.13 Reduced saposin D/prosaposin immunoreactivity seen in β -III ^{-/-} spectrin mice	157
Figure 7.14 No reduction in prosaposin/saposin D expression in β -III ^{-/-} spectrin mice at 6-weeks or 1-year	158
Figure 7.15 No renal pathology observed in β -III spectrin mice	160

Figure 7.16 Interaction of clathrin light chain with amino terminus β -III spectrin requires exon 7 and downstream protein sequence	162
Figure 7.17 Full length clathrin light chain 1 may be important for interaction with amino-terminus β -III spectrin	163
Figure 7.18 β -III spectrin and clathrin light chain 1 interact in mammalian cells using BiFC assay	165
Figure 7.19 Discrete localisation of fluorescence in BiFC assay when β -III spectrin exon 7 is missing or mutated	166
Figure 8.1 Schematic diagram of β -III spectrin function	179

TABLE LIST

Table 1.1	Clinical and molecular features of autosomal dominant spinocerebellar ataxias	3
Table 1.2	Functions controlled by the cerebellar nuclei	10
Table 1.3	Details of disease in families with <i>SPTBN2</i> mutations	16
Table 7.1	Sequence results of clones detected with the yeast-two hybrid screen	140

ABBREVIATIONS

ADCA	autosomal dominant forms of cerebellar ataxia
ABCD2	ATP-binding cassette transporter
AD	activation domain
AIS	axon initiation segment
AP	adaptor proteins
Arp1	actin related protein 1
BD	binding domain
BDNF	brain-derived neurotrophic factor
CACNA1A	gene encoding Cav2.1 voltage-gated calcium channel
<i>Calb1</i>	gene encoding calmodulin
<i>Car8</i>	gene encoding the binding partner of IP ₃ receptor
<i>C.elegans</i>	<i>Caenorhabditis elegans</i>
CH	calponin-homology
CIC	capicua
CIP	calf intestinal phosphatase
CK	casein kinase
CNS	central nervous system
Cy2	cyanine 2
Cy3	cyanine 3
DAPI	4',6-Diamidino-2-Phenylindole
DCN	deep cerebellar nuclei
<i>D. melanogaster</i>	<i>Drosophila melanogaster</i>
DMEM	Dulbecco's modified Eagle's medium
EAAC1	excitatory amino acid carrier 1

EAAT4	excitatory amino acid transporter type 4
ECL	enhanced chemiluminescence
EDTA	ethylenediaminetetra-acetic acid
ER	endoplasmic reticulum
EV	empty vector
FGF14	fibroblast growth factor 14
FITC	fluorescein isothiocyanate
GFAP	glial fibrillary acidic protein
GLAST	glutamate aspartate transporter
GLT1	glutamate transporter type 1
GluR δ 2	δ 2 glutamate receptor
<i>Grm1</i>	gene encoding metabotropic glutamate receptor
HEK	human embryonic kidney
HFA	hydroxyl fatty acids
HIP	huntingtin-interacting protein
HIP1R	HIP1-related protein
HB	homogenisation buffer
iFGF	intracellular fibroblast growth factor
<i>Itp1</i>	gene that encodes IP ₃ receptor
IVCs	individual ventilated cages
KCNC3	gene that encodes a potassium channel
<i>KLHL1</i>	Kelch-like 1 gene
KO	knockout
LB	luria broth
LiAc	lithium acetate
MBNL1	muscleblind-like 1
MJD	Machado-Joseph disease
MRI	magnetic resonance imaging

NCAM	neural cell adhesion molecule
NES	nuclear export signal
Neuro 2a	neuronal 2a
NGS	normal goat serum
NLS	nuclear localisation signal
NMD	nonsense-mediated mRNA decay
OCT	optical cutting temperature compound
OPNG	o-nitrophenyl β -D- galactoside
PAGE	polyacrylamide gel electrophoresis
PCR	polymerase chain reaction
PBS	phosphate buffered saline
pcd	Purkinje cell degeneration
<i>Pcp2</i>	gene encoding modulator of voltage-gated calcium channels
<i>Pcp4</i>	gene encoding calmodulin regulator
PD	postnatal day
PFA	paraformaldehyde
PH	Pleckstrin homology
PMSF	phenylmethylsulfonyl fluoride
PRKCG	gene that encodes protein kinase C
PtdIns (4,5) P ₂	phosphatidylinositol 4,5-bisphosphate
RBM17	RNA-binding motif protein 17
REST/NRSF	RE1 silencing transcription factor/neuron-restrictive silencer factor
ROR α	orphan nuclear hormone receptor gene
RT-PCR	reverse transcription-polymerase chain reaction
SCA	spinocerebellar ataxia
SD	synthetic defined
SDS	sodium dodecyl sulfate

SEM	standard error of the mean
<i>Slc1a6</i>	gene encoding EAAT4
S1P	sphingosine 1 phosphate
SPHK1	Sphingosine kinase 1
SPTBN2	gene which encodes β -III spectrin
STWS	Scotch tap water substitute
TAE	Tris-acetate EDTA
TIRF	total internal reflection fluorescence
TTBK2	tau tubulin kinase 2
UPR	unfolded protein response
VGPCs	voltage gated potassium channels
VGSCs	voltage gated sodium channels
WT	wild type
X-gal	5-bromo-4-chloro-3-indolyl- β -D-galactoside
YFP	yellow fluorescent protein

ACKNOWLEDGEMENTS

First and foremost I would like to express my eternal gratitude to my supervisor, Dr Mandy Jackson. I thank her for giving me this opportunity and for being such an amazing role model. She has provided me with an invaluable experience and without her help, patience, and guidance I would not be where I am today. I have thoroughly enjoyed my PhD studies and this is entirely due to her and her commitment.

It is impossible to mention everyone who has helped me over the course of my studies but there are several to whom I owe especial thanks. These people have helped me and contributed to various important aspects of my work.

Firstly, to Dr. David Wyllie and Dr. Paul Skehel. I have been privileged to work in the same lab as Paul who has given much time and allowed me to “borrow” many of his own resources; to Dr. Trudi Gillespie for her invaluable help with confocal microscopy; to Grace Grant and Vivian Allison for their assistance; to Yu Cheng for help with generating BiFC plasmids; to Dr. Ying Sun and Dr Masao Hiraiwa for providing me with saposin C and D antibodies and finally Professor Stephen Michnick for the BiFC plasmids.

Thanks also must go to Laura Ranum and Jeffrey Rothstein for their help, resources and useful discussions.

My years at the University of Edinburgh have allowed me to develop lasting friendships and I would like to make special mention of Dr. Melanie White and Laura Comley because without their help and advice, I would have been totally lost.

I would also like to thank Dr Emma Perkins, whose help throughout this time has been greatly appreciated. She has been a great friend whose patience and kindness will never be forgotten.

I am very grateful to the Medical Research Council for providing the financial support that has enabled me to complete my studies and I would also like to thank the Edinburgh Alumni fund for enabling me to travel to America to establish valuable collaborations and to meet key scientific researchers.

Last, but definitely not least, I would like to thank my family. I am indebted to them and I cannot thank them enough for all of the wonderful support that they have given me throughout the course of my studies. We have finally made it.

CHAPTER 1

INTRODUCTION

1.1 Definition of ataxia

The term ‘ataxia’ is Greek in descent and literally translates to ‘without order’ and is used clinically to describe a lack of motor co-ordination or posture that cannot be explained by motor weakness or sensation deficits (Garcin, 1969; Trouillas et al., 1997). Ataxia can be a consequence of immune diseases, cancer, hypothyroidism, drug abuse, a cerebellar abscess, other infectious diseases, or an inherited neurodegenerative disorder.

The topic of this thesis focuses on the dominantly inherited ataxias, also known as the spinocerebellar ataxias (SCAs). They are a group of progressive, typically late onset, neurodegenerative disorders that arise from dysfunction within the spinocerebellum, the region of the cerebellar cortex that receives somatosensory input from the spinal cord (Oscarsson, 1965). Clinically cerebellar signs are oculomotor disturbances (abnormal eye movements), dysarthria (difficulties with speech), deficits of limb movements and abnormalities of gait and posture (Trouillas et al., 1997). In most cases the degeneration of the cerebellum is accompanied by damage within other brain regions, including brainstem, basal ganglia, spinal cord and the peripheral nervous system. Originally the SCAs, previously known as autosomal dominant forms of cerebellar ataxia (ADCA) were classified according to these extracerebellar phenotypes (Table 1.1) (Harding, 1993). This placed most

CHAPTER 1 INTRODUCTION

forms into type I due to brainstem and/or spinal cord involvement. Whereas type II was classified by the occurrence of retinal degeneration and type III were the pure cerebellar forms, with or without vestibular symptoms. The latter cases of pure cerebellar atrophy may be more appropriately termed familial cortical cerebellar atrophy and it is SCA5, a subtype falling into this category, that forms the basis of the work reported here.

1.2 The cerebellum

1.2.1 Motor coordination

Marie-Jean-Pierre Flourens was the first person to suggest the function of the cerebellum was to coordinate movement. She predicted that any interference with the cerebellum would affect the ability of the animal to control motor coordination and if the entire cerebellum was removed the ability to control movement would be lost (Flourens, 1824). Her initial studies involved cerebellar ablations in pigeons and from this work she was able to state *“the will, the senses, the perception remained, but the coordination of movement, the ability for controlled and determined movement, was lost”*.

It is now known that the cerebellum integrates and combines sensory inputs from the periphery, fine-tuning movement and postural control so that automatic motor skills are performed rapidly and smoothly every time (Holmes, 1939). Damage to the cerebellum results in slow and irregular movement as the action of muscles are no

CHAPTER 1 INTRODUCTION

Table 1.1 Clinical and molecular features of autosomal dominant spinocerebellar ataxias

Disease	Distinguishing features (all have gait ataxia)	Harding Classification	Average Duration	Protein or chromosomal locus	Type of mutation	Reference
SCA1	Cognitive impairment, peripheral neuropathy	I	15 years	Ataxin-1	CAG repeat	Orr et al., 1993; Banfi et al., 1994; Zoghbi and Orr, 1995
SCA2	Slow saccadic eye movements, peripheral neuropathy, dementia	I	10 years	Ataxin-2	CAG repeat	Imbert et al., 1996; Pulst et al., 1996; Sanpei et al., 1996
SCA3	Decreased saccade velocity, sensory loss, pyramidal and extrapyramidal signs	I	10 years	Ataxin-3	CAG repeat	Kawaguchi et al., 1994
SCA4	Sensory axonal neuropathy, deafness	I	Decades	16q22.1		Flanigan et al., 1996
SCA5	Early onset, slow progression	III	> 25 years	β -III spectrin	In-frame deletions, missense mutations	Ikeda et al., 2006
SCA6	Very slow progression, sometimes episodic ataxia	III	>25 years	Voltage-dependent P/Q-type calcium channel alpha-1A subunit	CAG repeat	Zhuchenko et al., 1997
SCA7	Visual loss with retinopathy	II	20 years	Ataxin-7	CAG repeat	David et al., 1997
SCA8	Slowly progressive, decreased vibration sense, rare cognitive impairment	I	Normal lifespan	13q21	CAG.CTG repeat	Koob et al., 1999

CHAPTER 1 INTRODUCTION

Table 1.1 Continued Clinical and molecular features of autosomal dominant spinocerebellar ataxias

Disease	Distinguishing features (all have gait ataxia)	Harding Classification	Average Duration	Protein or chromosomal locus	Type of mutation	Reference
SCA10	Epilepsy	I	9 years	Ataxin-10	ATTCT repeat	Matsuura et al., 2000
SCA11	Mild, remain ambulatory, abnormal eye signs	III	Normal lifespan	Tau-tubulin kinase 2	Insertions and deletions	Worth et al., 1999; Houlden et al., 2007
SCA12	Slowly progressive, Parkinson's, cognitive impairments, action tremor of upper extremities	I		Phosphatase 2A regulatory subunit	CAG repeat	Holmes et al., 1999
SCA13	Mild mental retardation, seizures	I	Normal lifespan	Potassium voltage-gated channel	Missense mutations	Waters et al., 2006
SCA14	Early axial myoclonus	III	Decades	Protein kinase C gamma	Missense mutations	Chen et al., 2003
SCA15	Very slow progression	III	Decades	Inositol 1,4,5- trisphosphate receptor type 1	Deletion of 5' part of gene	Matsumoto et al., 1996; Knight et al., 2003; Gardner et al., 2005; van de Leemput et al., 2007; Hara et al., 2008
SCA16	Head tremor	III	Decades			Miyoshi et al., 2001
SCA17	Mental deterioration, dystonia, epilepsy	I	>8 years	TATA-box binding protein	CAA/CAG repeat	Nakamura et al., 2001

CHAPTER 1 INTRODUCTION

Table 1.1 Continued Clinical and molecular features of autosomal dominant spinocerebellar ataxias

Disease	Distinguishing features (all have gait ataxia)	Harding Classification	Average Duration	Protein or chromosomal locus	Type of mutation	Reference
SCA18				7q22-q32		Devos et al., 2001
SCA19	Cognitive impairment	I	Decades	1p21-q21		Verbeek et al., 2002
SCA20	Early dysarthria, hyperflexia, bradykinesia	I	Decades	11q12.2- 11q12.3	260-kb duplication	Knight et al., 2004
SCA21	Mild cognitive impairment	I	Decades	7p21-p15.1		Vuillaume et al., 2002
SCA22	Slowly progressive	I	Decades	1p21-q23		Chung et al., 2003
SCA23	Dysarthria, abnormal eye movements, reduced vibration senses	I	>10 years	20p13-p12.3		Verbeek et al., 2004
SCA25	Sensory neuropathy	I	Unknown	2p21-p13		Stevanin et al., 2005
SCA26	Dysarthria, irregular visual pursuits	III	Unknown	19p13.3		Yu et al., 2005
SCA27	Early onset tremor, dyskinesia, cognitive deficits	I	Decades	Fibroblast growth factor 14	Missense mutations	van Swieten et al., 2003
SCA28	Nystagmus, increased tendon reflexes	I	Decades	AFG3-like protein 2	Missense mutations	Cagnoli et al., 2006; Di Bella et al., 2010
SCA31	Adult onset, pure cerebellar	III		16q22.1	TGGAA repeat	Nagaoka et al., 2000; Ishikawa et al., 2005; Sato et al., 2009

CHAPTER 1 INTRODUCTION

longer coordinated in timing, duration and amplitude. Instead the frontal cerebral cortex has to think out every movement.

1.2.2 Neurons in the cerebellar cortex

The structure of the cerebellum can be divided into two parts – the cerebellar cortex and the cerebellar nuclei. The cerebellar cortex comprises three layers (granule cell, Purkinje cell and molecular layers) and contains five types of neurons (stellate, basket, Purkinje, Golgi and granule cells; Figure 1.1). The granule cell layer contains a huge number of neurons, mainly excitatory granule cells but also a few Golgi interneurons. In contrast the Purkinje cell layer is a single layer of Purkinje cell bodies lying between the granule cell and molecular layers. The latter layer has very few cell bodies, only those of inhibitory stellate and basket cells, and instead is mainly composed of the dendritic arborizations of the inhibitory Purkinje cells. The Purkinje cells receive input from a range of sources throughout the central nervous system (CNS) but in turn they are the sole output of the cerebellar cortex, targeting the deep cerebellar nuclei (fastigius, interpositus and dentate; refer to section 1.2.5).

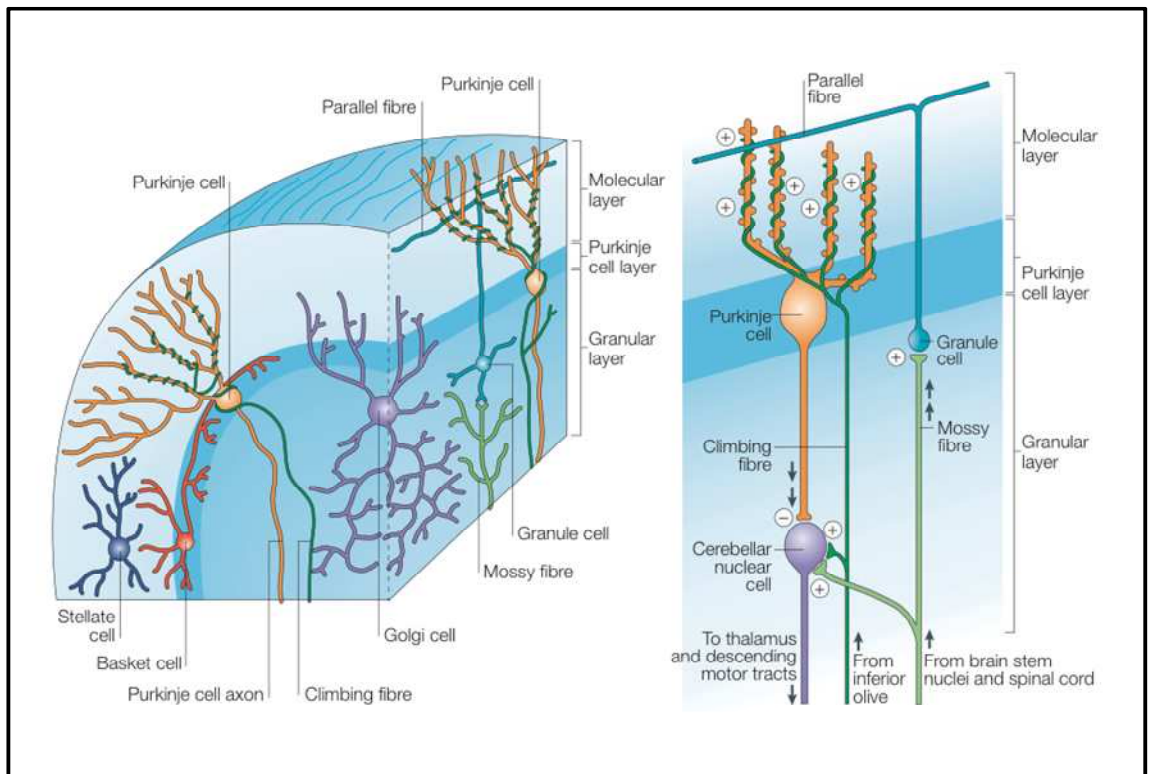


Figure 1.1 Basic structure of the cerebellar cortex. A schematic representation of the three layers of the cerebellar cortex composed of five types of neurons (Apps and Garwicz, 2005).

1.2.3 Purkinje cell innervation and modulation

Parallel and climbing fibers form the two excitatory (glutamatergic) inputs to Purkinje cells (Figure 1.1). Climbing fibers originate from the medulla, within the inferior olivary nucleus, and each fiber forms hundreds of excitatory synapses on the cell body and proximal dendrites of 1-10 Purkinje cells. Each individual Purkinje cell however only receives input from one climbing fiber. Nevertheless the action potential produced by a climbing fiber is incredibly large, activating the Purkinje cell every time and producing a complex spike. This contains a large-amplitude spike that

CHAPTER 1 INTRODUCTION

is followed by a burst of smaller-amplitude action potentials due to prolonged conductance within the Purkinje cell soma and dendrites (Eccles, 1967; Thach, 1967). In contrast parallel fibers, the axons of granule cells, synapse with a large number of Purkinje cells. These fibers are situated at right angles to the Purkinje cell dendrites and a single Purkinje cell can form synaptic contacts with as many as one million granule cells. It is excitation from parallel fibers that modulates the tonic simple spike firing frequency such that it can exceed 100 Hz (Eccles, 1967; Thach, 1967). A third glutamatergic synapse exists between mossy fibers, originating from the spinal cord and brainstem, and the dendrites of granule cells. This conveys to the cerebellum information from the cerebral cortex and sensory inputs from a variety of sources.

The removal of glutamate by postsynaptic neuronal (excitatory amino acid carrier 1 (EAAC1) and excitatory amino acid transporter type 4 (EAAT4)) and glial (glutamate transporter type 1 (GLT1) and glutamate aspartate transporter (GLAST)) glutamate transporters is critical for terminating the excitatory signal and preventing diffusion of glutamate into neighbouring synapses (Chaudhry et al., 1995; Takahashi et al., 1996; Bergles et al., 1997; Clark and Barbour, 1997; Otis et al., 1997; Dzubay and Jahr, 1999; Auger and Attwell, 2000; Diamond, 2001). GLAST and EAAT4 are thought to be responsible for the majority of cerebellar uptake with GLT1 only contributing a small amount (Furuta et al., 1997). Glutamate transporters have an essential role in protecting neurons from excitotoxic injury by maintaining low concentrations of extracellular glutamate (Danbolt, 2001). Malfunction, aberrant

expression or insufficient capacity of glutamate transporters can lead to high extracellular concentrations of glutamate and neuronal death (Choi, 1988; Rothstein et al., 1996).

As well as excitatory inputs Purkinje cells receive inhibitory input from three interneurons (stellate, basket and Golgi cells). The axons of stellate and basket cells directly contact Purkinje cells whereas Golgi cells form synapses with the granule cells. All three interneurons are activated by parallel fibers.

1.2.4 Motor learning

The involvement of the cerebellum in motor learning was a theory proposed by David Marr and James Albus (Marr, 1969; Albus, 1971). They stated the modulation of Purkinje cell input results in a new movement being learnt or an old one adapted. Animal studies have since provided evidence that the cerebellum does have a role in motor learning as removal of the cerebellar cortex prevents adaptation and learning (Robinson, 1976; McCormick et al., 1981; McCormick and Thompson, 1984; Yeo et al., 1984). The mechanism appears to involve trial-and-error with climbing fibers signaling an error in movement that weakens the strength of concurrently active parallel fiber-Purkinje cell synapses (Simpson and Alley, 1974; Gilbert and Thach, 1977; Gellman et al., 1985; Dugas and Smith, 1992; Ojakangas and Ebner, 1994). This allows signals from the correct movement to emerge and influence Purkinje cell output (Ito et al., 1982; Ekerot and Kano, 1985; Strata, 1985; Kano and Kato, 1987).

1.2.5 The cerebellar nuclei

The deep cerebellar nuclei (DCN) and the vestibular nuclei are responsible for the output of the cerebellum. When there is no movement, the DCN spontaneously fire at rates between 40-50 Hz but during movement the firing rate can either increase or decrease from this baseline frequency (Bastian and Thach, 2002). It is the changes of firing frequency that result in the modulation of target structures and each nucleus appears to control different motor systems and their respective functions (Asanuma et al., 1983a; Asanuma et al., 1983b, c, d; Orioli and Strick, 1989) (Table 1.2).

Table 1.2 Functions controlled by the cerebellar nuclei.

Cerebellar nuclei	Functions	Effect on inactivating the nucleus
Fastigius (Vestibular and medial)	Eye movements, equilibrium, upright stance and gait	Animal unable to sit, stand or walk with recurrent falls to the side of the lesion (Botterell and Fulton, 1938; Kane et al., 1988, 1989; Sprague and Chambers, 1953; Thach et al., 1990, 1992).
Interpositus (Intermediate)	Stretch, contact, placing and other reflexes	Development of a severe action tremor during reaching (Kane et al., 1988, 1989; Thach et al., 1990, 1992).
Dentate (Lateral)	Voluntary movements of the extremities including reaching and grasping	Over angulation of the shoulder and elbow when reaching (Kane et al., 1988, 1989; Thach et al., 1990, 1992).

1.3 Genetic causes of SCA

The prevalence of SCAs in several populations can be as high as 5 – 7 in 100 000 (van de Warrenburg et al., 2002; Craig et al., 2004), making these diseases as common as Huntington's or motor neuron disease. Currently, over 30 different genetic loci have been identified as associating with SCA and are numbered in order of discovery (Table 1.1). However, the disease-causing mutations and their respective genes have only been identified for sixteen SCA subtypes (Carlson et al., 2009). This means that 20 – 50% of families with autosomal dominant forms of ataxia are still of unknown genetic origin (A Brice, personal communication). The SCA subtypes of known genetic origin can be classified into three main subgroups.

1.3.1 CAG repeat expansions

The first genetic defect to be identified in a family with SCA was the discovery of an expanded CAG-repeat sequence in the ataxin 1 gene, which leads to an abnormally long poly-glutamine tract being present in the encoded protein (Orr et al., 1993). A further five SCA subtypes (SCA 2, 3, 6, 7 and 17) have since been found to be associated with coding CAG repeat expansions (reviewed in (Duenas et al., 2006)). These six polyglutamine SCAs account for over 50% of all SCA families, with SCA3 being the most common form (Bird, 1998).

1.3.2 Repeat expansions outwith the protein coding region

The second category, comprising SCA 8, 10 and 12, are due to repeat expansions that occur outside of the protein-encoding region of the relevant disease gene. There is therefore no polyglutamine tract expansion or any other amino acid repeat within the disease protein. In the case of SCA10 it is a large pentanucleotide expansion within an intron (Matsuura et al., 2000), for SCA12 it is a small CAG repeat expansion within the 5' untranslated region of the disease gene (Holmes et al., 1999) and in SCA8 a CTG repeat that is bidirectionally transcribed resulting in a non-coding CUG transcript and possibly a polyQ protein (Koob et al., 1999).

1.3.3 Conventional mutations

The remaining seven SCAs comprise an expanding third category due to the identification of mutations in rarer forms of dominantly inherited ataxia. These subtypes are not caused by dynamic repeat expansions, but instead by conventional mutations. The conventional mutations are deletion, missense, nonsense or frameshift mutations in the corresponding genes. Mutations in the genes that encode β -III-spectrin (Ikeda et al., 2006), tau tubulin kinase 2 (TTBK2) (Houlden et al., 2007), a potassium channel (KCNC3) (Waters et al., 2006), protein kinase C (PRKCG) (Chen et al., 2003), type 1 inositol 1,4,5-triphosphate receptor (ITPR1) (van de Leemput et al., 2007; Iwaki et al., 2008) and fibroblast growth factor 14 (FGF14) (van Swieten et al., 2003) give rise to SCA5, 11, 13, 14, 15/16 and 27, respectively.

1.4 Spinocerebellar ataxia type 5

1.4.1 Clinical symptoms

In 1992 a large family, descended from the paternal grandparents of United States President Abraham Lincoln, was identified as having a clinically mild form of SCA (Ranum et al., 1994). Linkage to all known ataxia loci was excluded and instead genetic linkage analysis mapped the disease locus to the centromeric region of the long arm of chromosome 11 (11q13), identifying a new SCA subtype, coined SCA5.

Clinically SCA5 is more benign (Ranum et al., 1994) than other SCAs (Gouw et al., 1994; Yagishita and Inoue, 1997) and is classified as ADCA type III due to it primarily affecting the cerebellum, with the brainstem usually being spared (Table 1.1). SCA5 cases show severe atrophy of the cerebellum by magnetic resonance imaging (MRI) scans (Figure 1.2) and autopsy examination shows significant Purkinje cell loss, shrinkage of the molecular layer, mild loss of granular neurons and frequent empty basket fibers (Manto and Pandolfo, 2002; Ikeda et al., 2006). The DCN (see section 1.2.5) were found to be gliotic, but this was not accompanied by neuronal loss. Another clinical distinction between SCA5 and other SCAs is that disease progression is much slower and is typically not fatal (Ranum et al., 1994). This difference is thought to result from the lack of bulbar paralysis in SCA5, which in the other SCAs results in a poorer ability to fight recurrent pneumonia (Zoghbi, 1991).

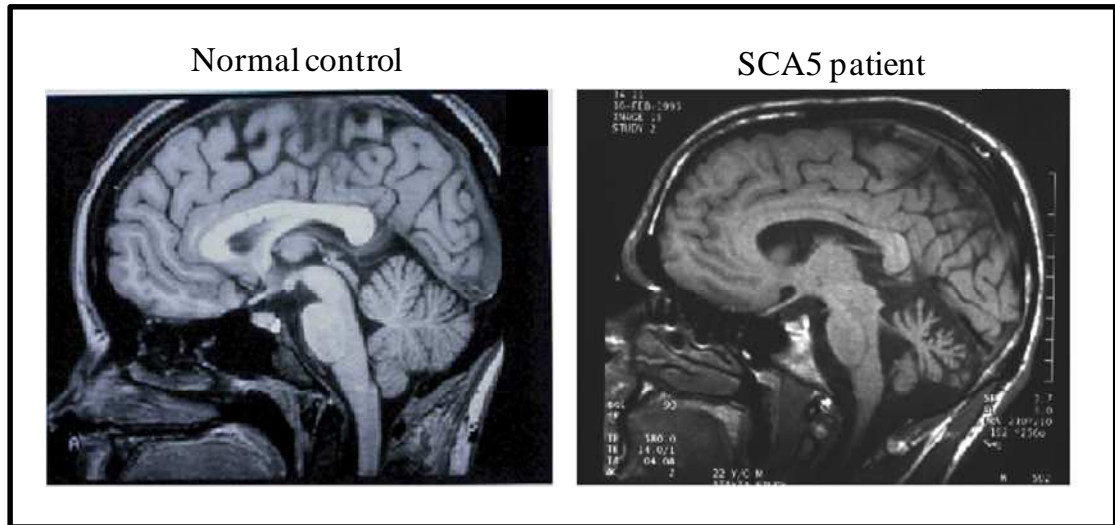


Figure 1.2 MRI scan shows cerebellar atrophy in SCA5 patient. MRI scan of a normal control and a patient with SCA5. The SCA5 patient shows severe cerebellar atrophy with sparing of the brainstem. Images obtained from Laura Ranum, personal communication.

Average age of onset of SCA5 is later in life, typically in the third or fourth decade but symptoms can manifest between 10 and 68 years of age (Ranum et al., 1994; Stevanin et al., 1999; Burk et al., 2004). Mild disturbance of gait, incoordination of limbs, abnormal eye movements, and slurred speech are the initial symptoms, which gradually progress over several decades to wheelchair dependency in some instances. However, patients with early onset (before the age of 20) also show signs of mild bulbar involvement and it may be that these individuals will go on to develop a more severe form of disease.

1.4.2 Genetic mutations that underlie SCA5

In 2006 Ranum and colleagues found mutations in the gene *SPTBN2*, which encodes β -III spectrin, in affected members of the Lincoln pedigree and two additional families but not in 1000 control chromosomes (Table 1.3) (Ikeda et al., 2006). The mutation associated with the Lincoln pedigree was a 39-bp in-frame deletion resulting in a 13-amino acid deletion within the third spectrin repeat of β -III spectrin (see section 1.5.4). A shorter in-frame deletion (15 bp) in the same spectrin repeat was observed in a French family and this deletion also resulted in the introduction of a missense mutation (R634W). The third family possessed a single missense mutation (L253P) within the second of two calponin-homology (CH) domains.

Historical literature had suggested President Lincoln may have suffered from SCA5. In 1861 William Russell, a reporter from the London Times, wrote of Abraham Lincoln “*Soon afterwards there entered, with a shambling, loose, irregular, almost unsteady gait, a tall, lank, lean man..*” depicting a man with characteristic features of ataxia. But recently, using handwriting analysis, Dr. Sotos has refuted this possibility. He believes Lincoln’s handwriting was perfect when he drafted the Gettysburg Address in 1864 (a year before he died), so, ruling out SCA5, in his opinion since the most common complaint of patients is deterioration in handwriting and fine finger dexterity (Sotos, 2009).

CHAPTER 1 INTRODUCTION

Table 1.3 Details of disease in families with *SPTBN2* mutations

Family	Disease onset (yr)	Clinical Symptoms	Pathology	Reference
Lincoln	10-68	Disturbance of gait, incoordination of upper extremities, slurred speech Juvenile onset evidence of pyramidal tract dysfunction	Cerebellar atrophy, greater involvement of superior hemispheres and anterior vermis No change basal ganglia, cerebral cortex	Ranum et al., 1994
French	14-40	Slowly progressive, gait instability, horizontal nystagmus, brisk reflexes Slight facial myokymia, decreased vibration sense No extrapyramidal signs or swallowing difficulties	Universal cerebellar atrophy, sparing of pons	Stevanin et al., 1999
German	15-50	Downbeat nystagmus, ataxia of stance and gait, dysarthria, intention tremor Normal vestibular function No cognitive impairment, dysphagia, hearing loss, pyramidal tract signs or facial myokymia	Cerebellar atrophy, intact brainstem structures	Burk et al., 2004

1.5 Spectrin

1.5.1 Structure of spectrin

Spectrins are heterotetramers comprising two α - and two β -subunits (Figure 1.3). These proteins were first discovered in human erythrocytes, being the most abundant protein found within the membrane skeleton of red blood cells (Cohen, 1983). The majority of each spectrin polypeptide consists of a series of repeats, each one approximately 106 amino acids (Speicher and Marchesi, 1984) and forming a triple helix (Yan et al., 1993; Pascual et al., 1996). The α - and β -subunits associate laterally, forming anti-parallel heterodimers which interact head-to-head to form the functional heterotetramer (Ungewickell and Gratzer, 1978; Shotton et al., 1979)(Figure 1.3). Short actin filaments then link the spectrin tetramers together forming a flexible spectrin network attached to the inner leaf of the membrane bilayer.

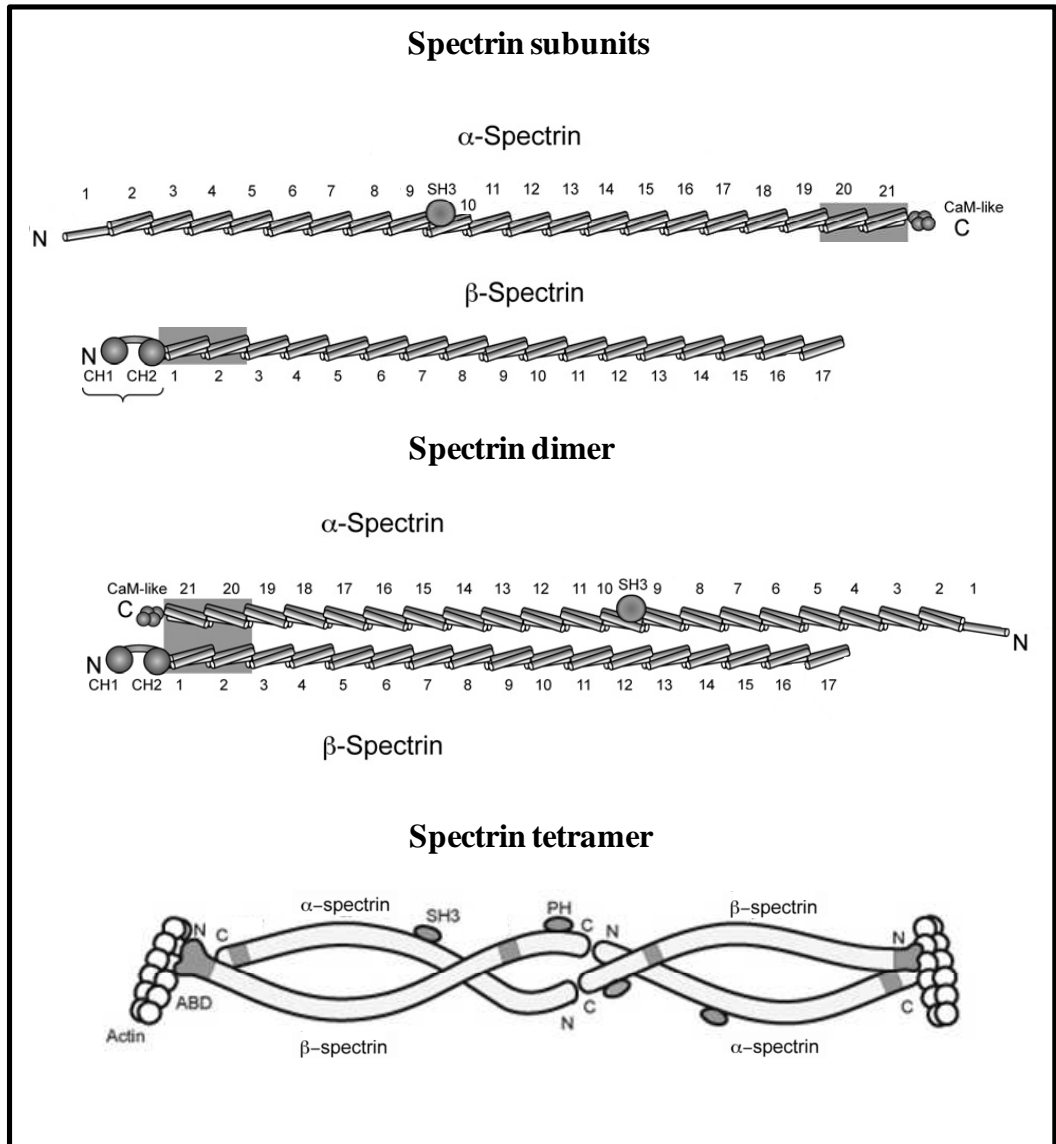


Figure 1.3 The formation of spectrin. Spectrin is composed of two α - and two β -spectrin subunits. Dimers are generated when non-covalent bonds form between an α - and a β -subunit which lie antiparallel to one another (Shotton et al., 1979). Tetramers form when dimers are joined together with the N' terminus of every α subunit linking to the C' terminus of every β subunit (Ungewickell and Gratzer, 1978). Image modified from originals (Baines and Pinder, 2005; Baines, 2009).

CHAPTER 1 INTRODUCTION

It is known that vertebrates have two α - ($\alpha I/\alpha II$), four β - ($\beta I-\beta IV$) and a β -H subunit, which creates diversity and specialization of function (Bennett and Baines, 2001). $\alpha I/\beta I$ polypeptides form mammalian erythrocyte spectrin and are also found in striated muscle and a subset of neurons. $\alpha II/\beta II$, $\alpha II/\beta III$ and $\alpha II/\beta IV$ polypeptides are the major forms in nonerythroid vertebrate tissues.

1.5.2 Erythrocyte spectrin

Characterization of the erythrocyte membrane has provided clues as to the organization and role of the spectrin skeleton. The assembly of a spectrin-actin filamentous network at the plasma membrane is critical for mechanical support and maintenance of structural membrane integrity. Mutations within spectrin subunits, in both mice (Greenquist et al., 1978; Lux et al., 1979) and humans (Agre et al., 1982; Agre et al., 1985), cause hereditary spherocytosis, a type of haemolytic anaemia. The mutations result in loss of spectrin and unsupported membranes leading to fragmentation of erythrocytes when placed under mechanical stress in the circulation.

Accessory proteins have also been identified as associating with erythrocyte spectrin and being important for the maintenance of the filamentous network. Protein 4.1 binds to the actin-binding domain of the β polypeptide and is thought to initiate and strengthen the interaction between spectrin and actin (Cohen, 1983; Bennett, 1985). Interaction of protein 4.1 with members of the glycophorin family (particularly glycophorin C) also links spectrin to the lipid bilayer stabilizing the whole structure. A stronger interaction between spectrin and the lipid bilayer arises from ankyrin-R

binding to spectrin repeats 14 and 15 of the β polypeptide and the cytoplasmic domain of the membrane-bound anion exchanger (Bennett and Stenbuck, 1980; Speicher et al., 1982; Kennedy et al., 1991). Interaction with ankyrin-R also increases the affinity of spectrin self-association, enhancing formation of the spectrin lattice (Cianci et al., 1988). The majority of human cases of hereditary spherocytosis actually result from mutations of ankyrin-R and not spectrin per se, but the common feature is a defective spectrin lattice (Eber and Lux, 2004; Gallagher, 2005).

1.5.3 Neuronal spectrin

Studies using *Caenorhabditis elegans*, *Drosophila melanogaster* and mice have demonstrated several functions of spectrin in the nervous system. Unlike vertebrates *C. elegans* and *D. melanogaster* have only one α , one β and one β -H subunit. Loss of β spectrin in *C. elegans*, encoded by *unc-70*, has revealed it is vital for axonal integrity (Hammarlund et al., 2000; Hammarlund et al., 2007). Without spectrin the worms are paralyzed, axons are unable to withstand strain initiated by movement, and muscle structure becomes disordered, eventually detaching from the body wall (Moorthy et al., 2000). The presence of β -spectrin therefore protects against spontaneous breaks in neuronal processes that would otherwise arise from movement.

In postembryonic *Drosophila* the knockdown of either α or β presynaptic spectrin results in synaptic retraction and consequently synapse elimination at the neuromuscular junction (Pielage et al., 2005). A decrease in two cell adhesion

CHAPTER 1 INTRODUCTION

molecules, neuroglian and Fasciclin II, is observed in flies lacking presynaptic spectrin suggesting that a loss in cell-cell contact is an early event in synapse retraction and a consequence of spectrin loss. Disorganization and retraction of microtubules, along with axonal transport defects, are also observed when spectrin protein levels are drastically reduced or absent (Pielage et al., 2005). A resulting disruption to normal retrograde transport of critical trophic factors (McCabe et al., 2003) may be a factor in the observed synapse retraction. Furthermore, a requirement for dynactin-mediated axonal transport has been shown to be required for synapse stabilization at the *Drosophila* neuromuscular junction (Eaton et al., 2002) and disruption to this transport has been associated with motor neuron disease in humans and mice (LaMonte et al., 2002; Hafezparast et al., 2003; Puls et al., 2003; Munch et al., 2004). Therefore, an important role of spectrin may be to link cell adhesion molecules to the microtubule as an interaction with microtubules for both α and β spectrin has been reported (Sisson et al., 2000).

Two mouse models have shown the importance of β -IV spectrin in the nervous system. Mice created to have a null mutation within the gene encoding β -IV spectrin were found to have tremors and clasp their hindlimbs when held in the air (a characteristic feature of ataxia). Severity of the phenotype increases with age and by 6-10 months of age the mice are no longer ambulatory (Komada and Soriano, 2002). The *quivering* mouse, resulting from a spontaneous mutation in the β -IV spectrin gene, also displays ataxia with hindlimb paralysis, deafness and tremor when homozygous for the mutation (Parkinson et al., 2001). These mice have ectopically

placed voltage gated sodium and potassium channels (VGSCs & VGPCs) as instead of being situated at the nodes of Ranvier they are redistributed along the lengths of the axons resulting in changes to the firing and propagation of axon potentials. A critical role of β -IV spectrin appears to be the localization and stabilization of ion channels to specific regions of the neuron.

Findings from animal studies have therefore demonstrated important roles for spectrin in stabilizing cell-cell contacts and localizing ion channels, cell-adhesion molecules and other transmembrane proteins within specific subdomains of the plasma membrane.

1.5.4 β -III spectrin

β -III spectrin is expressed primarily in the nervous system with the highest level of protein expression seen in the soma and dendrites of cerebellar Purkinje cells (Ohara et al., 1998; Sakaguchi et al., 1998; Stankewich et al., 1998; Jackson et al., 2001). Low levels of transcript have been detected in other tissues including kidney, liver, testes, prostate, pituitary, adrenal and salivary glands (Stankewich et al., 1998). It was originally thought β -III spectrin associated with the Golgi, maintaining its structure through an association with phosphatidylinositol 4,5-bisphosphate (PtdIns (4,5)P₂) (Beck et al., 1994; Stankewich et al., 1998). Loss of PtdIns (4,5)P₂ was proposed to result in phosphorylation of spectrin, cellular redistribution and subsequent fragmentation of the Golgi (Siddhanta et al., 2003). However, the Golgi

localization is now thought to have arisen from antibody cross-reactivity detecting another protein with spectrin repeats, syne1 (Gough et al., 2003).

β -III spectrin has been shown to interact with the carboxy-terminus of EAAT4, the glutamate transporter found in Purkinje cell soma and dendrites, and stabilize it at the plasma membrane (Jackson et al., 2001; Ikeda et al., 2006), the result being an increase in cell surface expression and enhanced glutamate uptake. Therefore, β -III spectrin appears to play an important role in the clearance of glutamate from the synaptic cleft, regulating glutamatergic neurotransmission and preventing glutamate-mediated excitotoxicity (see section 1.2.3). Yeast two-hybrid studies have shown the actin binding domain of β -III spectrin binds directly to actin related protein 1 (Arp 1), a subunit of the dynactin complex (Holleran et al., 2001). Dynactin is the accessory protein that mediates the association of dynein with vesicular cargo, suggesting β -III spectrin may participate in vesicular transport along microtubules. All three proteins have been co-purified from vesicles isolated from rat brain and it is thought that both β -III spectrin and dynactin are involved in organelle and vesicular transport, mediated by dynein (Karki et al., 1998; Holleran et al., 2001; Lorenzo et al., 2010).

1.6 Mouse models of ataxia

Clinically, the phenotype observed in SCA patients is well understood (Table 1.1). However the cellular processes that underlie cerebellar dysfunction and degeneration in SCA remain unclear. Mice have become an important tool for identifying gene

function and unravelling mechanisms of disease, as 99% of mouse genes have homologues in man and of these 96% are found in the same syntenic location (same chromosomal order) as their human homologue (MacAndrew., 2003). They are also relatively cheap to maintain, large numbers can be bred rapidly and they have short life spans. Therefore mouse models, either generated by genetic manipulation or a result of spontaneous mutations, have been used to gain insights into Purkinje cell degeneration and cerebellar ataxia.

1.6.1 Naturally occurring cerebellar mutants

Because unlike other brain regions the majority of cerebellar development occurs postnatally (Dobbing and Sands, 1973; Altman and Bayer, 1997), the cerebellum is much more vulnerable to developmental and environmental insults. This has led to more than 50 mutants being identified and analysed but only 4 are discussed in detail here (Sidman et al., 1965; Sidman et al., 1982; Sotelo et al., 1990). These spontaneous mutations in the mouse have proved excellent tools for studying Purkinje cell degeneration and elucidating the effects loss of certain elements of the cerebellar circuitry have on the formation and/or maintenance of the cerebellum. This has highlighted a tight interplay between Purkinje cell, granule cell and inferior olive cell survival.

1.6.1.1 *Purkinje cell degeneration mutant*

The autosomal recessive Purkinje cell degeneration (*pcd*) mutant is characterized by dramatic Purkinje cell degeneration, which starts at about postnatal day (PD) 18 and

CHAPTER 1 INTRODUCTION

rapidly progresses over the next 14 days (Mullen et al., 1976). Prior to Purkinje cell degeneration, all the normal cerebellar synaptic connections are made (Landis and Mullen, 1978) but following Purkinje cell degeneration there is a substantial loss of granule cells, deep cerebellar nuclear cells and neurons of the inferior olive (Chang and Ghetti, 1993; Triarhou, 1998). Given the gross loss of Purkinje cells severe motor impairment would be expected but instead only moderate ataxia is observed in *pcd* mutants. This is thought to be due to altered inhibition in the vestibular and deep cerebellar nuclei compensating for the lack of normal tonic inhibition from Purkinje cells (Mullen et al., 1976).

Mutations in the gene encoding Nna1, a member of a large protein family with conserved zinc-dependent carboxypeptidase domains (Harris et al., 2000), were found to underlie Purkinje cell degeneration in *pcd* mice (Fernandez-Gonzalez et al., 2002). The exact role this protein plays in Purkinje cell degeneration is not fully understood but there is evidence for endoplasmic reticulum (ER) stress and apoptosis in cell death. The cerebellar expression of BiP, an ER specific chaperone and CHOP, a transcription factor related to ER stress (Oyadomari and Mori, 2004), were found to be elevated in mutant Purkinje cells (Kyuhou et al., 2006). A change in the ratio of anti-apoptotic to pro-apoptotic factors was also observed in *pcd* mice with a 5-fold increase in levels of *c-fos*, *junB* and *krox24*, three cell death effector genes and a reduction in the levels of the anti-apoptotic protein Bcl-2 (Gillardon et al., 1995). Activated caspase 3 and caspase 12 were also detected along with signs of DNA fragmentation, all characteristics of apoptotic cell death (Kyuhou et al., 2006).

1.6.1.2 *Staggerer* mouse

In contrast to *pcd* mouse, severe cerebellar ataxia is observed in *staggerer* mice that have a cell autonomous defect in the maturation of Purkinje cells (Sidman et al., 1962; Herrup and Mullen, 1979a, b; Herrup, 1983). There is also a large reduction in granule cell proliferation and substantial death of granule cells in the first postnatal weeks, revealing an important interplay between Purkinje cell and granule cell survival.

The *staggerer* phenotype results from a 122 bp deletion in the orphan nuclear hormone receptor gene (*ROR α*) preventing the formation of the ROR α ligand binding domain and resulting in a loss-of-function (Hamilton et al., 1996). Gene expression microarrays and chromatin immunoprecipitation assays have identified a number of genes regulated by ROR α that are downregulated in *staggerer* Purkinje cells (Gold et al., 2003). Within the top ten are eight genes involved in glutamatergic and calcium signaling. These are the metabotropic glutamate receptor (*Grm1*), EAAT4 the Purkinje cell glutamate transporter (*Slc1a6*), β -III spectrin (*Spnb3*), the IP₃ receptor (*Itpr1*), its binding partner (*car8*), calmodulin (*Calb1*), a calmodulin regulator (*Pcp4*) and a modulator of voltage-gated calcium channels (*Pcp2*). The fact that *Spnb3* (β -III spectrin) and *Itpr1* (IP₃ receptor), the genetic causes of SCA5 and SCA15/16, respectively are downregulated in the *staggerer* mouse highlights a convergence of disease mechanisms in Purkinje cell degeneration and cerebellar ataxia. Furthermore, microarray analysis of the SCA1 transgenic mouse model (refer

CHAPTER 1 INTRODUCTION

to section 1.6.2.1) also shows a downregulation of *Slc1a6*, *Spnb3*, and *Itpr1* prior to onset of pathology (Lin et al., 2000).

The loss of granule cells is thought to arise from a downregulation in Purkinje cells of *Sonic hedgehog* (Gold et al., 2003), another gene regulated by ROR α and a mitogen for granule cell precursors in the embryonic cerebellum (Dahmane and Ruiz i Altaba, 1999; Wallace, 1999; Wechsler-Reya and Scott, 1999). Analysis of the staggerer mouse has therefore shown that Purkinje cells control both the proliferation of granule cells and their ability to respond to granule cell glutamatergic inputs by ROR α -dependent gene transcription.

1.6.1.3 *Lurcher* mouse

The lurcher mouse was identified in 1954 due to its wobbly, lurching gait (Philips, 1960) and more recently found to arise from a missense mutation in the gene encoding the $\delta 2$ glutamate receptor (GluR $\delta 2$) (Zuo et al., 1997). The function of the $\delta 2$ glutamate receptor is still unknown as it does not bind glutamate or glutamate agonists (Araki et al., 1993; Lomeli et al., 1993; Mayat et al., 1995) but it has been proposed that GluR $\delta 2$ stabilizes Purkinje cell-granule cell synapses and is involved in cerebellum-dependent motor learning (Kashiwabuchi et al., 1995; Kurihara et al., 1997; Yuzaki, 2004). Homozygote animals die in the early neonatal period due to immense neuronal death in the mid and hindbrain (Cheng and Heintz, 1997; Resibois et al., 1997) but cerebellar development begins normally in heterozygous animals. However, Purkinje cell abnormalities appear shortly after birth (PD 3-4) in

CHAPTER 1 INTRODUCTION

heterozygous animals (Swisher and Wilson, 1977) and Purkinje cell degeneration begins between PD 8-10. This is closely followed by death of granule cells and olivary neurons (Caddy and Biscoe, 1975; Wilson, 1975; Caddy and Biscoe, 1976; Wilson, 1976). By 3 months of age the cerebellum of heterozygous animals is practically devoid of Purkinje cells and at death only 10% and 25% of granule cells and olivary neurons remain, respectively (Caddy and Biscoe, 1979). There is no, or very little loss of deep cerebellar nuclei. The *lurcher* mutation is a missense mutation that changes an alanine to threonine resulting in a large constitutive cationic current. Different studies implicate necrosis, autophagy or apoptosis in *lurcher* Purkinje cell death (reviewed in (Vogel et al., 2007)). The mechanism for autophagy may arise from loss of interaction with Beclin-1, a mammalian ortholog of the yeast autophagy gene *apg6/vps30* (Liang et al., 1999), releasing it to associate with proteins involved in the formation of autophagosomes (Kihara et al., 2001). However, there are studies that indicate the constitutive leak current is necessary and sufficient to induce autophagy and cell death (Yamada et al., 2003a,b). The leak current may also lead to increased oxidative stress and excitotoxicity due to enhanced mitochondrial oxidative respiration in response to an increased demand for ATP in depolarized *lurcher* Purkinje cells (Caddy and Biscoe, 1979; Dumesnil-Bousez and Sotelo, 1992; Vogel et al., 2001)

1.6.1.4 Weaver mouse

Unlike the other mutants described a complete loss of granule cells precedes a secondary loss of Purkinje cells in the *weaver* mouse. Although about 50% of Purkinje cells survive in the *weaver* mouse it exhibits a more severe form of ataxia compared to the *pcd* mutant that lacks almost all Purkinje cells. This is thought to arise from an irregular output due to regions where Purkinje cells survive. In fact, removal of the cerebellum improves the motor performance of the *weaver* mouse (Grusser-Cornehls et al., 1999).

1.6.2 Mouse models generated by genetic manipulation

A number of transgenic and knockout mice have been generated to create animal models for several SCA subtypes. These mouse models have revealed whether a gain-of-function, haploinsufficiency or a loss-of-function with a dominant negative effect underly disease pathogenesis. The work has also highlighted the interplay between different cell populations and identified several common cellular mechanisms in Purkinje cell dysfunction and death including altered gene transcription, excitotoxicity, autophagy, apoptosis, and ER stress. A few of the *in vivo* studies are described in more detail in the following sections.

1.6.2.1 CAG repeat expansion models

Harry Orr and colleagues generated the first mouse model of SCA by creating transgenic mice that expressed the human *SCA1* gene (Burrigh et al., 1995). The mice were engineered to express human *SCA1* with either a normal or an expanded CAG repeat sequence, 30 or 82 repeats, respectively. They found that mice expressing human ataxin 1 with the expanded, but not the normal CAG repeat showed a severe loss of Purkinje cells, thinning of the molecular layer and an ataxic phenotype, mimicking the human phenotype (Burrigh et al., 1995; Zoghbi and Ballabio.,1995; Zoghbi and Orr, 1995). This showed that the CAG expansion is pathogenic. The presence of ubiquitinated nuclear aggregates, a pathological hallmark of SCA1 (Skinner et al., 1997), was also observed in the SCA1 transgenic mouse model (Cummings et al., 1998). However, subsequent mouse models have shown that these nuclear inclusions, long believed to be important in disease pathology (Taroni and DiDonato, 2004), are not involved in polyglutamine-mediated pathogenesis as signs of disease are still seen in mouse models that have no inclusions within Purkinje cells (Klement et al., 1998; Cummings et al., 1999; Watase et al., 2002). Instead, what appears to be fundamental for mutant ataxin 1 to cause disease is the nuclear localization of protein. Mice expressing a mutated nuclear localisation signal (NLS), lysine 772 replaced with threonine, thus disrupting entry into the nucleus, do not develop disease (Klement et al., 1998). Other *in vivo* studies have also revealed that phosphorylation of Ser776 is required for toxicity (Emamian et al., 2003). This is thought to be due to altered protein interactions that are regulated by phosphorylation, with some being enhanced and others decreased.

CHAPTER 1 INTRODUCTION

The binding of an mRNA splicing factor (RNA-binding motif protein 17, RBM17) appears to be enhanced by phosphorylation of Ser776 whereas interaction with the transcriptional repressor capicua (CIC) is reduced (Lim et al., 2008). Thus the balance of ataxin 1-containing complexes is changed by the phosphorylation status of Ser776, which appears to be affected by the size of the polyglutamine tract. Mouse models have therefore revealed that the polyglutamine expansion found in SCA1 patients is pathogenic, but importantly they have highlighted that other protein regions are also required for toxicity and both a gain-of-function and loss-of-function mechanism likely play a role in SCA1 pathogenesis through dysregulating gene expression and protein function.

Insights for SCA3, also known as Machado-Joseph disease (MJD) have also been gained from *in vivo* studies. Transgenic mouse models have revealed that, similar to SCA1, the nuclear localization of ataxin-3 protein is essential for manifestation of the disease phenotype (Bichelmeier et al., 2007). Normally ataxin-3 is found in the cytoplasm of neurons but nuclear inclusions are observed in patients with SCA3 (Paulson et al., 1997; Schmidt et al., 1998). This difference in subcellular localization was investigated by creating different mouse models. When transgenic mice expressed ataxin-3 with an expanded polyglutamine repeat but with a nuclear export signal (NES) attached they had mild or no behavioural phenotype and very few nuclear inclusions. In contrast when a NLS was attached, targeting the protein into the nucleus, an earlier and more severe phenotype was observed when compared to mice expressing the untagged transgene (Bichelmeier et al., 2007). Therefore nuclear

CHAPTER 1 INTRODUCTION

localization, a toxic gain-of-function, would appear to be an important aspect in SCA3 pathogenesis. Analysis of another mouse model suggests that Purkinje cell dysfunction, and not cell loss, is important in disease phenotype (Chou et al., 2008). The mice express full-length mutant ataxin-3 and display a severe behavioural phenotype when homozygous for the transgene but show very little cerebellar atrophy.

It is worth mentioning that although expression of mutant full-length protein is thought to recapitulate human disease most accurately, the initial mouse models of SCA3, showing a much more severe phenotype, only expressed a C-terminal region of ataxin-3 containing the expanded polyQ repeat (Ikeda et al., 1996). This led to the proposal that the production of toxic proteolytic fragments may be important in SCA3 pathogenesis. Carboxy-terminal ataxin-3 fragments are seen in the mouse expressing full-length protein (Chou et al., 2008) and so the possibility proteolytic cleavage of ataxin-3 is important cannot be ruled out.

In the case of SCA6, the trinucleotide repeat expansion is found within exon 47 of the *CACNA1A* gene, encoding the $\alpha 1A$ subunit of the (P/Q) $Ca_v2.1$ voltage-gated calcium channel (Garg and Sanchette, 1999; Pietrobon, 2002). However, a critical genetic feature of SCA6 is that the *CACNA1A* gene undergoes alternative splicing and so only one splice variant encodes the polyglutamine tract. The functions associated with the different isoforms are not clearly understood but they are thought

CHAPTER 1 INTRODUCTION

to be involved in regulating synaptic transmission (Sheng et al., 1994; Rettig et al., 1996).

The creation of three knock-in mouse models carrying normal, expanded or hyperexpanded CAG tracts in the *Cacna1a* locus revealed that, like SCA1 and SCA3, disease severity was linked to repeat length and expression level of the mutant protein (Watase et al., 2008). Cell culture experiments had suggested that the expanded CAG repeat affected the conductance of the Ca_v2.1 channel (Matsuyama et al., 1999; Restituito et al., 2000; Toru et al., 2000; Piedras-Renteria et al., 2001). However, the *in vivo* models show no change in the voltage sensitivity of either activation or inactivation of the Ca_v2.1 channel in Purkinje cells but rather decreased channel abundance and aggregation of mutant Ca_v2.1 (Watase et al., 2008). Similarly knockdown of Ca_v2.1 calcium channels has been shown to be sufficient to induce ataxia and progressive cerebellar atrophy (Saito et al., 2009). Therefore the *in vivo* data indicate that a loss-of-function may be a factor in disease, either a consequence of aggregation or altered splicing events that result in decreased levels of specific isoforms, whereas expression in heterologous systems suggest proteolytic cleavage of the C-terminal region produces a fragment that is translocated to the nucleus, causing toxicity (Kubodera et al., 2003; Kordasiewicz et al., 2006).

1.6.2.2 Non-coding repeat expansion models

A CTG repeat believed to be linked to SCA8 is found at the 3' end of a non-coding transcript (Koob et al., 1999). Both a noncoding CUG transcript and a pure polyglutamine protein expressed from a novel gene in the opposite direction (*ATXN 8*) are thought to be produced from the locus. Transgenic mice expressing the human CTG expanded repeat tract (CTG₁₁₆) at high copy number exhibit an ataxic phenotype and possess intranuclear inclusions positive for polyglutamine expansion proteins, whereas control lines expressing normal repeat tracts (CTG₁₁) show no disease phenotype and no inclusions (Moseley et al., 2006). These findings suggested that a gain-of-function at the protein level played a role in pathogenesis.

However, the CUG transcript could also cause disease by two separate mechanisms. One mechanism being that the non-coding RNA functions as an endogenous antisense RNA to regulate the expression of the Kelch-like 1 (*KLHL1*) gene on the opposite strand. *KLHL1*, homologous to *Drosophila* Kelch, an actin-binding protein implicated in cytoskeletal regulation (Robinson and Cooley, 1997) is the only encoded protein in the vicinity of the SCA8 mutation, making it a strong candidate for playing a key role in pathogenesis. *Klhl 1* knockout mice do show a subtle motor phenotype and marginal molecular layer thinning but do not recapitulate the more severe phenotype seen in patients with SCA8 (He et al., 2006). The other possibility is a toxic gain-of-function RNA mechanism similar to other RNA-mediated neurological disorders such as myotonic dystrophy (Ranum and Cooper, 2006). Here the repeat expansions sequester some splicing regulators, e.g. muscleblind-like 1

(MBNL1) but also prevent the binding of other RNA proteins that only bind to short single-stranded CUG repeats (e.g. CUG-BP1). The result is the misregulation of alternative splicing events in several genes due to altered activities of the RNA splicing proteins. One example of a CUG-BP1/MBNL1 regulated target gene found to be upregulated in the SCA8 transgenic mouse expressing the human CTG expanded repeat tract (CTG₁₁₆) and in human autopsy tissue is *GABA-A transporter 4* (Daughters et al., 2009). This upregulation of *Gab4* may explain the loss of GABAergic inhibition seen in the SCA8 transgenic mouse by reducing GABA at the synapse (Moseley et al., 2006). However, no Purkinje cell degeneration or any other neurodegenerative change is observed in this mouse model.

1.6.2.3 Conventional mutation models

In the case of SCA15, the mouse model preceded identification of the gene and is a good example of how spontaneous mouse mutations have been used to understand human disease. A knockout line of mice with a progressive movement disorder was shown through linkage and sequence analysis to be due to an in-frame deletion of 18 bp within exon 36 of *Itpr1*, the gene encoding inositol 1,4,5-triphosphate receptor (van de Leemput et al., 2007). A similar ataxic phenotype is observed in another spontaneous mutant mouse (*opt*), which is due to an in-frame deletion of exons 43 and 44 of *Itpr1* (Street et al., 1997). In 2001 the disease locus for a new autosomal dominant pure cerebellar ataxia (SCA15) was linked to the syntenic region of the human genome (Storey et al., 2001) leading van de Leemput and colleagues to identify a large (~ 200 Kb in length) genomic deletion encompassing one third of

CHAPTER 1 INTRODUCTION

ITPR1 and the first half of a neighbouring gene, *SUMF1* as the genetic cause of SCA15 (van de Leemput et al., 2007). The fact that heterozygous parents of children with multiple sulfatase deficiency due to a homozygous *SUMF1* mutation show no signs of ataxia indicate that heterozygosity for the deletion of *SUMF1* in SCA15 patients is unlikely to underlie disease pathogenesis. Instead a heterozygous loss (haploinsufficiency) of *ITPR1* protein and the resulting disruption to intracellular Ca^{2+} signalling in Purkinje cells would appear to be important in SCA15. Recent linkage analysis has now shown that the locus for SCA16 overlaps with the SCA15 locus indicating that these phenotypically similar diseases, are probably genetically identical (Knight et al., 2003; Miura et al., 2006).

Similarly, the discovery of ataxia in mice with a targeted disruption of the *Fgf14* (fibroblast growth factor 14) locus led to the identification of mutations in the human *FGF14* gene as the underlying cause of SCA27 (van Swieten et al., 2003). Members of the intracellular fibroblast growth factor subfamily (iFGF) have been shown to colocalize with voltage-gated sodium (Na_v) channels and modulate cell excitability (Liu et al., 2001; Liu et al., 2003; Wittmack et al., 2004; Lou et al., 2005; Goldfarb et al., 2007; Laezza et al., 2007). Analysis of *Fgf14*^{-/-} mice has revealed impaired Purkinje cell spontaneous firing and it has been proposed that a reduced expression of the $\text{Na}_v1.6$ channel underlies the deficit.

1.7 Aims and approaches

The overall aim of my thesis was to investigate the physiological role of β -III spectrin and identify mechanisms involved in Purkinje cell dysfunction and degeneration. This was achieved by the analysis of homozygous (β -III^{-/-}) and heterozygous (β -III^{+/-}) β -III spectrin deficient mice, which were generated by Dr Mandy Jackson, at The University of Edinburgh. This analysis is presented in Chapters 3, 4 and 5. Cell culture studies were employed to investigate the effect mutations associated with SCA5 have on β -III spectrin function and this data is reported in Chapter 6. A second approach to understand the normal function of β -III spectrin was to identify proteins that interact with β -III spectrin directly. This was achieved by carrying out a yeast two-hybrid screen using the amino terminus as bait. Two proteins, prosaposin and clathrin light chain, were considered the most promising candidates and further experiments to confirm the interaction were performed, detailed in Chapter 7.

CHAPTER 2

MATERIALS AND EXPERIMENTAL METHODS

2.1 Mammalian cell culture

2.1.1 Cell maintenance

Human embryonic kidney (HEK) 293T cells were grown in minimum essential media (Sigma) containing 10% fetal bovine serum, 10 mM glutamine, 1× non-essential amino acids and antibiotics (penicillin and streptomycin, Sigma). HEK-rEAAT4 cells were maintained in 75 µg/ml hygromycin (Invitrogen). Both cell lines were maintained in T-75 flasks at 37°C and 5% CO₂. Media was changed every 3 days and cells were split on reaching 85-90% confluence. Media was aspirated off, cells were washed with 4 ml of pre-warmed PBS and 2 ml 0.05% trypsin (Sigma) was added. After 1-2 minutes at 37°C 4 ml of media were added to the dissociated cells and centrifuged for 2 minutes at 800 rpm. The cell pellet was re-suspended in 1 ml of media and proportions used to seed fresh flasks and/or plates. Mouse neuronal 2a (Neuro 2a) cells were grown in Dulbecco's modified Eagle's medium (DMEM), supplemented with 4.5g/l glucose and 0.11g/l sodium pyruvate (Gibco), 10% fetal bovine serum, 10 mM glutamine, and antibiotics (penicillin and streptomycin). To split Neuro 2a cells, media was aspirated off and 6 ml of fresh media was pipetted up and down to dissociate the cells. Proportions of the cell suspension were used to seed fresh flasks and/or plates.

CHAPTER 2 MATERIALS AND EXPERIMENTAL METHODS

2.1.2 DNA transfection

For microscopic observation, cells were plated at less than 50% confluency onto glass coverslips (VWR) in 35 mm wells and transfected with 0.5 to 4 μg DNA. Prior to transfection the coverslips, stored under ethanol, were washed twice with autoclaved MQ water and coated overnight at 37°C with poly-L-lysine (50 $\mu\text{g}/\text{ml}$) (Sigma). FuGENE 6, and latterly FuGENE HD transfection reagents were used according to manufacturer's instructions (Roche), generally using a 3:2 ratio of μl transfection reagent : μg total DNA. To obtain cell homogenates HEK 293T cells were plated at 80-90% confluency onto 35-mm dishes and transfected with 4 μg of DNA using lipofectamine 2000 (Invitrogen). Transfections were carried out in accordance with the manufacturer's instructions and prior to transfection cell media was replaced with antibiotic free media. Media was also changed 2 hours post-transfection to remove lipofectamine. 24 hours post-transfection cells were either harvested for Western blot analysis (refer to section 2.4), fixed with 4% paraformaldehyde (PFA) for immunostaining (section 2.1.3) or either treated with 2 $\mu\text{g}/\text{ml}$ tunicamycin for 12 hours or maintained at 37 °C or 25 °C for an additional 12 hours before harvesting/fixation.

2.1.3 Immunostaining of transfected mammalian cells

24 hours post-transfection cells were fixed for 20 minutes with 4% PFA and after washing with 0.1 M Sorensen's Phosphate Buffer pH 7.4 coverslips were either directly mounted onto glass slides using hardset vectashield (Vector Laboratories) or

CHAPTER 2 MATERIALS AND EXPERIMENTAL METHODS

permeabilised with 0.4% Triton X-100 in phosphate buffered saline (PBS) for 15 minutes. Following two 5 min washes in PBS, cells were blocked with 5% normal goat serum (NGS)/0.1% Triton X-100 in PBS for one hour. Cells were then washed twice with PBS and incubated with primary antibody for 1 hour at room temperature (2% NGS/0.1% Triton X-100 in PBS). Following three 5 min washes in PBS cells were incubated with secondary antibody (1:200 in PBS) for 1 hour at room temperature, washed three times with PBS and once with dH₂O before mounting coverslips. Primary antibodies used were mouse anti-c-myc (Ab-1, Calbiochem), rabbit anti-carboxy terminus β -III spectrin, -EAAT4 and -GLAST (all kind gift of Jeffrey Rothstein), rabbit anti-GADD153 (Santa Cruz) and rabbit anti-mGluR1 (Calbiochem). Secondary antibodies used were cyanine 3 (Cy3)- or cyanine 2 (Cy2)-conjugated goat anti-mouse IgG (Jackson laboratories) and fluorescein isothiocyanate (FITC)-conjugated goat anti-rabbit IgG (Cappel). Coverslips were mounted using hard set vectashield containing 4',6-Diamidino-2-Phenylindole (DAPI) (Vector Laboratories) unless Cy2-conjugated goat anti-mouse IgG was used, in which case vectashield was the chosen mounting agent. Images were captured with the Zeiss Axiovert confocal microscope and processed using Image J.

CHAPTER 2 MATERIALS AND EXPERIMENTAL METHODS

2.1.4 Solubilisation assay

Transfected cells were harvested in ice cold homogenization buffer [HB, 20 mM HEPES pH 7.4, 1 mM ethylenediaminetetra-acetic acid (EDTA), protease inhibitor cocktail (Calbiochem) and 1 mM phenylmethylsulfonyl fluoride (PMSF)] containing 1% Triton X-100. Cell suspension was rotated for 2 hours at 4°C before centrifuging at 6000 rpm for 2 minutes at 4°C. An equal volume of 2 × loading dye [125 mM Tris-HCl pH 6.8, 20% glycerol, 4% sodium dodecyl sulfate (SDS), 10% β-mercaptoethanol, 0.25% pyroyin Y dye] was added to the supernatant and pellet. Additional cell pellets were re-suspended in HB containing 8M Urea and 4% SDS and rotated for 2 hours at 4°C before centrifuging at 6000 rpm for 2 minutes. Again an equal volume of 2 × loading dye was added to supernatant and pellet. All samples were resolved by SDS-polyacrylamide gel electrophoresis (PAGE) (refer to section 2.4).

2.1.5 Stability assay

HEK 293T cells were treated with 10 µg/ml cyclohexamide (Sigma) 24 hours after transfection. Cells were harvested in HB at 0 hours and 3 hours following cycloheximide treatment and protein concentrations determined using Coomassie-Plus Reagent and bovine serum albumin as standard (Pierce). Samples were resolved by SDS-PAGE and protein levels expressed as percentage of 0 hours.

CHAPTER 2 MATERIALS AND EXPERIMENTAL METHODS

2.1.6 Biotinylation

HEK-rEAAT4 cells were washed twice with 1 mM MgCl₂ and 0.1 mM CaCl₂ in PBS, pre-warmed to 37 °C. Cells were incubated with sulpho-biotin (1 mg/ml in PBS, Pierce) for 20 minutes at 4°C with gentle agitation, washed twice with 100 mM glycine (in PBS) and excess biotin quenched with 100 mM glycine in PBS for 45 minutes at 4°C. Cells were lysed for 1 hour at 4 °C with vigorous shaking (20 mM HEPES pH 7.4, 150 mM NaCl, 1 mM EDTA, 1% Triton, 1 mM PMSF and protease inhibitor cocktail) and lysates centrifuged at 13000 rpm for 15 minutes at 4°C. An aliquot of supernatant was added to an equal volume of 2 × loading dye (total cell lysate). The remainder was incubated with an avidin bead suspension (Pierce) for 1 hour with gentle agitation at room temperature. The suspension was centrifuged for 15 minutes at 13000 rpm at 4°C and supernatant was added to an equal volume of 2 × loading dye (intracellular lysate). The beads were washed 4 times with lysis buffer and an equal volume of 2 × loading dye added to form the membrane fraction. Total, intracellular and membrane fractions were resolved by SDS-PAGE.

2.1.7 Glutamate uptake assay

Cells grown in 6-well plates were washed twice with ice cold tissue buffer (50 mM Tris-HCl and 320 mM sucrose, pH 7.4) before being incubated for 10 minutes at 37°C in either sodium plus or sodium free Krebs buffers containing 5 µM cold glutamate and 0.03 µCi/µl ³H-glutamatic acid (sodium plus, 120 mM NaCl, 25 mM NaHCO₃, 5 mM

CHAPTER 2 MATERIALS AND EXPERIMENTAL METHODS

KCl, 2mM CaCl₂, 1mM KH₂PO₄ and 1 mM MgSO₄, pH 7.4; sodium free, 120 mM Choline Cl, 25 mM Tris-HCl, 5 mM KCl, 2 mM CaCl₂, 1 mM KH₂PO₄ and 1 mM MgSO₄, pH 7.4). Glutamate uptake was terminated by placing the cells back on ice and cells were washed twice with ice cold wash buffer (50 mM Tris-HCl, 160 mM NaCl, pH 7.4). Cells were lysed with 0.1 M NaOH and radioactivity measured using a scintillation counter. Na⁺-dependent uptake was determined by subtracting Na⁺-free counts.

2.2 Polymerase chain reaction (PCR)-based techniques

2.2.1 Primer design for PCR

Primers (refer to appendix 1) were designed by the author, if possible with regard to the following rules:

- a) Forward and reverse primers should have similar annealing temperatures *ie.* equivalent numbers of (A + T) and (C + G) residues.
- b) There should be no complementarity in the 4 nucleotides most 3' in each primer, to reduce the formation of primer dimers.
- c) Primers should not have extensive stretches of internal complementarity, and with regard to site directed mutagenesis:
- d) Primers should have either a G or C at 3' end.

CHAPTER 2 MATERIALS AND EXPERIMENTAL METHODS

2.2.2 PCR

PCR reactions were carried out in a volume of 50 μ l using Expand High Fidelity buffer (2 mM Tris-HCl pH 7.5, 1.5 mM MgCl₂) (Roche), dNTPs each at 200 μ M, 0.3 μ M of each primer (MWG), 2.6 U Expand High Fidelity enzyme mix (Roche) and 50 ng of template DNA. Following an initial denaturation step of 94 °C for 2 minutes, 24 cycles of denaturing at 94 °C for 15 seconds, annealing at 55-65°C for 30 seconds and extension at 68°C or 72°C (between 30 seconds and 20 minutes), with a final extension time of 10 minutes was used. The precise annealing temperature and extension time varied according to the predicted T_m of the primers and size of the amplified product, respectively. Conditions for each primer pair are detailed in appendix 1.

2.2.3 Purification of PCR products

Specific PCR products were purified away from amplification primers and nucleotides by gel extraction using the QIAEX II gel extraction kit (Qiagen) according to manufacturer's instructions. Products were mixed with loading buffer (30% glycerol, 0.25% bromophenol blue) and resolved on a 1% Tris-acetate EDTA (TAE) agarose gel. The band of interest was excised using a sterile scalpel blade and the agarose solubilized at 55°C in 3 volumes of QX1 buffer (7 M Na PO₄, 10 mM NaAc, pH 5.3). The DNA binds to QIAEX II silica-gel particles and after washing away excess agarose and salt, is eluted with TE (10 mM Tris-HCl, 1 mM EDTA, pH 8.0).

CHAPTER 2 MATERIALS AND EXPERIMENTAL METHODS

2.2.4 Site-directed mutagenesis

Mutations were introduced using the QuickChange site-directed mutagenesis kit (Stratagene) according to the manufacturer's instructions using pRK5-myc-tagged β -III spectrin and pCDNA-YC- β -III295 as template DNA. Refer to appendix 1 for primer sequence and PCR conditions.

2.3 Methods used to subclone DNA fragments

2.3.1 Preparation of DNA

2 μ g of vector DNA was digested for 2 hours and gel purified PCR products were cut overnight at 37 °C with the appropriate restriction enzyme (Promega). Restriction enzymes were heat-inactivated at 70 °C for 10 minutes and cut plasmid was treated with calf intestinal phosphatase (CIP, Promega) for 30 minutes at 37 °C and then heat-inactivated at 70 °C for 10 minutes. All digested DNA was resolved by electrophoresis on a 1% TAE agarose gel and gel-purified with QIAEX II gel extraction kit (Qiagen).

2.3.2 DNA ligations and bacterial transformations

Ligation reactions were performed either overnight at 4 °C or at room temperature for 1 hour with 3 U of T4 DNA ligase and T4 DNA ligase buffer (30 mM Tris-HCl pH7.8, 10 mM MgCl₂, 10 mM DTT, 1 mM ATP) in a final volume of 10 μ l. DH5 α subcloning efficiency competent cells (Invitrogen) were transformed with 5 μ l of ligation mix

CHAPTER 2 MATERIALS AND EXPERIMENTAL METHODS

followed by heat shocking. DNA was added to 50 µl competent cells and left on ice for 30 minutes, heat shocked at 42 °C for 45 seconds and placed back on ice for 2 minutes. 450 µl Luria broth (LB) medium (1% Bacto[®] tryptone, 0.5% yeast extract, 0.5% NaCl) was added and incubated at 37 °C for 1 hour with shaking. Aliquots of the transformation were plated onto agar plates, supplemented with kanimycin (30 µg/ml) or ampicillin (50 µg/ml). If pGEM-T Easy vector (Promega) was used to directly clone PCR products then 0.02% 5-bromo-4-chloro-3-indolyl-β-D-galactoside (X-gal) was also added to ampicillin plates for colour selection.

2.3.3 Isolation of plasmid DNA

Single bacterial colonies (white colonies if using pGEM-T Easy) were picked and inoculated into 5 ml LB medium. Cultures were supplemented with ampicillin or kanimycin and grown overnight at 37 °C with shaking. The following day plasmid DNA was extracted using QIAprep Spin Miniprep Kit (QIAGEN) according to manufacturer's protocol. Bacteria are lysed under alkaline conditions, then the lysate is neutralized and adjusted to a high salt concentration allowing the absorption of DNA onto the QIAprep silica membrane. Pure plasmid DNA can then be eluted from the membrane with TE. A 5 ml culture reliably yields 5 µg of high-copy plasmid DNA.

CHAPTER 2 MATERIALS AND EXPERIMENTAL METHODS

2.3.4 Mammalian expression vectors

Full length rat β III spectrin and the amino terminus of WT and L253P β III spectrin were amplified by PCR using primers that introduced either *Bsp* EI and *Xba* I restriction sites or *Not* I and *Cla* I restriction sites (refer to appendix 1). The PCR products, following digestion with the appropriate restriction enzymes and gel purification, were cloned into the appropriately cut pCDNA3.1 (zeo) -YC vectors (kind gift of Stephen Michnick). Full length Arp1, full length prosaposin and full length clathrin light chain were amplified using Quickclone rat cDNA (Clontech) as template and cloned into either the *Bsp* EI and *Xba* I sites or *Not* I and *Cla* I sites of pCDNA3.1 (zeo) -YN. Other mammalian expression vectors used were pCDNA3.1-EAAT4 (Jackson et al., 2001), pCDNA3.1-GLAST, pRK5-mGluR1, pRK5-myc-tagged mGluR5, pCDNA3.1-myc-tagged human β -III spectrin (WT and mutant forms, Ikeda et al., 2006), pECFP-golgi and pDsRed2-ER (Clontech).

2.3.5 DNA sequencing

500 ng of double stranded plasmid DNA, in a final volume of 30 μ l dH₂O, and primers (MWG) at a concentration of 3.2 μ M were sent to the DNA Sequencing Service at the University of Dundee. Sequencing results were analysed using MacVector software.

CHAPTER 2 MATERIALS AND EXPERIMENTAL METHODS

2.3.6 Glycerol stocks

For long-term storage, glycerol stocks were made by adding 180 μ l of sterile 50% glycerol to 820 μ l of bacterial culture grown overnight. Samples were mixed, snap frozen in a dry ice/ethanol bath and stored at -80°C .

2.4 SDS-PAGE and Western blotting

Samples in $2 \times$ loading dye were boiled for 10 minutes and centrifuged briefly before being run on either a 4-20% gradient gel (Invitrogen), or a 6% or 12% acrylamide gel in Tris-Glycine/SDS running buffer (25 mM Tris-HCl, 52 mM glycine, 0.1% SDS). After electrophoresis (gradient gels, 120 V for 90 minutes; single percentage gels, 200 V for 40 minutes) proteins were transferred for 1 hour at 100 V to a nitrocellulose membrane (Amersham Biosciences) in Tris-Glycine/methanol buffer (25 mM Tris-HCl, 192 mM glycine, 20% methanol). Membranes were blocked for 1 hour at room temperature with 5% wt/vol non-fat dry milk (Marvel) in Tris-buffered saline/Tween 20 (TBS/T, 20 mM Tris-HCl, 200 mM NaCl, (pH 7.6 with 0.1% v/v Tween-20). Blots were incubated overnight at 4°C with either rabbit anti- β -III spectrin (1:200), anti-EAAT4 (1:200), anti-GLAST (1:200), anti-GLT1 (1:4000), anti-GFP (1:8000), anti-p38 (1:1000), anti-GADD153 (1:500), mouse anti-actin (1:1600 Sigma), anti-calbindin (1:1600 Sigma), anti-HA (1:1600, Covance), anti-c-myc (1:400, Calbiochem), or goat anti- β -III spectrin (1:2000, Santa Cruz) in blocking buffer. After washing 5 times, each for 5 minutes with TBS/T, the blots were incubated for 1 hour at room temperature with HRP-conjugated

CHAPTER 2 MATERIALS AND EXPERIMENTAL METHODS

donkey anti-rabbit IgG (1:4000; Amersham Pharmacia), HRP-conjugated sheep anti-mouse IgG (1:4000; Amersham Pharmacia) or HRP-conjugated donkey anti-goat IgG (1:4000; Santa Cruz). Immunoreactive proteins were visualized by autoradiography using enhanced chemiluminescence (ECL) according to manufacturer's protocol (Santa Cruz Biotechnology).

2.5 Animal procedures

2.5.1 Husbandry

Mice were housed in either individual ventilated cages (IVCs) or conventional cages. All animals were kept in a pathogen free environment and maintained in a 12 hour light/dark cycle. Food and water were available *ad libitum*.

2.5.2 Genotyping

DNA was extracted from mouse ear notches using ChargeSwitch[®] gDNA micro tissue kit (Invitrogen) and animals genotyped by PCR analysis. Amplification used a common upstream primer (5'- gagcgagaagccgtgcagaag - 3') as well as primers specific to the WT allele (5' - aggatgatgtccacactagcc- 3') and the *PGK-neo* cassette (5' - ctaccggtggatgtggaatg - 3') from the mutant allele. PCR products from the WT allele (710 bp) and the mutant allele (562 bp) were resolved by electrophoresis on a 1% TAE agarose gel.

CHAPTER 2 MATERIALS AND EXPERIMENTAL METHODS

2.5.3 Behaviour tests

Prior to testing, mice were handled for 10 minutes per day for 7 days and habituated to the test environment. All behaviour tests were carried out in low lighting and with constant background noise. Mice were handled, habituated, trained and tested at the same time of day for each experiment. As far as possible all tests were carried out blind to mouse genotype.

2.5.3.1 Footprint analysis

Mice had their hind paws dipped in non-toxic, water-soluble black ink (Indian Ink, Winsor and Newton) before being allowed to walk down an enclosed runway, lined with white paper (80 cm by 10.5 cm wide). After each trial, paws were washed with water. Three consecutive strides were measured for each animal. Stride length measurements were taken from the base of two consecutive paw prints on the same side and the base width was measured as the distance between the centre of one paw print to the centre of the next on the opposite side.

2.5.3.2 Rotarod

Mice were placed on a stationary (maximum time 60 seconds) and rotating rod (3, 5 and 10 rpm, maximum time 2 minutes) and the latency to fall off was recorded (TSE rotarod, 3 cm diameter). On the same day each animal was given four consecutive trials with a minimum of 30 minutes rest between trials.

CHAPTER 2 MATERIALS AND EXPERIMENTAL METHODS

2.5.3.3 Elevated Beam

Mice were placed on a narrow horizontal beam (2 cm wide, 80 cm long), held approximately 30 cm above the bench, and the number of hind paw slips the animal made whilst traversing the beam were counted.

2.5.3.4 Inverted Grid

Animals were placed on a cage lid, which was then slowly turned upside down, and the latency to fall was measured. A maximum time of 60 seconds was given for each of the 4 consecutive trials.

2.5.3.5 Novel Object Recognition

Each mouse was placed inside a dark maze (40 cm x 40 cm) and monitored by a video camera linked to the Anymaze programme. Various plastic objects were used, constructed to be of equal height, weight and interest to the mice. Every trial started with a 5 min habituation phase where the mouse was placed in the centre of the empty maze and allowed to explore. The mouse was removed for 5 min and 2 plastic objects were placed centrally into the maze. The mouse was then re-introduced for a further 5 min, removed for 5 min and one object replaced before the mouse was allowed to explore the already familiar and novel object for a further 5 min. Data was expressed as a ratio of the time exploring novel object to time exploring familiar object (termed exploratory

CHAPTER 2 MATERIALS AND EXPERIMENTAL METHODS

preference). Exploration was recorded when the mouse was in close proximity to the object, had its head orientated towards it and demonstrated an active interest in the object by either intensively smelling it or having its limbs up against it. Climbing on the object was not recorded as exploration. Mice were given 3 trials, with each trial separated by 48 hours, and each time two different objects were used. Between trials, the maze and objects were thoroughly cleaned with ethanol to remove olfactory cues.

2.6 Analysis of mouse tissue

2.6.1 Protein homogenates

Tissue was homogenised in ice cold HB with a Teflon-glass homogenizer. Protein concentrations were determined using Coomassie-plus reagent and bovine serum albumin as standard (Pierce).

2.6.2 Freezing tissue

Animals were killed with an overdose of anaesthetic, tissue removed and immersion-fixed overnight at 4°C in 4% PFA/0.1 M sodium phosphate buffer pH 7.4 before cryoprotecting in 30% sucrose/0.1 M sodium phosphate buffer pH 7.4. Tissue was snap-frozen on dry-ice and stored at -80°C.

CHAPTER 2 MATERIALS AND EXPERIMENTAL METHODS

2.6.3 Transcardial perfusions

Mice were anaesthetised with sodium pentobarbitol and perfused through the left cardiac ventricle with physiological saline followed by 4% PFA in 0.1 M sodium phosphate buffer pH 7.4. Brain and kidneys were removed and immersed in 4% PFA overnight at 4°C. Brain tissue was cryoprotected by immersion in 0.1 M sodium phosphate buffer pH 7.4 containing 30% sucrose, snap-frozen on dry-ice and stored at -80°C, whereas kidneys were embedded in paraffin (refer to section 2.6.5).

2.6.4 Frozen sections

Fixed brain tissue was mounted onto a chuck, coated in optical cutting temperature compound (OCT), and placed in a cryochamber (Leica CM 1900), the temperature of which was maintained at -23°C. 10 µm thick sagittal sections were cut, using a blade cleaned with ethanol, and electrostatically attached to poly-L-lysine coated Super Frost glass slides (VWR). Sections were stored at -20°C prior to staining.

2.6.5 Paraffin sections

Kidneys were removed from 4% PFA and placed in plastic cassettes (VWR) which were immersed in 50% ethanol for 2 hours and then maintained in 70% ethanol until embedded in paraffin by Grace Grant and Vivian Allison. After processing, paraffin blocks were attached to metal chucks, mounted and orientated in a microtome so that the

CHAPTER 2 MATERIALS AND EXPERIMENTAL METHODS

front side of the block was parallel with the cutting blade. Ribbons of 10 μm wax sections were cut, floated in a water bath (40°C) and mounted onto poly-L-lysine coated Super Frost glass slides (VWR). Slides were heated in an oven overnight at 37°C.

2.6.6 Histological techniques

2.6.6.1 Haematoxylin and eosin staining

Paraffin sections were first de-waxed in xylene for 30 minutes and then rehydrated through alcohol (100% to 90% to 70% EtOH), washed in dH₂O and stained with haematoxylin for 5 minutes. Sections were then washed in dH₂O, dipped in 70% acid alcohol (2 ml glacial acetic acid in 200 ml 70% EtOH), washed in dH₂O and submerged in Scotch tap water substitute (STWS) for 3 minutes. After a 3 min dH₂O wash, sections were stained with alcohol-based acidic eosin, washed in dH₂O and placed in potassium alum before another dH₂O wash. Sections were then processed through 70%, 90%, 95% and 100% alcohol, washed twice in mounting xylene and mounted using DPX mountant (VWR). All incubations were for 2 minutes unless otherwise stated and haematoxylin and eosin solutions were filtered before use. Mounted sections were left overnight at room temperature before being imaged using Olympus IX70 microscope and Openlab software (Improvision). All images were processed using Image J.

CHAPTER 2 MATERIALS AND EXPERIMENTAL METHODS

2.6.6.2 Cresyl violet staining

Frozen sections were air dried for 30 minutes before being rehydrated through alcohol (100% to 90% to 70% EtOH), washed in dH₂O and then stained with cresyl violet solution (0.25%) for 3 minutes. Sections were then washed in dH₂O before being placed in 70% acid alcohol. Sections were dehydrated through alcohol (70% to 90% to 100% EtOH), placed in xylene and mounted with DPX mountant. All incubations were for 2 minutes. Sections were imaged using the Zeiss Axiovert confocal microscope and images processed using Image J.

2.6.6.3 Immunostaining

Frozen sections were air dried for 30 minutes before being immunostained as described in section 2.1.3. Primary antibodies used were mouse anti-calbindin D28K (Sigma), mouse anti-glial fibrillary acidic protein (GFAP, Sigma), rabbit anti-saposin D (kind gift of Ying Sun) and rabbit anti- β -III spectrin (kind gift of Jeffrey Rothstein). Secondary antibodies used were Cy3-conjugated goat anti-mouse IgG (Jackson Laboratories) and FITC-conjugated goat anti-rabbit IgG (Cappel). Images were captured using the Zeiss Axiovert confocal microscope and processed using Image J.

2.6.6.4 Quantification of cerebellar morphology

Quantification was carried out on cresyl violet stained cerebellar sections by counting the number of Purkinje cells along a 1 mm linear length in folia II, III, IV, VI and VIII (the most consistent folia between animals) and the counts averaged for each animal. The molecular layer thickness was also measured at 3 specific points within each of the aforementioned folia and the fifteen measurements averaged for each animal.

2.7 Co-immunoprecipitations

Cerebellums were rapidly dissected and homogenized in 800 μ l of HB with a Teflon-glass homogenizer. The protein concentration was calculated using Coomassie-Plus Reagent and bovine serum albumin as standard (Pierce). HB and 10% Triton X-100 were added to obtain a final concentration of 2 μ g protein/ μ l and 1% Triton X-100 (v/v). Homogenate was rotated for 2 hr at 4°C before centrifugation at 13000 rpm for 20 min at 4 °C to remove cellular debris. An equal volume of 2 \times loading dye was added to 25 μ l of lysate. 500 μ l of lysate was incubated with either 1 μ g of anti-sapoin D antibody or 1 μ g of rabbit IgG. After rotating overnight at 4°C 150 μ l of 50% protein A sepharose slurry in PBS (Amersham Biosciences) was added to each sample and rotated for a further 2 hr at 4°C. Protein A sepharose was pelleted by centrifugation for 2 min at 6000 rpm (4 °C) and resin washed with 500 μ l HB. Wash procedure was repeated a further three times and after the final wash, an equal volume of 2 \times loading dye was

CHAPTER 2 MATERIALS AND EXPERIMENTAL METHODS

added to the resin. Bound proteins were resolved by SDS-PAGE and immunoblotted with anti- β -III spectrin antibody.

2.8 Methods used in yeast two-hybrid assay

2.8.1 Yeast two-hybrid assay

In the MATCHMAKER GAL4 Two-Hybrid system (Clontech) the bait gene (β -IIIInt295) was expressed as a fusion to the GAL4 DNA-binding domain (BD) and the prey protein (a rat library) was expressed as a fusion to the GAL4 DNA-activation domain (AD). Upon interaction between the bait and prey proteins, the reporter gene, *Lac Z*, which tested positive for β -galactosidase activity was activated.

2.8.2 Library screen

The bait plasmid was introduced into yeast strain Y190 by the small-scale lithium acetate (LiAc)-mediated method according to manufacturer's protocol (Yeast Protocols Handbook, Clontech 2001). Yeast expressing the bait protein was sequentially transformed with an adult rat brain MATCHMAKER cDNA library constructed in pACT2 (Clontech), and plated on synthetic defined (SD) agar deficient in leucine, tryptophan and histidine and containing 30 mM 3-amino-1,2,4-triazole.

CHAPTER 2 MATERIALS AND EXPERIMENTAL METHODS

2.8.3 Preparation of yeast protein extracts

Yeast protein extracts were prepared using the urea/SDS method according to manufacturer's instructions (Yeast Protocols Handbook, Clontech 2001). Cells were lysed by vortexing with glass beads in cracking buffer (8 M Urea, 5% SDS, 40 mM Tris-HCl pH 6.8, 0.1 mM EDTA, 0.89% β -mercaptoethanol, protease inhibitor cocktail, PMSF and 0.25% pyroyin Y dye) and then centrifuged at 13000 rpm for 5 minutes at 4°C to pellet debris and unbroken cells. Supernatants were boiled and resolved by SDS-PAGE.

2.8.4 β -galactosidase activity assays

Colonies were screened for β -galactosidase activity using a colony lift assay and quantification was obtained using a liquid o-nitrophenyl β -D- galactoside (OPNG) assay, both according to manufacturer's instructions (Yeast Protocols Handbook, Clontech 2001). Cells were lysed by freeze-thawing in liquid nitrogen and in the former case the cells were incubated on a filter soaked in Z buffer/X-gal (8 mM $\text{Na}_2\text{HPO}_4 \cdot 7\text{H}_2\text{O}$, 4 mM $\text{NaH}_2\text{PO}_4 \cdot \text{H}_2\text{O}$, 0.1 mM KCl, 0.1 mM $\text{MgSO}_4 \cdot 7\text{H}_2\text{O}$, (pH 7) 2.7 % β -mercaptoethanol and 20 mg/ml X-gal stock solution) solution and in the latter incubated with 4 mg/ml OPNG in Z buffer/ β -mercaptoethanol (0.27 %).

CHAPTER 2 MATERIALS AND EXPERIMENTAL METHODS

2.8.5 Recovery of plasmid DNA from yeast

Yeast colonies were grown in 2 ml of –Leu/Trp SD media overnight at 30 °C with shaking. The pellet from 1.5 ml of culture, centrifuged for 5 minutes at 13000 rpm, was re-suspended in 200 µl of breaking buffer (2% Triton X-100, 1% SDS, 100 mM NaCl, 10 mM Tris-HCl pH 8, 1mM EDTA). Samples were vortexed vigorously for 2 minutes with an equal volume of glass beads (Sigma) and phenol/ chloroform to break open cells and then centrifuged for 5 minutes at 13000 rpm. A second phenol/chloroform extraction was carried out on 175 µl of the aqueous layer. DNA was precipitated from 150 µl of the second aqueous layer by adding 2.5 volumes of 100% ethanol and centrifuging for 20 minutes at 13000 rpm. Pellets were washed with 70% ethanol, air-dried and re-suspended in 30 µl TE. Library efficiency competent cells (Invitrogen) were transformed with 10 µl of plasmid DNA.

2.8.6 Yeast Expression Vectors

Different β -III spectrin constructs (β -IIIInt219, β -IIIInt258, β -III220-851 and β -III259-851) were amplified by PCR using primers that introduced *Eco* RI restriction sites (refer to appendix 1). The PCR products, following digestion with the appropriate restriction enzymes and gel purification, were cloned into the appropriately cut pGBKT7 vector. Different clathrin constructs (CLC374, CLC375-746 and CLC246-500) were amplified by PCR using primers that introduced *Eco* RI and *Xho* I restriction sites (refer to appendix 1) and cloned into the respective sites of the pACT2 vector.

CHAPTER 2 MATERIALS AND EXPERIMENTAL METHODS

2.9 Statistics

Statistical analysis was performed using a Mann-Whitney test or a two sample Student's t-test, assuming unequal variance. In certain instances, the Kriskal-Wallis H' test preceded the Mann-Whitney test with Bonferroni correction for comparison within groups. For densitometry analysis of Western blots a one sample t-test was used with predicted value of 100% for WT.

CHAPTER 3

ANALYSIS OF $\Delta 2-6$ β -III SPECTRIN

3.1 Background

The targeting strategy used by Dr. Mandy Jackson to generate a β -III spectrin knockout mouse involved replacing exons 3 to 6 with the neomycin-resistance gene. This disrupted the open reading frame in the recombinant allele by introducing a premature stop codon at the beginning of exon 7 due to exon 2 being spliced onto exon 7. Western blot analysis of whole cerebellar homogenates, using a previously characterised anti- β -III spectrin antibody (Jackson et al., 2001), confirmed the loss of full-length β -III spectrin (270 KDa) in β -III^{-/-} spectrin mice and revealed its quantity was approximately halved ($58.4 \pm 7.4\%$ of full length β -III spectrin) in β -III^{+/-} spectrin animals (asterix Figure 3.1A). However, a smaller molecular weight protein was detected at low levels in β -III^{+/-} and β -III^{-/-} spectrin mice but not in WT mice ($18.8 \pm 2.2\%$ of full-length β -III spectrin) (arrowhead Figure 3.1A).

Additional work in the Jackson lab revealed, using semi-quantitative reverse transcription-polymerase chain reaction (RT-PCR), a novel β -III spectrin transcript was expressed in β -III^{+/-} and β -III^{-/-} spectrin mice (Figure 3.1B). Sequencing revealed this arose from exon 1, not exon 2, being spliced onto exon 7 in the recombinant allele. Consequently no premature stop codon is introduced and the open reading frame is retained. Therefore β -III^{+/-} and β -III^{-/-} spectrin mice appeared to express a truncated form

CHAPTER 3 ANALYSIS OF $\Delta 2-6$ β -III SPECTRIN

of β -III spectrin (~ 250 KDa) that lacks most of the actin-binding domain encoded by exons 2-6.

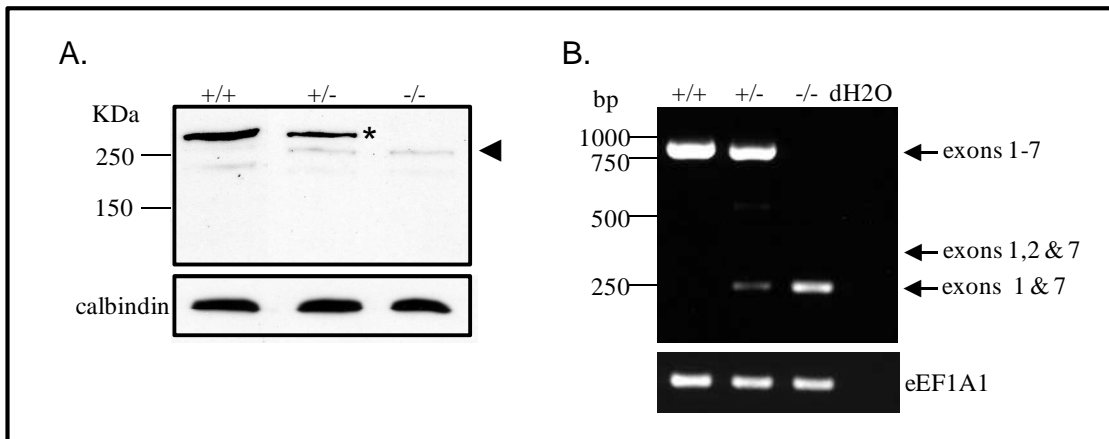


Figure 3.1 Low level of smaller molecular weight protein expressed in β -III^{+/-} and β -III^{-/-} spectrin mice. **A)** Total cerebellar homogenates resolved by SDS-PAGE and probed with polyclonal antibody raised against C-terminal epitope of β -III spectrin. Calbindin used as protein loading control. **B)** Semi-quantitative RT-PCR analysis using forward primer in exon 1 and reverse primer in exon 7. Predicted PCR products for exon 1 to 7, exon 1, 2 & 7 and exon 1 & 7 are 772- 423- and 260-bp, respectively. Amplification of elongation factor (eEF1A1) controlled for template levels.

The initial aim of this thesis was to confirm the truncated protein expressed in β -III^{+/-} and β -III^{-/-} spectrin mice was in fact protein lacking exons 2-6 ($\Delta 2-6$ β -III spectrin) and determine whether this truncated protein possessed any obvious gain-of-function or adverse properties compared to full-length β -III spectrin. *In vitro* experiments were carried out to compare cellular localisation, solubility, stability and ability to stabilise EAAT4, a known interactor of β -III spectrin (refer to section 1.5.4).

3.2 Results

3.2.1 Cloning and expression of $\Delta 2-6$ β -III spectrin

The cloning of $\Delta 2-6$ β -III spectrin cDNA was a 4-step process and utilised the unique *Sph* I restriction site at amino acid (aa) 1108 of rat β -III spectrin and the *Sph* I restriction site in the vector backbone of pGEM-T easy (Figure 3.2A). Briefly, a *Sph* I restriction digest of full-length β -III spectrin cDNA in pGEM-T easy released an amino-terminal fragment containing 1-1108 aa, leaving the remainder of β -III spectrin cDNA attached to the plasmid backbone (step 1). The RT-PCR product of exon 1 spliced onto exon 7 amplified from β -III^{-/-} mice was used as one of two DNA templates in an overlapping PCR to replace the normal amino terminus with exons 1 & 7 (step 2). This PCR product was then subcloned into pGEM-T easy vector and colonies with the insert in correct orientation identified (step 3). The cloned insert was released by digestion with *Sph* I and ligated into the previously *Sph* I cut pGEM-T easy vector containing the 3' end of β -III spectrin cDNA (step 4). Finally, amplification of the cloned insert by PCR using primers that introduced *Not* I restriction sites allowed $\Delta 2-6$ β -III spectrin cDNA to be cloned into two mammalian expression vectors, pCDNA3.1 and pRK5, the latter resulting in the addition of an N-terminal myc-tag.

Cell homogenates from HEK 293T cells transfected with the newly generated pCDNA3.1 $\Delta 2-6$ β -III spectrin construct were run alongside total cerebellar

CHAPTER 3 ANALYSIS OF $\Delta 2-6$ β -III SPECTRIN

homogenates from β -III^{+/-} and β -III^{-/-} spectrin mice (Figure 3.2B). The expressed protein was found to co-migrate on a SDS-polyacrylamide gel with the smaller molecular weight protein detected in genetically modified mice, indicating the remaining protein was β -III spectrin lacking exons 2-6. Endogenous β -III spectrin in HEK 293T cells was shown to be smaller than full-length mouse β -III spectrin by probing cell homogenates from cells transfected with empty vector.

3.2.2. Characterisation of $\Delta 2-6$ β -III spectrin protein

Cellular localisation

Rat β -III spectrin was previously shown to localise with actin at the cell membrane (Jackson et al., 2001). Neuro2a cells were transfected with myc-tagged full length and myc-tagged $\Delta 2-6$ β -III spectrin to determine whether the loss of exons 2-6 resulted in an abnormal cellular distribution. Immunostaining of fixed cells with an anti-c-myc antibody showed that like full length β -III spectrin (Figure 3.3A), $\Delta 2-6$ β -III spectrin was predominantly found at the cell membrane (Figure 3.3B). Images were captured in 3 planes and all confirmed that both full length and $\Delta 2-6$ β -III spectrin were associated with the cell membrane. No cytoplasmic or nuclear aggregates were observed. As a negative control Neuro2a cells were transfected with empty vector, immunostained using anti-c-myc antibody and no immunofluorescence was detected (data not shown). Moreover, confocal immunofluorescence microscopy by Emma Perkins revealed that

CHAPTER 3 ANALYSIS OF $\Delta 2-6$ β -III SPECTRIN

$\Delta 2-6$ β -III spectrin in β -III^{-/-} spectrin mice was still located throughout the Purkinje cell dendritic tree but, consistent with results from Western blot analysis, at a substantially reduced level when compared with WT β -III spectrin (Figure 3.3C).

CHAPTER 3 ANALYSIS OF $\Delta 2-6$ β -III SPECTRIN

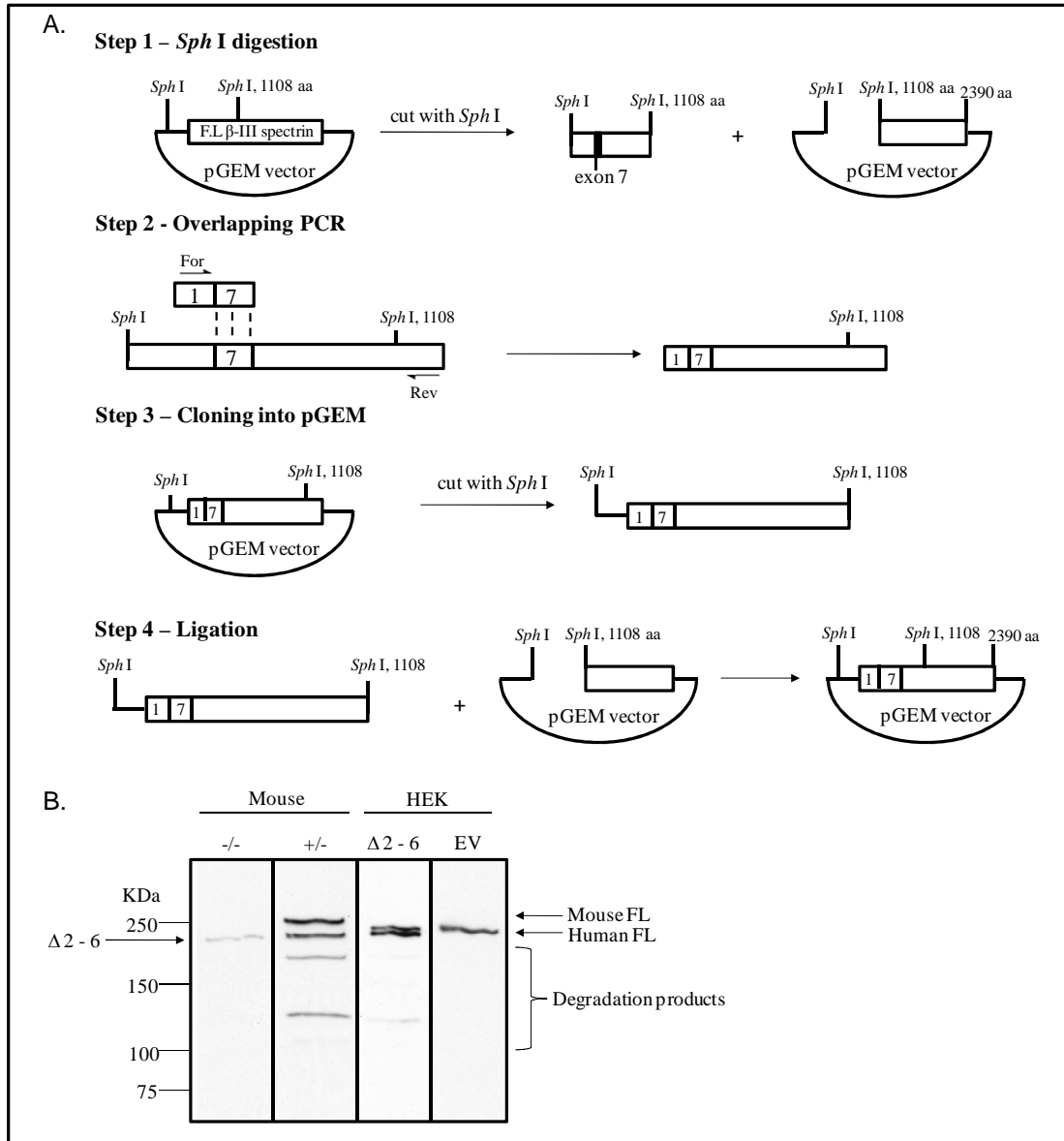


Figure 3.2 Cloning and expression of $\Delta 2-6$ β -III spectrin. A) Schematic diagram of steps used to clone $\Delta 2-6$ β -III spectrin. **B)** Homogenates of HEK 293T cells transfected with empty vector (EV), or pCDNA3.1 $\Delta 2-6$ β -III spectrin ($\Delta 2-6$) and total cerebellar homogenates from homozygous (β -III^{-/-}) and heterozygous (β -III^{+/-}) mice resolved by SDS-PAGE and probed with polyclonal antibody raised against C-terminal epitope of β -III spectrin. (FL = full-length).

CHAPTER 3 ANALYSIS OF $\Delta 2-6$ β -III SPECTRIN

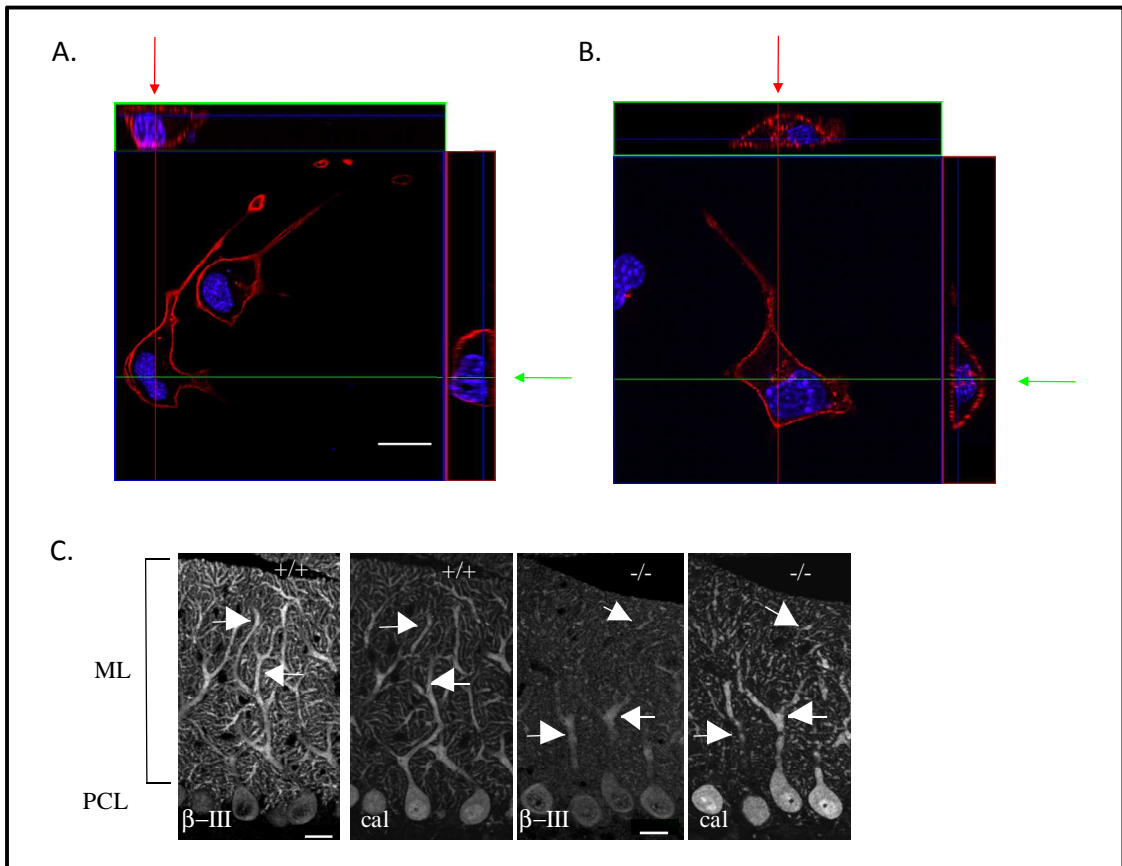


Figure 3.3 $\Delta 2-6$ β -III spectrin is located at the cell membrane. Neuro2a cells transfected with myc-tagged full length (red) **(A)** and myc-tagged $\Delta 2-6$ β -III spectrin (red) **(B)**. Red arrow indicates the xz orthogonal view and green arrow the yz orthogonal view of the same cell. Nucleus was stained with DAPI (blue). Bar, 50 μ m. **(C)** Cerebellar sections from 3-week old WT (+/+) and β -III^{-/-} spectrin mice immunostained with anti- β -III spectrin and anti-calbindin antibody. Arrow indicates dendrites. ML = molecular layer, PCL = Purkinje cell layer. All images are representative of three independent experiments. Bar, 50 μ m.

CHAPTER 3 ANALYSIS OF $\Delta 2-6$ β -III SPECTRIN

Protein Solubility

The solubility of $\Delta 2-6$ β -III spectrin was compared to that of full length β -III spectrin. HEK 293T cells were transfected with either myc-tagged full length or myc-tagged $\Delta 2-6$ β -III spectrin and 24 hours post transfection cell samples were homogenised in an extraction buffer containing 1% Triton (refer to section 2.1.4) and separated into soluble and insoluble fractions by centrifugation. Western blot analysis using an anti-c-myc antibody confirmed that the levels of $\Delta 2-6$ β -III spectrin protein found in the supernatant and insoluble pellet fractions were similar to that of full length β -III spectrin. Even when transfected cells were solubilised in buffer containing 8 M Urea and 4% SDS there was no difference between levels of full length and $\Delta 2-6$ β -III spectrin in the insoluble membrane pellet fraction (Figure 3.4).

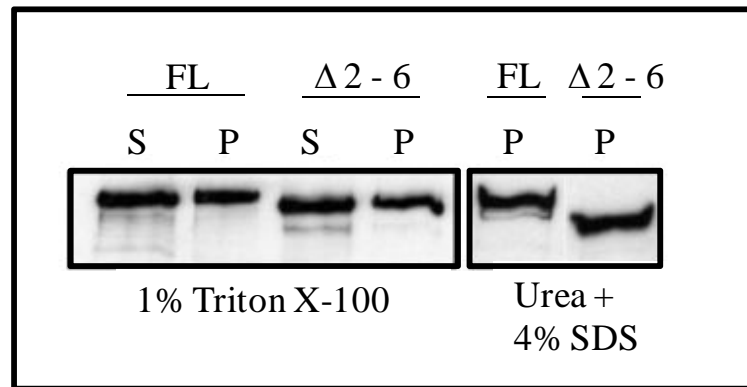


Figure 3.4 No difference in solubility between full length and $\Delta 2-6$ β -III spectrin. Transfected cell homogenates solubilised in buffer containing either 1% Triton or 8M Urea and 4% SDS and supernatant (S) and pellet (P) fractions resolved by SDS-PAGE. Blots probed with anti-c-myc antibody.

CHAPTER 3 ANALYSIS OF $\Delta 2-6$ β -III SPECTRIN

Stability

The stability of full length and $\Delta 2-6$ β -III spectrin was compared by treating transfected HEK 293T cells with cyclohexamide (10 μ g/ml), an inhibitor of protein synthesis, 24 hours after transfection. Cells were harvested at 0-hours and 3-hours post treatment and samples resolved by SDS-PAGE. Western blot and densitometry analysis using an anti-c-myc antibody revealed that three hours after addition of cyclohexamide there was a 29 ± 6 % reduction in the level of $\Delta 2-6$ β -III spectrin protein but no reduction in full length protein ($108 \pm 7\%$; $P = 0.018$) (Figure 3.5).

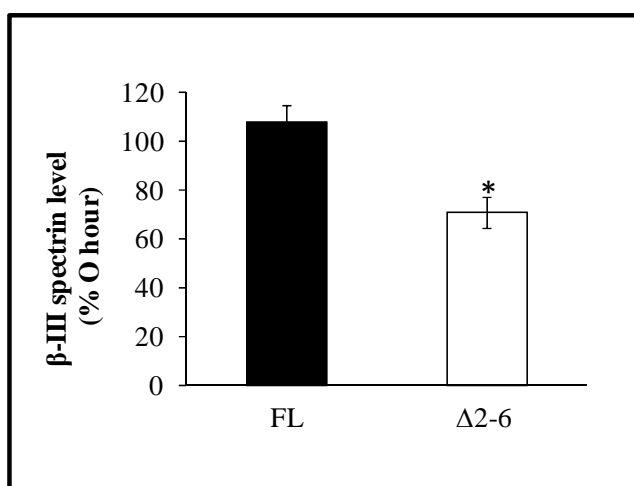


Figure 3.5 $\Delta 2-6$ β -III spectrin is less stable than WT. Quantification of Western blot analysis. Level of protein remaining 3-hours after administration of cyclohexamide expressed as percentage of protein level at 0-hours. All data are given as means \pm SEM (N = 3; * $P = 0.018$).

CHAPTER 3 ANALYSIS OF $\Delta 2-6$ β -III SPECTRIN

Cell surface expression of EAAT4

Previously it was shown that β -III spectrin increases EAAT4 glutamate uptake by stabilising the transporter at the plasma membrane (Jackson et al., 2001). HEK-r-EAAT4 cells were either transfected with empty vector (EV), full length β -III spectrin or $\Delta 2-6$ β -III spectrin and 24 hours after transfection, a biotinylation assay was performed to investigate whether $\Delta 2-6$ β -III spectrin stabilised EAAT4 at the cell membrane (refer to section 2.1.6). Total, intracellular and membrane fractions were resolved by SDS-PAGE and immunoblotted using anti-EAAT4 serum (Figure 3.6A). Quantification revealed that $\Delta 2-6$ β -III spectrin failed to increase cell surface expression of EAAT4 (104 ± 1.8 % of EV), unlike full length β -III spectrin (117 ± 1.6 % of EV) ($P = 0.002$) (Figure 3.6B).

CHAPTER 3 ANALYSIS OF $\Delta 2-6$ β -III SPECTRIN

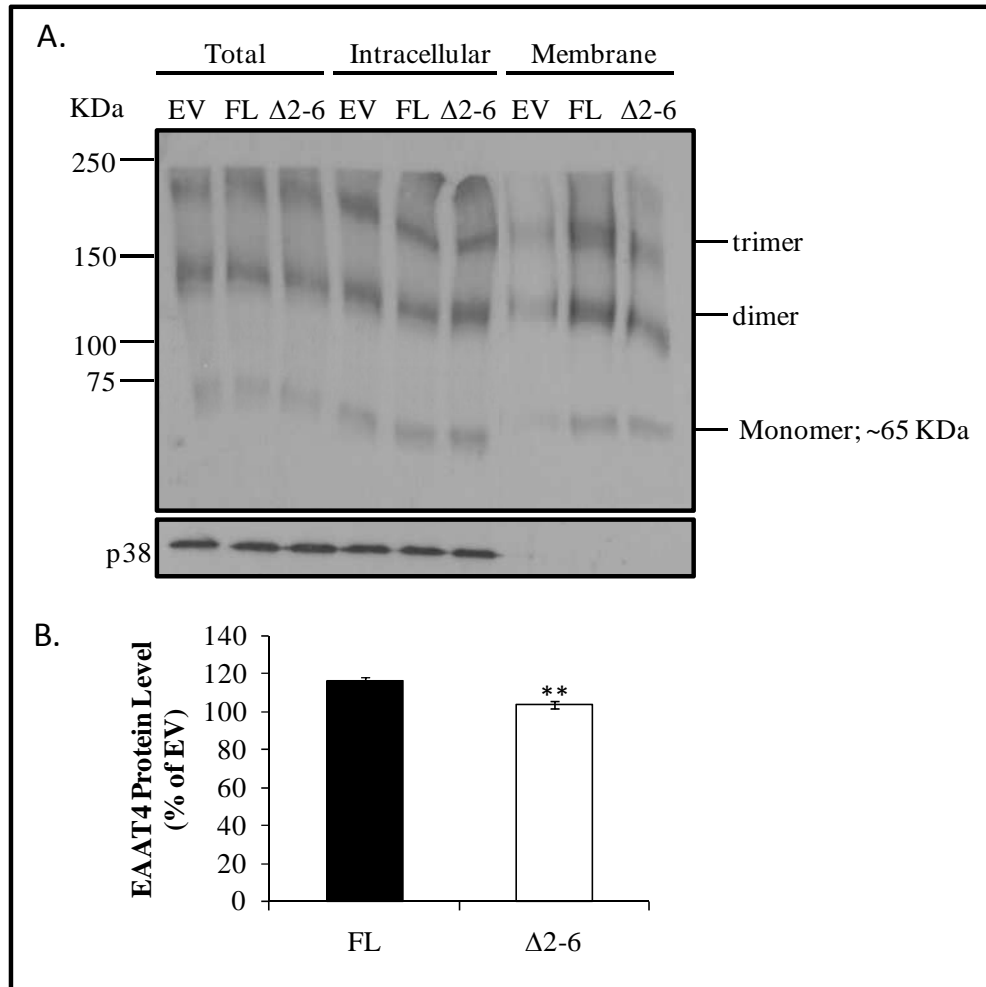


Figure 3.6 $\Delta 2-6$ β -III spectrin fails to increase EAAT4 cell surface expression. (A) A representative immunoblot using anti-EAAT4 serum to detect total, intracellular and membrane bound EAAT4 in HEK-rEAAT4 cells transfected with empty vector (EV), full length (FL) β -III spectrin and $\Delta 2-6$ β -III spectrin. p38 was used as a loading control. (B) Densitometry data quantifying levels of EAAT4 in membrane fraction. All data are given as means \pm SEM (N = 3; ** P = 0.002).

3.3 Discussion

The main aim in generating a knockout mouse is to abolish the expression of a protein of interest. However it is possible that targeting strategies, although resulting in loss of full-length protein, give rise to the production of truncated proteins due to aberrant splicing events or utilisation of different start codons. Yet the occurrence of various protein isoforms can go unnoticed either simply due to the lack of characterisation or as a consequence of lack of multiple or good antibodies for protein analysis.

The work reported in this chapter has tried to address what is a difficult but potentially fairly common issue in genetically modified mice. Since a transcript was still expressed in the β -III^{-/-} spectrin mouse it was necessary to clone and express the aberrant protein in order to identify or rule out the occurrence of a toxic gain-of-function. Expression of $\Delta 2-6$ β -III spectrin in Neuro2a cells revealed the loss of exons 2-6 does not appear to have any adverse effect on its cellular distribution, with the truncated protein still being located at the plasma membrane, similar to WT protein. This indicates that the targeting and trafficking of the truncated protein was not disrupted, confirmed by the fact $\Delta 2-6$ β -III spectrin was located throughout the Purkinje cell dendritic tree in the β -III^{-/-} spectrin mouse. As further evidence that $\Delta 2-6$ β -III spectrin protein did not possess a toxic gain-of-function, there was no sign of cytosolic or nuclear aggregates, which are a common phenomenon of the SCAs caused by trinucleotide expansions (Paulson et al., 1997; Skinner et al., 1997; Holmberg et al., 1998; Schmidt et al., 1998; Koyano et al., 2000;

CHAPTER 3 ANALYSIS OF $\Delta 2-6$ β -III SPECTRIN

Nakamura et al., 2001; Moseley et al., 2006). The fact there was no difference in the amount of $\Delta 2-6$ β -III spectrin protein solubilized by 1% Triton X-100 or 8 M Urea and 4% SDS, compared to full-length β -III spectrin, indicated no difference in solubility. What the *in vitro* experiments did reveal was that $\Delta 2-6$ β -III spectrin was significantly less stable than full length β -III spectrin, with less protein remaining after treatment with a protein synthesis inhibitor. In addition, possibly as a consequence of its own reduced stability, $\Delta 2-6$ β -III spectrin failed to stabilize EAAT4 at the cell surface to the same extent as full-length β -III spectrin.

In conclusion the results from *in vitro* experiments identified no obvious gain-of-function or adverse property for the truncated protein $\Delta 2-6$ β -III spectrin. Instead it appears, if anything, to be less functional than full-length β -III spectrin. These data provide convincing evidence that the β -III^{-/-} spectrin mouse can be considered a functional knockout.

3.3.1 *Spnb3*^{-/-} mouse

The characterization of aberrant proteins is not routinely performed in knock-out mouse studies and so it is highly probable that a number of published knockout mice are not actually true nulls. This raises the question of whether the observed phenotype is due the

CHAPTER 3 ANALYSIS OF $\Delta 2-6$ β -III SPECTRIN

presence of an aberrant protein isoform rather than a consequence of loss of protein. This may be the case for another β -III spectrin knockout mouse (*Spnb3*^{-/-}), which lacks full-length β -III spectrin but expresses a protein lacking the last 12 exons (~ 110 KDa) (Stankewich et al., 2010). Unfortunately, no *in vitro* experiments were performed to analyse the properties of this truncated protein, even though it was found to have an aberrant expression pattern, being found in punctate accumulations within the soma, in membrane bounded aggregates along the proximal dendritic shafts and along the initial axon segment (Stankewich et al., 2010). Therefore it is possible that the myoclonic seizures observed in *Spnb3*^{-/-} mice are not a consequence of loss of β -III spectrin function but are due to the aberrant expression and downstream effects of the truncated protein (Stankewich et al., 2010), especially since no seizures are seen in our β -III^{-/-} spectrin mouse.

3.3.2 Deleterious effects of β spectrin fragments

The need for careful analysis of truncated forms of β -III spectrin is highlighted by the fact there are several studies reporting dominant-negative effects of truncated forms of β -I spectrin (Devarajan et al., 1997; Pradhan and Morrow, 2002; Leshchyns'ka et al., 2003). The expression of region 1 and the MAD 1 domain of β -I spectrin (β I_{N-5}) results in the disruption of endogenous Golgi spectrin-ankyrin skeleton and reduced cell surface expression of Na,K-ATPase (Devarajan et al., 1997). Similarly expression of β I_{N-5} and

CHAPTER 3 ANALYSIS OF $\Delta 2-6$ β -III SPECTRIN

$\beta_{I_{14,15}}$ results in cytosolic aggregates and reduced plasma membrane expression of CD45, a membrane phosphotyrosine phosphatase expressed in cells of the hematopoietic lineage (Pradhan and Morrow, 2002). Finally spectrin fragments $\beta_{I_{N-5}}$ and $\beta_{I_{2-3}}$ (which lacks the pleckstrin homology (PH) domain and the binding site for PKC β_2) prevents PKC β_2 from interacting with neural cell adhesion molecule (NCAM) clusters at the cell surface thus suppressing NCAM-mediated neurite outgrowth (Leshchyn'ska et al., 2003).

Similarly various truncated forms of β spectrin are known to be pathogenic, underlying hereditary elliptocytosis (Dhermy et al., 1982; Ohanian et al., 1985; Pothier et al., 1987; Eber et al., 1988; Yoon et al., 1991; Garbarz et al., 1992). This is thought to arise from loss of the carboxy-terminus preventing phosphorylation and dimer self-association. Consequently there is membrane instability resulting in spontaneous fragmentation, spherocytosis and permanent shape deformation (Coetzer and Zail, 1982; Liu et al., 1982; Liu et al., 1990; Palek and Lambert, 1990).

3.3.3 Expression of truncated proteins in other mouse models

One example of where a truncated protein has a detrimental effect due to a toxic gain-of-function is in the megencephaly (*mceph/mceph*) mouse, which displays seizures and an increased brain volume (Persson et al., 2005). However, in this instance the truncated protein, arising from a frame shift and the introduction of a premature stop codon in the

CHAPTER 3 ANALYSIS OF $\Delta 2-6$ β -III SPECTRIN

gene encoding potassium channel $K_v1.1$ (Petersson et al., 2003), was fully characterised. It is thought the transcripts escape nonsense-mediated mRNA decay (NMD), a process whereby mRNAs that have a premature stop codon undergo degradation (Hentze and Kulozik, 1999), due to the lack of introns in the *Kv1* genes (Brocke et al., 2002). The study demonstrated the truncated protein is trapped within the ER and has a dominant-negative effect on K_v1 subunits in both oocytes and cell culture. Furthermore, the fact the $K_v1.1$ knockout mouse does not have an enlarged brain, whereas brain overgrowth is observed in the *mceph/mceph* mice suggests that it is the truncated protein that has the pathological effect on brain size. A similar truncated protein has been identified in a patient with episodic ataxia type 1 and it too has been shown to possess dominant-negative effects (Eunson et al., 2000).

In contrast there appears to have been no analysis of the proteins remaining in the mouse lacking the peroxisomal ATP-binding cassette (ABCD2) transporter (Pujol et al., 2004). Western blot analysis reportedly shows complete loss of protein however the blot shown in the original paper shows only one band's width of a gel and a subsequent publication reveals the detection of additional bands with the anti-ABCD2 antibody, with only one band missing in *aldr*^{-/-} mice (Ferrer et al., 2005). Although quantitative RT-PCR confirmed the absence of full-length transcript it did identify shorter, smir-type and low expressed fragments, indicative of NMD. However, there was no mention of what the other bands detected by the anti-ABCD2 antibody were and no further work was done to

CHAPTER 3 ANALYSIS OF $\Delta 2-6$ β -III SPECTRIN

analyse whether any of the truncated transcripts were translated. Therefore truncated forms of ABCD2 may remain in the $aldr^{-/-}$ mouse.

Finally, SCA3 is caused by a polyglutamine expansion in ataxin-3 (Kawaguchi et al., 1994) as mentioned in section 1.6.2.1. Over expression of just the polyglutamine expansion, and not full-length mutant ataxin-3, resulted in Purkinje cell degeneration and a severe ataxic phenotype (Ikeda et al., 1996). This indicates that the truncated protein is actually more toxic and potent at inducing Purkinje cell death than full length protein.

3.3.4 Conclusions

It is evident that truncated protein isoforms can have unpredictable and deleterious effects on cell function and survival. This highlights why in knockout mice a thorough analysis of remaining transcripts and proteins is essential before phenotypic interpretation. The fact no abnormal property was identified for $\Delta 2-6$ β -III spectrin strongly indicates that the β -III^{-/-} spectrin mouse is a hypomorph (functional knockout). Nevertheless, the generation of a transgenic mouse that over expresses the truncated $\Delta 2-6$ β -III spectrin protein would be an alternative approach to examine whether this protein has a toxic gain-of-function. However taking into consideration the data

CHAPTER 3 ANALYSIS OF $\Delta 2-6$ β -III SPECTRIN

presented in this chapter, the ethics of utilising additional mice is questionable given the prediction these mice would have no obvious phenotype.

CHAPTER 4

CHARACTERISATION OF β -III^{-/-} SPECTRIN MOUSE

4.1 Background

The data shown in chapter 3 indicates the β -III^{-/-} spectrin mouse can be considered a functional knockout (hypomorph) as the remaining protein appears to be less functional than full-length β -III spectrin and more importantly was found not to have any obvious toxic gain-of-function property. This chapter reports the behavioural analyses carried out on β -III^{-/-} spectrin mice to determine whether loss of β -III spectrin function gives rise to a phenotype consistent with ataxia and cerebellar dysfunction.

4.2 Results

4.2.1 Behavioural Analyses

Body Weight

Male and female mice of both genotypes were weighed at 3-weeks, 6-months and 1-year of age. There was no significant difference in weight between WT and β -III^{-/-} spectrin mice at any age (Figure 4.1).

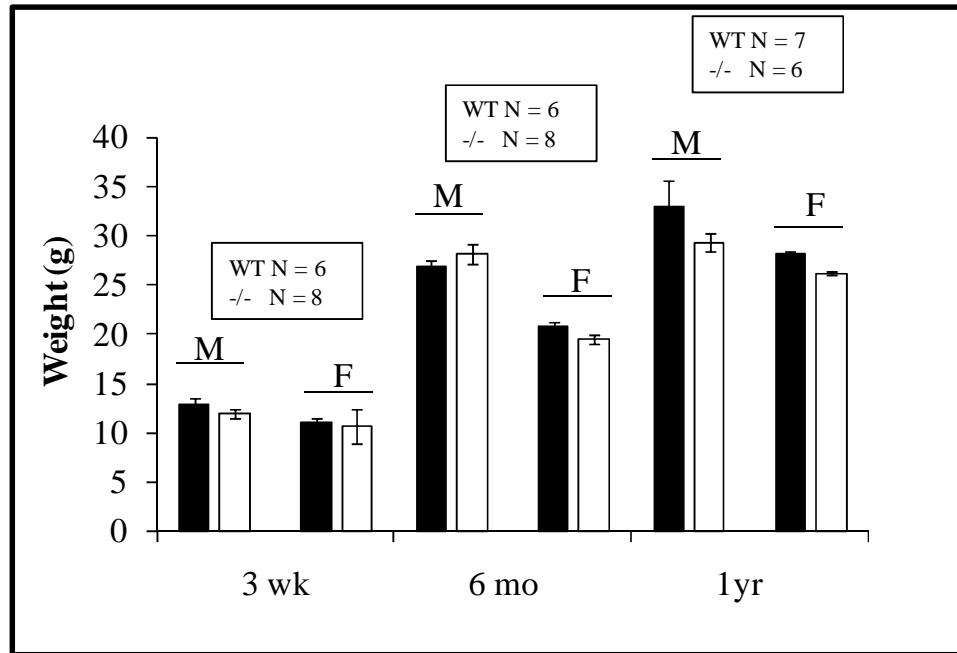


Figure 4.1 No difference in body weight between β -III^{-/-} spectrin and WT mice. Body weight of WT mice (black) and β -III^{-/-} spectrin animals (white). All data are given as means \pm SEM (M, male; F, female).

Gait analysis

Footprint analysis (representative trace shown in Figure 4.2A) performed on animals from 6-weeks to 1-year of age indicated that hind-limb gait of β -III^{-/-} spectrin mice became progressively wider than that of WT littermates (Figure 4.2B), with no significant difference in stride length at any age (Figure 4.2C). However, the latter result might have occurred through mice walking at varying speeds down the runway, thus introducing heterogeneity in stride length, which could have masked any genotype-dependent differences.

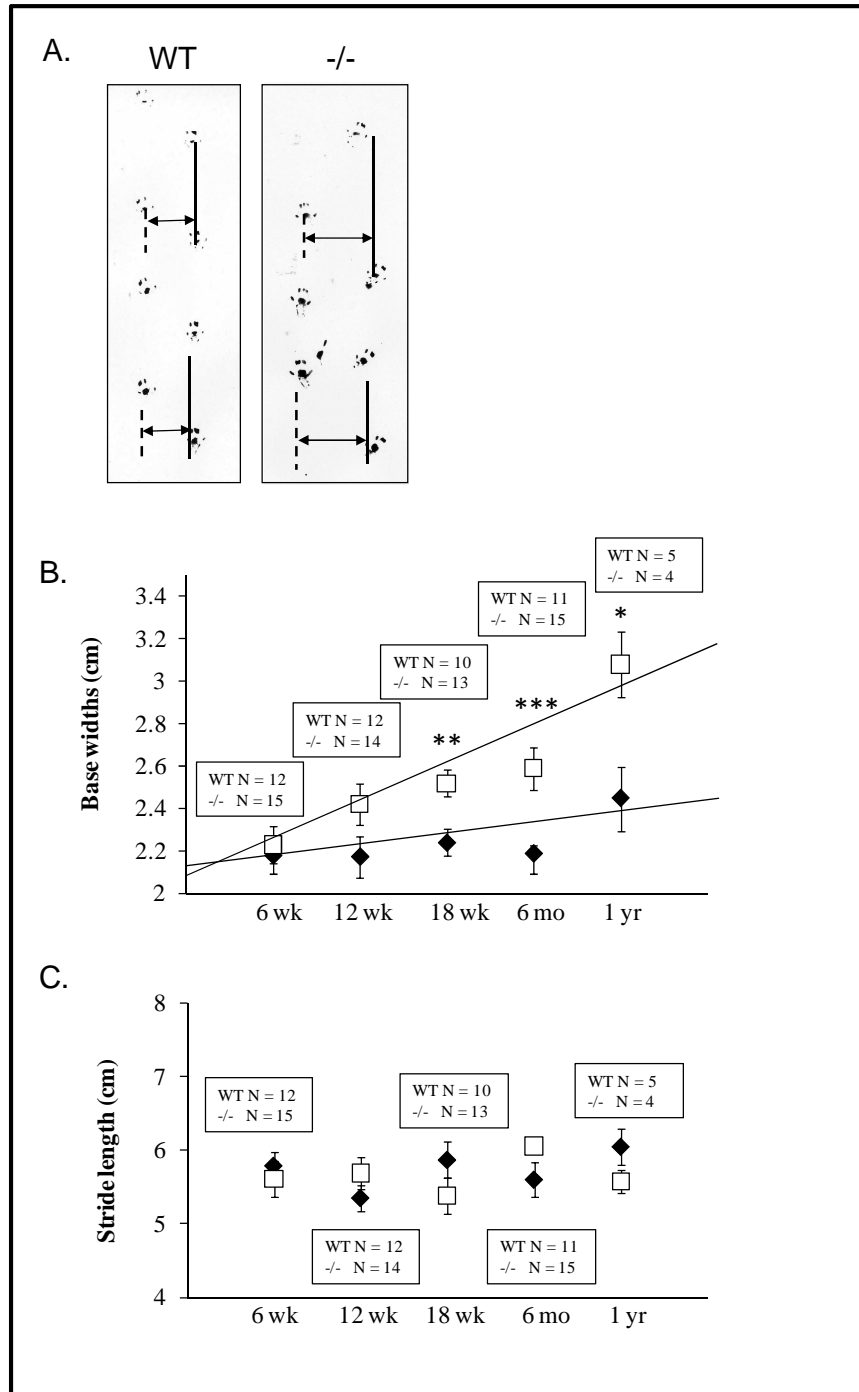


Figure 4.2 Abnormal Gait in β -III^{-/-} spectrin mice. (A) Representative footprints from 18-week old WT and β -III^{-/-} spectrin littermates. Stride length shown by solid lines and base width by double headed arrows. **(B)** Quantification of footprint patterns in β -III^{-/-} (white square) and WT littermates (black diamonds) at 18-weeks (**P=0.0078), 6-months (**P=2.82E⁻⁶) and 1-year (*P=0.02). **(C)** Quantification of stride length. All data given as means \pm SEM.

Stationary Rod

Assessment of balance, measured by the ability of WT and β -III^{-/-} spectrin mice to remain on a stationary rod, showed no significant difference between the performance of WT and β -III^{-/-} spectrin mice at 3-weeks of age (Figure 4.3). However at 6-months ($P = 0.004$) and 1-year of age ($P = 0.0007$) β -III^{-/-} spectrin mice struggled to maintain their balance and were significantly worse than their WT littermates.

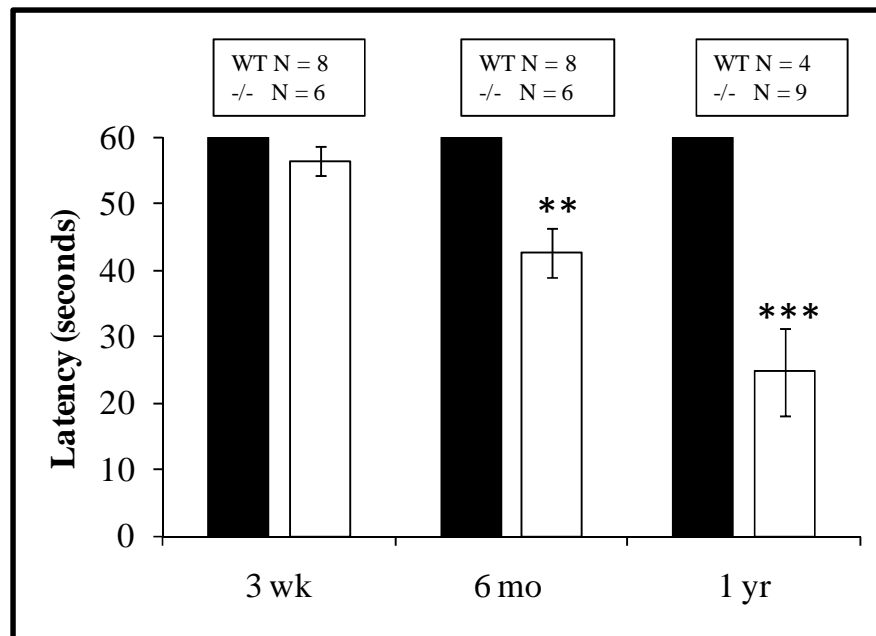


Figure 4.3 Progressive loss of balance in β -III^{-/-} spectrin mice. The latency for WT (black) and β -III^{-/-} spectrin mice (white) to remain on a stationary rod. All data given as means \pm SEM. ** $P < 0.01$; *** $P < 0.001$.

Rotating Rod

To increase the intensity of the motor task, mice were examined on a rotating rotarod at 3 different speeds (3, 5 and 10 rpm). The 3-week β -III^{-/-} spectrin mice initially performed significantly worse than their WT littermates at 3 rpm (Figure 4.4A). However, their performance improved and on the third and fourth days of testing β -III^{-/-} spectrin mice could perform almost as well as WTs. Again at 5 rpm although β -III^{-/-} spectrin mice were significantly worse than their WT littermates on every day, they were able to improve performance, whereas at 10 rpm β -III^{-/-} spectrin mice showed no improvement with consecutive days of testing. In contrast, 6-month old β -III^{-/-} spectrin mice were unable to remain for more than 20 seconds on the rotating rod even at 3 rpm and showed no improvement (Figure 4.4B).

Elevated Beam

Balance and coordination was also measured using the elevated beam. Mice traversed the 2 cm wide beam and impaired coordination was measured by counting the number of hind limb slips. β -III^{-/-} spectrin mice were generally more nervous and hesitant to cross the beam. Frequently they would try to turn around while on the beam and, in so doing, lost their balance and fell off. WT animals never fell off. From 12-weeks of age, β -III^{-/-} spectrin mice not only made significantly more slips than WT littermates (Figure 4.5) but the slips were generally bigger. Finally a tremor, characteristic of some ataxias, was also observed in β -III^{-/-} spectrin mice (refer to appendix 3 (bound-in DVD); video of mice on rotating rod, elevated beam

CHAPTER 4 CHARACTERISATION OF β -III^{-/-} SPECTRIN MOUSE

and tremor). Significance was obtained both with a two sample Student's t-test (12-wk – 6-months $P = 0.001$; 1-year $P = 0.0006$) and a Mann-Whitney test (12-wk – 6-months $P = 0.003$; 1-year $P = 0.004$). Furthermore, there was a significant difference ($P = 0.02$) between 12-week – 6-month and 1-year old animals demonstrating a progressive decline in motor coordination. Significance was obtained using a Kriskal-Wallis H' test, followed by Mann-Whitney test with Bonferroni correction for comparison within groups.

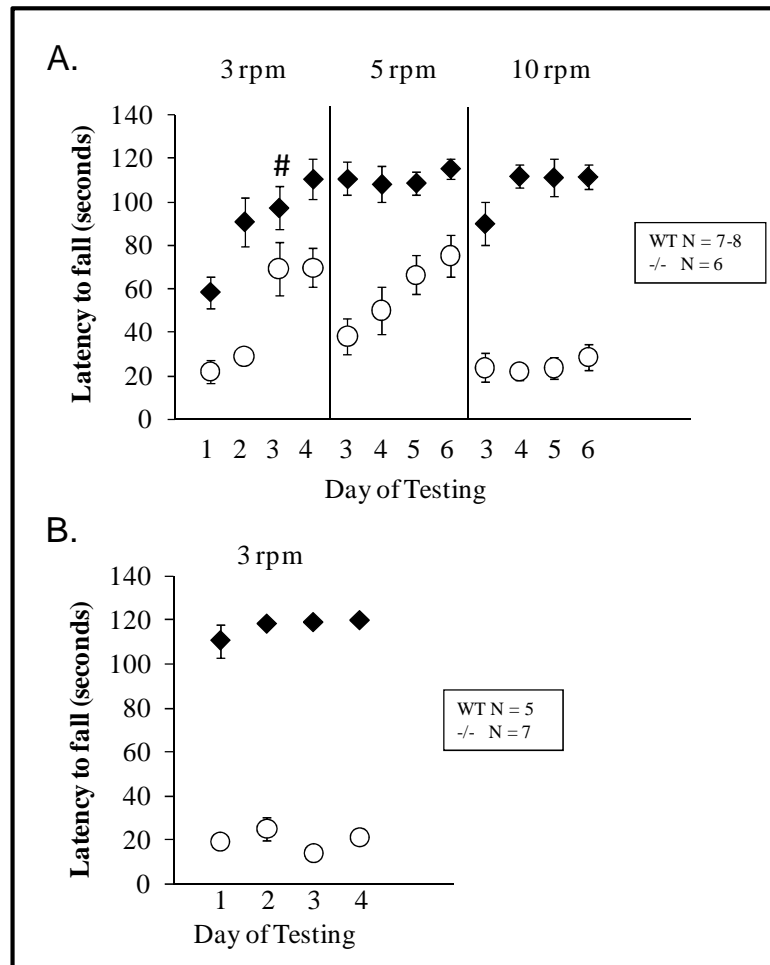


Figure 4.4 Progressive motor deficits in β -III^{-/-} spectrin mice. (A) Latency for 3-week WT (black diamonds) and β -III^{-/-} spectrin (white circles) mice to fall from rotating rod at 3-, 5- and 10-rpm. Latency to fall was always significantly different between genotypes apart from day 3 at 3-rpm (# P=0.218). **(B)** Performance of 6-month WT and β -III^{-/-} spectrin mice at 3-rpm. All data given as means \pm SEM.

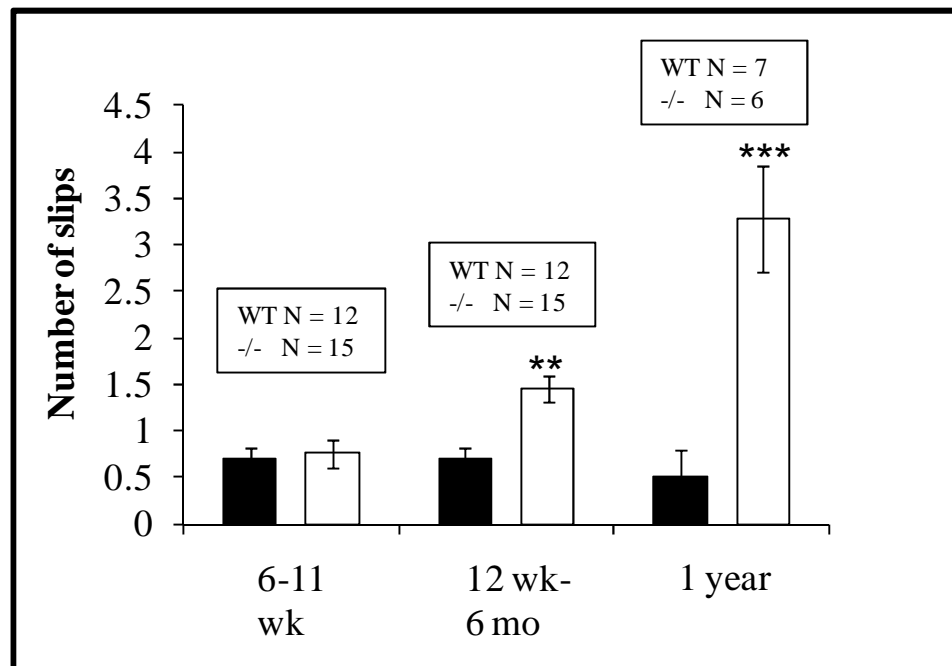


Figure 4.5 Loss of balance in β -III^{-/-} spectrin mice. The number of slips made while traversing a narrow, elevated beam were counted for β -III^{-/-} spectrin mice (white) and WT animals (black). (** P = 0.001 and *** P = 0.0006, two sample Student's t-test). All data are given as means \pm SEM.

Inverted Grid

There was no significant difference in muscle strength between WT β -III spectrin and β -III^{-/-} spectrin mice at any point in their development, as measured by their ability to hold onto the inverted grid at 3-weeks, 6-months and 1-year of age (Figure 4.6).

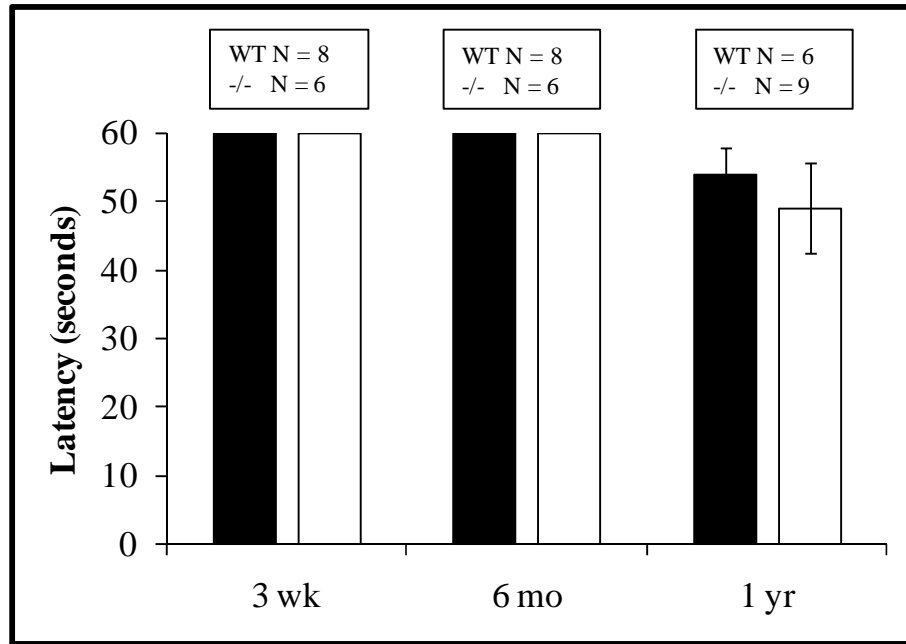


Figure 4.6 No muscle weakness in β -III^{-/-} spectrin mice. The latency for WT animals (black) and β -III^{-/-} spectrin mice (white) to fall from an inverted grid was recorded. All data are given as means \pm SEM.

Novel Object Recognition

β -III spectrin has been detected in the hippocampus (Jackson et al., 2001) and therefore the novel object recognition task was performed to test if there was a difference in learning ability between WT and β -III^{-/-} spectrin mice. The novel object recognition task takes advantage of a rodents' natural instinct to explore novel items instead of familiar ones. The amount of time that the mouse spends investigating the novel object, instead of the familiar one, is a measure of object recognition (refer to section 2.5.3.5). The exploratory preference of 3-week-old WT and β -III^{-/-} spectrin mice was measured (Figure 4.7).

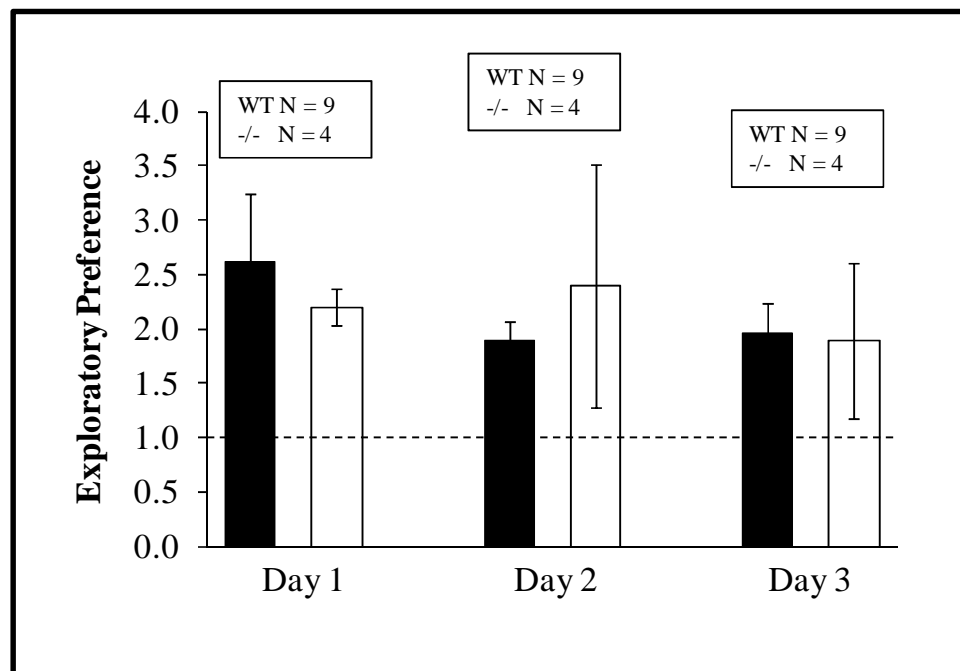


Figure 4.7 β -III^{-/-} spectrin mice display no deficit in object recognition. Preference of WT (black) and β -III^{-/-} (white) spectrin mice to explore a novel object. All data are given as means \pm SEM.

4.3 Discussion

In this chapter quantification of motor behaviour revealed that β -III^{-/-} spectrin mice develop a progressively splayed hind-limb gait and show progressive motor deficits on three separate motor tasks. This phenotype mirrors the wider stance and progressive motor incoordination observed in human cases (Stevanin et al., 1999; Burk et al., 2004; Ikeda et al., 2006), making the β -III^{-/-} spectrin mouse a good animal model of ataxia. Furthermore analysis of the β -III^{-/-} spectrin mouse has provided key insights into SCA5 pathogenesis, more specifically indicating that a

CHAPTER 4 CHARACTERISATION OF β -III^{-/-} SPECTRIN MOUSE

loss of β -III spectrin function, rather than a toxic gain-of-function, gives rise to ataxia.

The young β -III^{-/-} animals (3-weeks of age) were found to have no problem in maintaining balance on a stationary rod, the least demanding motor task, whereas by 6-months of age this task was more challenging and by 1-year the β -III^{-/-} animals were dramatically impaired. Similarly there was a progressive deterioration in their ability to maintain balance on a rotating rod. At 3-weeks of age β -III^{-/-} mice, although worse than age-matched controls, were found to improve their performance at 3 and 5 rpm, eventually remaining on the rotating rod for 60-80 seconds, whereas by 6-months of age they were unable to remain on the rod for longer than 20 seconds at 3-rpm. The fact young β -III^{-/-} spectrin mice were able to improve their rotarod performance demonstrated that they could overcome the relatively mild motor defects evident at that stage.

The poorer rotarod performance of β -III^{-/-} spectrin mice could have been a consequence of muscle weakness rather than a loss of balance and coordination. However, this possibility was ruled out by the finding that their performance on an inverted grid test was the same as WT littermates. Similarly, differences in body weight could not have accounted for the poorer rotarod performance, as there was no difference between genotypes at any age. Therefore all the data pointed towards the motor deficits being due to cerebellar dysfunction and/or degeneration, and not

somatic defects, an assumption corroborated by the observed loss of Purkinje cells and thinning of the molecular layer in older β -III^{-/-} spectrin mice. However, a thorough examination of other brain regions including the substantia nigra and corpus striatum is required to rule out any other deficiencies that could contribute to the observed phenotype.

Finally to investigate whether cognitive deficits might have contributed to the poorer motor performance, a measure of their cognitive ability was obtained using the novel object recognition task. The exploratory preference was greater than 1 for both genotypes, indicating no cognitive deficit in β -III^{-/-} spectrin mice, with all animals spending more time investigating the novel object rather than the familiar one. The lack of involvement of other brain regions is also indicated by the absence of neuronal loss in cortex, hippocampus, dentate gyrus and deep cerebellar nuclei (Perkins et al., 2010).

4.3.1 Loss-of-function in disease pathogenesis

The finding reported here, that loss-of- β -III spectrin function underlies SCA5 pathogenesis, provides additional evidence to support the emerging theory that at least some autosomal dominant diseases are not due to a toxic gain-of-function. Another example is SCA1 where originally the aggregation of the polyQ-expanded protein was thought to underlie toxic gain-of-function properties (Zoghbi and Orr, 2000), whereas recent evidence suggests the disease to be due to an altered balance

CHAPTER 4 CHARACTERISATION OF β -III^{-/-} SPECTRIN MOUSE

of normal protein activities (Lim et al., 2008). There is a decreased formation of wild type ataxin 1-capicua protein complex and an increased formation of mutant ataxin 1- RBM17 complex. This results in both a partial loss-of-function and enhancement of another normal activity, the two effects contributing to a disease phenotype. The involvement of a loss-of-function in SCA1 pathogenesis was also indicated by the fact that disease severity and lethality are greater in mice carrying a polyQ-expanded protein but lacking wild type ataxin 1 compared to animals with both mutant protein and normal levels of ataxin 1 (Lim et al., 2008).

Similar results have also been found for other animal models of autosomal dominant diseases. For example, the elimination of wild type huntingtin protein (Van Raamsdonk et al., 2005) or androgen receptor function (Thomas et al., 2006) enhances neurodegeneration in the transgenic models of Huntington's disease and spinobulbar muscular atrophy, respectively. Likewise increased levels of wild type huntingtin protein have been found to reduce the apoptotic cell death caused by expression of mutant huntingtin, further suggesting a role for loss-of-function in cell death (Leavitt et al., 2001). One postulated loss-of-function of mutant huntingtin is the inability to promote brain-derived neurotrophic (*BDNF*) gene transcription, due to the inability to repress the function of RE1 silencing transcription factor/neuron-restrictive silencer factor (REST/NRSF) an inhibitor of *BDNF* gene transcription (Zuccato et al., 2001; Zuccato et al., 2003; Zuccato et al., 2007).

CHAPTER 4 CHARACTERISATION OF β -III^{-/-} SPECTRIN MOUSE

A loss-of-function in prion diseases has also been suggested, since the overexpression of normal PrP protects cultured neurons from cell-death-inducing stimuli (Li and Harris, 2005) and moreover, coexpression of subphysiological levels of wild-type PrP prevents neurodegeneration in mice expressing truncated forms of PrP (Behrens and Aguzzi, 2002). Although mice lacking the neuronal cell-surface PrP protein are normal (Bueler et al., 1992) this is not incompatible with a loss-of-function mechanism as the cytoprotective functions of PrP may only be critical when cells are compromised.

There is also emerging evidence to suggest that Alzheimer's disease (AD) may be the consequence of a loss of presenilin functions rather than the accumulation of β -amyloid peptides in the form of amyloid plaques (Shen and Kelleher, 2007). One key finding that supports this hypothesis is that hallmarks of AD pathology are observed following the conditional inactivation of both presenilins (PS1 and PS2) in the adult mouse cerebral cortex (Saura et al., 2004) whereas mouse models overexpressing β -amyloid peptides appear to show no neurodegeneration (Irizarry et al., 1997). The fact that a large number of disease causing mutations have been found throughout the structure of presenilin (Bertram and Tanzi, 2008) also suggests that a loss of protein function accounts for pathogenesis since all alterations have a detrimental effect, which would be highly improbable if a toxic gain-of-function were responsible.

A loss-of-function caused by the creation of premature stop codons in the gene encoding tau tubulin kinase (TTBK2), a casein kinase (CK) that phosphorylates tau,

is also thought to underlie SCA11 (Houlden et al., 2007). The mechanism is thought to involve the deposition of unphosphorylated tau and knockdown data from *C. elegans* supports a loss of TTBK2 function in tau toxicity (Kraemer et al., 2006).

Therefore, although previously believed to be associated with recessive forms of disease, there are a number of reports that suggest the loss of normal protein function is an important factor in a variety of dominant neurodegenerative diseases, in accordance with the findings of the present study in relation to SCA5.

4.3.2 Disease pathogenesis in other SCA5 models

Currently there are only two other proposed animal models of SCA5. One is the previously mentioned Spnb3^{-/-} mouse (Stankewich et al., 2010) and the other is a *Drosophila* model that over expresses either mutant forms of human β -III spectrin or fly β -spectrin (Lorenzo et al., 2010).

The Spnb3^{-/-} mouse model is reported to develop ataxia but, in contrast to both the β -III^{-/-} spectrin mouse and SCA5 patients, the symptoms observed are mild and non-progressive, suggesting that this mouse is a poor match to the disease phenotype and, therefore, a poor disease model. Notably, the behaviour task that showed greatest impairment in Spnb3^{-/-} animals was the wire-hanging test, which is not a test for balance, but rather muscle and grip strength. Moreover, myoclonic seizures were observed in Spnb3^{-/-} mice, a phenotype not reported in any SCA5 individual and there was also no loss of Purkinje cells, even at 1.5 years in the Spnb3^{-/-} mice. Taken

CHAPTER 4 CHARACTERISATION OF β -III^{-/-} SPECTRIN MOUSE

together these data provide further evidence that the Spnb3^{-/-} mouse is probably not a good model for SCA5 pathogenesis, despite the authors claiming that their mouse mirrors the pathology of human SCA5. Instead it may be that the truncated protein still expressed in this mouse model has a toxic gain-of-function property that underlies some or all of the disease phenotype. Additional work to fully analyse the function of the truncated protein is required before interpretation of a disease mechanism can be made for the Spnb3^{-/-} mouse. Clearly careful consideration needs to be given as to whether this mouse should actually be considered a model of ataxia at all.

In contrast, data from the fly models, where effects of ectopic expression of mutant forms of β -III spectrin are enhanced when endogenous levels of wild type β spectrin are reduced, suggests that mutant β spectrin interferes with the normal function of spectrin but ultimately loss-of-function underlies the phenotype (Lorenzo et al., 2010). This is supported by the fact that even in the absence of mutant forms of β -III spectrin similar phenotypic defects are observed when β spectrin levels are reduced by RNAi (Lorenzo et al., 2010 and T. Hays personal communication).

4.3.3 Conclusions

This chapter reports the careful analysis of a new animal model of ataxia and clearly demonstrates a progressive motor phenotype, a characteristic of human ataxia. The work demonstrates that a loss-of β III-spectrin is pathogenic, providing key insights

CHAPTER 4 CHARACTERISATION OF β -III^{-/-} SPECTRIN MOUSE

into disease pathogenesis. Furthermore, Purkinje cell loss is observed in the β -III^{-/-} mouse making this model an excellent tool for future study, as a number of other SCA mouse models fail to recapitulate this important aspect of the human disease (He et al., 2006; Moseley et al., 2006; Chou et al., 2008; Watase et al., 2008).

CHAPTER 5

ANALYSIS OF β -III^{+/-} SPECTRIN DEFICIENT MICE

5.1. Background

The previous chapter reported the behavioural analysis of β -III^{-/-} spectrin mice and the results demonstrated that a loss of β -III spectrin function underlies ataxia and cerebellar degeneration. Since SCA5 is an autosomal dominant disease this finding indicated that either, the mutant forms of β -III spectrin are simply inactive and the disease arises from haploinsufficiency or, in addition to being non-functional, the mutant subunits also have a dominant negative effect and suppress the function of wild type spectrin. There is evidence from other mouse models and SCA literature to suggest other forms of ataxia (SCA15 & 28) arise from haploinsufficiency (van de Leemput et al., 2007; Maltecca et al., 2009). To address whether β -III spectrin haploinsufficiency could be pathogenic, heterozygote β -III^{+/-} spectrin mice were studied for signs of motor deficits and cerebellar degeneration. The same behavioural tests and histological analysis used to characterise the β -III^{-/-} spectrin mouse were performed on 6-month to 2-year-old heterozygous animals.

5.2 Results

5.2.1 Behavioural Analyses

Body Weight

The body weight between genotypes was not found to differ at any age (Figure 5.1).

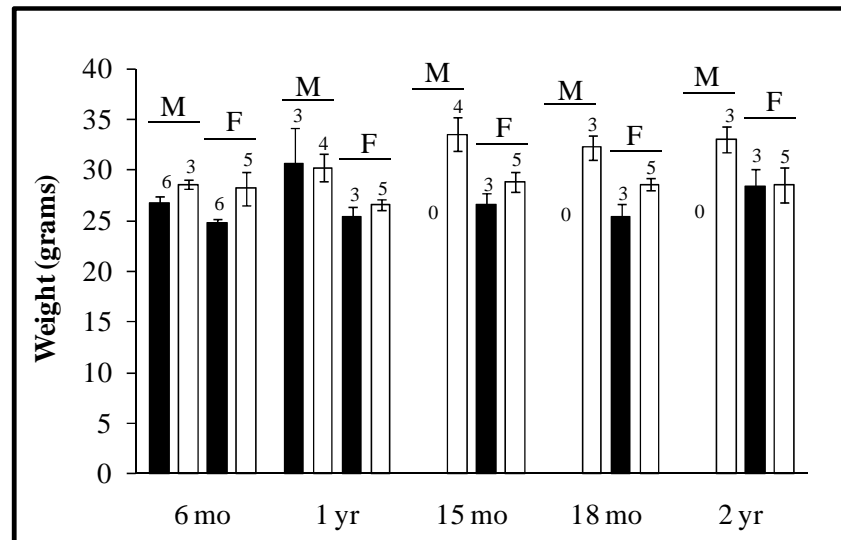


Figure 5.1 No difference in body weight between WT and β -III^{+/-} spectrin mice. Body weight of male (M) and female (F) mice measured for WT (black) and β -III^{+/-} spectrin mice at different ages. All data are given as means \pm SEM. The exact number of animals used (N) at each age point is shown above each genotype.

Gait analysis

Analysis of footprint patterns showed that, unlike β -III^{-/-} spectrin mice, β -III^{+/-} spectrin mice did not display an increase in base width at any age, when compared to WT littermates (Figure 5.2A). Similarly, there was no significant difference in stride length between WT and β -III^{+/-} spectrin mice at any of the ages examined (Figure 5.2B).

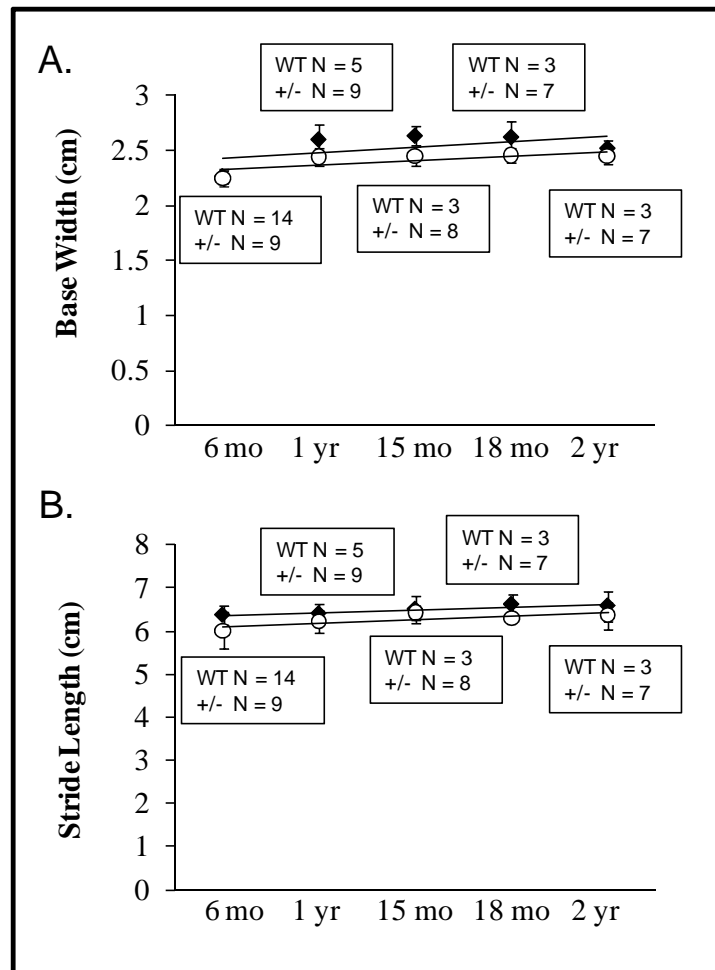


Figure 5.2 β -III^{+/-} spectrin mice have normal gait. Quantification of base width (**A**) and stride length (**B**) between WT (black diamonds) and β -III^{+/-} spectrin (white circles) mice from 6-months to 2-years of age. All data are given as means \pm SEM.

Stationary Rod

There was no significant difference in the ability of WT and β -III^{+/-} spectrin mice to remain on the stationary rod and even at 2-years of age β -III^{+/-} spectrin mice performed as well as their WT littermates (Figure 5.3).

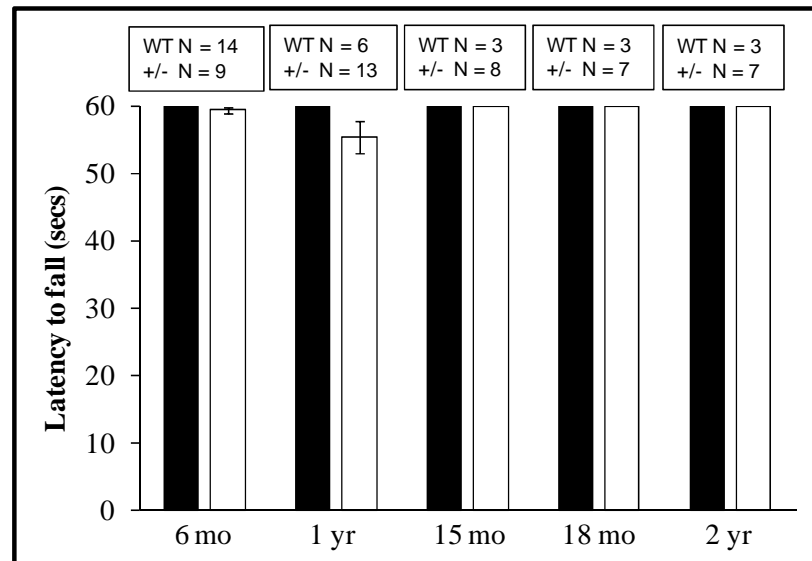


Figure 5.3 Progressive loss of balance not seen in β -III^{+/-} spectrin mice. Quantification of the latency for WT (black) and β -III^{+/-} spectrin (white) mice to fall from the stationary rod. Data from 4 consecutive trials, with a maximum time of 60 seconds, are given as means \pm SEM.

Rotating Rod

Neither genotype had any difficulty to remain on a rotating rod at the less intensive speeds of 3 and 5 rpm but when the speed was increased to 10 rpm, their performance was initially compromised (Figure 5.4). However, their performance did improve with consecutive days of testing and there was never any significant

CHAPTER 5 ANALYSIS OF β -III^{+/-} SPECTRIN DEFICIENT MICE

difference between genotypes. Only on the first trial day of each speed at 2-years of age were β -III^{+/-} spectrin mice obviously worse than their WT littermates but this never reached significance (P = 0.077, 0.070 and 0.056). By the second day they performed as well as WT littermates.

Elevated Beam

The number of slips made, when crossing the elevated beam were counted for WT and β -III^{+/-} spectrin mice (Figure 5.5). There was never any hesitation in crossing the beam for either genotype. By 18-months and 2-years of age, there was very little difference in the number of slips made by WT and β -III^{+/-} spectrin mice and at no age did the β -III^{+/-} spectrin mice make as many slips as symptomatic β -III^{-/-} spectrin mice (refer to section 4.2.1).

Inverted Grid

There was no difference in the ability of β -III^{+/-} spectrin mice and WT littermates to do the inverted grid test (Figure 5.6).

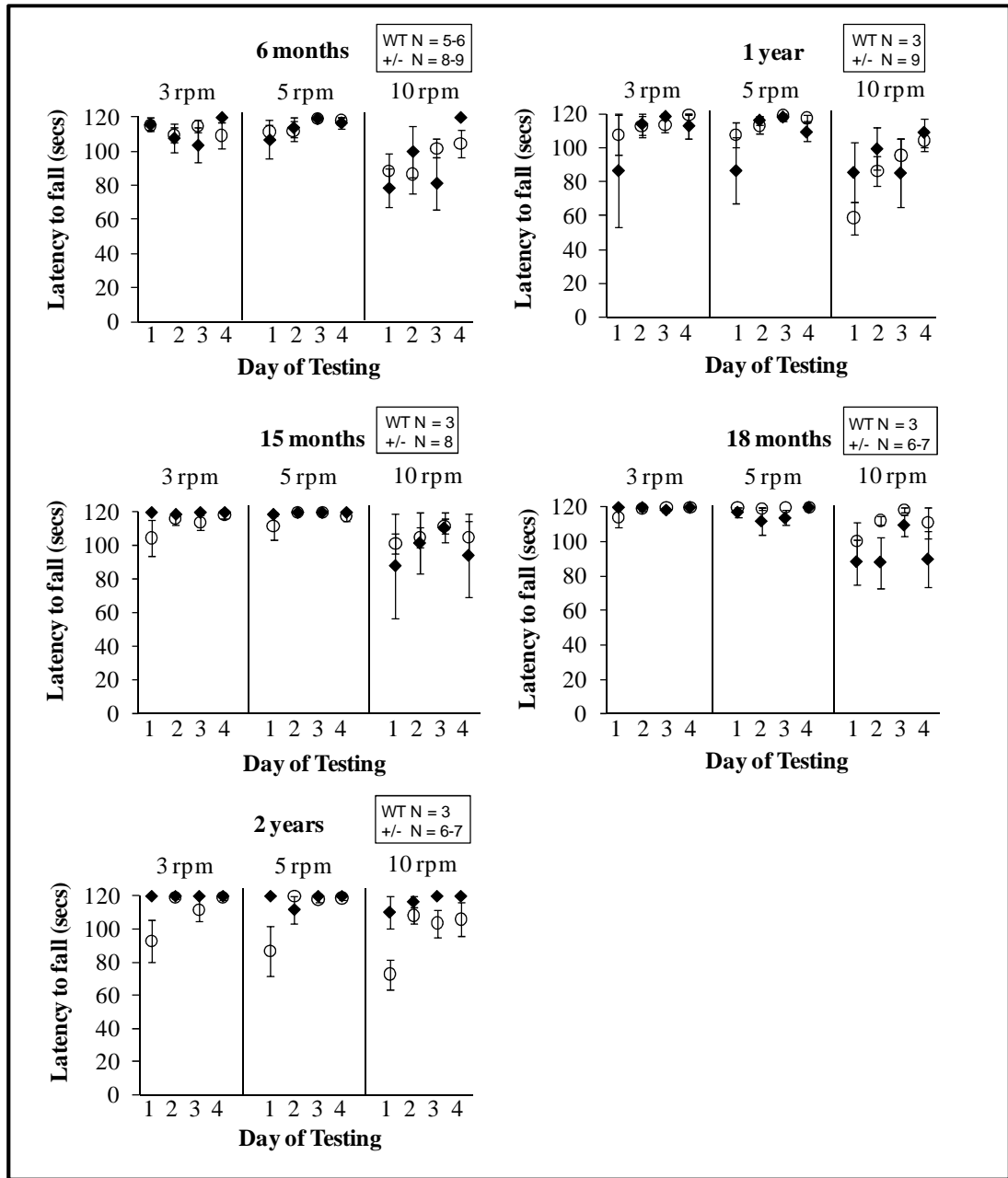


Figure 5.4 No progressive motor deficits in β -III^{+/-} spectrin mice. Latency of WT (black diamonds) and β -III^{+/-} (white circles) spectrin mice to fall from rotarod at 3, 5 and 10 rpm. Motor performance was recorded at 6-months, 1-year, 15-months and 2-years of age. Mice were given 4 trials per day and allowed a maximum time of 120 seconds per trial. All data are given as means \pm SEM.

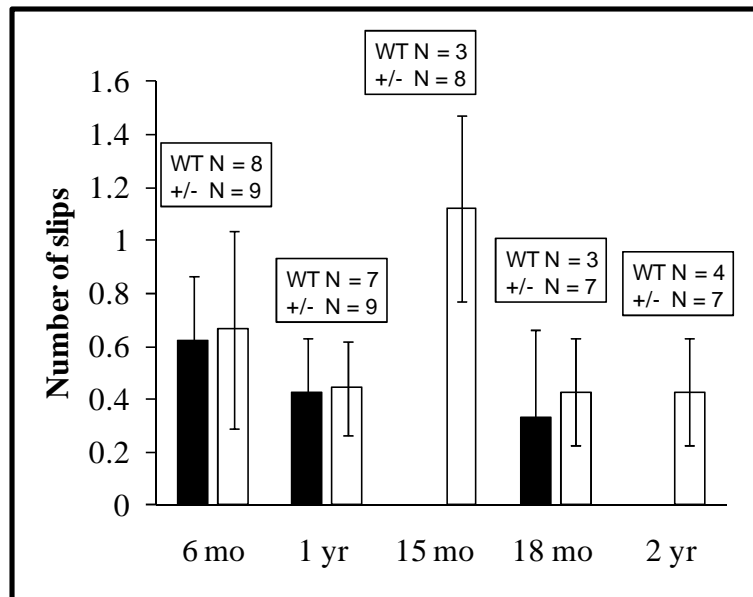


Figure 5.5 No loss of balance in β -III^{+/-} spectrin mice. The number of slips made while traversing an elevated beam were counted for WT (black) and β -III^{+/-} spectrin mice from 6-months to 2-years of age. All data are given as means \pm SEM.

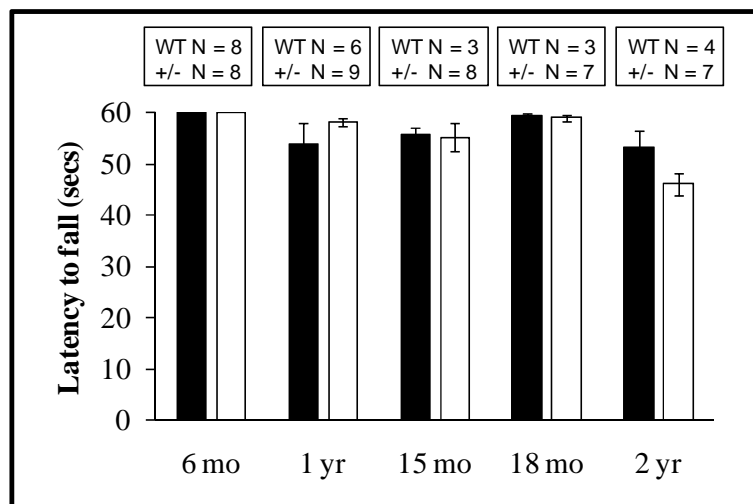


Figure 5.6 No muscle weakness in β -III^{+/-} spectrin mice. The latency for WT (black) and β -III^{+/-} spectrin (white) to fall from an inverted grid was recorded. Mice were given 4 trials and a maximum time of 60 seconds allowed. All data are given as means \pm SEM.

Novel Object Recognition

The novel object recognition task was performed on 3-week old WT and β -III^{+/-} spectrin mice and the exploratory preference measured (Figure 5.7). There was no discernable difference between the ability of WT and β -III^{+/-} spectrin mice in recognising the novel object.

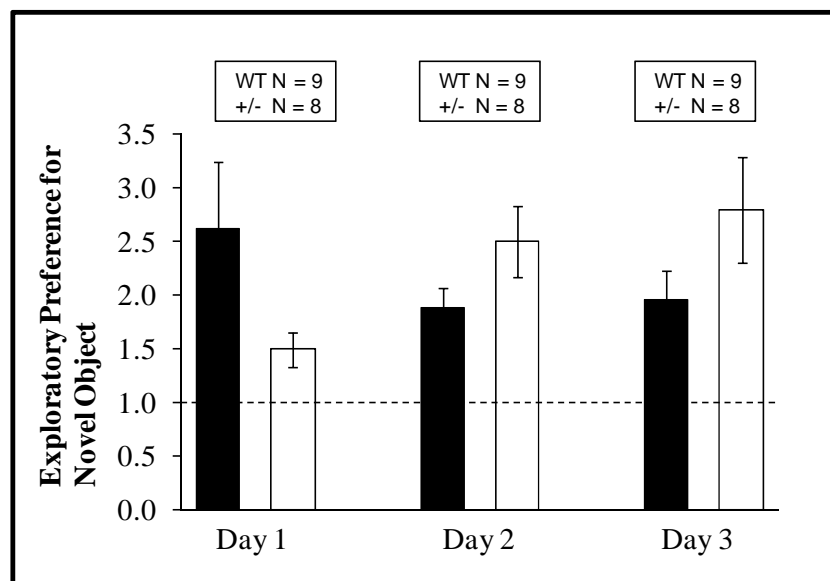


Figure 5.7 β -III^{+/-} spectrin mice display no deficit in object recognition. Preference of WT (black) and β -III^{+/-} (white) spectrin mice to explore a novel object. All data are given as means \pm SEM.

5.2.2 Histological Analysis

In order to examine cerebellar morphology sections from 2-year old WT and β -III^{+/-} spectrin mice were stained for Nissl. The over all cerebellar size and morphology appeared normal in β -III^{+/-} spectrin mice apart from a slight difference in folia 1 and 2 compared to WT (arrow Figure 5.8A). Quantification revealed no molecular layer thinning or Purkinje cell loss in β -III^{+/-} spectrin mice (Figure 5.8B). Cerebellar

sections from 2-year old WT and β -III^{+/-} spectrin mice were also immunostained for calbindin D28K to examine Purkinje cell morphology. The staining revealed no obvious difference in the cell body or dendritic tree of β -III^{+/-} spectrin Purkinje cells compared to WT (Figure 5.8C,D).

5.2.3 Analysis of glutamate transporter levels

A loss of EAAT4 and GLAST was observed in β -III^{-/-} spectrin mice (Perkins et al., 2010) and dramatic changes in EAAT4 distribution were reported in SCA5 autopsy tissue (Ikeda et al., 2006). Therefore glutamate transporter expression levels were examined in β -III^{+/-} spectrin mice. Total cerebellar homogenates from 1- and 2-year old WT and β -III^{+/-} spectrin mice were resolved by SDS-PAGE and immunoblotted for EAAT4, GLAST and GLT1 (Figure 5.9A). Quantification revealed no significant difference in any glutamate transporter at 1-year or 2-years of age in β -III^{+/-} spectrin mice (Figure 5.9B). Levels of the neuronal transporter EAAT4 were normalised to calbindin whereas levels of the astroglial transporters GLAST and GLT1 were normalised to actin.

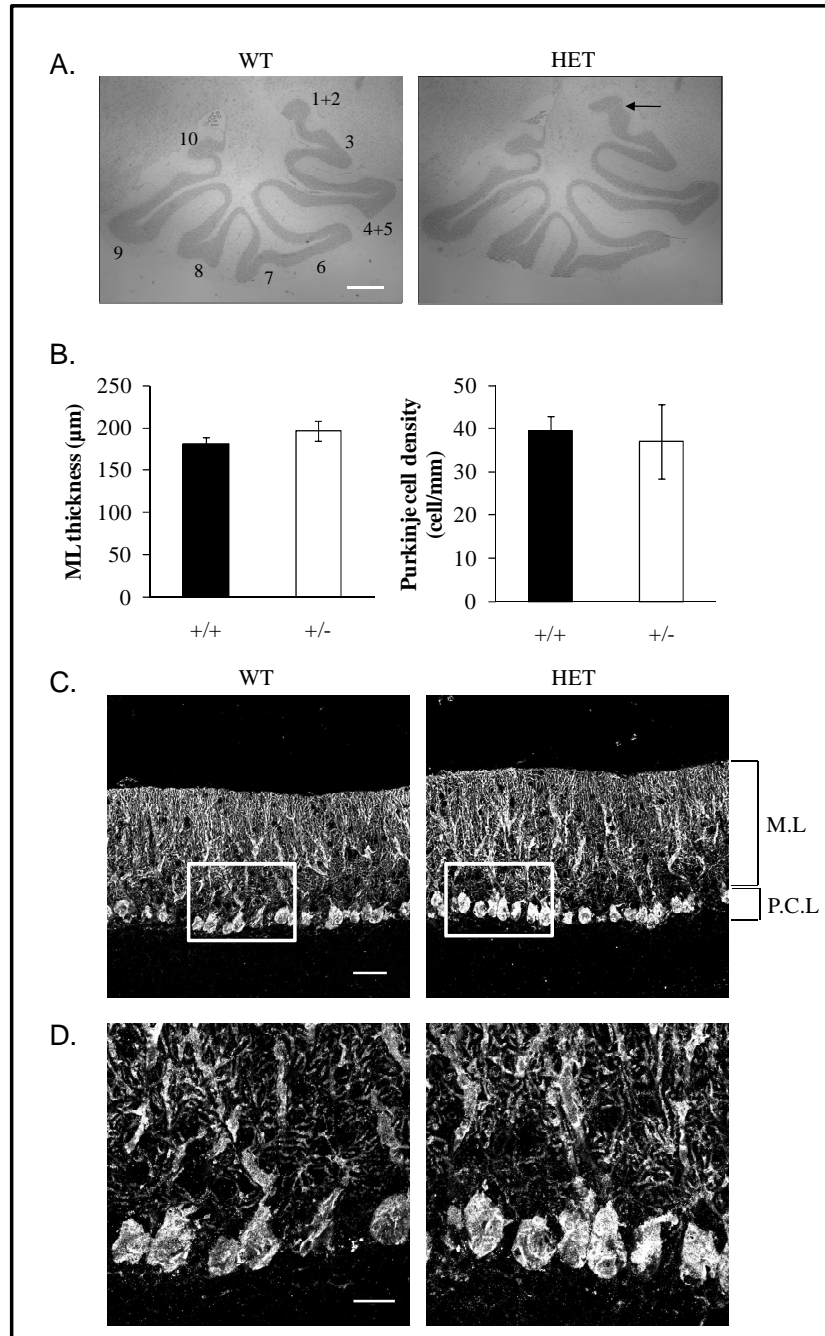


Figure 5.8 No cerebellar pathology in β -III^{+/-} spectrin mice. (A) Cerebellar sections stained with cresyl violet. Numbers correspond to folia. Bar, 500 μ m. (B) Left, Quantification of the mean molecular layer thickness at 2-years of age. Right, Quantification of the mean Purkinje cell density in 2-year old WT and β -III^{+/-} spectrin mice. All data are given as means \pm SEM (WT N = 3; β -III^{+/-} N = 3). (C,D) Cerebellar sections immunostained with anti-calbindin D28K antibody. (ML, molecular layer; PCL, Purkinje cell layer; Bar, 50 μ m (C); Bar, 20 μ m (D)).

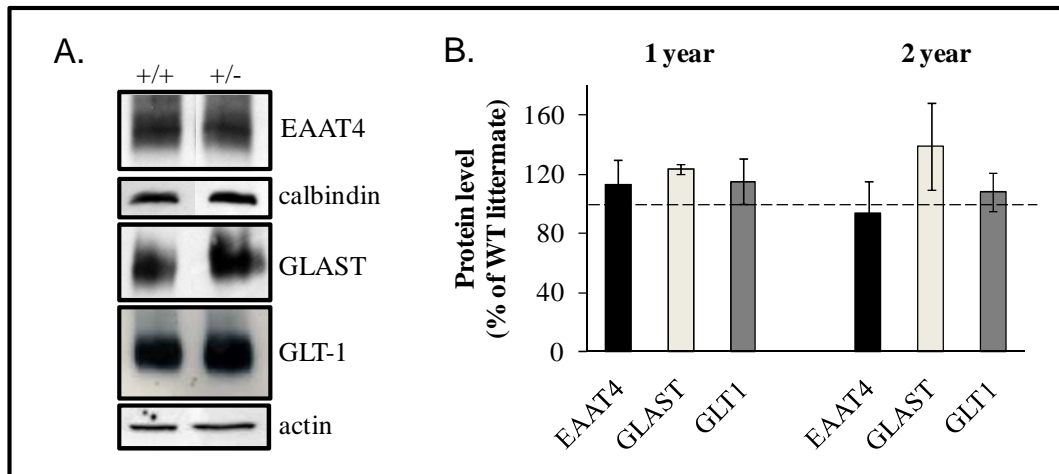


Figure 5.9 No loss of neuronal or astroglial transporters in β -III^{+/-} spectrin mice. (A) Representative Western blots of cerebellar homogenates from 2-year old WT and β -III^{+/-} spectrin mice immunoblotted using anti-EAAT4, anti-GLAST and anti-GLT1 antibody. (B) Quantification of transporter expression from 1- and 2-year old WT and β -III^{+/-} spectrin mice. Data plotted as a percentage of WT littermate values. Dotted line represents 100%. All data are given as means \pm SEM (N = 3 of each genotype).

5.3 Discussion

The data shown in this chapter argue against haploinsufficiency as a disease mechanism since even at 2-years of age β -III^{+/-} spectrin mice show no signs of ataxia or cerebellar degeneration. Furthermore, the discovery that there is no change in the levels of EAAT4 and GLAST in β -III^{+/-} spectrin mice, the two transporters found to be reduced in β -III^{-/-} spectrin mice (Perkins et al., 2010), suggests that a loss of EAAT4 and GLAST may play a role in disease pathogenesis.

5.3.1 Haploinsufficiency as a disease mechanism

Haploinsufficiency has been shown to underlie a number of dominantly inherited human diseases (Santarosa and Ashworth, 2004; Veitia and Birchler, 2004; Zephir et al., 2005; Dang et al., 2008; Iwaki et al., 2008) and more recently other forms of ataxia (SCA15 & 28) are thought to arise from haploinsufficiency (van de Leemput et al., 2007; Maltecca et al., 2009). Often the genes involved in these diseases encode proteins where a correct stoichiometry is imperative for normal function and a single wild type copy is insufficient. Transcription factors and proteins that form macromolecular complexes are examples of such proteins.

In the case of SCA15 it is *ITPR1* haploinsufficiency that is believed to be responsible for a disease phenotype (van de Leemput et al., 2007). *ITPR1* is found coupled to calcium channels and mediates calcium release from the ER following binding of inositol 1,4,5-triphosphate, an intracellular second messenger (Berridge, 1993; Mikoshiba, 1993; Matsumoto and Nagata, 1999). A pathogenic gain-of-function resulting from the large gene deletion across the first one-third of the *ITPR1* gene and across the first half of a neighbouring gene, *SUMF1*, is not supported by the findings as *ITPR1* levels were dramatically reduced in cells derived from SCA15 patients and no disease specific truncated *ITPR1* products were detected (van de Leemput et al., 2007). Instead the observations are consistent with haploinsufficiency, as mice homozygous for *Itp1* deletions display an early onset disorder whereas humans heterozygous for the deletion have a much later onset. Analysis of aged heterozygous mice is required to reveal whether they eventually

CHAPTER 5 ANALYSIS OF β -III^{+/-} SPECTRIN DEFICIENT MICE

show signs similar to SCA15 patients, which would lend further support to haploinsufficiency as a mechanism. In addition, the fact ITPR1 is downregulated in other neurodegenerative diseases such as Alzheimer's disease, Huntington's disease and Friedreich's ataxia (Zecevic et al., 1999) indicates that the dysregulation of calcium homeostasis, through loss of this protein, may be a convergent disease mechanism in neuronal degeneration.

In the case of SCA28, there is clearer evidence to support haploinsufficiency of a nuclear encoded mitochondrial protein, *Afg3l2*, as the underlying cause of ataxia (Maltecca et al., 2009). Although homozygous *Afg3l2* mutant mice were found to have widespread neuromuscular dysfunction in the CNS and PNS with impaired axonal maturation, delayed myelination and death occurring at postnatal day 14 (Maltecca et al., 2008; Maltecca et al., 2009), heterozygous *Afg3l2* mutant mice showed characteristics of ataxia including progressive gait abnormalities, motor deficits and cerebellar degeneration from 4-months of age (Maltecca et al., 2009). This is thought to be due to respiratory chain dysfunction resulting in elevated reactive oxygen species production, a consequence of altered mitochondrial calcium homeostasis, and ultimately dysfunction and dark cell degeneration of Purkinje cells (Maltecca et al., 2009; Di Bella et al., 2010).

With respect to SCA5, all patients to date have been found to be heterozygous for mutations in β -III spectrin (Ikeda et al., 2006 and LPW Ranum personal

CHAPTER 5 ANALYSIS OF β -III^{+/-} SPECTRIN DEFICIENT MICE

communication). It is therefore possible that SCA5 arises from haploinsufficiency, especially since spectrin functions as a heterotetramer and assembly appears to be rate limited by the β subunit (Hanspal and Palek, 1987). One possibility is that the mutant β -III polypeptides fail to associate with other subunits of the tetramer. However, based on the findings reported here it does not appear that β -III spectrin haploinsufficiency is responsible for either ataxia or cerebellar degeneration. It is possible that mice do not live long enough for a phenotype to manifest itself in β -III^{+/-} spectrin mice, or that the behavioural tasks used were not sensitive enough to detect minor motor deficits. However, the motor tests used were consistent with other studies (Dunham and Miya, 1957; Crawley, 1999). One other complicating issue is that the β -III^{+/-} spectrin mice will also be expressing a very low level of Δ 2-6 β -III spectrin (refer to Chapter 3). However, this is thought unlikely to provide sufficient function to occlude the appearance of any phenotype. Therefore, from the analysis of β -III^{+/-} spectrin mice it would appear that β -III spectrin haploinsufficiency is not likely to give rise to either ataxia or cerebellar degeneration.

In contrast, work by Stankewich et al., (2010) reported an ataxic phenotype in *Spnb3*^{+/-} mice, but, as mentioned previously, this was based on a wire-hanging test which is not generally considered appropriate as a method for assessment of motor performance. Furthermore, no data were collected from *Spnb3*^{+/-} mice to rule out any potential toxic gain-of-function associated with the truncated β -III spectrin protein

still being expressed in these mice (Stankewich et al., 2010). Consequently, the relevance of these mice as an accurate model of SCA5 must remain open to question.

5.3.2 Lack of glutamate transporter loss in β -III^{+/-} spectrin mice

The lack of disease phenotype and glutamate transporter loss in β -III^{+/-} spectrin mice provides evidence that EAAT4 and GLAST may be important in the development of ataxia. In β -III^{-/-} spectrin mice there is an early and consistent loss of EAAT4, the Purkinje cell specific transporter, and with age there is a progressive loss of the Bergmann glial transporter GLAST (Perkins et al., 2010). Furthermore there is a correlation of disease severity with degree of Purkinje cells undergoing dark cell degeneration, a characteristic of glutamate-mediated excitotoxicity (Barenberg et al., 2001; Strahlendorf et al., 2003). The fact no glutamate transporter loss, dark cell degeneration or motor deficits were seen in β -III^{+/-} spectrin mice supports the correlation between reduction in clearance of glutamate due to loss of EAAT4 and GLAST and excitotoxic damage to Purkinje cells resulting in dysfunction and disease.

A loss of GLAST, glutamate uptake and dark cell degeneration was also observed in the SCA7 transgenic mouse, where mutant ataxin-7 was expressed specifically in Bergmann glia, supporting a role for reduced astroglial uptake in Purkinje cell toxicity (Custer et al., 2006). The importance of a non-cell autonomous mechanism in Purkinje cell degeneration is also highlighted by the discovery that the conditional

ablation of Bergmann glia in adult mice results in ataxia and degeneration of Purkinje cell dendrites (Cui et al., 2001). Further evidence that GLAST dysfunction plays a role in cerebellar ataxia comes from the discovery that a complete loss-of-function mutation in EAAT1 (GLAST), with a dominant negative effect on wild type protein, underlies episodic and progressive ataxia (Jen et al., 2005), and a GLAST knockout mouse possesses motor deficits (Watase et al., 1998).

In contrast although EAAT4 loss does not correlate with disease progression, as the same level of loss is observed in older animals with more pronounced deficits, an early loss of EAAT4 may be a common feature in the onset of ataxia as two other mouse models also show a loss of both EAAT4 and β -III spectrin before any overt phenotype (Lin et al., 2000; Gold et al., 2003).

5.3.4 Conclusions

The analysis of β -III^{+/-} spectrin mice reported in this chapter provides no evidence for β -III spectrin haploinsufficiency in ataxia. However, in conjunction with the data presented in chapter 4 that loss of β -III spectrin function underlies pathogenesis, the results indicate that the mutations associated with SCA5 have dominant negative effects on WT β -III spectrin function in addition to partial loss of normal function. The fact no non-sense mutations have been identified in SCA5 patients would support the hypothesis that haploinsufficiency is not pathogenic and that the mutations interfere with the normal function of β -III spectrin. Furthermore the

CHAPTER 5 ANALYSIS OF β -III^{+/-} SPECTRIN DEFICIENT MICE

analysis of both β -III^{+/-} and β -III^{-/-} spectrin mice has revealed that a reduction in glutamate transporter protein levels correlates with disease and may be an important aspect of disease pathogenesis.

CHAPTER 6

HUMAN MUTATIONS ASSOCIATED WITH SCA5

6.1 Background

Originally two separate in-frame deletions and a missense mutation in β -III spectrin were found to associate with SCA5 in three independent families ((Ikeda et al., 2006); Figure 6.1). Subsequently, the screening of the same regions of β -III spectrin in more than 6587 unclassified ataxic individuals identified a further twelve missense mutations, (D Lorenzo and LPW Ranum, personal communication). Of the residues affected, leucine 253, alanine 486, arginine 634, arginine 658 and arginine 1278 are conserved between human and rat. This chapter reports a series of cell culture experiments to investigate the effect mutations associated with SCA5 have on normal β -III spectrin function.

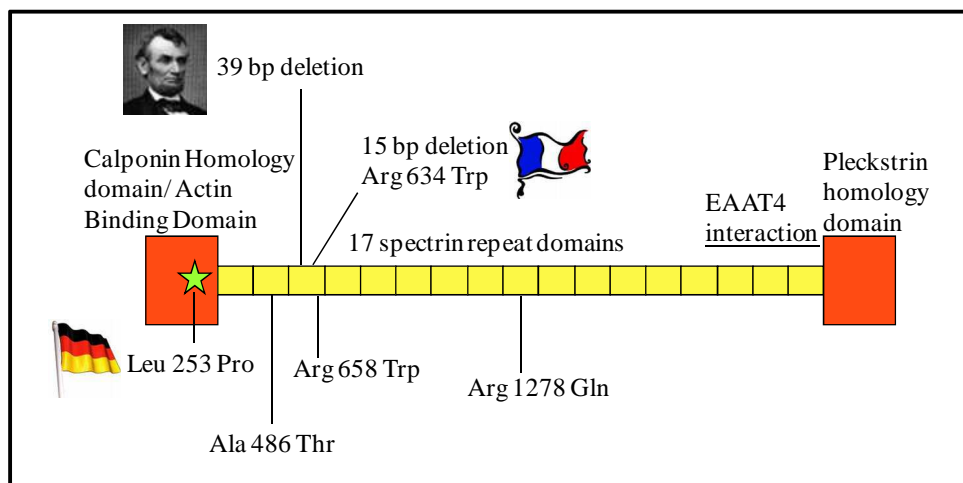


Figure 6.1 Human mutations associated with SCA5. A schematic representation of β -III spectrin annotated with the location of mutations found in individuals with ataxia that are at conserved residues in rat.

6.2 Results

6.2.1 Generation, expression and cellular localisation of β -III spectrin mutant constructs

Using site-directed mutagenesis (refer to section 2.2.4) five missense mutations, identified in individuals with ataxia that altered residues conserved between human and rat, were introduced into a construct encoding myc-tagged rat β -III spectrin. Western blot analysis confirmed the expression of mutant proteins upon transfection of HEK 293T cells, but the level of expression varied and L253P was always expressed at a lower level (Figure 6.2).

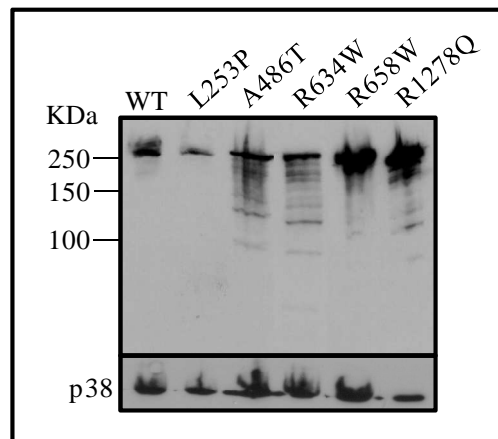


Figure 6.2 Expression of full length rat β -III spectrin with mutations associated with SCA5. Cell homogenates from HEK 293T cells transfected with various myc-tagged β -III spectrin constructs resolved by SDS-PAGE and probed with anti-c-myc antibody. p38 was used as a loading control.

Confocal immunofluorescence microscopy revealed that, unlike WT, L253P β -III spectrin was not found at the plasma membrane in either HEK 293T or Neuro 2a cells, but instead accumulated in a discrete intracellular location (Figure 6.3). To

further elucidate the intracellular distribution, L253P was co-expressed with either a Golgi (Figure 6.4A) or an ER marker (Figure 6.4B). This revealed that L253P β -III spectrin appears to associate with the Golgi apparatus (Figure 6.4A). Expression of myc-tagged β -III spectrin constructs encoding an original human mutation Δ 39 bp or Δ 15 bp + R634W found in the Lincoln and French pedigree respectively (Ikeda et al., 2006), revealed no difference in cellular distribution compared to WT β -III spectrin (Figure 6.5). All other mutant forms of rat β -III spectrin were also found at the plasma membrane and did not associate with the Golgi apparatus (Figure 6.6).

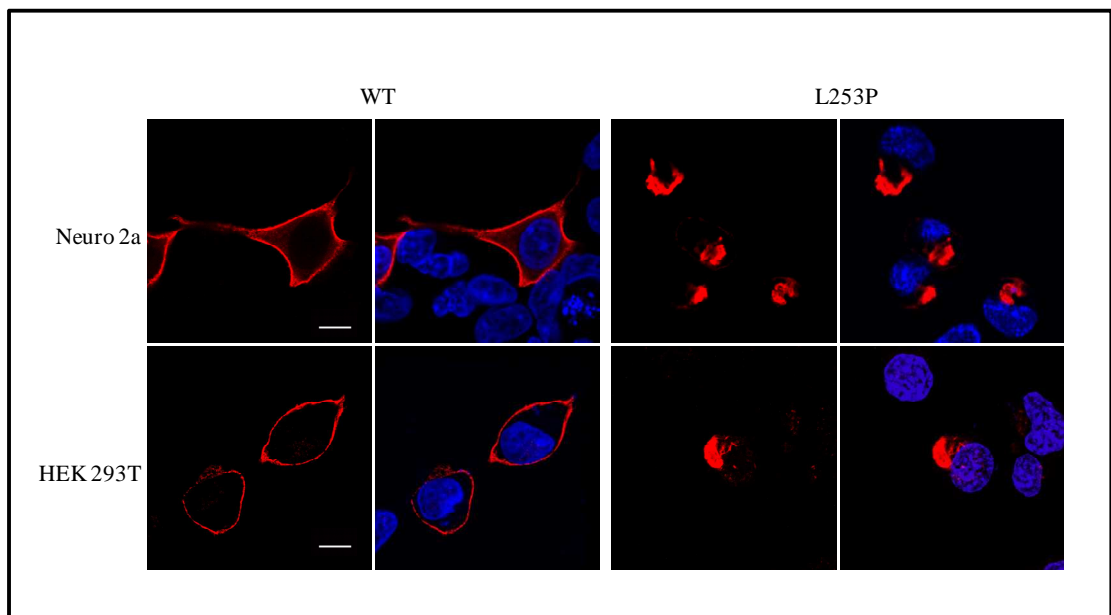


Figure 6.3 Lack of expression of L253P β -III spectrin at plasma membrane. Neuro 2a and HEK 293T cells transfected with either myc-tagged WT or L253P β -III spectrin (red). Nucleus was stained with DAPI (blue). All images are representative of three independent experiments. Bar, 10 μ m.

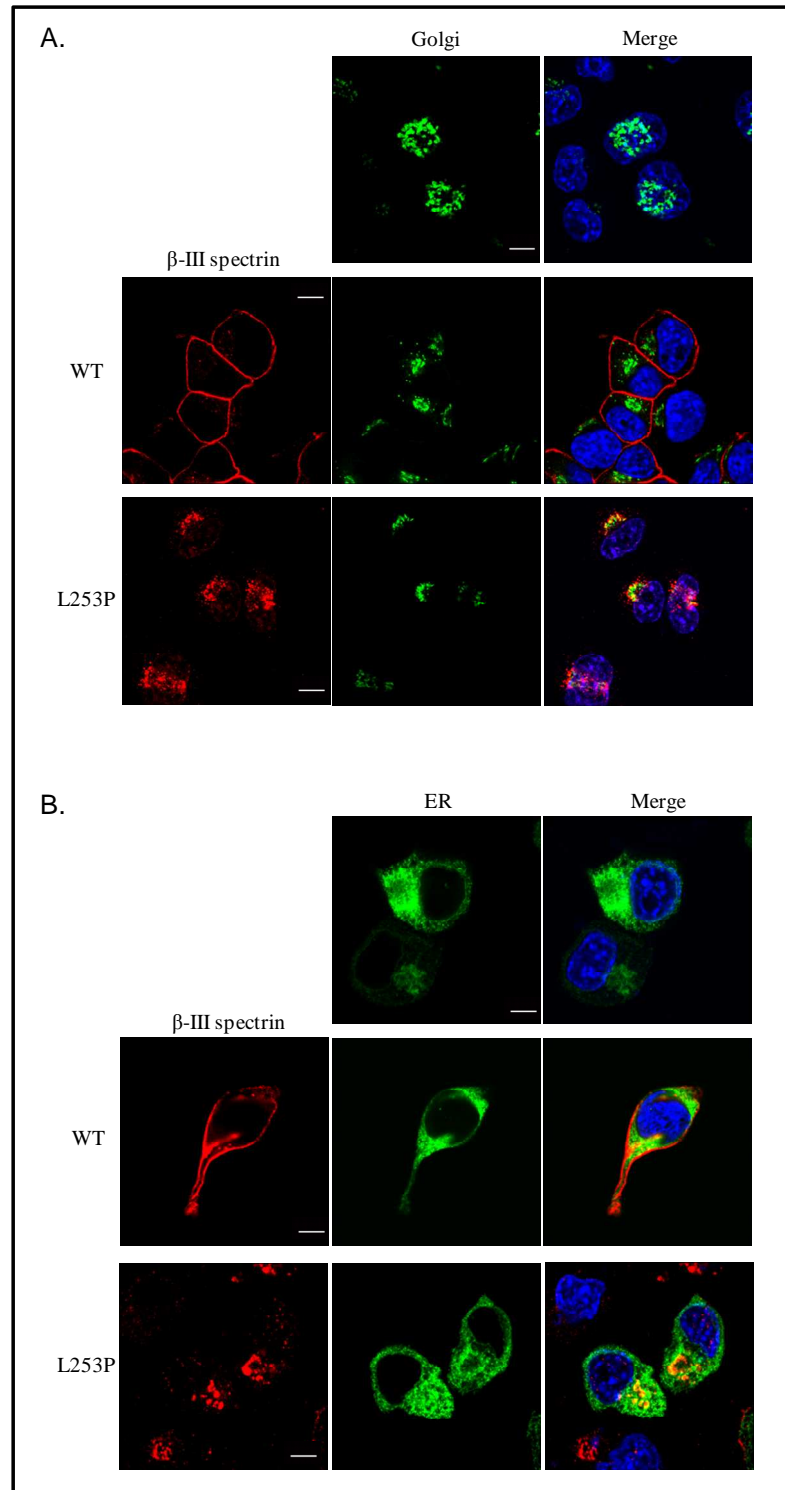


Figure 6.4 L253P β -III spectrin associates with a Golgi marker. Neuro 2a cells transfected with either myc-tagged WT or L253P β -III spectrin (red) and either **(A)** a Golgi (green) or **(B)** an ER (green) marker. Nucleus was stained with DAPI (blue). All images are representative of three independent experiments. Bar, 10 μ m.

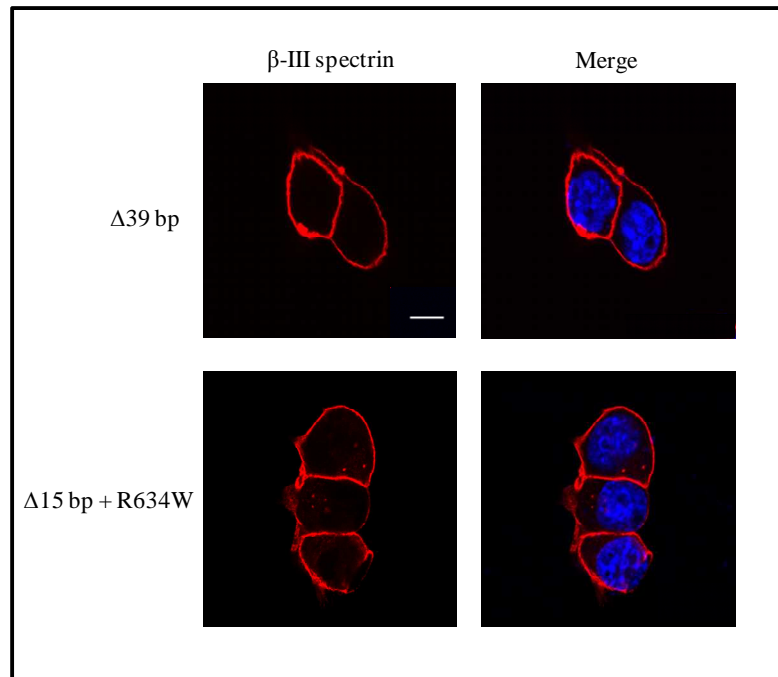


Figure 6.5 $\Delta 39$ bp and $\Delta 15$ bp + R634W β -III spectrin associate with the plasma membrane. Neuro 2a transfected with either myc-tagged $\Delta 39$ bp and $\Delta 15$ bp + R634W β -III spectrin (red). Nucleus was stained with DAPI (blue). All images are representative of three independent experiments. Bar, 10 μ m.

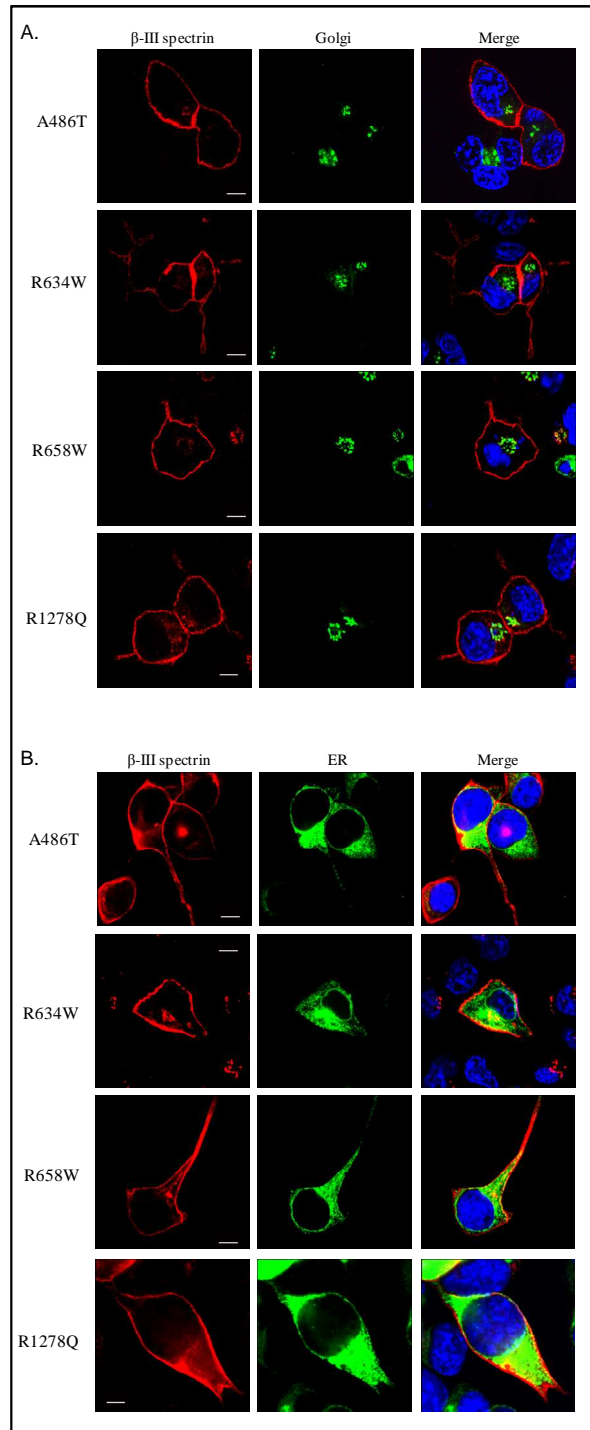


Figure 6.6 Other SCA5 missense mutations associate with the cell membrane. Neuro 2a cells cotransfected with either a Golgi (green) **(A)** or ER (green) marker **(B)** and myc-tagged β -III spectrin constructs (red). Nucleus was stained with DAPI (blue). All images are representative of three independent experiments. Bar, 10 μ m.

At the time of this work it was found that unlike WT, the amino terminus of human L253P β -III spectrin was cleaved (K Dick-Krueger and LPW Ranum). Western blot analysis using antibodies against both the N-terminus of β -III spectrin and the N-terminal c-myc tag confirmed that the amino terminus of rat L253P β -III spectrin was cleaved, similar to human L253P β -III spectrin (Figure 6.7A). In contrast no cleavage was seen for the other two human mutations, Δ 39 bp and Δ 15 bp + R634W β -III spectrin. Confocal immunofluorescence microscopy revealed that for all three mutant constructs the polyclonal antibody raised against the C-terminal region of β -III spectrin recognised the same protein as the antibody directed against the N-terminal myc-tag (Figure 6.7B). This demonstrated that it was full length L253P β -III spectrin that was associated with the Golgi and not the N-terminal proteolytic fragment.

To determine whether increasing the expression of L253P β -III spectrin had any effect on the cellular distribution of the mutant protein Neuro 2a cells were transfected with different amounts of DNA (0.5 μ g – 4 μ g). This had very little effect on the amount of L253P protein that reached the plasma membrane and instead more protein appeared trapped at the Golgi apparatus (Figure 6.8A). Similarly, increasing the length of time for protein expression did not result in more L253P protein reaching the plasma membrane (Figure 6.8B).

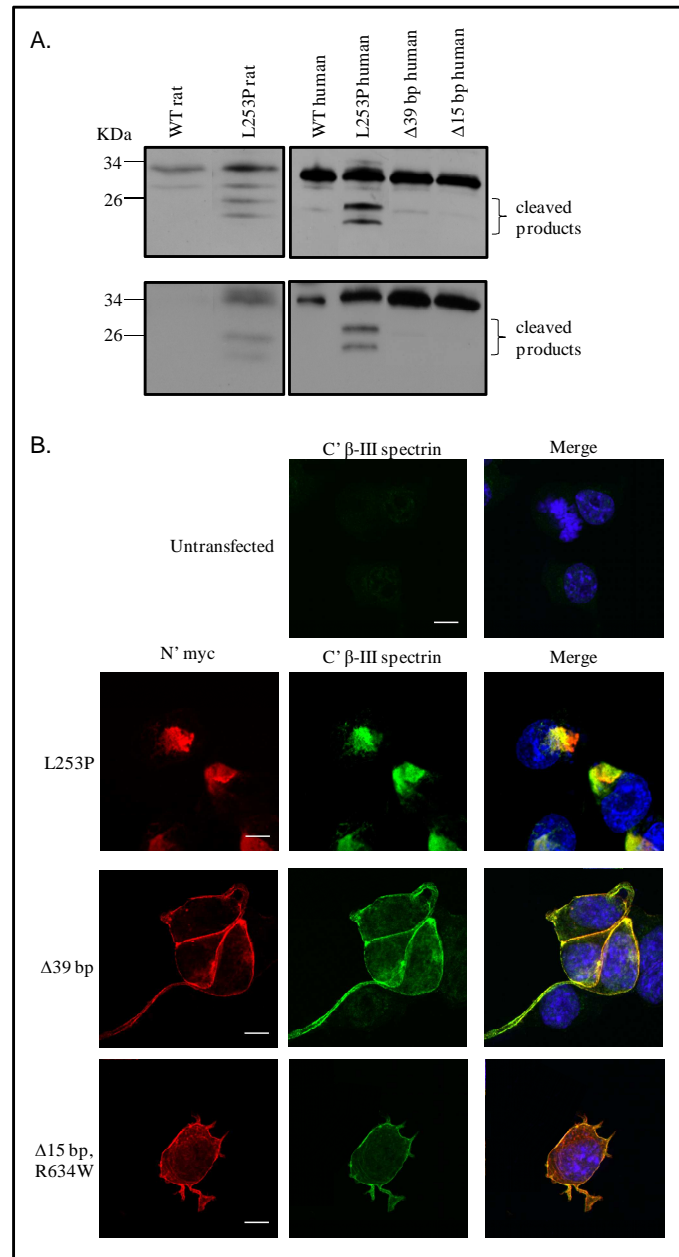


Figure 6.7 Full length L253P β -III spectrin associated with Golgi. (A) Neuro 2a cellular homogenates immunoblotted using antibodies against either N-terminus of β -III spectrin (top panel) or c-myc epitope (bottom panel). **(B)** Neuro 2a cells transfected with myc-tagged L253P, Δ 39 bp and Δ 15 bp + R634W β -III spectrin and immunostained with a carboxy-terminal anti- β -III spectrin antibody (green) and an anti-c-myc antibody (red) to detect amino terminal myc-tag. Nucleus stained with DAPI (blue). All images are representative of three independent experiments. Bar, 10 μ m.

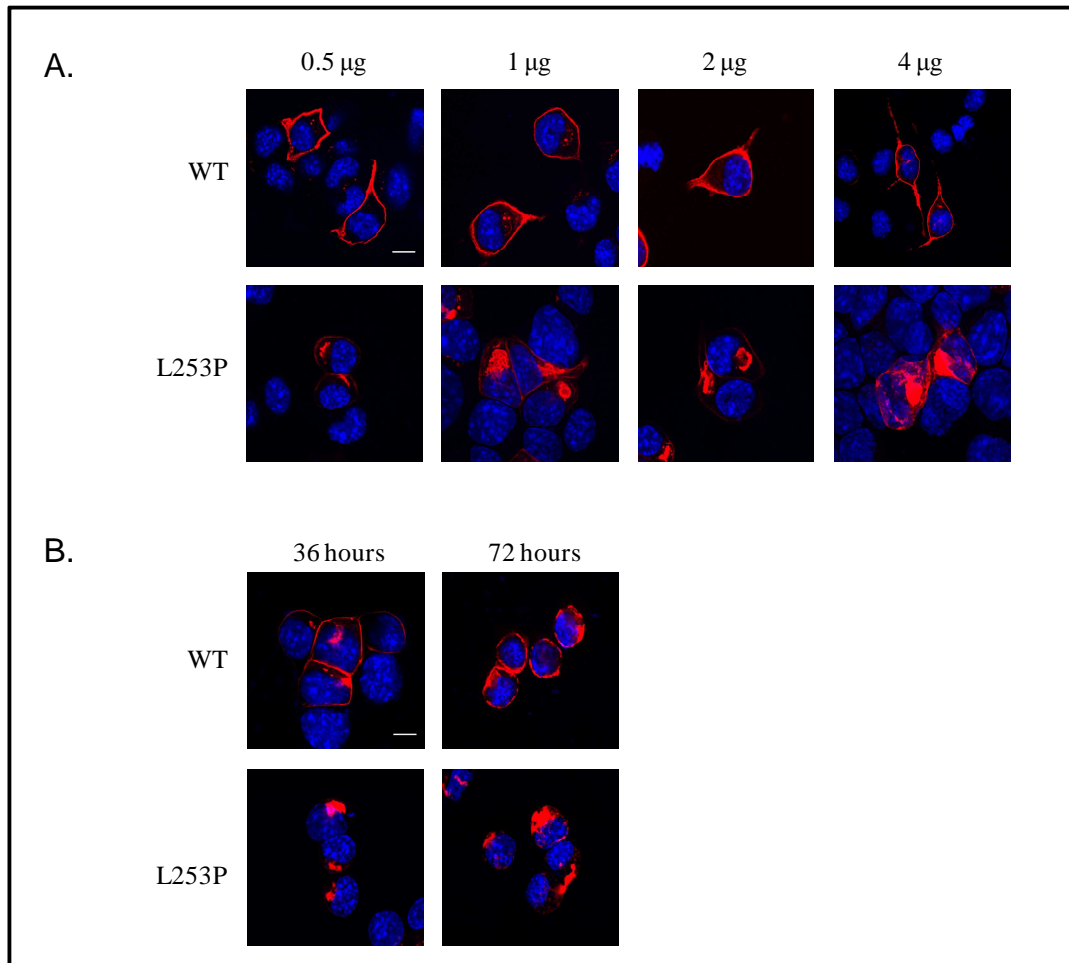


Figure 6.8 Increased protein levels or longer time for protein expression does not result in normal cellular distribution of L253P β -III spectrin. (A) Neuro 2a cells transfected with different amounts of myc-tagged WT or L253P β -III spectrin construct DNA. β -III spectrin (red), nucleus (blue). (B) Neuro 2a cells transfected with either myc-tagged WT or L253P β -III spectrin and left for 36- or 72-hours before fixation and immunostaining. Nucleus stained with DAPI (blue). All images are representative of three independent experiments. Bar, 10 μ m.

6.2.2 Dominant negative effect of L253P on WT β -III spectrin

To determine what effect L253P β -III spectrin had on WT protein, YFP-tagged WT β -III spectrin was co-expressed in Neuro 2a cells with myc-tagged L253P β -III spectrin. Immunostaining with antibodies against the c-myc and GFP tags revealed that the presence of L253P β -III spectrin resulted in WT β -III spectrin being abnormally located and found in the same cellular localisation as L253P β -III spectrin (Figure 6.9). However, when YFP-tagged WT β -III spectrin was co-expressed with myc-tagged β -III spectrin both constructs were located at the cell membrane (Figure 6.9).

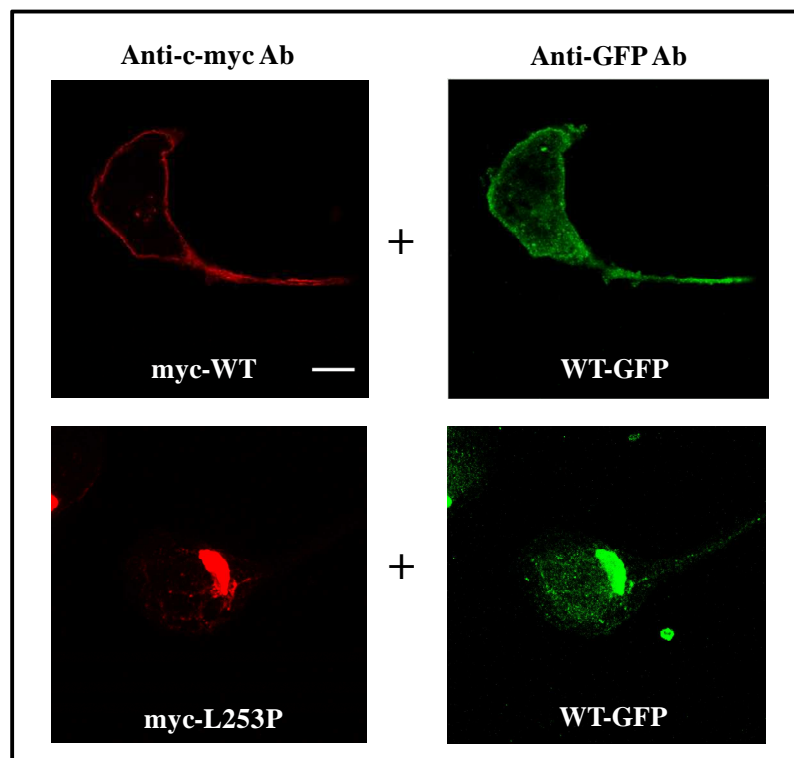


Figure 6.9 L253P β -III spectrin has a dominant negative effect on WT β -III spectrin. Neuro 2a cells co-transfected with YFP-tagged WT β -III spectrin and either myc-tagged WT or L253P β -III spectrin. Immunostaining used anti-c-myc antibody (red) and anti-GFP antibody (green). All images are representative of three independent experiments. Bar, 10 μ m.

6.2.3 Trafficking of membrane proteins disrupted by L253P β -III spectrin

To examine what effect L253P β -III spectrin had on the trafficking of other proteins Neuro 2a cells were co-transfected with either myc-tagged WT or L253P β -III spectrin and EAAT4, a protein known to interact with and be stabilised at the cell surface by WT β -III spectrin ((Jackson et al., 2001); refer to section 1.5.4). EAAT4 was found at the cell membrane when WT β -III spectrin was coexpressed, whereas in the presence of L253P β -III spectrin EAAT4 had the same intracellular distribution as L253P β -III spectrin (Figure 6.10).

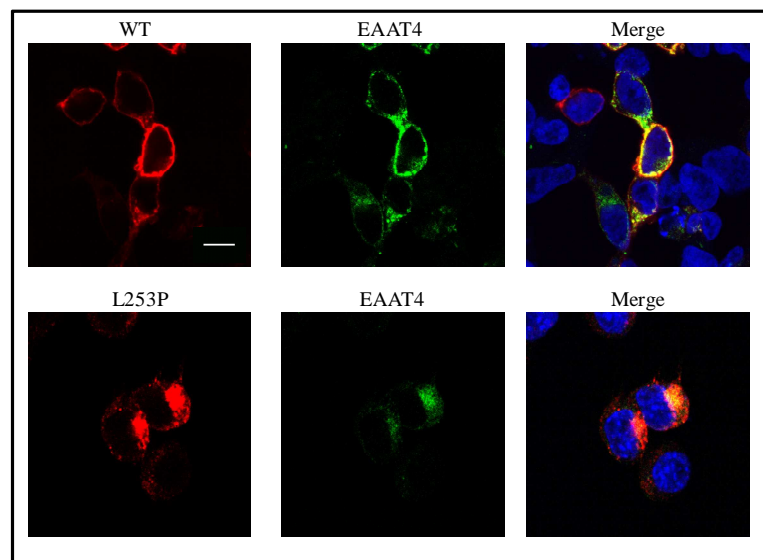


Figure 6.10 L253P β -III spectrin reduces EAAT4 cell surface expression.

Neuro 2a cells co-transfected with EAAT4 and either myc-tagged WT or L253P β -III spectrin. Cells immunostained using anti-c-myc (red), anti-EAAT4 antibody (green) and nucleus stained with DAPI (blue). All images are representative of three independent experiments. Bar, 10 μ m.

To determine whether the defect in protein trafficking was specific to β -III spectrin, and proteins it interacted with, the same experiment was repeated using constructs that encoded GLAST, mGluR1 and mGluR5. To date, there is only evidence to suggest that mGluR1 directly interacts with β -III spectrin (K. Armbrust and LPW Ranum, personal communication). Confocal immunofluorescence microscopy revealed that, like EAAT4, the cellular distributions of GLAST (Figure 6.11A), mGluR1 (Figure 6.11B) and mGluR5 (Figure 6.11C) were altered when co-expressed with L253P β -III spectrin. However, with EAAT4 there was a complete loss of membrane staining but GLAST, mGluR1 and mGluR5 were still partially associated with the membrane. Furthermore the morphology of cells transfected with L253P β -III spectrin was substantially different to that of WT as they had a more rounded appearance.

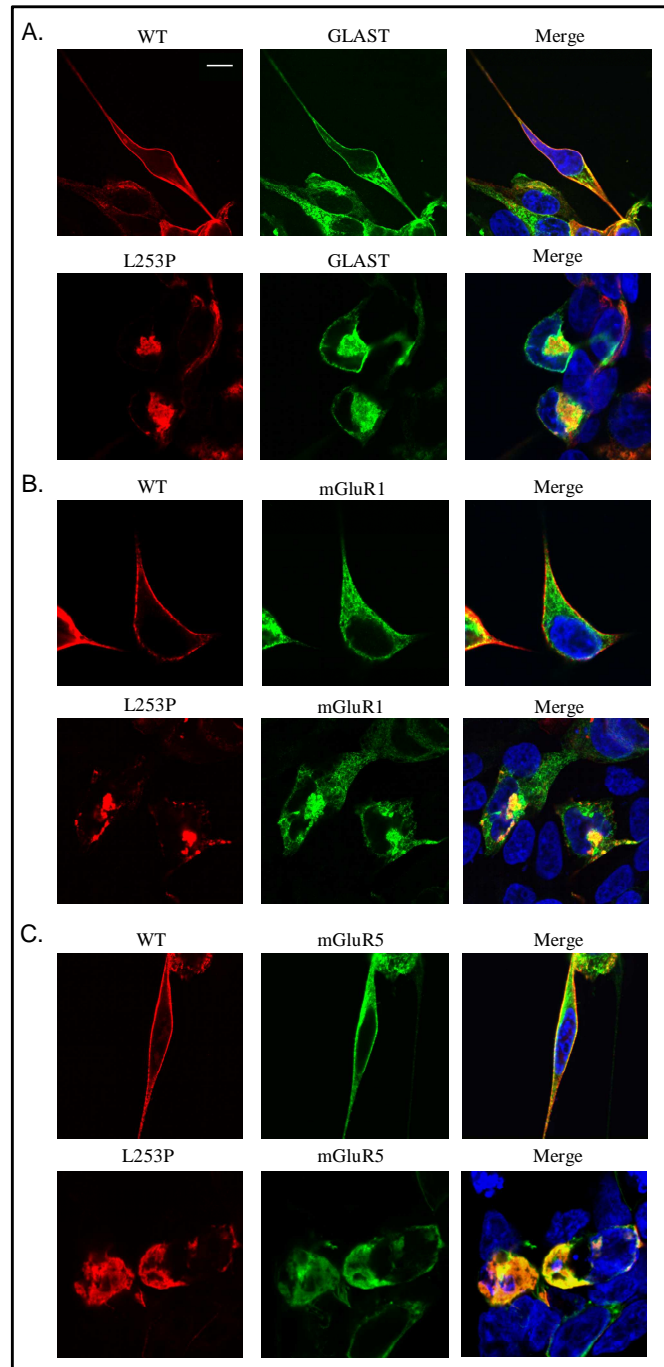


Figure 6.11 Trafficking of proteins from the Golgi disrupted when L253P β -III spectrin expressed. Neuro 2a cells co-transfected with either myc-tagged WT or L253P β -III spectrin and GLAST **(A)** or mGluR1 **(B)**. **(A,B)** Cells immunostained using anti-c-myc (red), anti-GLAST (green) and anti-mGluR1 antibody (green). **(C)** Cells transfected with either untagged WT or L253P β -III spectrin and myc-tagged mGluR5. Cells immunostained with anti-c-myc (green) and carboxy-terminal anti- β -III spectrin antibody (red). Nucleus stained with DAPI (blue). Colours applied using Image J. All images are representative of three independent experiments. Bar, 10 μ m.

6.2.3.1 Membrane trafficking and interaction with Arp1 rescued by temperature shift

Prior to immunostaining transfected cells were incubated for a further 12 hours at a lower temperature (25 °C) and the temperature shift was found to rescue the trafficking defect of L253P β -III spectrin. At the permissive temperature L253P β -III spectrin, like WT, was now localized at the cell membrane (Figure 6.12A). Western blot analysis revealed that the temperature shift did not enhance protein levels and in fact showed that at 25 °C L253P β -III spectrin levels were still lower than that of WT (Figure 6.12B). The disruption to EAAT4 trafficking was also rescued by incubating at the lower temperature (Figure 6.12C).

Previously it was shown that β -III spectrin interacts with Arp1, a subunit of the dynactin complex and copurifies with dynein and dynactin on intracellular vesicles from rat brain (Holleran et al., 2001). A biomolecular fluorescence complementation (BiFC) assay (refer to section 7.2.2) was used to investigate whether the L253P mutation interfered with the ability of the N-terminus of β -III spectrin to interact with Arp1. Full length Arp1 and the amino-terminus of β -III spectrin (amino acids 1-295) were cloned downstream of the N-terminal (YN) and C-terminal fragments (YC) of YFP respectively and HEK 293T cells transfected with the expression vectors. Coexpression of YN-Arp1 and WT YC- β -III spectrin yielded fluorescence but no fluorescence was observed when L253P YC- β -III spectrin was coexpressed with YN-Arp1 (Figure 6.13A), indicating that the mutation does indeed eliminate the interaction between β -III spectrin and Arp1. However, incubation at 25°C for an

additional 12 hours produced a fluorescent signal (Figure 6.13A). Western blot analysis confirmed all proteins were expressed at 37°C (Figure 6.13B).

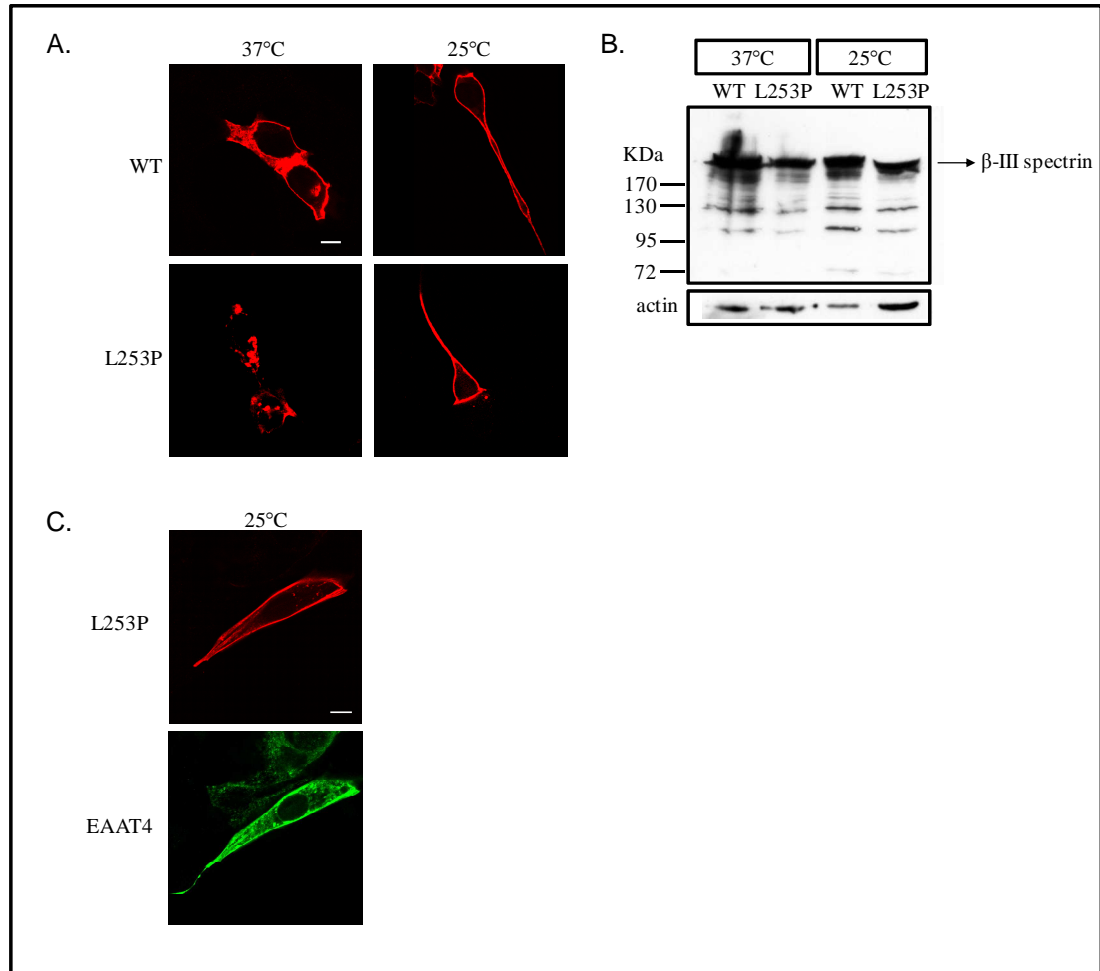


Figure 6.12 Membrane localisation rescued by temperature shift. (A) Cells transfected with either myc-tagged WT or L253P β-III spectrin and 24 hours after transfection cells incubated for a further 12 hours at 37°C or 25°C before immunostaining with anti-c-myc antibody (red). **(B)** Western blot analysis of HEK 293T cell homogenates probed with anti-c-myc antibody. Actin was used as a protein loading control. **(C)** HEK 293T cells expressing myc-tagged L253P β-III spectrin and EAAT4. 24 hours post-transfection cells were incubated for a further 12 hours at 25°C. Cells immunostained using anti-c-myc antibody (red) and anti-EAAT4 antibody (green). All images are representative of three independent experiments. Bar, 10 μm.

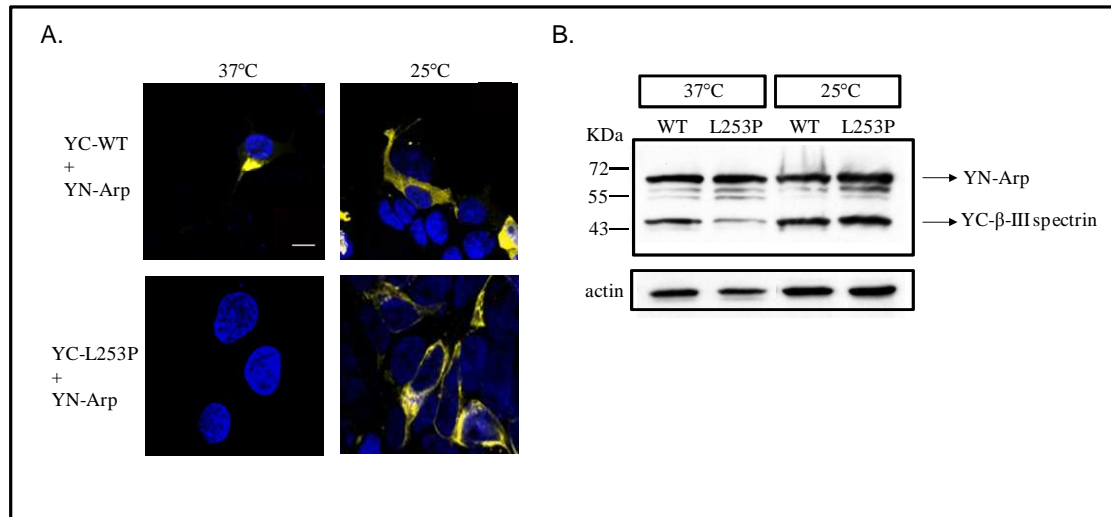


Figure 6.13 Interaction with Arp1 rescued by temperature shift. (A) BiFC assay using HEK 293T cells transfected with Arp1 fused to the N-terminal half of YFP (YN-Arp) and the amino terminus of β -III spectrin, with or without the L253P substitution, fused to the C-terminal half of YFP (YC- β III). 24 hours after transfection cells were incubated at 37°C or 25°C for a further 12 hours. Nucleus was stained with DAPI (blue). All images are representative of three independent experiments. Bar, 10 μ m. **(B)** Western blot analysis of HEK 293T cell homogenates probed with anti-GFP antibody. Actin was used as a protein loading control.

6.2.4 L253P β -III spectrin does not induce the unfolded protein response

A number of neurodegenerative diseases like amyotrophic lateral sclerosis (ALS) (Atkin et al., 2006; Nagata et al., 2007) and Alzheimer's disease (Salminen et al., 2009) have been shown to be associated with accumulation of abnormal protein, impaired ER homeostasis and activation of the ER unfolded protein response (UPR). The UPR can be triggered by a block in trafficking at the ER and Golgi, as well as the accumulation of unfolded or misfolded proteins in the ER. ER stress induces the expression of CHOP (GADD153), a transcription factor growth arrest and DNA damage/C/EBP-homologous protein, which is believed to be a downstream effector

of all three UPR pathways (Oyadomari and Mori, 2004; Xu et al., 2005). Therefore, it was investigated whether the expression of L253P β -III spectrin induced the UPR given its detrimental effect on membrane protein trafficking. Neuro 2a cells were transfected with either GFP, WT β -III spectrin, L253P β -III spectrin, EAAT4, WT β -III spectrin and EAAT4 or L253P β -III spectrin and EAAT4. Western blot and densitometry analysis revealed that CHOP expression induced by L253P β -III spectrin overexpression was not significantly different to that of cells overexpressing GFP (Figure 6.14A). Western blot analysis and immunofluorescence microscopy confirmed the pharmacological induction of CHOP expression in Neuro 2a cells by tunicamycin, a blocker of N-linked glycosylation (Figure 6.14B,C). In contrast no nuclear staining for CHOP was observed in Neuro 2a cells transfected with either WT or L253P β -III spectrin (Figure 6.14C).

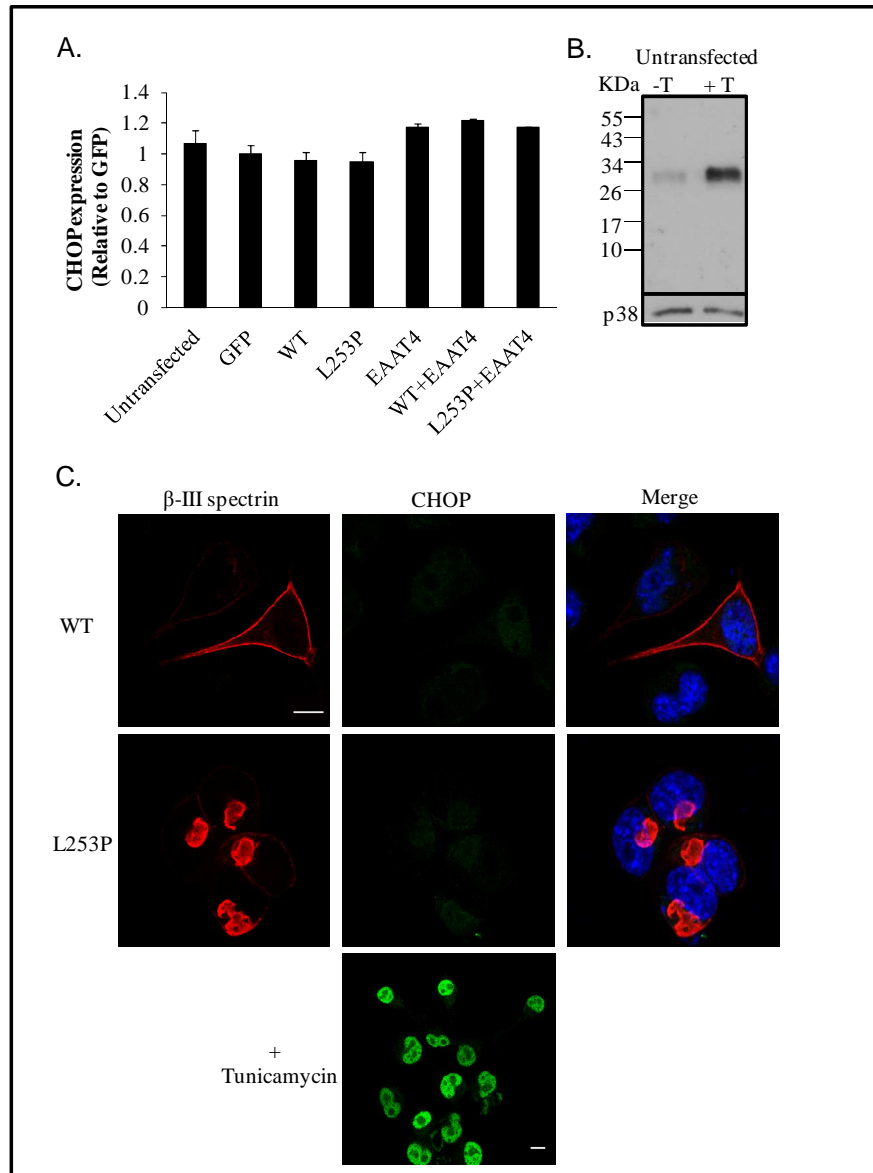


Figure 6.14 L253P β -III spectrin does not induce unfolded protein response. **(A)** Neuro 2a cells transfected with constructs encoding either GFP, WT β -III spectrin, L253P β -III spectrin, EAAT4, WT β -III spectrin and EAAT4 or L253P β -III spectrin and EAAT4. Total cellular homogenates resolved by SDS-PAGE and immunoblotted using anti-CHOP antibody. Data quantified by densitometry and expressed relative to level of GFP expressing cells (means \pm S.E.M, N = 3). **(B)** Total cellular homogenates of untreated (-T) and cells treated with tunicamycin (+T) for 12 hours resolved by SDS-PAGE and immunoblotted using anti-CHOP antibody. **(C)** Confocal microscopy of cells transfected with myc-tagged WT or L253P β -III spectrin using an anti-c-myc antibody (red), an anti-CHOP antibody (green) and nucleus stained with DAPI (blue). All images are representative of three independent experiments. Bar, 10 μ m.

6.3 Discussion

The data presented in this chapter indicate there is a dominant-negative effect on wild-type β -III spectrin function for the L253P missense mutation found within the β -III spectrin calponin homology domain of individuals with SCA5. Instead of being primarily localised at the cell membrane, mutant L253P β -III spectrin was found associated with the Golgi apparatus and furthermore disrupted the normal trafficking of WT β -III spectrin and a number of transmembrane proteins. The fact that the disruption to protein trafficking was rescued by incubating at a lower temperature suggests the missense mutation L253P alters the protein conformation of β -III spectrin (Payne et al., 1998; Gelman and Kopito, 2002; Thomas et al., 2003; Anderson et al., 2006; Rusconi et al., 2007; Rennolds et al., 2008). This assumption is supported by the fact circular dichroism shows a loss of α helical content in the amino terminus of human L253P β -III spectrin (KA Dick Krueger and LPW Ranum, personal communication).

Furthermore the results presented here are the first to directly show an SCA5 mutation can interfere with the ability of spectrin to interact with Arp1, a component of the dynactin complex, thus providing mechanistic insights into how protein trafficking defects may arise. Nevertheless, despite the intracellular accumulation of proteins due to expression of L253P β -III spectrin, there was no sign of the UPR suggesting that the loss of normal transmembrane protein function is more critical for SCA5 pathogenesis rather than an intracellular accumulation of protein. This is in contrast to other neurodegenerative diseases and mouse models that have been shown

to be associated with an intracellular accumulation of proteins in conjunction with the UPR (Atkin et al., 2006; Kim et al., 2006; Nagata et al., 2007; Salminen et al., 2009).

6.3.1 Loss of transmembrane proteins in SCA5 pathogenesis

6.3.1.1 Mutant β -III spectrin proteins disrupt vesicular trafficking of membrane proteins

A role for β -III spectrin in vesicular trafficking was previously proposed based on its ability to interact with Arp1, a subunit of the dynactin complex, and copurify with dynein and dynactin from rat brain vesicles (Holleran et al., 2001). Dynactin is a multi-subunit complex that binds to the microtubule motor dynein (Karki and Holzbaur, 1995; Vaughan and Vallee, 1995) and so by also binding spectrin it forms a link between the spectrin coat of transport vesicles and the motor (Presley et al., 1997; Holleran et al., 1998; Holleran et al., 2001; Muresan et al., 2001). Work with *Drosophila* confirms a role for β spectrin in protein trafficking as knockdown by RNAi treatment disrupted the subcellular localization of a number of synaptic proteins and resulted in the accumulation of axonal cargoes (Featherstone et al., 2001; Pielage et al., 2005, 2006; Lorenzo et al., 2010). In addition, a role in vesicular transport is suggested by the ultrastructural analysis of Purkinje cells lacking β -III spectrin where a large number of vesicles are observed surrounding the Golgi cisternae (Perkins et al., 2010).

There is also evidence from work with *Drosophila* to indicate that two mutations associated with SCA5 (Δ 39 bp and L253P) disrupt vesicle transport. Live imaging of larval axons shows a disruption to vesicle movement when human β -III spectrin harbouring one or other of these mutations is overexpressed (Lorenzo et al., 2010). Furthermore their work in *Drosophila* indicated a link between defects in the dynein-dynactin complex and SCA5 pathogenesis (Lorenzo et al., 2010). When flies overexpressing human β -III spectrin harbouring the Δ 39 bp mutation were crossed with either a hypomorphic dynein heavy chain allele or a dominant mutation in the p150^{Glued} subunit of dynactin the larvae displayed exacerbated posterior paralysis and slowing of vesicle transport, inferring a synergistic effect between spectrin and dynein-dynactin (Lorenzo et al., 2010). Similarly the rough eye phenotype was enhanced in flies overexpressing either the Δ 39 bp or the L253P mutation by the dynein-dynactin mutants (Lorenzo et al., 2010).

Here we directly show that the L253P mutation interferes with the ability of spectrin to interact with Arp1, and therefore highlight how normal vesicular trafficking can be disrupted in some cases of SCA5 due to disrupting the link between vesicles and the microtubule motor dynein. Similar to the study in the SCA1 transgenic mouse, where one interaction of ataxin-1 is lost and another enhanced by the polyQ expansion (Lim et al., 2008), the presence of the L253P mutation has also been shown to result in an enhanced interaction with actin (KA Dick Krueger and LPW Ranum, personal communication). Therefore, a change in protein conformation due to the substitution

of leucine 253 by proline may alter the balance of normal β -III spectrin interactions, enhancing its ability to bind actin and reducing its ability to interact with Arp1, resulting in protein trafficking defects.

Importantly, a direct role for dynein in the transport of proteins into dendrites has recently been shown (Kapitein et al., 2010), supporting the findings from this chapter which suggest that interfering with the binding between β -III spectrin and Arp1 could result in defects to protein trafficking within the Purkinje cell dendritic tree of SCA5 patients. Due to Purkinje cells being among the largest neurons in the human CNS (Paley and Chan-Paley, 1974) the trafficking of macromolecules, vesicles and organelles are essential for the maintenance and survival of the elaborate dendritic tree.

Although a similar disease phenotype was observed in *Drosophila* for both the Δ 39 bp and L253P mutations (Lorenzo et al. 2010), an association with the Golgi apparatus was only observed in the present study for the L253P mutant protein. All other mutant forms of β -III spectrin analyzed here were found to possess the same plasma membrane distribution as WT β -III spectrin. Similarly, only β -III spectrin harbouring the L253P mutation was found to be cleaved at the N-terminus, whereas neither the Δ 39 bp nor Δ 15 bp + R634W mutations showed such cleavage, indicating different effects of the mutations on protein structure and function. This

raises the question of what effect do the other mutations have on the normal function of β -III spectrin?

6.3.1.2 Failure of mutant β -III spectrin proteins to stabilize transmembrane proteins

As mentioned previously β -III spectrin is thought to stabilize EAAT4 at the plasma membrane (Jackson et al., 2001) and using total internal reflection fluorescence (TIRF) microscopy Ranum and colleagues have shown the in-frame deletion found in the Lincoln SCA5 pedigree to stabilize EAAT4 at the plasma membrane of HEK cells to a lesser extent than wild-type β -III spectrin (Ikeda et al., 2006). Therefore, the other mutant forms of β -III spectrin, although present at the plasma membrane, may be ineffective at retaining or stabilizing transmembrane proteins at the cell surface. This could be due to the loss of a direct interaction with the transmembrane protein or instead with the adaptor proteins 4.1 and ankyrin that form a membrane skeleton and are essential for the stable cell surface expression of numerous transmembrane proteins (Anderson and Lovrien, 1984; Coleman et al., 2003; Lin et al., 2009). Further studies are required to investigate whether other mutations associated with SCA5 interfere with the binding of β -III spectrin to 4.1, ankyrin and/or other interacting partners.

6.3.4 Conclusions

This chapter clearly identifies an abnormal cellular distribution and loss-of-function for the L253P mutant form of β -III spectrin associated with SCA5, namely the loss of interaction with Arp1 and disruption to protein trafficking. Furthermore as the results from analysis of the heterozygous β -III spectrin deficient mice suggested (refer to chapter 5) this mutation does have has a dominant-negative effect on WT β -III spectrin function, preventing its expression at the plasma membrane. The detrimental effects of other mutations associated with SCA5 still remain elusive and require further investigation.

CHAPTER 7

IDENTIFICATION OF PROTEINS THAT INTERACT WITH THE AMINO TERMINUS OF β -III SPECTRIN

7.1 Background

For over a decade the yeast-two hybrid assay (as described in section 2.8) has identified interacting partners for a large number of different proteins (Chien et al., 1991; Okura et al., 1996; Shen et al., 1996; Coates and Hall, 2003; Nallani and Sullivan, 2005; Park et al., 2009). To shed light on the normal functions of β -III spectrin, especially the region missing from the protein expressed in β -III^{-/-} spectrin mice (Δ 2-6 β III spectrin), an adult rat brain cDNA library was screened using the amino-terminus of β -III spectrin as bait. The two proteins thought to be the most promising candidates, and analysed in more detail, were prosaposin/saposin D and clathrin light chain 1 (CLC1). Prosaposin (PSAP) is the precursor protein for a family of four lysosomal glycoproteins (saposins A, B, C and D) (Vielhaber et al., 1996) and strong evidence to support the further analysis of prosaposin/saposin D comes from a paper by Matsuda et al., (2004) where a saposin D KO mouse was shown to develop ataxia and dramatic Purkinje cell loss. With respect to CLC1 and clathrin's well-documented involvement in vesicle trafficking (Brodsky et al., 1991; Kirchhausen, 2000; Brodsky et al., 2001; Fotin et al., 2004; Robinson, 2004; Poupon et al., 2008), it too was considered suitable for further study due to the postulated role of β -III spectrin in protein trafficking (refer to chapter 6).

CHAPTER 7 IDENTIFICATION OF PROTEINS THAT INTERACT WITH THE AMINO TERMINUS OF β -III SPECTRIN

7.2 Results

7.2.1 Yeast two-hybrid assay

Exons 1 to 7 of rat β -III spectrin (amino acid residues 1-295) were used as bait and were amplified by PCR using primers that introduced *Eco* RI restriction sites (see appendix 1). Protein extracts were obtained from yeast strain Y190 transformed with the bait construct pGBKT7- β -IIIInt295 and expression of the fusion protein (~ 56kDa) confirmed by Western blot analysis (Figure 7.1).

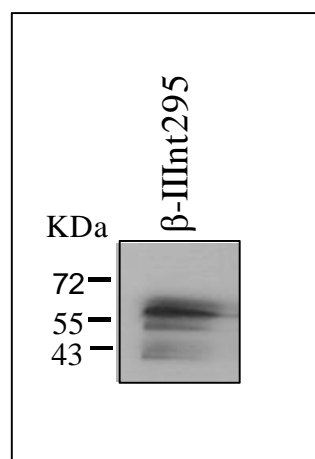


Figure 7.1 Expression of amino-terminus β -III spectrin fusion protein used as bait in yeast two-hybrid screen. Protein extract from Y190 cells transformed with bait construct (pGBKT7- β -IIIInt295) resolved by SDS-PAGE and probed with anti-c-myc antibody. Size of protein markers shown on the left.

In the yeast two-hybrid screen, protein interactions were detected by the ability of transformed yeast to grow on dropout media and by blue colouration of yeast colonies in the presence of 5-bromo-4-chloro-3-indolyl- β -D-galactopyranoside. Of the 210 clones that grew on dropout media, 60 turned blue. Plasmid DNA was rescued from all sixty positive clones and sequencing of 21 revealed the majority to

CHAPTER 7 IDENTIFICATION OF PROTEINS THAT INTERACT WITH THE AMINO TERMINUS OF β -III SPECTRIN

be false positives, containing inserts that were either out-of-frame or were part of untranslated regions (Table 7.1). Of the plasmids sequenced the potential clones of interest were clathrin light chain 1 (Genbank Accession number NM 031974) and the last 79 amino acids of prosaposin (Genbank Accession number NM 002778) (Figure 7.2). Although an interaction between Arp1 and the amino-terminus of β -III spectrin was first reported in yeast (Holleran et al., 2001) and an interaction was observed in the BiFC assay (refer to chapter 6), no clone encoding Arp1 was evident in the present yeast two-hybrid screen.

CHAPTER 7 IDENTIFICATION OF PROTEINS THAT INTERACT WITH THE
AMINO TERMINUS OF β -III SPECTRIN

Table 7.1 Sequence results of clones detected with the yeast-two hybrid screen

pACT clone	Insert Size (bp)	Sequence
3	138	guanylate kinase (out of frame)
8	427	Enolase
30	201	transmembrane protein 151 cDNA (out of frame)
34	20	ribosomal protein S27a (out of frame)
37	24	cytochrome oxidase (out of frame)
43	206	tumour protein (out of frame)
44	146	3' UTR of predicted apoptosis-associated tyrosine kinase
78	203	5' UTR of neurogranin
85	29	3' UTR of mKIAA0128
86	200	3' UTR of epsin 2
93	383	3' UTR of microtubule associated protein
97	833	clathrin light chain 1
125	98	5' UTR of mitochondrial ribosomal protein L55
130	98	5' UTR of predicted mitochondrial ribosomal protein L55
149	38	ATPase (out of frame)
166	170	3' UTR of discs, large homolog 2 (Drosophila)
170	17	3' UTR of metallothionein 3
181	131	protein similar to TNF intracellular domain-interacting protein (out of frame)
186	530	zinc finger protein RP-8 (out of frame)
199	272	prosaposin/saposin D
210	26	procollagen, type 1, alpha 1 (out of frame)

UTR – untranslated region

CHAPTER 7 IDENTIFICATION OF PROTEINS THAT INTERACT WITH THE AMINO TERMINUS OF β -III SPECTRIN

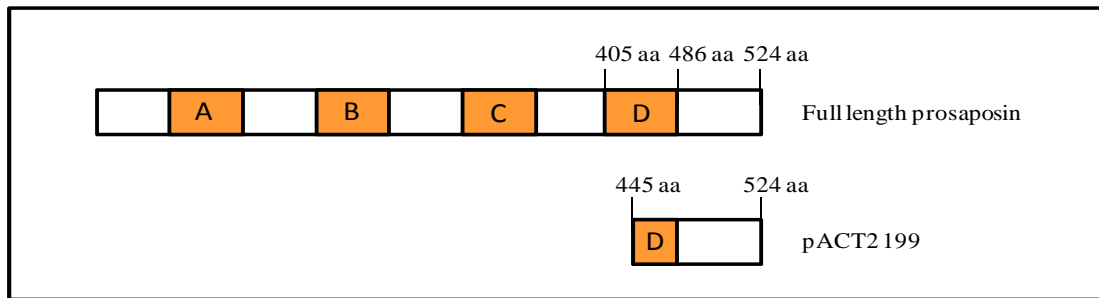


Figure 7.2 Carboxy terminus of prosaposin/saposin D. A schematic representation of full length prosaposin and the carboxy terminus of prosaposin/saposin D pulled out in the yeast two-hybrid assay. aa, amino acid.

7.2.1.1 Carboxy-terminus of prosaposin/saposin D interacts with β -III spectrin in yeast

An interaction between the amino-terminus of β -III spectrin and the carboxy-terminus of prosaposin/saposin D was confirmed by measuring β -galactosidase activity in yeast retransformed with the rescued plasmid pACT-199 and pGBKT7- β -IIIInt295 (COOH-prosaposin and β -IIIInt295 in Figure 7.2A). Activity was found to be substantially higher than when pGADT7-T and pGBKT-53 were transformed, these being control prey and bait constructs, respectively. Even higher β -galactosidase activity levels were obtained when a larger bait protein (β -IIIInt851; amino acids 1-851), similar to that used by Holleran et al., (2001) was used in the assay. In contrast, no β -galactosidase activity above control levels was observed when full length Arp1 was coexpressed with the larger bait protein (Figure 7.3A), although Western blot analysis confirmed expression of full length Arp1 (Figure 7.3B).

CHAPTER 7 IDENTIFICATION OF PROTEINS THAT INTERACT WITH THE AMINO TERMINUS OF β -III SPECTRIN

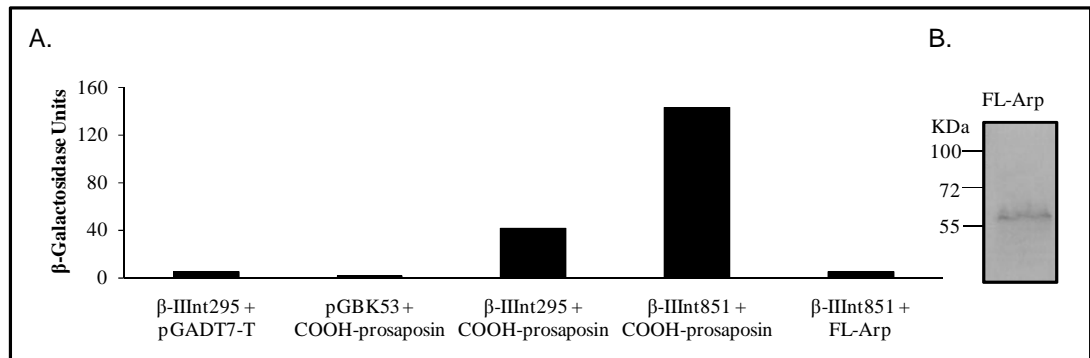


Figure 7.3 Carboxy-terminus of prosaposin/saposin D interacts with amino-terminus β -III spectrin in yeast. (A) β -galactosidase activity of yeast expressing GAL4 (BD) – β IIIInt295 or GAL4 (BD) – β IIIInt851 and GAL4 (AD) - COOH – prosaposin quantified using OPNG liquid assay. Activity of control bait (pGBKT-53), control prey (pGADT7-T) and full length (FL) Arp1, a protein previously reported to interact with β -IIIInt851, also measured. **(B)** Protein extract prepared from yeast transformed with GAL4 (AD) – Arp1, analysed by SDS-PAGE and immunoblotted with anti-HA antibody.

7.2.1.2 Region of β -III spectrin required for interaction narrowed down to exon

7

Additional bait proteins (exons 1-5 (β IIIInt219), exons 1-6 (β IIIInt258), exon 6 – amino acid 851 (β III220-851) and exon 7 – amino acid 851 β -III spectrin (β III259-851)) were generated (refer to section 2.8.6) to narrow down the region of β -III spectrin that interacted with carboxy terminus of prosaposin/saposin D (Figure 7.4A). Western blot analysis of yeast extracts confirmed all bait and prey proteins were expressed and migrated according to their predicted molecular weights (refer to appendix 2) (Figure 7.4B). Bait proteins were fused to the myc-tagged GAL4 DNA binding domain (19kDa) whereas prey proteins were fused to the HA-tagged GAL4 activation domain (15 kDa).

CHAPTER 7 IDENTIFICATION OF PROTEINS THAT INTERACT WITH THE AMINO TERMINUS OF β -III SPECTRIN

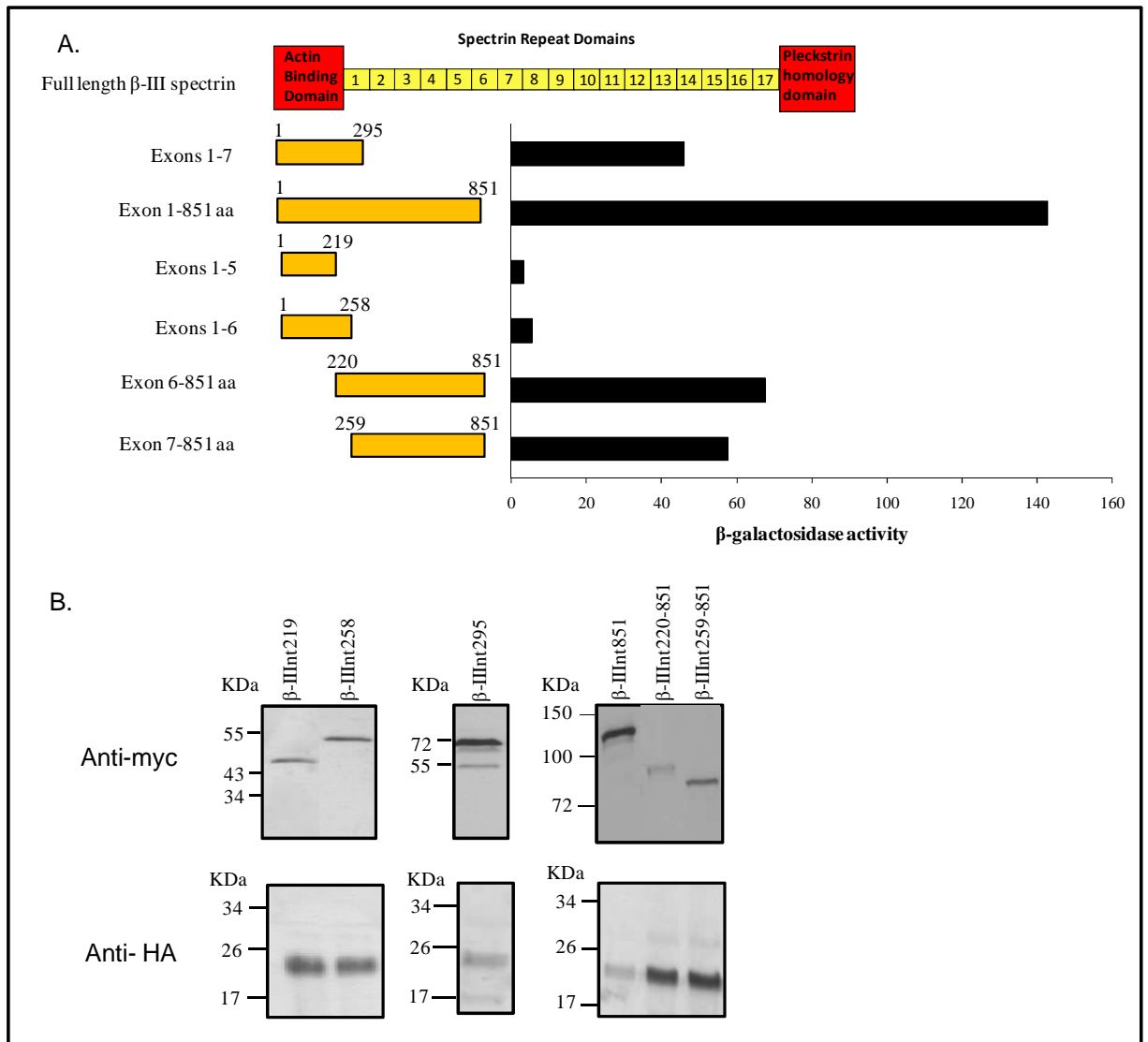


Figure 7.4 Interaction with carboxy-terminus prosaposin/saposin D requires β -III spectrin exon 7. (A) Left, Schematic representation of bait proteins used to narrow down region of interaction. Right, Quantification of β -galactosidase activity using OPNG liquid assay. (B) Protein extracts from transformed yeast resolved by SDS-PAGE and immunoblotted with antibodies against myc-epitope (bait) and HA-epitope (prey).

CHAPTER 7 IDENTIFICATION OF PROTEINS THAT INTERACT WITH THE AMINO TERMINUS OF β -III SPECTRIN

7.2.2 Bimolecular fluorescence complementation (BiFC) assay

7.2.2.1 Prosaposin/saposin D and the amino-terminus β -III spectrin interact in mammalian cells

Bimolecular fluorescence complementation (BiFC) assay is a technique that allows the direct visualisation of protein interactions within mammalian cells (Hu et al., 2002) and was utilised to confirm the protein interactions identified in the yeast-two hybrid screen. The technique is based on the generation of a fluorescent signal when the two halves (YN, amino acids 1-154 and YC, amino acids 155-234) of enhanced yellow fluorescent protein (YFP) are brought together, mediated by the association of two interacting partners fused to YN and YC (Figure 7.5A). Individually the two halves do not emit fluorescence.

CHAPTER 7 IDENTIFICATION OF PROTEINS THAT INTERACT WITH THE AMINO TERMINUS OF β -III SPECTRIN

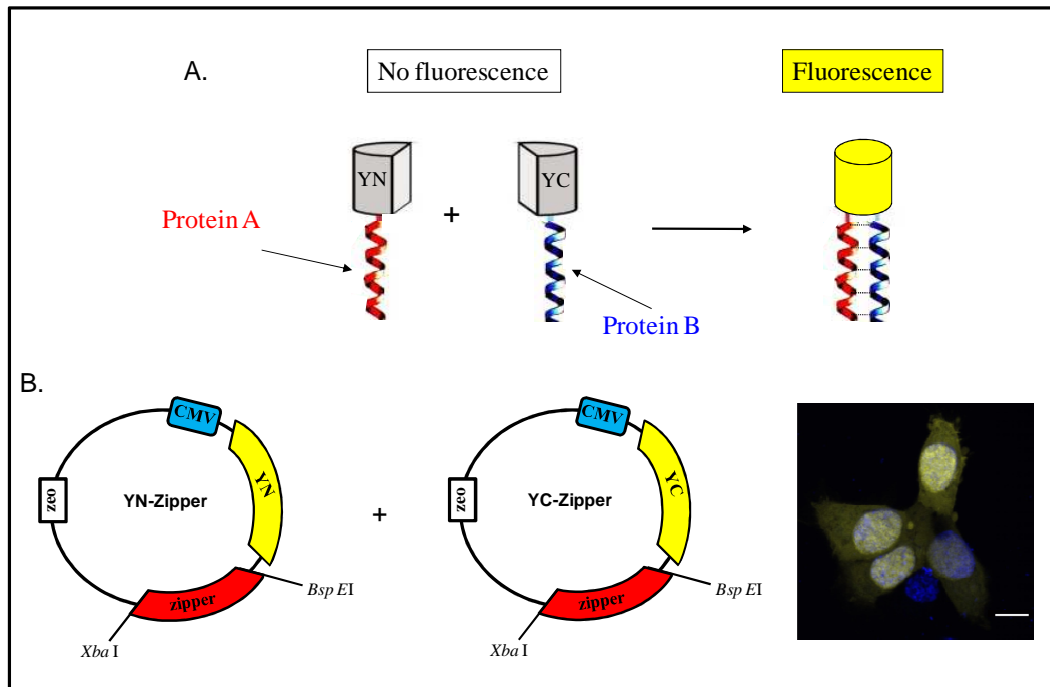


Figure 7.5 Bimolecular fluorescence complementation assay. (A) Schematic diagram showing principle of BiFC (adapted from Hu et al., 2002). (B) Left, Diagrammatical representation of positive control vectors with leucine-zippers as cloned inserts. Right, Confocal immunofluorescence image of HEK 293T cells transfected with positive control vectors. Nucleus stained with DAPI (blue). Bar, 10 μ m.

cDNAs encoding proteins of interest were amplified by PCR to introduce either *Not* I – *Cla* I or *Bsp* EI and *Xba* I restriction sites (refer to appendix 1) and cloned upstream or downstream of the YFP fragments, respectively replacing the positive control leucine zipper inserts (Figure 7.5B). HEK 293T cells were transfected with four vector combinations:

- 1) YN-prosaposin + YC- β III295
- 2) prosaposin-YN + β III295-YC
- 3) prosaposin-YN + YC- β III295

CHAPTER 7 IDENTIFICATION OF PROTEINS THAT INTERACT WITH THE AMINO TERMINUS OF β -III SPECTRIN

4) YN-prosaposin + β III295-YC

When prosaposin and β -III295 (exons 1-7) were cloned downstream of the YFP fragments, fluorescence was observed throughout the cytoplasm (Figure 7.6A). However, no fluorescence was seen with any other vector combination (Figure 7.6A) even though all fusion proteins were expressed. The expression of full length β -III spectrin cloned upstream or downstream of YC (Figure 7.7A) also failed to yield a fluorescent signal despite the proteins being expressed (Figure 7.7B).

CHAPTER 7 IDENTIFICATION OF PROTEINS THAT INTERACT WITH THE AMINO TERMINUS OF β -III SPECTRIN

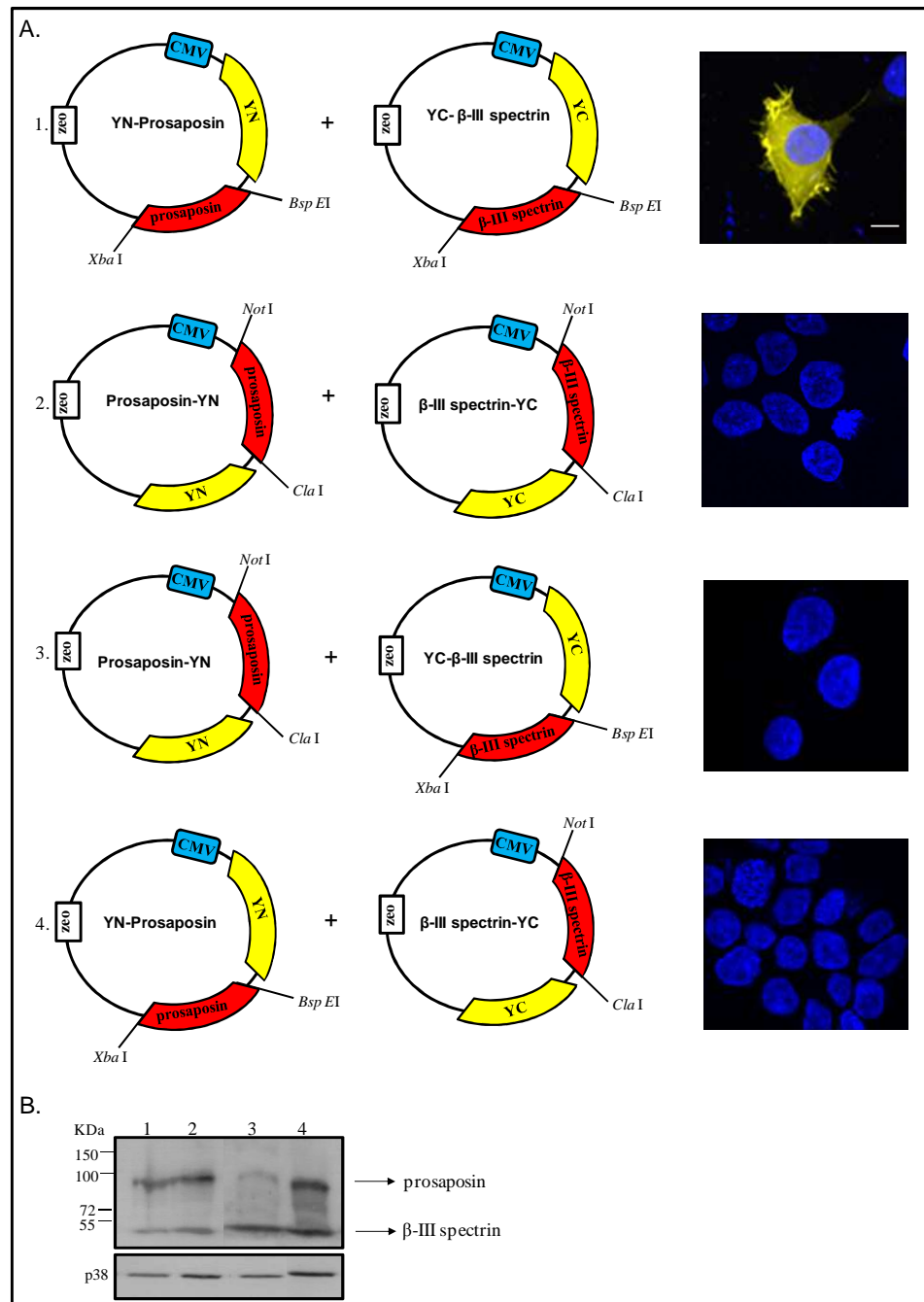


Figure 7.6 BiFC assay shows amino-terminus of β -III spectrin and prosaposin interact in mammalian cells. (A). Left, Schematic representation of the four vector combinations. Right, Confocal immunofluorescence images of representative HEK 293T cells transfected with plasmid combinations shown on left. Nucleus stained with DAPI (blue). Bar, 10 μ m. **(B)** Total HEK 293T cell homogenates from the four different vector combinations resolved by SDS-PAGE and immunoblotted using either anti-GFP antibody that recognises both carboxy- and amino-terminus of YFP (top panel, fusion proteins indicated) or anti-p38 antibody for protein loading control (bottom panel).

CHAPTER 7 IDENTIFICATION OF PROTEINS THAT INTERACT WITH THE AMINO TERMINUS OF β -III SPECTRIN

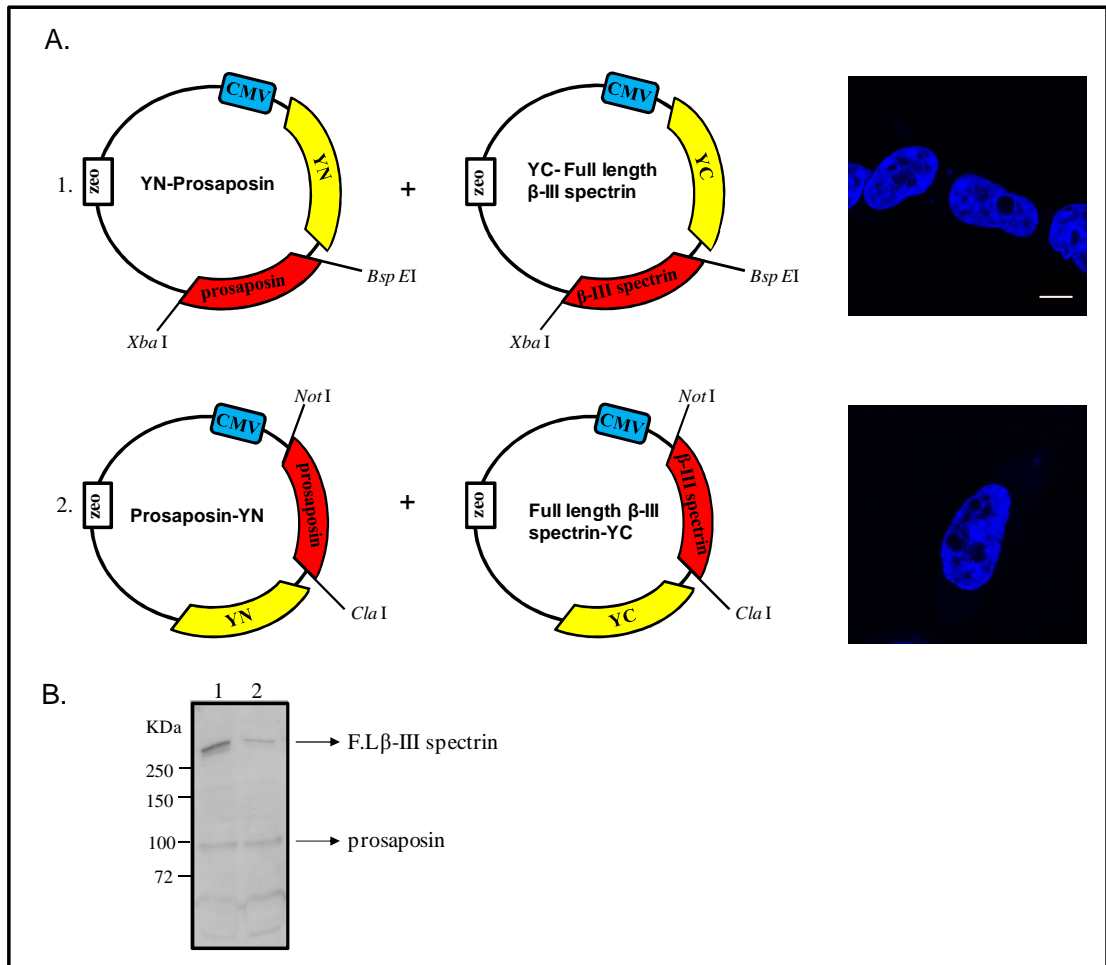


Figure 7.7 No interaction observed between full-length β -III spectrin and prosaposin in BiFC assay. (A) Left, Schematic representation of the two vector combinations used to transfect HEK 293T cells. Right, Confocal immunofluorescence images of representative cells. Nucleus stained with DAPI (blue). Bar, 10 μ m. (B) Total HEK 293T cell homogenates from the two vector combinations resolved by SDS-PAGE and immunoblotted using anti-GFP antibody that recognises both carboxy- and amino- terminus of YFP (fusion proteins indicated).

CHAPTER 7 IDENTIFICATION OF PROTEINS THAT INTERACT WITH THE AMINO TERMINUS OF β -III SPECTRIN

7.2.2.2 β -III spectrin exon 7 required for protein trafficking from Golgi apparatus

In addition to exons 1-7 of β -III spectrin, exons 1-5 (β -III219), exons 1-6 (β -III258), and L253P exon1-7 β -III spectrin were cloned downstream of YC, the configuration of the exon 1-7 construct shown to elicit an interaction with prosaposin (vector combination 1 in Figure 7.6A). The missense mutation L253P β -III spectrin was introduced into the exon 1-7 construct of β -III spectrin by site-directed mutagenesis (refer to section 2.2.4). Co-expression of these new YC- β -III spectrin constructs with prosaposin resulted in an altered pattern of fluorescence, compared to YC-exon 1-7. The fluorescent signal was no longer observed throughout the cytoplasm but instead overlapped with a Golgi marker (Figure 7.8A). Western blot analysis revealed all proteins migrated at their predicted molecular weights (refer to appendix 2) (Figure 7.8B).

7.2.2.3 Interaction between amino terminus β -III spectrin and Arp1 in mammalian cells

In contrast to the yeast experiments (Figure 7.3A) an interaction between Arp1 and the amino terminus of β -III spectrin was detected in mammalian cells using the BiFC assay, but not with all vector combinations (Figure 7.9A,B and refer to Chapter 6). Similar to the studies with prosaposin (Figure 7.8) the fluorescent signal was observed associated with the Golgi apparatus when exons 1-5 and exons 1-6 of β -III spectrin were coexpressed with Arp1 (Figure 7.10A). In contrast no fluorescence was

CHAPTER 7 IDENTIFICATION OF PROTEINS THAT INTERACT WITH THE AMINO TERMINUS OF β -III SPECTRIN

observed when L253P exon 1-7 was expressed along with Arp1 (refer to Chapter 6 Figure 6.13). Protein expression for all constructs was confirmed by Western blot analysis and all proteins migrated according to their predicted molecular weights (refer to appendix 2) (Figures 6.13B and 7.10B).

CHAPTER 7 IDENTIFICATION OF PROTEINS THAT INTERACT WITH THE AMINO TERMINUS OF β -III SPECTRIN

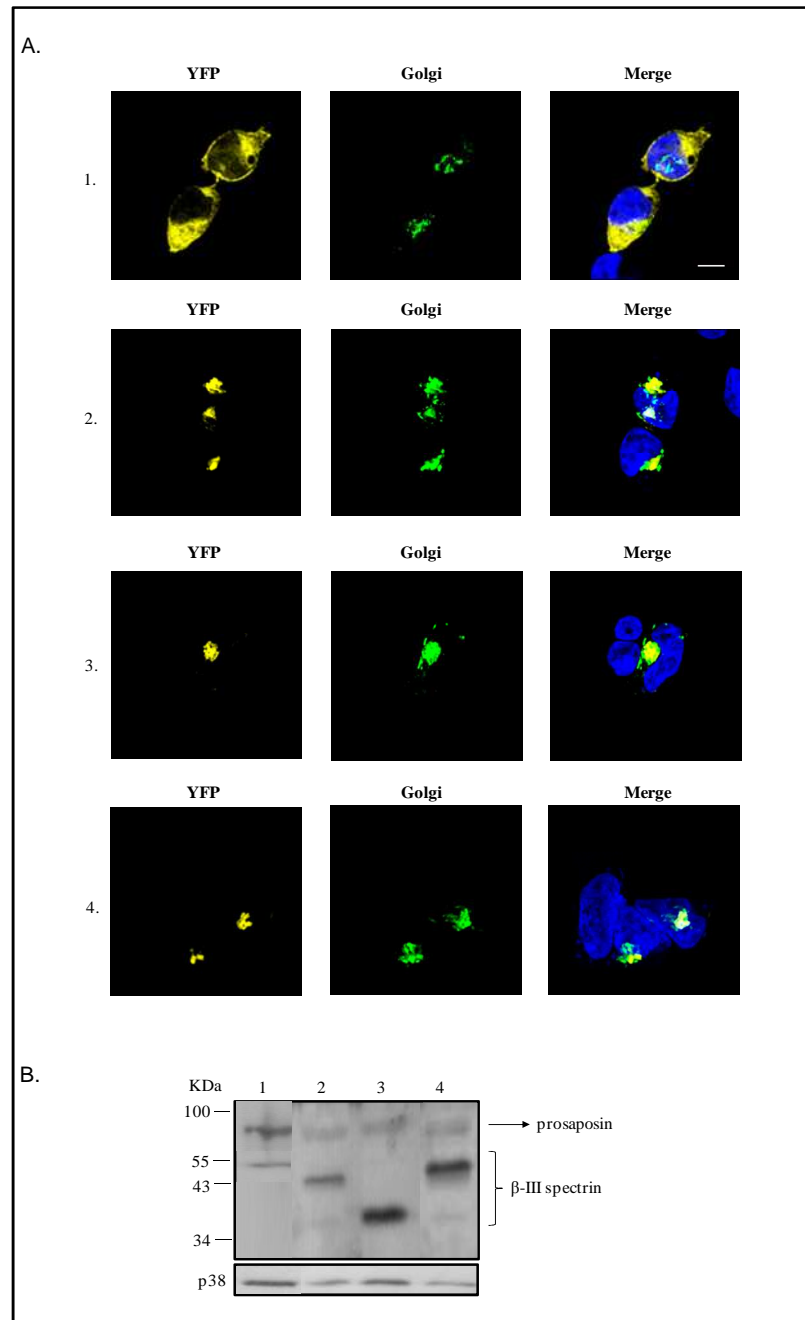


Figure 7.8 Golgi associated fluorescence when β -III spectrin exon 7 missing or mutated. **(A)** Confocal immunofluorescence images of representative HEK 293T cells co-transfected with YN-Prosaposin and either YC- β -III295 **(1)**, YC- β -III258 **(2)**, YC- β -III219 **(3)** or L253P YC β -III295 **(4)**. YFP fluorescence (yellow), Golgi marker (green) and nucleus stained with DAPI (blue). Bar, 10 μ m. **(B)** Total HEK 293T cell homogenates from the four different vector combinations resolved by SDS-PAGE and immunoblotted using either anti-GFP antibody that recognises both carboxy- and amino-terminus of YFP (top panel, fusion proteins indicated) or anti-p38 antibody for protein loading control (bottom panel).

CHAPTER 7 IDENTIFICATION OF PROTEINS THAT INTERACT WITH THE AMINO TERMINUS OF β -III SPECTRIN

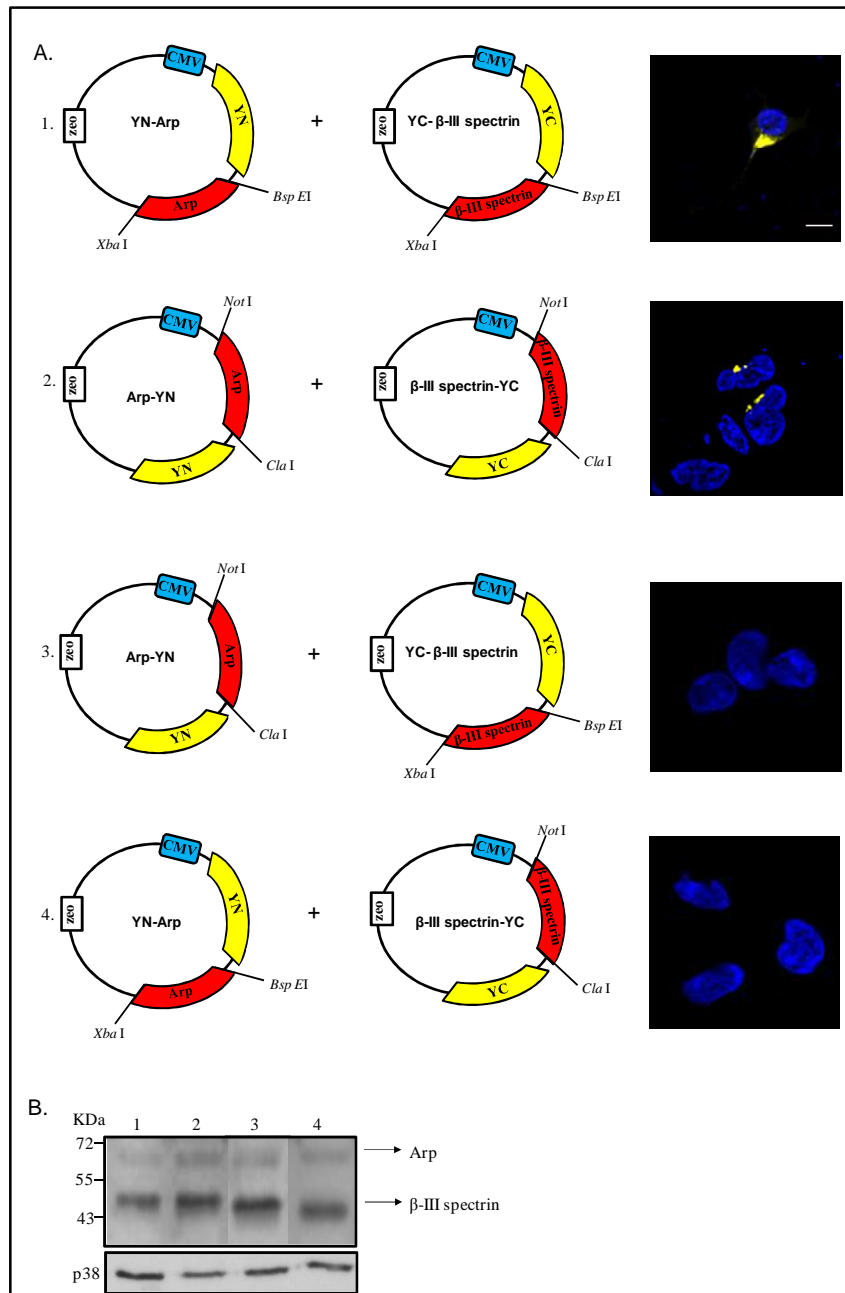


Figure 7.9 Interaction of Arp1 with amino-terminus of β -III spectrin in mammalian cells using BiFC assay. (A) Left, Schematic representation of the four vector combinations used to transfect HEK 293T cells. Right, Confocal immunofluorescence images of representative HEK 293T cells transfected with plasmid combinations shown on left. Nucleus stained with DAPI (blue). Bar, 10 μ m. **(B)** Total HEK 293T cell homogenates from the four different vector combinations resolved by SDS-PAGE and immunoblotted using either anti-GFP antibody that recognises both carboxy- and amino-terminus of YFP (top panel, fusion proteins indicated) or anti-p38 antibody for protein loading control (bottom panel).

CHAPTER 7 IDENTIFICATION OF PROTEINS THAT INTERACT WITH THE AMINO TERMINUS OF β -III SPECTRIN

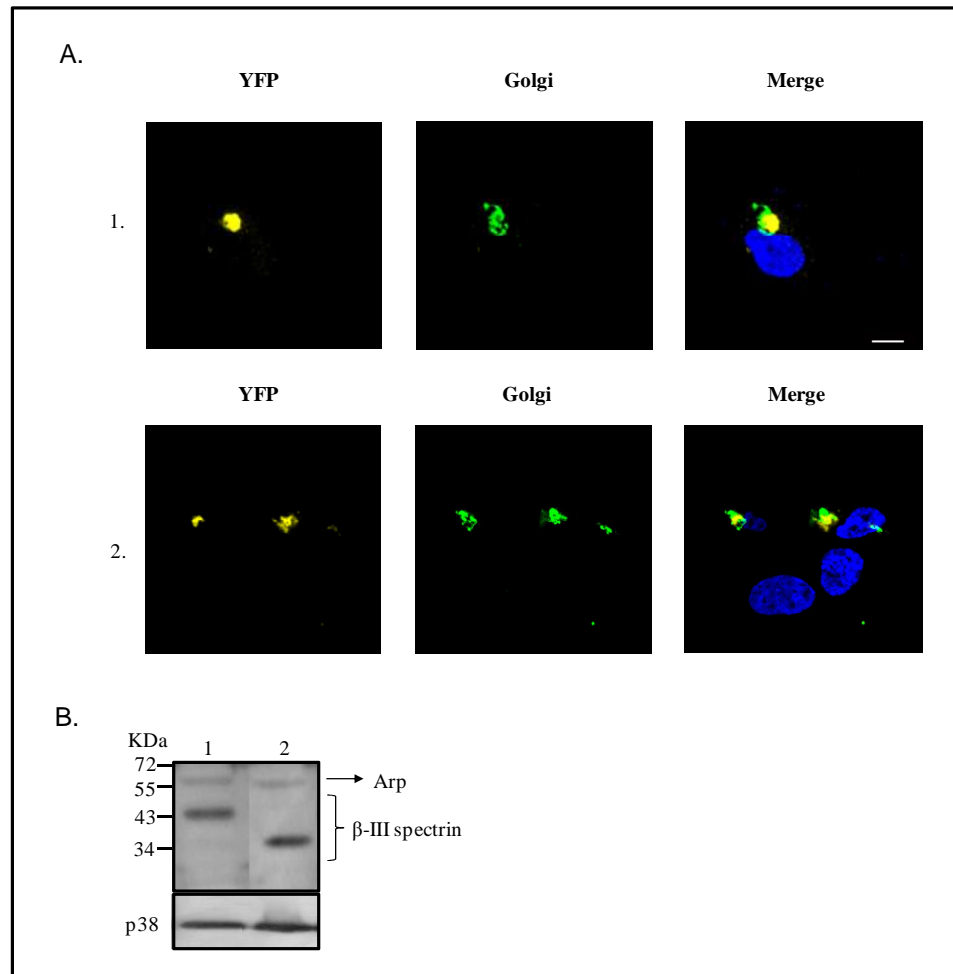


Figure 7.10 Loss of exon 7 results in Golgi associated fluorescence with Arp1 and β -III spectrin . (A) Confocal immunofluorescence images of representative HEK 293T cells co-transfected with YN-Arp and either YC- β -III258 (**1**) or YC- β -III219 (**2**). YFP fluorescence (yellow), Golgi marker (green) and nucleus stained with DAPI (blue). Bar, 10 μ m. **(B)** Total HEK 293T cell homogenates from the two vector combinations resolved by SDS-PAGE and immunoblotted using either anti-GFP antibody that recognises both carboxy- and amino-terminus of YFP (top panel, fusion proteins indicated) or anti-p38 antibody for protein loading control (bottom panel).

7.2.3 Interaction of β -III spectrin and prosaposin/saposin D *in vivo*

Having confirmed the interaction of prosaposin/saposin D with the amino terminus of β -III spectrin in both yeast and mammalian cells the next step was to examine whether the proteins interacted *in vivo*. Cerebellar mouse homogenates were

CHAPTER 7 IDENTIFICATION OF PROTEINS THAT INTERACT WITH THE AMINO TERMINUS OF β -III SPECTRIN

incubated with either rabbit anti-saposin D or control rabbit IgG. After pelleting the antibody-protein complex with protein A sepharose, Western blot analysis confirmed the coimmunoprecipitation of β -III spectrin with anti-saposin D antibody but not the control IgG (Figure 7.11).

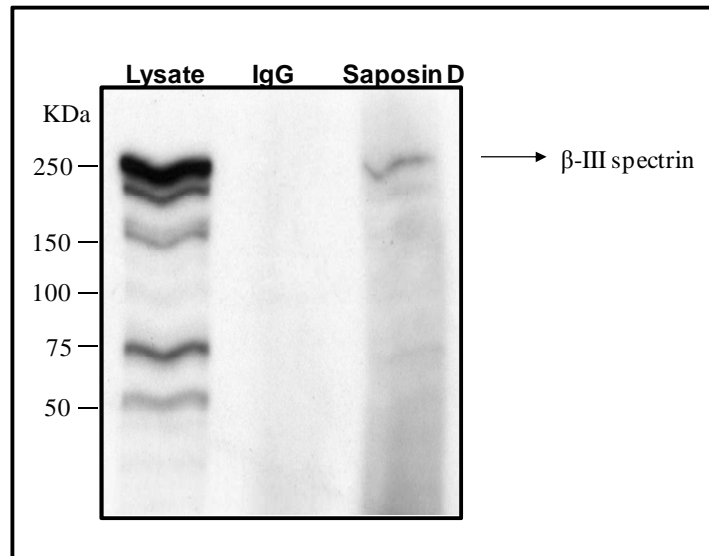


Figure 7.11 β -III spectrin interacts with carboxy-terminus prosaposin/saposin D *in vivo*. Mouse cerebellar homogenates immunoprecipitated with antibodies against saposin D and control rabbit IgG. The resulting precipitates and lysates resolved by SDS-PAGE and subjected to immunoblot analysis with antibodies against β -III spectrin.

7.2.4 Expression of prosaposin/saposin D reduced in Purkinje cells of β -III^{-/-} spectrin mice

The previously reported expression of prosaposin in Purkinje cells (Kreda et al., 1994; Sun et al., 1994) was confirmed by staining cerebellar sections with antibodies against the carboxy-terminus of prosaposin/saposin D, calbindin D28K, a Purkinje cell specific marker, and glial fibrillary acidic protein (GFAP), an astroglial marker

CHAPTER 7 IDENTIFICATION OF PROTEINS THAT INTERACT WITH THE AMINO TERMINUS OF β -III SPECTRIN

(Figure 7.12). Prosaposin/saposin D was found around the membrane of Purkinje cell somas and throughout the dendritic tree. Immunostaining of cerebellar sections from young (3-week-old) β -III^{-/-} spectrin mice revealed that although saposin D/prosaposin was still located within the cell body and dendritic tree of Purkinje cells, the intensity of staining was reduced (Figure 7.13).

To quantify the total cerebellar levels of prosaposin/saposin D in WT and β -III^{-/-} spectrin mice Western blot analysis was performed using protein homogenates from young (6-weeks of age) and old (1-year of age) mice (Figure 7.14A). An anti-saposin D antibody, kindly donated by Ying Sun, detected both saposin D (~10 kDa) and prosaposin (~72 kDa). Quantification of levels by densitometry, normalized to actin, revealed that at 6-weeks and 1-year of age the levels of saposin D and prosaposin in β -III^{-/-} spectrin mice were not significantly different to their WT littermates (6 weeks, saposin D 91 ± 7.9 %; prosaposin 103.8 ± 9.0 % of WT levels; 1 year, saposin D 88.3 ± 12.3 %; prosaposin 83.5 ± 6.6 % of WT levels; Figure 7.14B). There was also no significant difference in the expression ratios of saposin D to prosaposin in WT and β -III^{-/-} spectrin mice at the two ages.

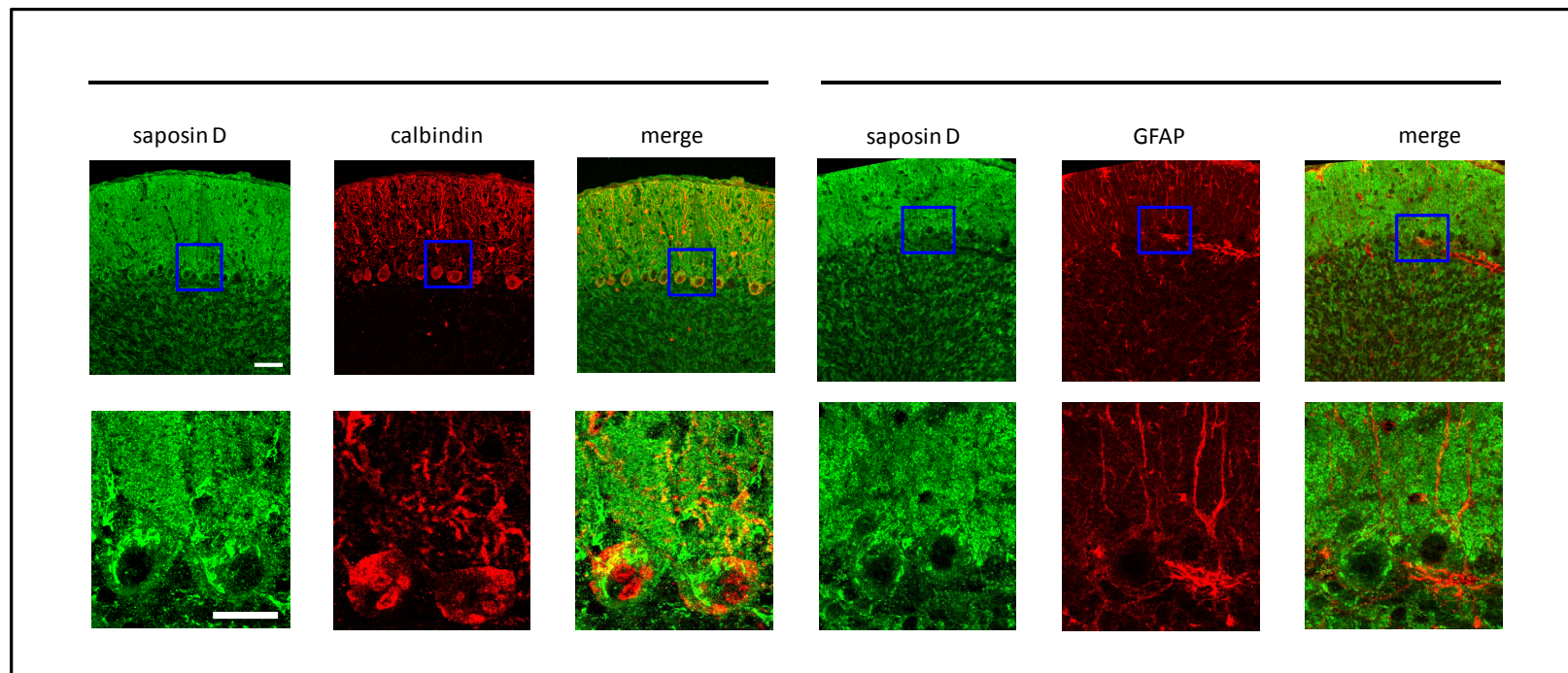


Figure 7.12 Expression pattern of saposin D/prosaposin in cerebellum. Cerebellar folia VI from 3-week old mice immunostained for calbindin (red), GFAP (red) or prosaposin/saposin D (green). Bar, 50 μ m (top panel), 20 μ m (bottom panel).

CHAPTER 7 IDENTIFICATION OF PROTEINS THAT INTERACT WITH THE
AMINO TERMINUS OF β -III SPECTRIN

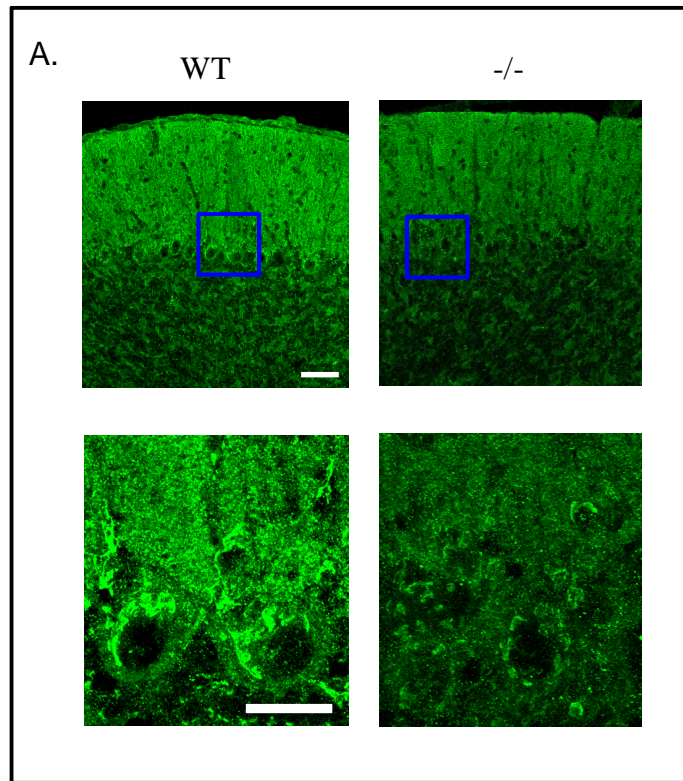


Figure 7.13 Reduced prosaposin/saposin D immunoreactivity in β -III^{-/-} spectrin mice. (A) Cerebellar sections from 3-week old WT and β -III^{-/-} spectrin mice immunostained with anti-COOH-prosaposin/ saposin D antibody (Bar, 50 μ m (top panel) and 20 μ m (bottom panel)).

CHAPTER 7 IDENTIFICATION OF PROTEINS THAT INTERACT WITH THE AMINO TERMINUS OF β -III SPECTRIN

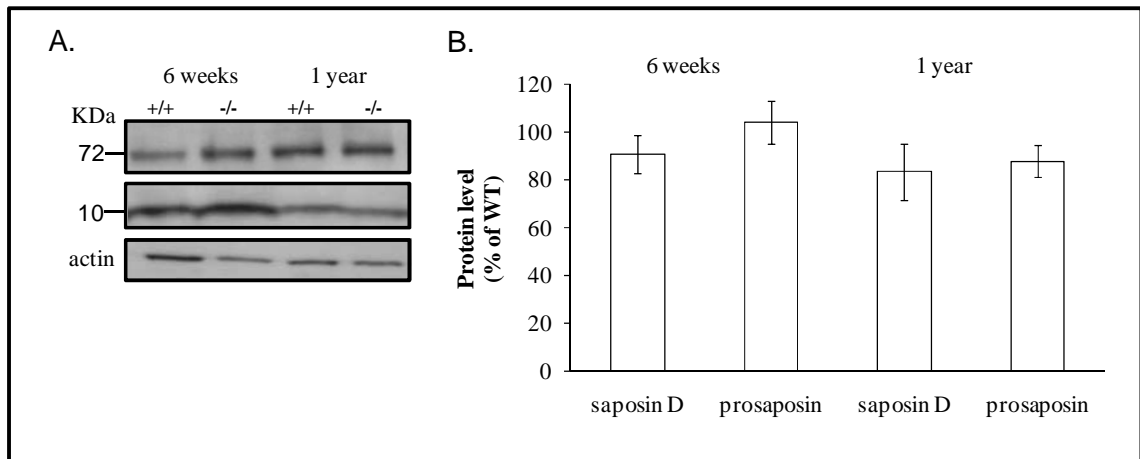


Figure 7.14 No reduction in prosaposin/saposin D expression in β -III^{-/-} spectrin mice at 6-weeks or 1-year. (A) Total cerebellar homogenates from 6-week and 1-year old mice resolved by SDS-PAGE and immunoblotted with antibodies against COOH-prosaposin/saposin D. Actin used as protein loading control. **(B)** Bands corresponding to saposin D and prosaposin quantified by densitometry, normalised against actin and expressed as percentage of WT levels at 6-weeks and 1-year of age. All data are given as means \pm SEM (N = 3 for each genotype).

7.2.5 Normal kidney morphology in β -III^{-/-} spectrin mice

Matsuda et al (2004) revealed that loss of saposin D results in ataxia and Purkinje cell loss but the other finding was that the saposin D^{-/-} mice develop renal tubular degeneration. Western blot analysis confirmed β -III spectrin is expressed in the kidney but at a much lower level compared to cerebellum (Figure 7.15A). To investigate whether β -III^{-/-} spectrin mice developed any kidney pathology, similar to saposin D^{-/-} mice, kidney sections from 1-year-old mice were stained with hematoxylin and eosin (H&E). This revealed the glomeruli were healthy and there was also no sign of renal tubular degeneration in β -III^{+/+} or β -III^{-/-} spectrin mice (Figure 7.15B). Western blot analysis and quantification by densitometry showed no significant difference in levels of saposin D or prosaposin in the kidneys of 6-week-

CHAPTER 7 IDENTIFICATION OF PROTEINS THAT INTERACT WITH THE AMINO TERMINUS OF β -III SPECTRIN

and 1-year-old animals (6 weeks, saposin D 112.3 ± 12 %; prosaposin 108.3 ± 11.3 % of WT levels; 1 year, saposin D 101 ± 15.2 %; prosaposin 104 ± 10.8 % of WT levels; Figure 7.15C,D). There was also no significant difference in the ratios of saposin D to prosaposin in WT and β -III^{-/-} spectrin mice at the two ages.

CHAPTER 7 IDENTIFICATION OF PROTEINS THAT INTERACT WITH THE AMINO TERMINUS OF β -III SPECTRIN

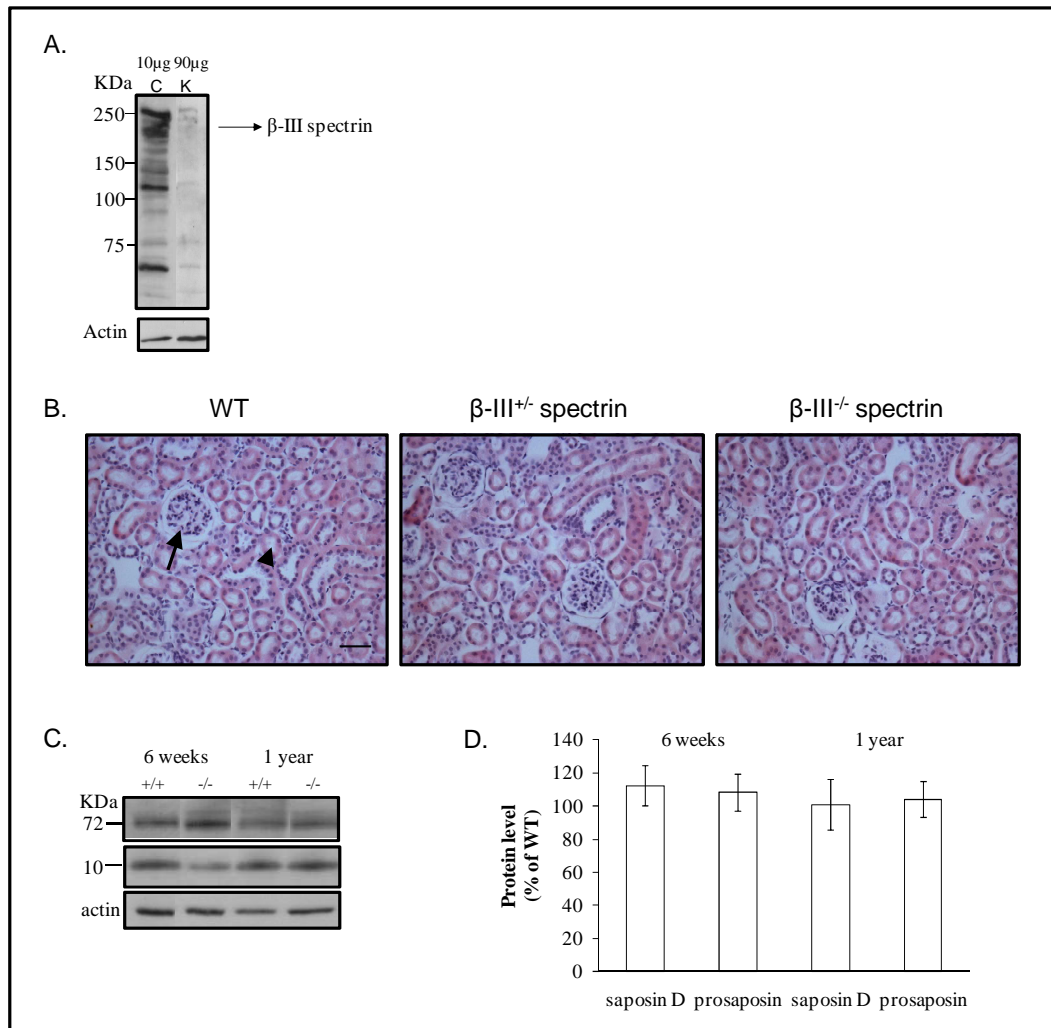


Figure 7.15 No renal pathology observed in β -III^{-/-} spectrin mice. (A) Homogenates from cerebellum (C; 10 μ g) and kidney (K; 90 μ g) resolved by SDS-PAGE and immunoblotted with antibody against β -III spectrin. (B) Sections from kidneys of 1-year-old WT, heterozygous and homozygous β -III spectrin deficient mice stained with H&E. (Arrow, glomeruli; arrowhead, renal tubule; Bar, 50 μ m). (C) Kidney homogenates from 6-week- and 1-year-old mice resolved by SDS-PAGE and immunoblotted with antibodies against COOH-prosaposin/saposin D. Actin used as protein loading control. (D) Bands corresponding to saposin D and prosaposin quantified by densitometry, normalised against actin and expressed as percentage of WT levels. All data are means \pm SEM (N = 3 for each genotype).

7.2.6 Confirmation that clathrin light chain 1 interacts with β -III spectrin

7.2.6.1 Quantification of β -galactosidase activity in retransformed yeast

The other protein identified in the yeast two-hybrid screen that was further investigated was clathrin light chain 1 (CLC1). First the interaction was confirmed by measuring β -galactosidase activity in Y190 cells transformed with the rescued plasmid pACT-97 and pGBKT7- β -IIIInt295 (Figure 7.16A). Then to narrow down the region of interaction other bait constructs were used [exons 1-5 (β IIIInt219), exons 1-6 (β IIIInt258), exon 6 – amino acid 851 (β III220-851) and exon 7 – amino acid 851 β -III spectrin (β III259-851)] (Figure 7.16A). Western blot analysis of yeast extracts confirmed all myc-tagged bait and HA-tagged prey proteins were expressed and migrated according to their predicted molecular weight (Refer to appendix 2)(Figure 7.16B).

To identify which region of CLC1 interacted with exons 1-7 of β -III spectrin, three shorter CLC1 products were generated by Ms Yu Cheng (1 – 374 bp (CLC374), 375 – 746 bp (CLC375-746) and 246 – 500 bp (CLC246-500) (refer to section 2.8.6) (Figure 7.17A). Western blot analysis confirmed that all bait and prey proteins were expressed and migrated according to their predicted molecular weights (Refer to appendix 2) (Figure 7.17B).

CHAPTER 7 IDENTIFICATION OF PROTEINS THAT INTERACT WITH THE AMINO TERMINUS OF β -III SPECTRIN

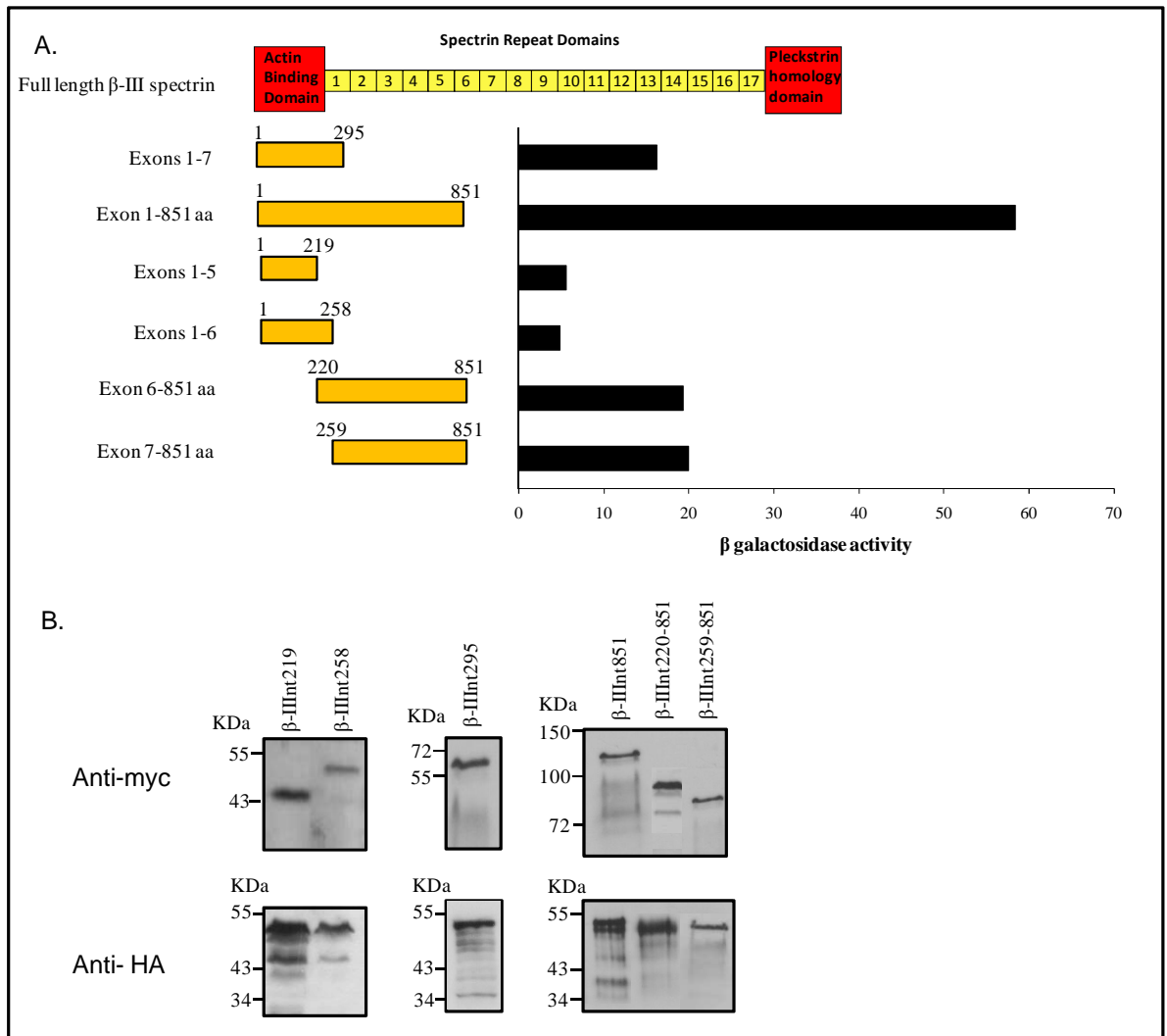


Figure 7.16 Interaction of clathrin light chain with amino terminus β -III spectrin requires exon 7 and downstream protein sequence. (A) β -galactosidase activity of yeast expressing GAL4(AD)-CLC and either GAL4 (BD)- β IIIInt295, GAL4(BD)- β IIIInt851 or deletion GAL4(BD)-baits and quantified using OPNG liquid assay. **(B)** Protein extracts from transformed yeast resolved by SDS-PAGE and immunoblotted with antibodies against myc-epitope (bait) and HA-epitope (prey).

CHAPTER 7 IDENTIFICATION OF PROTEINS THAT INTERACT WITH THE AMINO TERMINUS OF β -III SPECTRIN

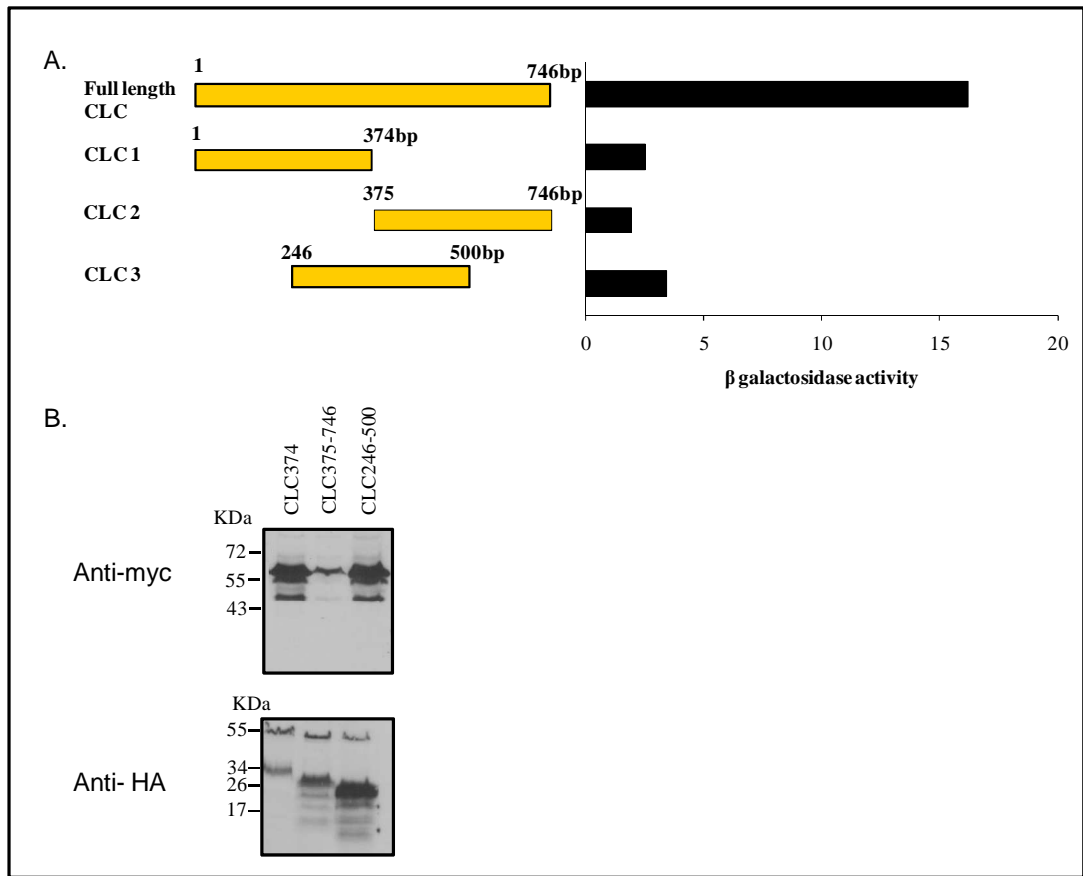


Figure 7.17 Full length clathrin light chain 1 may be important for interaction with amino-terminus β -III spectrin. (A) Schematic representation of prey proteins used to narrow down region of interaction. β -galactosidase activity quantified using OPNG liquid assay. **(B)** Protein extracts from transformed yeast resolved by SDS-PAGE and immunoblotted with antibodies against myc-epitope (bait) and HA-epitope (prey).

7.2.6.2 Interaction between clathrin light chain and amino-terminus β -III spectrin in mammalian cells

An interaction between the amino terminus of β -III spectrin and CLC1 was observed with every vector configuration of the BiFCc assay, although the level of fluorescent signal varied depending on the vector combination (Figure 7.18A). Western blot

CHAPTER 7 IDENTIFICATION OF PROTEINS THAT INTERACT WITH THE AMINO TERMINUS OF β -III SPECTRIN

analysis revealed a lower level of β -III spectrin fusion protein in cells with weaker fluorescence (Figure 7.18B).

The other β -III spectrin constructs (exons 1-5, exons 1-6 and L253P β -III spectrin) were used to determine the effect mutating or losing exon 7 had on the cellular distribution of fluorescent signal (refer to section 7.2.2.2). As before fluorescence was no longer seen throughout the cytoplasm but instead found to overlap with a Golgi marker (Figure 7.19A). Western blot analysis confirmed all proteins were expressed (Figure 7.19B).

CHAPTER 7 IDENTIFICATION OF PROTEINS THAT INTERACT WITH THE AMINO TERMINUS OF β -III SPECTRIN

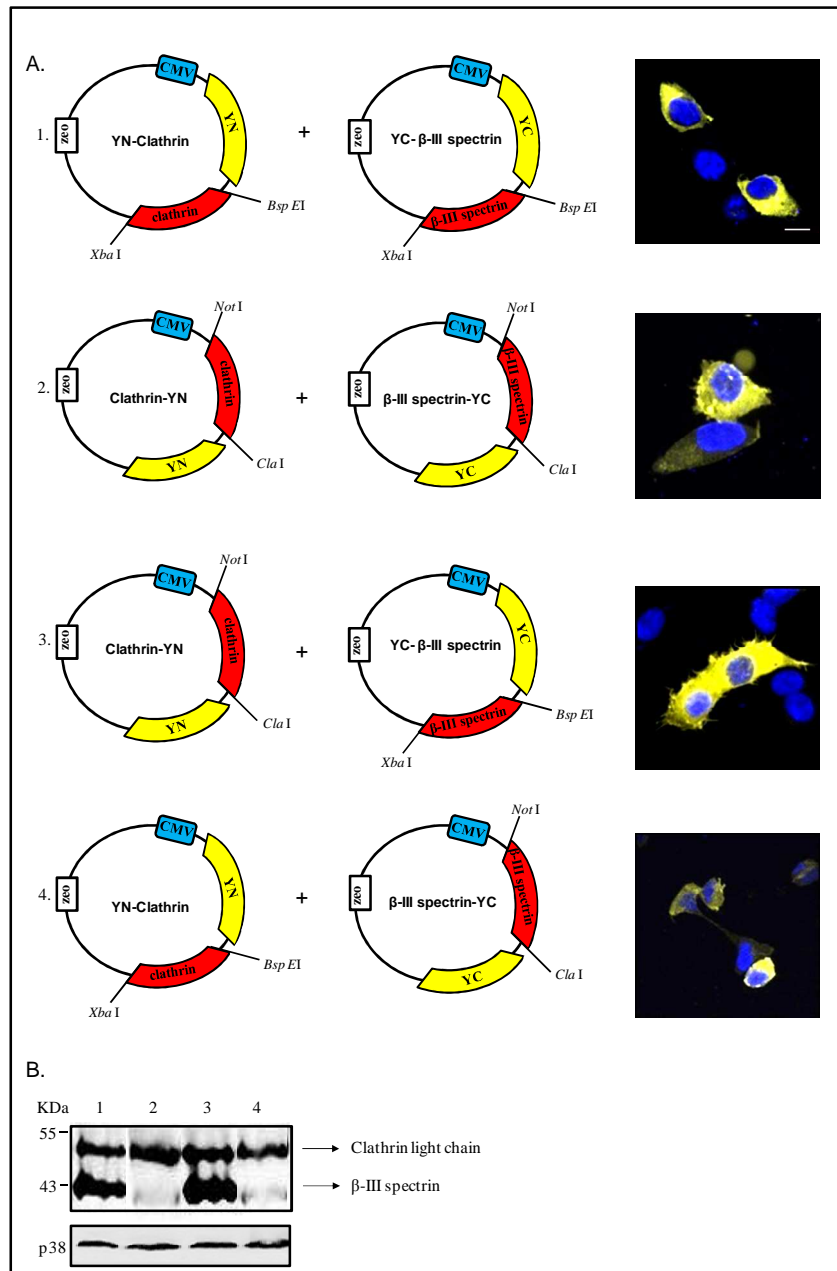


Figure 7.18 β -III spectrin and clathrin light chain 1 interact in mammalian cells using BiFC assay. (A). Left, Schematic representation of the four vector combinations used to transfect HEK 293T cells. Right, Confocal immunofluorescence images of representative HEK 293T cells transfected with plasmid combination shown on left. Nucleus stained with DAPI (blue). Bar, 10 μ m. **(B).** Total HEK 293T cell homogenates from the four different vector combinations resolved by SDS-PAGE and immunoblotted using either anti-GFP antibody that recognises both carboxy- and amino-terminus of YFP (top panel, fusion proteins indicated) or anti-p38 antibody for protein loading control (bottom panel).

CHAPTER 7 IDENTIFICATION OF PROTEINS THAT INTERACT WITH THE AMINO TERMINUS OF β -III SPECTRIN

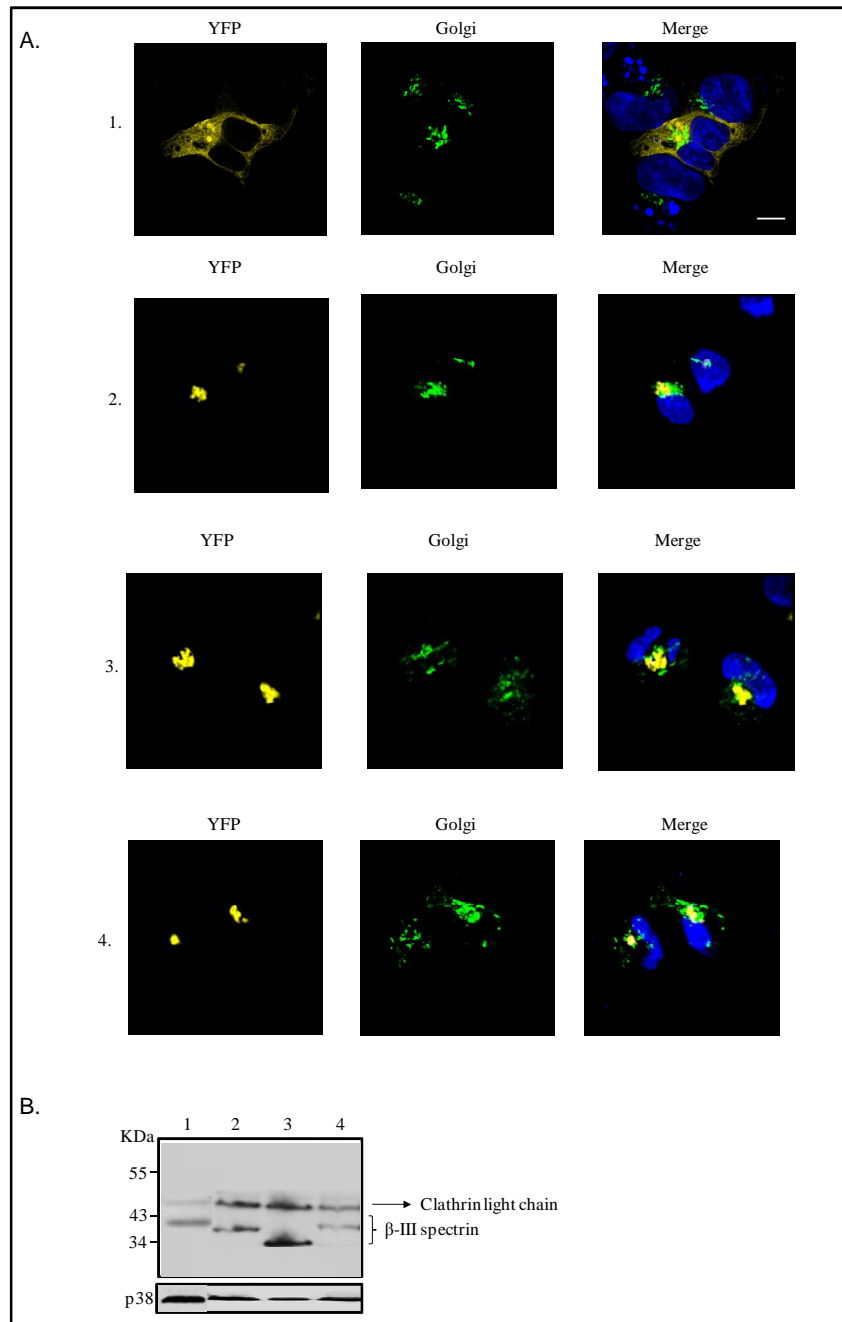


Figure 7.19 Discrete localisation of fluorescence in BiFC assay when β -III spectrin exon 7 is missing or mutated. (A) Confocal immunofluorescence images of representative HEK 293T cells co-transfected with YN-CLC1 and either YC- β -III295 (**1**), YC- β -III258 (**2**), YC- β -III219 (**3**) or L253P YC β -III295 (**4**). YFP fluorescence (yellow), Golgi marker (green) and nucleus stained with DAPI (blue). Bar, 10 μ m. **(B)** Total HEK 293T cell homogenates from the four different vector combinations resolved by SDS-PAGE and immunoblotted using either anti-GFP antibody that recognises both carboxy- and amino-terminus of YFP (top panel, fusion proteins indicated) or anti-p38 antibody for protein loading control (bottom panel).

CHAPTER 7 IDENTIFICATION OF PROTEINS THAT INTERACT WITH THE AMINO TERMINUS OF β -III SPECTRIN

7.3 Discussion

The results of a yeast two-hybrid screen, identifying prosaposin/saposin D and CLC1 as potential interacting partners with the amino-terminus of β -III spectrin, are presented in this chapter, along with cellular and *in vivo* analyses of prosaposin/saposin D. Both interactions (prosaposin/saposin D and CLC1) were confirmed in yeast and mammalian cells, and although a previously reported interaction of β -III spectrin with Arp1 (Holleran et al., 2001) was not detected in the present yeast two-hybrid screen it was observed using the BiFC assay. The reason for the lack, in the present study, of an interaction in yeast is not known, as although the bait used here in the initial screen was shorter compared to that used by Holleran et al. (2001), there was still no β -galactosidase activity observed even when the larger bait (β III-1-851) used by Holleran et al., (2001) was transformed with Arp1. Nevertheless, the results from the yeast two-hybrid and BiFC assays revealed that, for all interactions studied, exon 7 of β -III spectrin was required for β -galactosidase activity and a fluorescent signal throughout the cell, respectively. Deletion of exon 7 resulted in no β -galactosidase activity in yeast, indicating no protein-protein interaction, while the YFP fluorescent signal in the BiFC assay was no longer throughout the cell, but instead was found associated with the Golgi apparatus, suggesting a change to the cellular distribution of the proteins.

It was shown in chapter 6 that the interaction of β -III spectrin with Arp1 was completely lost in the BiFC assay when the missense mutation L253P associated

CHAPTER 7 IDENTIFICATION OF PROTEINS THAT INTERACT WITH THE AMINO TERMINUS OF β -III SPECTRIN

with SCA5 was introduced. In contrast the interaction with prosaposin/saposin D and clathrin light chain was still observed with L253P, but the fluorescent signal was only localised to the Golgi apparatus, similar to the studies when exon 7 was deleted. Taken together the data suggest that the inability of L253P to interact with endogenous Arp1 prevents the normal trafficking from the Golgi apparatus of β -III spectrin and proteins that interact with it. Furthermore, exon 7 appears to be required for movement away from the Golgi apparatus. With regard to the negative results obtained from the yeast two-hybrid assay, which are apparently contradictory to the BiFC assay results, it may be that these arose due to the inability of proteins to reach the nucleus and activate the β -galactosidase reporter gene rather than the complete loss of a protein-protein interaction.

The importance of protein conformation in the BiFC assay was highlighted in this study by the fact that for prosaposin and the amino-terminus of β -III spectrin a fluorescent signal was only observed for one of the four possible fusion protein configurations. Only when both YFP fragments were fused to the amino-termini of the two proteins was a fluorescent signal observed, for all other combinations it would appear the location of the YFP fragments was not optimal for interaction of the two halves. The lack of a fluorescent signal when full-length β -III spectrin was co-expressed with prosaposin is also likely to be due to structural interference due to the large size of β -III spectrin, preventing the two YFP fragments coming into close opposition with one another. In contrast full-length β -III spectrin was shown by

CHAPTER 7 IDENTIFICATION OF PROTEINS THAT INTERACT WITH THE AMINO TERMINUS OF β -III SPECTRIN

coimmunoprecipitation to interact with prosaposin/ saposin D *in vivo*, demonstrating a physiological interaction. However, although there was substantially reduced immunoreactivity of prosaposin/saposin D in Purkinje cells of β -III^{-/-} spectrin mice compared to age-matched littermates, no difference in expression levels was detected by Western blot analysis. Therefore it is still not clear whether there is a loss of saposin D or prosaposin in β -III^{-/-} spectrin mice that could play a role in the observed ataxic phenotype. However, from the fact no abnormal kidney morphology was observed in β -III^{-/-} spectrin mice, unlike saposin D^{-/-} mice which develop renal tubule degeneration and hydronephrosis (Matsuda et al., 2004), it would appear that β -III spectrin is not required for normal kidney morphology.

With respect to CLC1 it appears that full length CLC1 is required for an interaction with β -III spectrin, but due to a lack of both time and reliable antibodies against CLC1, no studies were able to be performed to confirm an interaction between the two proteins *in vivo*.

7.3.1 Role for saposin D loss in Purkinje cell degeneration

Prosaposin is the precursor of four sphingolipid activator proteins (saposins A, B, C and D, all about 80 amino acids), which are required for the hydrolysis of a variety of sphingolipids (O'Brien and Kishimoto, 1991; Kishimoto et al., 1992). Each saposin on its own is catalytically inactive but they interact with a specific glycosphingolipid

CHAPTER 7 IDENTIFICATION OF PROTEINS THAT INTERACT WITH THE AMINO TERMINUS OF β -III SPECTRIN

hydrolase or a membrane-bound sphingolipid, enhancing hydrolytic activity. In fact studies of human disorders of specific saposin deficiencies and work with specific saposin knockout mouse models has revealed loss of a particular saposin, in both human and mouse, elicits effects very similar to those caused by lack of the equivalent hydrolase, resulting in severe neurological defects (Matsuda et al., 2001; Matsuda et al., 2004; Kolter and Sandhoff, 2005; Spiegel et al., 2005). Saposin B deficiency leads to an accumulation of sulfatides and globotriaosylceramide and a metachromatic leukodystrophy-like disease, whereas saposin C deficiency leads to glucosylceramide accumulation and a Gaucher-like disease and the saposin A-deficient mouse is defective in the degradation of galactosylceramide, modelling late-onset Krabbe disease. In humans (Harzer et al., 1989; Hulkova et al., 2001; Elleder et al., 2005) and mice (Fujita et al., 1996) the loss of prosaposin and consequently all four saposins results in a severe, rapidly progressive neurological disease and the accumulation of multiple sphingolipids in the brain and other organs. Taken together these studies highlight the importance of prosaposin and the saposins in the nervous system.

In the case of saposin D there are no reported cases of deficiency in humans but from *in vitro* studies it is thought saposin D activates the degradation of sphingomyelin and ceramide, with the latter considered to be the predominant substrate (Morimoto et al., 1988; Azuma et al., 1994; Vaccaro et al., 1995). This *in vitro* work is corroborated by the fact that ceramides, particularly those containing hydroxyl fatty

CHAPTER 7 IDENTIFICATION OF PROTEINS THAT INTERACT WITH THE AMINO TERMINUS OF β -III SPECTRIN

acids (HFA), were found to accumulate in the cerebellum of saposin D knockout mice (Matsuda et al., 2004). One hypothesis, therefore, was that ceramide accumulation, due to loss of saposin D in the β -III^{-/-} spectrin mice, was toxic and played a role in the observed Purkinje cell degeneration and ataxic phenotype (Perkins et al., 2010). Interestingly, in saposin D KO mice the loss of Purkinje cells occurred in a striped pattern with the majority of surviving Purkinje cells being found in zebrin II positive bands (Matsuda et al., 2004). Sphingosine kinase 1 (SPHK1) phosphorylates sphingosine, the product of ceramide degradation, to sphingosine 1 phosphate (S1P) and this enzyme is found at high levels in zebrin II positive bands (Terada et al., 2004). Therefore, the relative levels of S1P and ceramide in Purkinje cells may determine whether a cell survives or dies. It is not yet known whether there is also a patterned loss of Purkinje cells in β -III^{-/-} spectrin mice.

However, from the present work it is unclear whether levels of saposin D are altered in β -III^{-/-} spectrin mice and hence might play a role in the disease phenotype. Confocal immunofluorescence studies, which cannot distinguish between prosaposin and saposin D, show apparently decreased immunoreactivity in β -III^{-/-} spectrin mice compared to WT, but Western blot analysis showed no change in levels of prosaposin or saposin D. One possibility is that, although the confocal images of WT and β -III^{-/-} spectrin mice were captured using the same settings, differences in tissue quality or membrane integrity, rather than protein levels *per se*, may give rise to different intensities of staining. On the other hand, the fact that total cerebellar

CHAPTER 7 IDENTIFICATION OF PROTEINS THAT INTERACT WITH THE AMINO TERMINUS OF β -III SPECTRIN

homogenates were analysed by Western blotting could preclude the detection of any change in protein levels confined to Purkinje cells, since high levels of expression have also been detected in granule cells and Bergmann glia (O'Brien et al., 1995; Matsuda et al., 2004; M Jackson unpublished data). A further factor may be antibody variability, since a number of antibodies against saposin D/prosaposin were initially tested and that supplied by Ying Sun was the only one to detect what was considered to be full length prosaposin and saposin D. However, the fact all four antibodies detected different sized proteins and showed variations from one another in protein distribution within the cerebellum suggests there may be issues with regard to antibody cross-reactivity. Another result which seems to conflict with the Western blotting data from β -III^{-/-} spectrin mice is that from the BiFC assay, where disruption of correct cellular trafficking of prosaposin from the Golgi apparatus by altering β -III spectrin (in this case as a consequence of the removal of exon 7) is indicated. This finding would suggest that the proportion of prosaposin converted to saposin D should be reduced when trafficking is disrupted, since the conversion to saposin D occurs in the lysosomes, a downstream destination of correctly trafficked prosaposin. Instead the Western blotting results indicated no difference in the proportions of prosaposin and saposin D in β -III^{-/-} spectrin mice compared to WT, although disrupted vesicular trafficking from the Golgi is suggested by transmission electron microscopy (TEM) data from the β -III^{-/-} spectrin mice (Perkins et al. 2010). However, in β -III^{-/-} spectrin mice the protein still expressed does possess exon 7 (exons 1-6 are missing), perhaps explaining the difference. Additional work is

CHAPTER 7 IDENTIFICATION OF PROTEINS THAT INTERACT WITH THE AMINO TERMINUS OF β -III SPECTRIN

required before any firm conclusions can be made regarding the involvement of saposin D in the Purkinje cell degeneration observed in β -III^{-/-} spectrin mice.

7.3.2 Role for prosaposin in Purkinje cell survival

Prosaposin, although not important in the hydrolysis of sphingolipids, is not simply a precursor protein but is found at high levels in the brain and muscle, unlike saposins which are ubiquitously expressed (Sano et al., 1988; Sano et al., 1989; Hineno et al., 1991; Kishimoto et al., 1992; Sano et al., 1992; Hiraiwa et al., 1993; Kreda et al., 1994; Sun et al., 1994; Sun et al., 2000). It is thought prosaposin functions as a secretory protein (Sylvester et al., 1989; Hineno et al., 1991; Kondoh et al., 1991; Hiraiwa et al., 1992; Hiraiwa et al., 1993) or as an integral membrane protein mediating the transfer of gangliosides across membranes (Rijnboutt et al., 1991). In cultured neuronal cells, gangliosides have been shown to promote neurite outgrowth (Tsuji et al., 1983; Schengrund, 1990) and there is growing evidence to support a role for prosaposin in neurite outgrowth, nerve regeneration and neuroprotection (O'Brien et al., 1994; Kotani et al., 1996a; Tsuboi et al., 1998; Calcutt et al., 1999).

Furthermore, the *in vitro* and *in vivo* neurotrophic properties of prosaposin have been narrowed down to a 21 amino acid linear sequence in the amino-terminus of saposin C (O'Brien et al., 1995; Qi et al., 1996; Qi et al., 1999). Prosapeptides, comprising this neurotrophic sequence, have been generated and found to stimulate neurite outgrowth and choline acetyl transferase activity *in vitro* and prevent neuronal cell

CHAPTER 7 IDENTIFICATION OF PROTEINS THAT INTERACT WITH THE AMINO TERMINUS OF β -III SPECTRIN

death induced by serum deprivation (O'Brien et al., 1995; Campana et al., 1996; Hiraiwa et al., 1997; Campana et al., 1998). Furthermore both prosaposin and prosapeptides were found to prevent apoptosis of cerebellar granule cells (Tsuboi et al., 1998), Schwann cells (Campana et al., 1999), ischemia induced death of hippocampal neurons in gerbils (Sano et al., 1994; Kotani et al., 1996b) and rats (Igase et al., 1999) and mediate sciatic nerve regeneration (Kotani et al., 1996a). The method of action may be a direct one on the neurons, involving ERK and P13K/Akt signalling and reduced phosphorylation of stress activated protein kinases (Ochiai et al., 2008) or it may act on glia preventing cell death by increasing sulfatide content (Hiraiwa et al., 1997; Campana et al., 1998). Therefore, it is feasible that changes to prosaposin levels or cellular distribution could have an important role in Purkinje cell survival. The effect of prosapeptides on the survival and morphology of dissociated cultured β -III^{-/-} spectrin Purkinje cells could address whether a loss of prosaposin plays a role in the loss of Purkinje cells in β -III^{-/-} spectrin mice. It may also be worth investigating whether the phosphorylation of Akt, JNK, p38 and ERK are altered in β -III^{-/-} spectrin mice compared to WT animals to determine if signalling downstream of prosaposin is altered. In addition a number of studies have revealed that alternative splicing is important in the sorting of prosaposin with an isoform possessing three extra residues (gln-asp-gln) being secreted and the isoform lacking the short exon 8 being targeted to lysosomes for proteolytic digestion (Igdoura et al., 1996; Madar-Shapiro et al., 1999). It may be that there are differences in the levels of the two isoforms in β -III^{-/-} spectrin mice compared to WT littermates.

7.3.3 Role for clathrin light chain 1 in neurodegeneration

Although clathrin coated vesicles were isolated 41 years ago (Kanaseki and Kadota, 1969) and their role in endocytosis and intracellular protein trafficking has been well studied (Kirchhausen, 2000; Brodsky et al., 2001; Fotin et al., 2004; Robinson, 2004), the exact function of the two light chains is not yet known. However, studies from yeast indicate that light chains are important for the oligomerization of heavy chains (Chu et al., 1996; Huang et al., 1997) as three clathrin heavy chains each associate with a light chain and form a triskelion (Kirchhausen and Harrison, 1981; Ungewickell and Branton, 1981; Blondeau et al., 2004; Girard et al., 2005). Adaptor proteins (AP) then link the clathrin coat to transmembrane cargo molecules (Kirchhausen, 2000; Nakatsu and Ohno, 2003; Owen et al., 2004; Robinson, 2004) with each AP involved in a distinct transport pathway within the post-Golgi and/or endocytic network. For example, AP-2 regulates the formation of clathrin coated vesicles during endocytosis (Nakatsu and Ohno, 2003; Owen et al., 2004; Traub, 2005) whereas AP-4 regulates the formation of vesicles from the trans-Golgi network to lysosomes (Aguilar et al., 2001).

Previously the huntingtin-interacting protein (HIP1) and HIP1-related protein (HIP1R), two actin-binding endocytic proteins, were found to interact with clathrin light chains (Bennett et al., 2001; Engqvist-Goldstein et al., 2001; Henry et al., 2002; Legendre-Guillemain et al., 2002). Therefore, defects in clathrin coat formation and downstream effects on vesicular trafficking, a consequence of altered light chain

CHAPTER 7 IDENTIFICATION OF PROTEINS THAT INTERACT WITH THE AMINO TERMINUS OF β -III SPECTRIN

activity, may be a factor in neurodegeneration. Clathrin-mediated endocytosis was indeed found to be disrupted when HIP proteins were depleted by RNA interference, with glutamate receptors being one cargo that failed to be correctly recycled, consequently affecting glutamatergic neurotransmission (Kaksonen et al., 2003; Metzler et al., 2003; Engqvist-Goldstein et al., 2004). Similarly the knockdown of clathrin light chain 1 was shown to result in the mislocalisation of HIP1R, the over assembly of actin, disruption to protein trafficking at the trans-Golgi network and an increase in endosome-targeted cargo, possibly a consequence of vesicles being trapped in an excessively stable actin network (Royle et al., 2005). Therefore it is apparent that interfering with the expression of proteins involved in the formation of clathrin coats has detrimental effects on vesicular transport. Of note, the trafficking of prosaposin, the other binding partner of β -III spectrin, from the Golgi apparatus to lysosomes, was found to be disrupted when the recruitment of clathrin to transport vesicles was prevented by expression of mutant adaptor proteins (Hassan et al., 2004).

In this study, using the BiFC assay, the normal cellular trafficking of CLC1 appears to be dependent on β -III spectrin, with the proteins remaining associated with the Golgi apparatus, rather than distributed throughout the cytoplasm, when mutant or truncated forms of the amino terminus of β -III spectrin were expressed. A potential link between clathrin and the spectrin-actin cytoskeleton was already proposed based on the fact the D4 region of ankyrin R binds with high affinity to the amino terminus

CHAPTER 7 IDENTIFICATION OF PROTEINS THAT INTERACT WITH THE AMINO TERMINUS OF β -III SPECTRIN

of clathrin heavy chain (Michaely et al., 1999). Whether β -III spectrin interacts with one or more ankyrin isoforms still needs to be investigated but ankyrin R, initially identified in the erythrocyte membrane (Bennett and Stenbuck, 1979), is found throughout the cell body and dendritic tree of Purkinje cells (Lambert and Bennett, 1993) and therefore possesses the same cellular distribution as β -III spectrin, making it a possible candidate. In contrast, ankyrin G localises to the axon initiation segment (AIS) and nodes of Ranvier where it has been shown to interact with sodium channels and β -IV spectrin (Zhou et al., 1998; Berghs et al., 2001; Jenkins and Bennett, 2001; Komada and Soriano, 2002). The fact that clathrin was recently shown to play a role in the correct sorting of basolateral proteins in epithelial cells (Deborde et al., 2008) does raise the question whether the CLC1- β -III spectrin interaction plays an important role in the selection and targeting of correct cargo to dendrites?

7.3.4 Conclusions

Two proteins, prosaposin/saposin D and CLC1, identified in a yeast two-hybrid screen as interacting with the amino-terminus of β -III spectrin were confirmed as binding partners in yeast and mammalian cells and for prosaposin/saposin D the interaction was further confirmed *in vivo*. The identification of these proteins as interactors provides further evidence that β -III spectrin plays important roles in protein trafficking and that defects to the transport of proteins within the Purkinje cell dendritic tree may be critical features of SCA5 pathogenesis.

CHAPTER 8

GENERAL DISCUSSION

8.1 Summary of findings

In summary, the work carried out in this thesis suggests that loss of β -III spectrin underlies SCA5 pathogenesis and that the mutations associated with disease have dominant-negative effects on wild type β -III spectrin function. Furthermore the work presented here confirms a role for β -III spectrin in vesicular trafficking and reveals that one mutation associated with SCA5 (L253P) interferes with protein transport from the Golgi apparatus. The deleterious effect of other disease causing β -III spectrin mutations was not obvious from the work carried out in this study, but all the data obtained to date would suggest that loss of membrane proteins, as a consequence of defects either in protein transport or in protein stabilisation at the membrane, is an important aspect of SCA5 pathogenesis (Figure 8.1).

The results presented here from *in vitro* experiments demonstrated that the truncated form of β -III spectrin (Δ 2-6 β -III spectrin), expressed at a low level in the β -III^{-/-} spectrin mouse, had no obvious adverse properties, but in fact appeared to be less functional than WT β -III spectrin inferring that the β -III^{-/-} spectrin mouse could be considered a functional knockout (hypomorph). Therefore, because the animals developed progressive motor deficits and cerebellar degeneration, it was concluded that a loss of β -III spectrin function recapitulates the clinical features of SCA5. In contrast β -III^{+/-} spectrin mice showed no signs of an ataxic phenotype, even at 2

years of age, arguing against haploinsufficiency as a causative mechanism and instead pointing towards the mutations in β -III spectrin possessing dominant negative effects on WT β -III spectrin function in addition to lacking normal function.

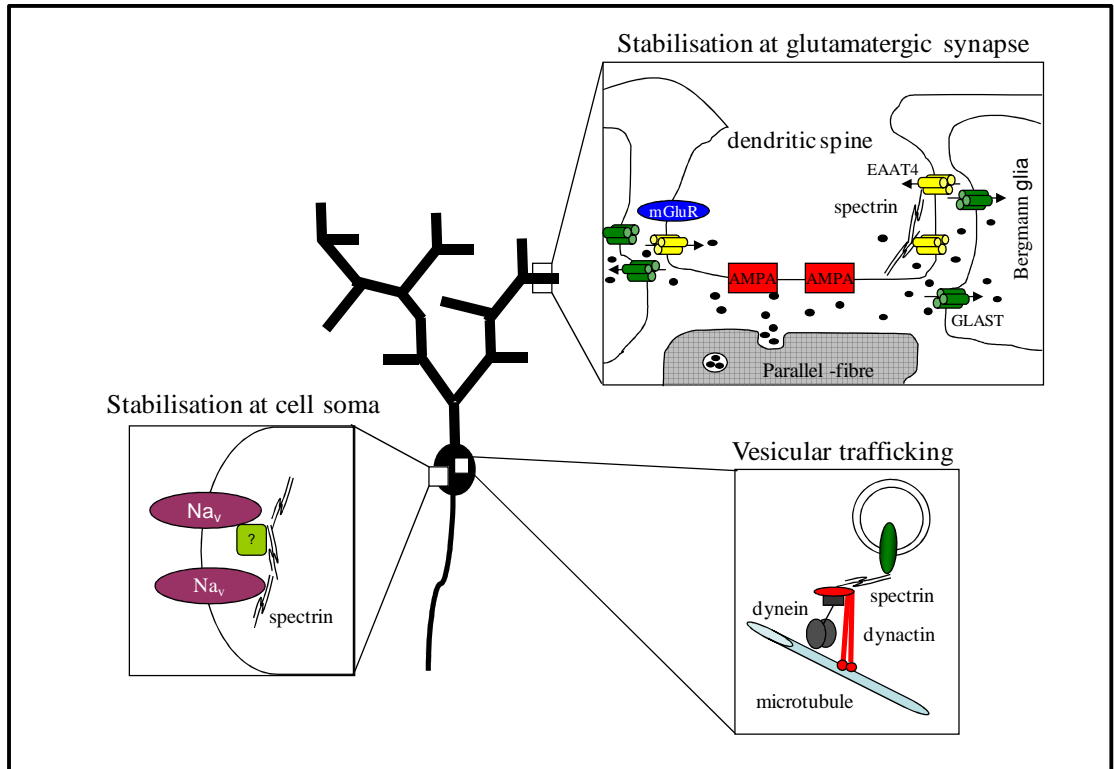


Figure 8.1 Schematic diagram of β -III spectrin function.

Cell culture studies were able to identify a dominant-negative effect of one mutation, the L253P missense mutation within the calponin homology domain of β -III spectrin. Expression of L253P β -III spectrin in two mammalian cell lines, HEK 293T and Neuro 2a cells, revealed an abnormal cellular localisation compared to that of WT. The L253P mutant protein appeared to remain associated with the Golgi apparatus,

CHAPTER 8 GENERAL DISCUSSION

rather than the plasma membrane, and furthermore interfered with the cell surface expression of WT β -III spectrin and other membrane proteins. The ability of β -III spectrin to interact with Arp1, a subunit of the dynactin-dynein complex, was also lost by the substitution of leucine 253 by proline. This finding revealed how a link between the microtubule motor dynein and β -III spectrin could be lost, accounting for the observed defects in vesicular protein trafficking. The fact that incubation at a lower temperature (25°C) rescued both the interaction with Arp1 and protein trafficking defects suggested that a conformational defect was responsible for the dominant-negative effect of L253P. But, despite the intracellular accumulation of proteins in cells expressing L253P β -III spectrin, there was no evidence for the induction of the unfolded protein response in cell culture or in β -III^{-/-} spectrin mice, indicating that the actual loss of proteins from the membrane was more important in initiating cell death than the accumulation of the mis-trafficked proteins.

Finally, a yeast two-hybrid screen identified prosaposin and/or saposin D (a neurotrophic factor and a protein involved in the degradation of ceramide, respectively) and clathrin light chain 1 (component of clathrin lattice) as interactors of β -III spectrin. Both interactions were confirmed in mammalian cells using a BiFC assay and for prosaposin/saposin D further corroboration was obtained from *in vivo* studies. Despite a reduced immunoreactivity of prosaposin/saposin D in β -III^{-/-} Purkinje cells compared to WT no difference in total cerebellar protein levels was observed by Western blot analysis. It therefore remains uncertain whether a loss of

saposin D or prosaposin underlies some aspects of the phenotype observed in β -III^{-/-} spectrin mice.

8.2 Outstanding questions

8.2.1 How are the β -III spectrin mutations associated with SCA5 pathogenesis?

Work presented in this thesis has begun to shed light on the pathogenic mechanism of the L253P missense mutation, with over expression in mammalian cells revealing a defect in protein trafficking and inability to interact with Arp1, one subunit of the dynactin-dynein complex. However, in this study the over expression of other mutations associated with SCA5 revealed no obvious difference in the cellular distribution compared to WT β -III spectrin. Unpublished work using the yeast-two hybrid system has suggested that the Lincoln mutation (Δ 39 bp) reduces the interaction between β -III spectrin and p150^{Glued} (another subunit of the dynactin complex) while the French mutation (Δ 15 bp + R634W) increases the interaction between β -III spectrin and α -II spectrin (LPW Ranum, personal communication). Therefore alterations in the balance of protein interactions involved in vesicular trafficking may be an important aspect of disease.

Two transgenic mouse models, expressing human β -III spectrin harbouring the Lincoln mutation, were also generated by Dr. Ranum and colleagues to elucidate disease-causing mechanisms. One model is a conditional transgenic mouse that expresses an untagged form of human Δ 39 bp β -III spectrin whereas the other is a

transgenic that constitutively expresses a FLAG-tagged version of the mutant protein. Both mutant transgenic lines were found to be slightly impaired on the rotarod but no Purkinje cell loss was observed in either line (LPW Ranum, personal communication). The mild phenotype and lack of cerebellar degeneration is in strong contrast to that observed in the β -III^{-/-} spectrin mice (Perkins et al., 2010), but based on the results reported in this thesis, that a loss of β -III spectrin function and dominant negative effects underlie disease pathogenesis, the fact that a high level of expression was not obtained for either transgene could explain why a mild phenotype was observed. Without sufficient knockdown of endogenous β -III spectrin function by the mutant protein a disease phenotype would not be obtained. This potential problem with regard to expression levels in transgenic mice raises an important issue as to what type of animal model is best for the future study of pathogenic mechanisms in SCA5. In many respects knock-in mouse models would be the most appropriate system, as they would simulate the human disease more closely, with one endogenous allele being mutated.

8.2.2 What role do glutamate transporters play in Purkinje cell survival?

The analysis of both β -III^{-/-} and β -III^{+/-} spectrin mice has revealed that a loss of EAAT4 and GLAST, the two predominant glutamate transporters in the cerebellum, correlates with Purkinje cells undergoing dark cell degeneration and an ataxic phenotype, suggesting that reduced glutamate uptake may be an important factor in Purkinje cell dysfunction and degeneration. In the future the generation of additional genetically modified mice could provide further insights into the role of EAAT4

and/or GLAST in SCA5 disease onset and progression. The abolition of EAAT4 or GLAST expression in mice heterozygous for the loss of β -III spectrin (β -III^{+/-}/EAAT4^{-/-} or β -III^{+/-}/GLAST^{-/-}) should reveal whether the loss of GLAST or EAAT4 is sufficient to cause disease in what should be asymptomatic mice. Similarly, determining whether the phenotype of β -III^{-/-} spectrin mice is emphasised by the early and complete loss of GLAST will address whether levels of GLAST are important in disease progression. Finally the creation of a double glutamate transporter knockout mouse (EAAT4^{-/-}/GLAST^{-/-}) will address which, if any, aspects of the β -III^{-/-} spectrin mouse phenotype are due to the loss of EAAT4 and GLAST. The fact that no severe phenotype has been reported for either EAAT4 (Huang et al., 2004) or GLAST (Watase et al., 1998) knockout mice indicates that the loss of one transporter can be compensated for by the other and it may only be when both are lost that a disease phenotype manifests itself. This would be consistent with analysis of the β -III^{-/-} spectrin mouse (Perkins et al., 2010).

8.2.3 Is a subpopulation of Purkinje cells more vulnerable to cell death?

Although Purkinje cell degeneration is a hallmark of SCAs a number of mouse studies have highlighted that the pattern of neuronal loss is often not uniform throughout the cerebellum with some regions of cells being preserved (Sarna and Hawkes, 2003). EAAT4, like sphingosine kinase 1 (refer to section 7.3.1), is one of a handful of proteins known-to-be differentially expressed in distinct Purkinje cell populations and has been shown to correlate with patterned neuroprotection (Welsh et al., 2002; Sachs et al., 2009). It will be worth investigating whether in β -III^{-/-}

spectrin mice a specific Purkinje cell population is initially more susceptible to or protected from degeneration and determine whether EAAT4, GLAST and/or prosaposin/saposin D levels correlate with the selectivity.

8.2.4 Which sodium channel subunit is involved in SCA5 pathogenesis?

Although not mentioned in this thesis, work from the Jackson lab has also shown that sodium currents from acutely dissociated Purkinje neurons are reduced in β -III^{-/-} spectrin mice (Perkins et al., 2010). Furthermore, the decrease in sodium currents likely underlies the two-fold reduction observed in the spontaneous firing rate of Purkinje cells lacking β -III spectrin (Perkins et al., 2010), since sodium channels along with potassium channels are essential for the sustained high-frequency tonic firing of Purkinje cells (Raman and Bean, 1999; Sacco et al., 2006; Zagha et al., 2008). Genetic defects for several other SCA subtypes result in loss of ion channel function associated with ataxia in humans (Browne et al., 1994; Ophoff et al., 1996; Zhuchenko et al., 1997; Waters et al., 2006). This is also reflected in mice lacking various ion channels (Sausbier et al., 2004; Akemann and Knopfel, 2006; Levin et al., 2006; Walter et al., 2006), suggesting that the observed loss of sodium currents in β -III^{-/-} spectrin mice may be an important factor in disease pathogenesis. Further work to determine the role of sodium channel dysfunction in SCA5 is required as a patient with cerebellar atrophy and ataxia has been found to have a mutation in the gene encoding Na_v1.6 (Trudeau et al., 2006), one of the two sodium channel alpha-subunits (Na_v1.1 and Na_v1.6) expressed in the cell body and dendritic tree of Purkinje cells (Kalume et al., 2007). Additional evidence to support an interaction

between β spectrin, sodium channels and ataxia comes from analysis of the β -IV spectrin knockout mouse, which develops progressive ataxia and shows mislocalisation of voltage gated sodium channels at both the AIS and nodes of Ranvier (Parkinson et al., 2001; Komada and Soriano, 2002). The β -III^{-/-} spectrin mouse will be a useful tool in identifying whether sodium channel subunits are lost and/or redistributed in the absence of β -III spectrin. Subsequently, the effect the β -III spectrin mutations associated with SCA5 have on the trafficking, cell surface expression and activity of the subunits identified as being altered in β -III^{-/-} spectrin mice will reveal whether sodium channel dysfunction is an important aspect of the human disease. Finally, it is well documented that the various isoforms of ankyrin (R, G, B) link transmembrane proteins such as sodium channels to the spectrin skeleton (Zhou et al., 1998; Jenkins and Bennett, 2001; Komada and Soriano, 2002) and so the expression and cellular distribution of such adaptor proteins could also be examined in β -III^{-/-} spectrin mice as potential factors in disease pathogenesis.

8.3 Common mechanisms in neurodegeneration

As detailed in section 1.6, the identification of SCA-associated genes has enabled the pathogenic mechanisms of some SCAs to be investigated using animal and cell culture models. This has led to several hypotheses being suggested as to the mechanism(s) of Purkinje cell death, including protein aggregation (consequence of trinucleotide repeat expansion or proteolytic cleavage of mutant proteins), alterations in Ca^{2+} homeostasis, defects in vesicle trafficking, glutamate-mediated excitotoxicity, impaired protein degradation/unfolded protein response and

interference with gene transcription (reviewed in (Duenas et al., 2006)). One or more of these pathways have been linked to the pathogenesis of other neurodegenerative disorders, including Alzheimer's (Stokin et al., 2005), Huntington's (DiFiglia et al., 1997; Sapp et al., 1999; Li et al., 2000; Trettel et al., 2000; Li et al., 2001; Lee et al., 2004), ALS (Rothstein et al., 1992; Rothstein et al., 1995; Shaw et al., 1995; Bruijn et al., 1997; Zhang et al., 1997; Lin et al., 1998; Williamson and Cleveland, 1999; Howland et al., 2002; Ligon et al., 2005), spinal and bulbar muscular atrophy (SBMA) (Piccioni et al., 2001) and epilepsy (Tanaka et al., 1997; Sepkuty et al., 2002) highlighting the convergence of disease mechanisms in neuronal cell death. With respect to this study, glutamate-mediated excitotoxicity and defects in protein trafficking are two mechanisms convergent with other neurodegenerative diseases identified as being important in SCA5, whereas the unfolded protein response was not found to play a role in pathogenesis here.

8.4 Conclusions

The present work has demonstrated that the $\Delta 2-6$ β -III spectrin protein doesn't have any toxic gain of function, confirming the β -III^{-/-} spectrin mouse to be a functional KO. Behavioural analysis demonstrated that these mice exhibit a phenotype similar to that of SCA5 patients. Furthermore, haploinsufficiency was ruled out as a disease mechanism by analysis of heterozygote (β -III^{+/-}) mice, while a dominant negative effect of a human SCA5 mutation (L253P) on WT β -III spectrin was demonstrated, leading to disruption of protein trafficking from the Golgi apparatus. Finally, new interactions of β -III spectrin with prosaposin/saposin D and clathrin light chain were

CHAPTER 8 GENERAL DISCUSSION

found, providing new avenues for further research into SCA5 pathogenesis. In conclusion, this work has demonstrated that SCA5, an autosomal dominant disease, results from a loss of β -III spectrin function and furthermore the loss of other proteins, either through disruption to vesicular trafficking or stabilisation at the membrane, appear to be important factors in disease pathogenesis.

REFERENCES

- Agre, P., Casella, J.F., Zinkham, W.H., McMillan, C., and Bennett, V. (1985). Partial deficiency of erythrocyte spectrin in hereditary spherocytosis. *Nature* 314, 380-383.
- Agre, P., Orringer, E.P., and Bennett, V. (1982). Deficient red-cell spectrin in severe, recessively inherited spherocytosis. *The New England journal of medicine* 306, 1155-1161.
- Aguilar, R.C., Boehm, M., Gorshkova, I., Crouch, R.J., Tomita, K., Saito, T., Ohno, H., and Bonifacino, J.S. (2001). Signal-binding specificity of the mu4 subunit of the adaptor protein complex AP-4. *The Journal of biological chemistry* 276, 13145-13152.
- Akemann, W., and Knopfel, T. (2006). Interaction of Kv3 potassium channels and resurgent sodium current influences the rate of spontaneous firing of Purkinje neurons. *J Neurosci* 26, 4602-4612.
- Albus, J.S. (1971). A theory of cerebellar function. *Math Biosci* 10: 25-61.
- Altman, J., and Bayer, S.A. (1997). *Development of the Cerebellar System*, CRC Press, New York.
- Anderson, C.L., Delisle, B.P., Anson, B.D., Kilby, J.A., Will, M.L., Tester, D.J., Gong, Q., Zhou, Z., Ackerman, M.J., and January, C.T. (2006). Most LQT2 mutations reduce Kv11.1 (hERG) current by a class 2 (trafficking-deficient) mechanism. *Circulation* 113, 365-373.
- Anderson, R.A., and Lovrien, R.E. (1984). Glycophorin is linked by band 4.1 protein to the human erythrocyte membrane skeleton. *Nature* 307, 655-658.

REFERENCES

- Apps, R., and Garwicz, M. (2005). Anatomical and physiological foundations of cerebellar information processing. *Nature reviews* 6, 297-311.
- Araki, K., Meguro, H., Kushiya, E., Takayama, C., Inoue, Y., and Mishina, M. (1993). Selective expression of the glutamate receptor channel delta 2 subunit in cerebellar Purkinje cells. *Biochemical and biophysical research communications* 197, 1267-1276.
- Asanuma, C., Thach, W.R., and Jones, E.G. (1983a). Anatomical evidence for segregated focal groupings of efferent cells and their terminal ramifications in the cerebellothalamic pathway of the monkey. *Brain Res* 286, 267-297.
- Asanuma, C., Thach, W.T., and Jones, E.G. (1983b). Brainstem and spinal projections of the deep cerebellar nuclei in the monkey, with observations on the brainstem projections of the dorsal column nuclei. *Brain Res* 286, 299-322.
- Asanuma, C., Thach, W.T., and Jones, E.G. (1983c). Cytoarchitectonic delineation of the ventral lateral thalamic region in the monkey. *Brain Res* 286, 219-235.
- Asanuma, C., Thach, W.T., and Jones, E.G. (1983d). Distribution of cerebellar terminations and their relation to other afferent terminations in the ventral lateral thalamic region of the monkey. *Brain Res* 286, 237-265.
- Atkin, J.D., Farg, M.A., Turner, B.J., Tomas, D., Lysaght, J.A., Nunan, J., Rembach, A., Nagley, P., Beart, P.M., Cheema, S.S., and Horne, M.K. (2006). Induction of the unfolded protein response in familial amyotrophic lateral sclerosis and association of protein-disulfide isomerase with superoxide dismutase 1. *The Journal of biological chemistry* 281, 30152-30165.
- Auger, C., and Attwell, D. (2000). Fast removal of synaptic glutamate by postsynaptic transporters. *Neuron* 28, 547-558.

REFERENCES

- Azuma, N., O'Brien, J.S., Moser, H.W., and Kishimoto, Y. (1994). Stimulation of acid ceramidase activity by saposin D. *Archives of biochemistry and biophysics* 311, 354-357.
- Baines, A.J. (2009). Evolution of spectrin function in cytoskeletal and membrane networks. *Biochemical Society transactions* 37, 796-803.
- Baines, A.J., and Pinder, J.C. (2005). The spectrin-associated cytoskeleton in mammalian heart. *Front Biosci* 10, 3020-3033.
- Banfi, S., Servadio, A., Chung, M.Y., Kwiatkowski, T.J., Jr., McCall, A.E., Duvick, L.A., Shen, Y., Roth, E.J., Orr, H.T., and Zoghbi, H.Y. (1994). Identification and characterization of the gene causing type 1 spinocerebellar ataxia. *Nature genetics* 7, 513-520.
- Barenberg, P., Strahlendorf, H., and Strahlendorf, J. (2001). Hypoxia induces an excitotoxic-type of dark cell degeneration in cerebellar Purkinje neurons. *Neuroscience research* 40, 245-254.
- Bastian, A and Thach W.T. (2002). Structure and function of the cerebellum. In *The cerebellum and its disorders*, ed. M.U. Manto and M. Pandolfo. Cambridge University Press. pg. 49-66.
- Beck, K.A., Buchanan, J.A., Malhotra, V., and Nelson, W.J. (1994). Golgi spectrin: identification of an erythroid beta-spectrin homolog associated with the Golgi complex. *The Journal of cell biology* 127, 707-723.
- Behrens, A., and Aguzzi, A. (2002). Small is not beautiful: antagonizing functions for the prion protein PrP(C) and its homologue Dpl. *Trends in neurosciences* 25, 150-154.

REFERENCES

- Bennett, E.M., Chen, C.Y., Engqvist-Goldstein, A.E., Drubin, D.G., and Brodsky, F.M. (2001). Clathrin hub expression dissociates the actin-binding protein Hip1R from coated pits and disrupts their alignment with the actin cytoskeleton. *Traffic (Copenhagen, Denmark)* 2, 851-858.
- Bennett, V. (1985). The membrane skeleton of human erythrocytes and its implications for more complex cells. *Annual review of biochemistry* 54, 273-304.
- Bennett, V., and Baines, A.J. (2001). Spectrin and ankyrin-based pathways: metazoan inventions for integrating cells into tissues. *Physiological reviews* 81, 1353-1392.
- Bennett, V., and Stenbuck, P.J. (1979). Identification and partial purification of ankyrin, the high affinity membrane attachment site for human erythrocyte spectrin. *The Journal of biological chemistry* 254, 2533-2541.
- Bennett, V., and Stenbuck, P.J. (1980). Human erythrocyte ankyrin. Purification and properties. *The Journal of biological chemistry* 255, 2540-2548.
- Berghs, S., Ferracci, F., Maksimova, E., Gleason, S., Leszczynski, N., Butler, M., De Camilli, P., and Solimena, M. (2001). Autoimmunity to beta IV spectrin in paraneoplastic lower motor neuron syndrome. *Proceedings of the National Academy of Sciences of the United States of America* 98, 6945-6950.
- Bergles, D.E., Dzubay, J.A., and Jahr, C.E. (1997). Glutamate transporter currents in bergmann glial cells follow the time course of extrasynaptic glutamate. *Proceedings of the National Academy of Sciences of the United States of America* 94, 14821-14825.
- Berridge, M.J. (1993). Inositol trisphosphate and calcium signalling. *Nature* 361, 315-325.

REFERENCES

- Bertram, L., and Tanzi, R.E. (2008). Thirty years of Alzheimer's disease genetics: the implications of systematic meta-analyses. *Nature reviews* 9, 768-778.
- Bichelmeier, U., Schmidt, T., Hubener, J., Boy, J., Ruttiger, L., Habig, K., Poths, S., Bonin, M., Knipper, M., Schmidt, W.J., *et al.* (2007). Nuclear localization of ataxin-3 is required for the manifestation of symptoms in SCA3: in vivo evidence. *J Neurosci* 27, 7418-7428.
- Bird TD. Hereditary ataxia overview. (1998)
<http://www.geneclinics.org/servlet/access?db=geneclinics&site=gt&id=8888891&key=UOEVCBakjvMZq&gry=&fcn=y&fw=ig9&filename=/profiles/ataxias/index.html>.
- Blondeau, F., Ritter, B., Allaire, P.D., Wasiak, S., Girard, M., Hussain, N.K., Angers, A., Legendre-Guillemin, V., Roy, L., Boismenu, D., *et al.* (2004). Tandem MS analysis of brain clathrin-coated vesicles reveals their critical involvement in synaptic vesicle recycling. *Proceedings of the National Academy of Sciences of the United States of America* 101, 3833-3838.
- Botterell, E.H. and Fulton, J.F. (1938). Functional localisation in the cerebellum of primates. II. Lesions of midline structures (vermis) and deep nuclei. *J Comp Neurol* 69: 47-62.
- Brocke, K.S., Neu-Yilik, G., Gehring, N.H., Hentze, M.W., and Kulozik, A.E. (2002). The human intronless melanocortin 4-receptor gene is NMD insensitive. *Human molecular genetics* 11, 331-335.
- Brodsky, F.M., Chen, C.Y., Knuehl, C., Towler, M.C., and Wakeham, D.E. (2001). Biological basket weaving: formation and function of clathrin-coated vesicles. *Annual review of cell and developmental biology* 17, 517-568.

REFERENCES

- Brodsky, F.M., Hill, B.L., Acton, S.L., Nathke, I., Wong, D.H., Ponnambalam, S., and Parham, P. (1991). Clathrin light chains: arrays of protein motifs that regulate coated-vesicle dynamics. *Trends in biochemical sciences* *16*, 208-213.
- Browne, D.L., Gancher, S.T., Nutt, J.G., Brunt, E.R., Smith, E.A., Kramer, P., and Litt, M. (1994). Episodic ataxia/myokymia syndrome is associated with point mutations in the human potassium channel gene, KCNA1. *Nature genetics* *8*, 136-140.
- Bruijn, L.I., Becher, M.W., Lee, M.K., Anderson, K.L., Jenkins, N.A., Copeland, N.G., Sisodia, S.S., Rothstein, J.D., Borchelt, D.R., Price, D.L., and Cleveland, D.W. (1997). ALS-linked SOD1 mutant G85R mediates damage to astrocytes and promotes rapidly progressive disease with SOD1-containing inclusions. *Neuron* *18*, 327-338.
- Bueler, H., Fischer, M., Lang, Y., Bluethmann, H., Lipp, H.P., DeArmond, S.J., Prusiner, S.B., Aguet, M., and Weissmann, C. (1992). Normal development and behaviour of mice lacking the neuronal cell-surface PrP protein. *Nature* *356*, 577-582.
- Burk, K., Zuhlke, C., Konig, I.R., Ziegler, A., Schwinger, E., Globas, C., Dichgans, J., and Hellenbroich, Y. (2004). Spinocerebellar ataxia type 5: clinical and molecular genetic features of a German kindred. *Neurology* *62*, 327-329.
- Burright, E.N., Clark, H.B., Servadio, A., Matilla, T., Feddersen, R.M., Yunis, W.S., Duvick, L.A., Zoghbi, H.Y., and Orr, H.T. (1995). SCA1 transgenic mice: a model for neurodegeneration caused by an expanded CAG trinucleotide repeat. *Cell* *82*, 937-948.
- Caddy, K.W., and Biscoe, T.J. (1975). Preliminary observations on the cerebellum in the mutant mouse Lurcher. *Brain Res* *91*, 276-280.

REFERENCES

- Caddy, K.W., and Biscoe, T.J. (1979). Structural and quantitative studies on the normal C3H and Lurcher mutant mouse. *Philosophical transactions of the Royal Society of London* 287, 167-201.
- Caddy, K.W., and Biscow, T.J. (1976). The number of Purkinje cells and olive neurones in the normal and Lurcher mutant mouse. *Brain Res* 111, 396-398.
- Cagnoli, C., Mariotti, C., Taroni, F., Seri, M., Brussino, A., Michielotto, C., Grisoli, M., Di Bella, D., Migone, N., Gellera, C., *et al.* (2006). SCA28, a novel form of autosomal dominant cerebellar ataxia on chromosome 18p11.22-q11.2. *Brain* 129, 235-242.
- Calcutt, N.A., Campana, W.M., Eskeland, N.L., Mohiuddin, L., Dines, K.C., Mizisin, A.P., and O'Brien, J.S. (1999). Prosaposin gene expression and the efficacy of a prosaposin-derived peptide in preventing structural and functional disorders of peripheral nerve in diabetic rats. *Journal of neuropathology and experimental neurology* 58, 628-636.
- Campana, W.M., Darin, S.J., and O'Brien, J.S. (1999). Phosphatidylinositol 3-kinase and Akt protein kinase mediate IGF-I- and prosaptide-induced survival in Schwann cells. *Journal of neuroscience research* 57, 332-341.
- Campana, W.M., Hiraiwa, M., Addison, K.C., and O'Brien, J.S. (1996). Induction of MAPK phosphorylation by prosaposin and prosaptide in PC12 cells. *Biochemical and biophysical research communications* 229, 706-712.
- Campana, W.M., Hiraiwa, M., and O'Brien, J.S. (1998). Prosaptide activates the MAPK pathway by a G-protein-dependent mechanism essential for enhanced sulfatide synthesis by Schwann cells. *Faseb J* 12, 307-314.
- Carlson, K.M., Andresen, J.M., and Orr, H.T. (2009). Emerging pathogenic pathways in the spinocerebellar ataxias. *Current opinion in genetics & development* 19, 247-253.

REFERENCES

- Chang, A.C., and Ghetti, B. (1993). Embryonic cerebellar graft development during acute phase of gliosis in the cerebellum of pcd mutant mice. *The Chinese journal of physiology* 36, 141-149.
- Chaudhry, F.A., Lehre, K.P., van Lookeren Campagne, M., Ottersen, O.P., Danbolt, N.C., and Storm-Mathisen, J. (1995). Glutamate transporters in glial plasma membranes: highly differentiated localizations revealed by quantitative ultrastructural immunocytochemistry. *Neuron* 15, 711-720.
- Chen, D.H., Brkanac, Z., Verlinde, C.L., Tan, X.J., Bylenok, L., Nochlin, D., Matsushita, M., Lipe, H., Wolff, J., Fernandez, M., *et al.* (2003). Missense mutations in the regulatory domain of PKC gamma: a new mechanism for dominant nonepisodic cerebellar ataxia. *American journal of human genetics* 72, 839-849.
- Cheng, S.S., and Heintz, N. (1997). Massive loss of mid- and hindbrain neurons during embryonic development of homozygous lurcher mice. *J Neurosci* 17, 2400-2407.
- Chien, C.T., Bartel, P.L., Sternglanz, R., and Fields, S. (1991). The two-hybrid system: a method to identify and clone genes for proteins that interact with a protein of interest. *Proceedings of the National Academy of Sciences of the United States of America* 88, 9578-9582.
- Choi, D.W. (1988). Glutamate neurotoxicity and diseases of the nervous system. *Neuron* 1, 623-634.
- Chou, A.H., Yeh, T.H., Ouyang, P., Chen, Y.L., Chen, S.Y., and Wang, H.L. (2008). Polyglutamine-expanded ataxin-3 causes cerebellar dysfunction of SCA3 transgenic mice by inducing transcriptional dysregulation. *Neurobiology of disease* 31, 89-101.

REFERENCES

- Chu, D.S., Pishvaei, B., and Payne, G.S. (1996). The light chain subunit is required for clathrin function in *Saccharomyces cerevisiae*. *The Journal of biological chemistry* *271*, 33123-33130.
- Chung, M.Y., Lu, Y.C., Cheng, N.C., and Soong, B.W. (2003). A novel autosomal dominant spinocerebellar ataxia (SCA22) linked to chromosome 1p21-q23. *Brain* *126*, 1293-1299.
- Cianci, C.D., Giorgi, M., and Morrow, J.S. (1988). Phosphorylation of ankyrin down-regulates its cooperative interaction with spectrin and protein 3. *Journal of cellular biochemistry* *37*, 301-315.
- Clark, B.A., and Barbour, B. (1997). Currents evoked in Bergmann glial cells by parallel fibre stimulation in rat cerebellar slices. *The Journal of physiology* *502* (Pt 2), 335-350.
- Coates, P.J., and Hall, P.A. (2003). The yeast two-hybrid system for identifying protein-protein interactions. *The Journal of pathology* *199*, 4-7.
- Coetzer, T., and Zail, S. (1982). Spectrin tetramer-dimer equilibrium in hereditary elliptocytosis. *Blood* *59*, 900-905.
- Cohen, C.M. (1983). The molecular organization of the red cell membrane skeleton. *Seminars in hematology* *20*, 141-158.
- Coleman, S.K., Cai, C., Mottershead, D.G., Haapalahti, J.P., and Keinanen, K. (2003). Surface expression of GluR-D AMPA receptor is dependent on an interaction between its C-terminal domain and a 4.1 protein. *J Neurosci* *23*, 798-806.
- Craig, K., Keers, S.M., Archibald, K., Curtis, A., and Chinnery, P.F. (2004). Molecular epidemiology of spinocerebellar ataxia type 6. *Annals of neurology* *55*, 752-755.

REFERENCES

- Crawley, J.N. (1999). Behavioral phenotyping of transgenic and knockout mice: experimental design and evaluation of general health, sensory functions, motor abilities, and specific behavioral tests. *Brain Res* 835, 18-26.
- Cui, W., Allen, N.D., Skynner, M., Gusterson, B., and Clark, A.J. (2001). Inducible ablation of astrocytes shows that these cells are required for neuronal survival in the adult brain. *Glia* 34, 272-282.
- Cummings, C.J., Mancini, M.A., Antalffy, B., DeFranco, D.B., Orr, H.T., and Zoghbi, H.Y. (1998). Chaperone suppression of aggregation and altered subcellular proteasome localization imply protein misfolding in SCA1. *Nature genetics* 19, 148-154.
- Cummings, C.J., Reinstein, E., Sun, Y., Antalffy, B., Jiang, Y., Ciechanover, A., Orr, H.T., Beaudet, A.L., and Zoghbi, H.Y. (1999). Mutation of the E6-AP ubiquitin ligase reduces nuclear inclusion frequency while accelerating polyglutamine-induced pathology in SCA1 mice. *Neuron* 24, 879-892.
- Custer, S.K., Garden, G.A., Gill, N., Rueb, U., Libby, R.T., Schultz, C., Guyenet, S.J., Deller, T., Westrum, L.E., Sopher, B.L., and La Spada, A.R. (2006). Bergmann glia expression of polyglutamine-expanded ataxin-7 produces neurodegeneration by impairing glutamate transport. *Nature neuroscience* 9, 1302-1311.
- Dahmane, N., and Ruiz i Altaba, A. (1999). Sonic hedgehog regulates the growth and patterning of the cerebellum. *Development (Cambridge, England)* 126, 3089-3100.
- Danbolt, N.C. (2001). Glutamate uptake. *Progress in neurobiology* 65, 1-105.
- Dang, V.T., Kassahn, K.S., Marcos, A.E., and Ragan, M.A. (2008). Identification of human haploinsufficient genes and their genomic proximity to segmental duplications. *Eur J Hum Genet* 16, 1350-1357.

REFERENCES

- Daughters, R.S., Tuttle, D.L., Gao, W., Ikeda, Y., Moseley, M.L., Ebner, T.J., Swanson, M.S., and Ranum, L.P. (2009). RNA gain-of-function in spinocerebellar ataxia type 8. *PLoS genetics* 5, e1000600.
- David, G., Abbas, N., Stevanin, G., Durr, A., Yvert, G., Cancel, G., Weber, C., Imbert, G., Saudou, F., Antoniou, E., *et al.* (1997). Cloning of the SCA7 gene reveals a highly unstable CAG repeat expansion. *Nature genetics* 17, 65-70.
- Deborde, S., Perret, E., Gravotta, D., Deora, A., Salvarezza, S., Schreiner, R., and Rodriguez-Boulan, E. (2008). Clathrin is a key regulator of basolateral polarity. *Nature* 452, 719-723.
- Devarajan, P., Stabach, P.R., De Matteis, M.A., and Morrow, J.S. (1997). Na,K-ATPase transport from endoplasmic reticulum to Golgi requires the Golgi spectrin-ankyrin G119 skeleton in Madin Darby canine kidney cells. *Proceedings of the National Academy of Sciences of the United States of America* 94, 10711-10716.
- Devos, D., Schraen-Maschke, S., Vuillaume, I., Dujardin, K., Naze, P., Willoteaux, C., Destee, A., and Sablonniere, B. (2001). Clinical features and genetic analysis of a new form of spinocerebellar ataxia. *Neurology* 56, 234-238.
- Dhermy, D., Lecomte, M.C., Garbarz, M., Bournier, O., Galand, C., Gautero, H., Feo, C., Alloisio, N., Delaunay, J., and Boivin, P. (1982). Spectrin beta-chain variant associated with hereditary elliptocytosis. *The Journal of clinical investigation* 70, 707-715.
- Diamond, J.S. (2001). Neuronal glutamate transporters limit activation of NMDA receptors by neurotransmitter spillover on CA1 pyramidal cells. *J Neurosci* 21, 8328-8338.

REFERENCES

- DiFiglia, M., Sapp, E., Chase, K.O., Davies, S.W., Bates, G.P., Vonsattel, J.P., and Aronin, N. (1997). Aggregation of huntingtin in neuronal intranuclear inclusions and dystrophic neurites in brain. *Science (New York, N.Y)* 277, 1990-1993.
- Di Bella, D., Lazzaro, F., Brusco, A., Plumari, M., Battaglia, G., Pastore, A., Finardi, A., Cagnoli, C., Tempia, F., Frontali, M., *et al.* (2010). Mutations in the mitochondrial protease gene AFG3L2 cause dominant hereditary ataxia SCA28. *Nat. Genetics*. 42 (4) : 313-321.
- Dobbing, J., and Sands, J. (1973). Quantitative growth and development of human brain. *Archives of disease in childhood* 48, 757-767.
- Duenas, A.M., Goold, R., and Giunti, P. (2006). Molecular pathogenesis of spinocerebellar ataxias. *Brain* 129, 1357-1370.
- Dugas, C., and Smith, A.M. (1992). Responses of cerebellar Purkinje cells to slip of a hand-held object. *Journal of neurophysiology* 67, 483-495.
- Dumesnil-Bousez, N., and Sotelo, C. (1992). Early development of the Lurcher cerebellum: Purkinje cell alterations and impairment of synaptogenesis. *Journal of neurocytology* 21, 506-529.
- Dunham, N.W., and Miya, T.S. (1957). A note on a simple apparatus for detecting neurological deficit in rats and mice. *Journal of the American Pharmaceutical Association* 46, 208-209.
- Dzubay, J.A., and Jahr, C.E. (1999). The concentration of synaptically released glutamate outside of the climbing fiber-Purkinje cell synaptic cleft. *J Neurosci* 19, 5265-5274.
- Eaton, B.A., Fetter, R.D., and Davis, G.W. (2002). Dynactin is necessary for synapse stabilization. *Neuron* 34, 729-741.

REFERENCES

- Eber, S., and Lux, S.E. (2004). Hereditary spherocytosis--defects in proteins that connect the membrane skeleton to the lipid bilayer. *Seminars in hematology* 41, 118-141.
- Eber, S.W., Morris, S.A., Schroter, W., and Gratzer, W.B. (1988). Interactions of spectrin in hereditary elliptocytes containing truncated spectrin beta-chains. *The Journal of clinical investigation* 81, 523-530.
- Eccles, J.C., Ito, M. and Szentagothai, J. (1967). *The Cerebellum as a Neuronal Machine*, New York, Heidelberg: Springer-Verlag.
- Ekerot, C.F., and Kano, M. (1985). Long-term depression of parallel fibre synapses following stimulation of climbing fibres. *Brain Res* 342, 357-360.
- Elleder, M., Jerabkova, M., Befekadu, A., Hrebicek, M., Berna, L., Ledvinova, J., Hulkova, H., Rosewich, H., Schymik, N., Paton, B.C., and Harzer, K. (2005). Prosaposin deficiency -- a rarely diagnosed, rapidly progressing, neonatal neurovisceral lipid storage disease. Report of a further patient. *Neuropediatrics* 36, 171-180.
- Emamian, E.S., Kaytor, M.D., Duvick, L.A., Zu, T., Tousey, S.K., Zoghbi, H.Y., Clark, H.B., and Orr, H.T. (2003). Serine 776 of ataxin-1 is critical for polyglutamine-induced disease in SCA1 transgenic mice. *Neuron* 38, 375-387.
- Engqvist-Goldstein, A.E., Warren, R.A., Kessels, M.M., Keen, J.H., Heuser, J., and Drubin, D.G. (2001). The actin-binding protein Hip1R associates with clathrin during early stages of endocytosis and promotes clathrin assembly in vitro. *The Journal of cell biology* 154, 1209-1223.
- Engqvist-Goldstein, A.E., Zhang, C.X., Carreno, S., Barroso, C., Heuser, J.E., and Drubin, D.G. (2004). RNAi-mediated Hip1R silencing results in stable association between the endocytic machinery and the actin assembly machinery. *Molecular biology of the cell* 15, 1666-1679.

REFERENCES

- Eunson, L.H., Rea, R., Zuberi, S.M., Youroukos, S., Panayiotopoulos, C.P., Liguori, R., Avoni, P., McWilliam, R.C., Stephenson, J.B., Hanna, M.G., *et al.* (2000). Clinical, genetic, and expression studies of mutations in the potassium channel gene KCNA1 reveal new phenotypic variability. *Annals of neurology* 48, 647-656.
- Featherstone, D.E., Davis, W.S., Dubreuil, R.R., and Broadie, K. (2001). Drosophila alpha- and beta-spectrin mutations disrupt presynaptic neurotransmitter release. *J Neurosci* 21, 4215-4224.
- Fernandez-Gonzalez, A., La Spada, A.R., Treadaway, J., Higdon, J.C., Harris, B.S., Sidman, R.L., Morgan, J.I., and Zuo, J. (2002). Purkinje cell degeneration (pcd) phenotypes caused by mutations in the axotomy-induced gene, *Nna1*. *Science (New York, N.Y)* 295, 1904-1906.
- Ferrer, I., Kapfhammer, J.P., Hindelang, C., Kemp, S., Troffer-Charlier, N., Broccoli, V., Callyzot, N., Mooyer, P., Selhorst, J., Vreken, P., *et al.* (2005). Inactivation of the peroxisomal ABCD2 transporter in the mouse leads to late-onset ataxia involving mitochondria, Golgi and endoplasmic reticulum damage. *Human molecular genetics* 14, 3565-3577.
- Flanigan, K., Gardner, K., Alderson, K., Galster, B., Otterud, B., Leppert, M.F., Kaplan, C., and Ptacek, L.J. (1996). Autosomal dominant spinocerebellar ataxia with sensory axonal neuropathy (SCA4): clinical description and genetic localization to chromosome 16q22.1. *American journal of human genetics* 59, 392-399.
- Flourens, P. (1824). *Rescherches experimentales sur les Proprietes et les Fonctions du Systeme Nerveux dans les Animaux Vertebres*. Paris: Crevot.
- Fotin, A., Cheng, Y., Sliz, P., Grigorieff, N., Harrison, S.C., Kirchhausen, T., and Walz, T. (2004). Molecular model for a complete clathrin lattice from electron cryomicroscopy. *Nature* 432, 573-579.

REFERENCES

- Fujita, N., Suzuki, K., Vanier, M.T., Popko, B., Maeda, N., Klein, A., Henseler, M., Sandhoff, K., Nakayasu, H., and Suzuki, K. (1996). Targeted disruption of the mouse sphingolipid activator protein gene: a complex phenotype, including severe leukodystrophy and wide-spread storage of multiple sphingolipids. *Human molecular genetics* 5, 711-725.
- Furuta, A., Rothstein, J.D., and Martin, L.J. (1997). Glutamate transporter protein subtypes are expressed differentially during rat CNS development. *J Neurosci* 17, 8363-8375.
- Gallagher, P.G. (2005). Hematologically important mutations: ankyrin variants in hereditary spherocytosis. *Blood cells, molecules & diseases* 35, 345-347.
- Garbarz, M., Boulanger, L., Pedroni, S., Lecomte, M.C., Gautero, H., Galand, C., Boivin, P., Feldman, L., and Dhermy, D. (1992). Spectrin beta Tandil, a novel shortened beta-chain variant associated with hereditary elliptocytosis is due to a deletional frameshift mutation in the beta-spectrin gene. *Blood* 80, 1066-1073.
- Garcin, R (1969). The ataxias. In *Handbook of Clinical Neurology*, ed. P.J. Vinken and G.W. Bruyn, pp.309-55. Amsterdam: North-Holland Publishing Company.
- Gardner, R.J., Knight, M.A., Hara, K., Tsuji, S., Forrest, S.M., and Storey, E. (2005). Spinocerebellar ataxia type 15. *Cerebellum (London, England)* 4, 47-50.
- Garg, M.K., and Sanchette, P.C. (1999). Ion channels and channelopathy. *The Journal of the Association of Physicians of India* 47, 436-439.
- Gellman, R., Gibson, A.R., and Houk, J.C. (1985). Inferior olivary neurons in the awake cat: detection of contact and passive body displacement. *Journal of neurophysiology* 54, 40-60.

REFERENCES

- Gelman, M.S., and Kopito, R.R. (2002). Rescuing protein conformation: prospects for pharmacological therapy in cystic fibrosis. *The Journal of clinical investigation* *110*, 1591-1597.
- Gilbert, P.F., and Thach, W.T. (1977). Purkinje cell activity during motor learning. *Brain Res* *128*, 309-328.
- Gillardot, F., Baurle, J., Wickert, H., Grusser-Cornehls, U., and Zimmermann, M. (1995). Differential regulation of bcl-2, bax, c-fos, junB, and krox-24 expression in the cerebellum of Purkinje cell degeneration mutant mice. *Journal of neuroscience research* *41*, 708-715.
- Girard, M., Allaire, P.D., McPherson, P.S., and Blondeau, F. (2005). Non-stoichiometric relationship between clathrin heavy and light chains revealed by quantitative comparative proteomics of clathrin-coated vesicles from brain and liver. *Mol Cell Proteomics* *4*, 1145-1154.
- Gold, D.A., Baek, S.H., Schork, N.J., Rose, D.W., Larsen, D.D., Sachs, B.D., Rosenfeld, M.G., and Hamilton, B.A. (2003). ROR α coordinates reciprocal signaling in cerebellar development through sonic hedgehog and calcium-dependent pathways. *Neuron* *40*, 1119-1131.
- Goldfarb, M., Schoorlemmer, J., Williams, A., Diwakar, S., Wang, Q., Huang, X., Giza, J., Tchetchik, D., Kelley, K., Vega, A., *et al.* (2007). Fibroblast growth factor homologous factors control neuronal excitability through modulation of voltage-gated sodium channels. *Neuron* *55*, 449-463.
- Gough, L.L., Fan, J., Chu, S., Winnick, S., and Beck, K.A. (2003). Golgi localization of Syne-1. *Molecular biology of the cell* *14*, 2410-2424.

REFERENCES

- Gouw, L.G., Digre, K.B., Harris, C.P., Haines, J.H., and Ptacek, L.J. (1994). Autosomal dominant cerebellar ataxia with retinal degeneration: clinical, neuropathologic, and genetic analysis of a large kindred. *Neurology* *44*, 1441-1447.
- Greenquist, A.C., Shohet, S.B., and Bernstein, S.E. (1978). Marked reduction of spectrinin hereditary spherocytosis in the common house mouse. *Blood* *51*, 1149-1155.
- Grusser-Cornehls, U., Grusser, C., and Baurle, J. (1999). Vermectomy enhances parvalbumin expression and improves motor performance in weaver mutant mice: an animal model for cerebellar ataxia. *Neuroscience* *91*, 315-326.
- Hafezparast, M., Klocke, R., Ruhrberg, C., Marquardt, A., Ahmad-Annuar, A., Bowen, S., Lalli, G., Witherden, A.S., Hummerich, H., Nicholson, S., *et al.* (2003). Mutations in dynein link motor neuron degeneration to defects in retrograde transport. *Science* (New York, N.Y. *300*, 808-812.
- Hamilton, B.A., Frankel, W.N., Kerrebrock, A.W., Hawkins, T.L., FitzHugh, W., Kusumi, K., Russell, L.B., Mueller, K.L., van Berkel, V., Birren, B.W., *et al.* (1996). Disruption of the nuclear hormone receptor RORalpha in staggerer mice. *Nature* *379*, 736-739.
- Hammarlund, M., Davis, W.S., and Jorgensen, E.M. (2000). Mutations in beta-spectrin disrupt axon outgrowth and sarcomere structure. *The Journal of cell biology* *149*, 931-942.
- Hammarlund, M., Jorgensen, E.M., and Bastiani, M.J. (2007). Axons break in animals lacking beta-spectrin. *The Journal of cell biology* *176*, 269-275.
- Hanspal, M., and Palek, J. (1987). Synthesis and assembly of membrane skeletal proteins in mammalian red cell precursors. *The Journal of cell biology* *105*, 1417-1424.

REFERENCES

- Hara, K., Shiga, A., Nozaki, H., Mitsui, J., Takahashi, Y., Ishiguro, H., Yomono, H., Kurisaki, H., Goto, J., Ikeuchi, T., *et al.* (2008). Total deletion and a missense mutation of ITPR1 in Japanese SCA15 families. *Neurology* *71*, 547-551.
- Harding, A.E. (1993). Clinical features and classification of inherited ataxias. *Advances in neurology* *61*, 1-14.
- Harris, A., Morgan, J.I., Pecot, M., Soumare, A., Osborne, A., and Soares, H.D. (2000). Regenerating motor neurons express Nna1, a novel ATP/GTP-binding protein related to zinc carboxypeptidases. *Molecular and cellular neurosciences* *16*, 578-596.
- Harzer, K., Paton, B.C., Poulos, A., Kustermann-Kuhn, B., Roggendorf, W., Grisar, T., and Popp, M. (1989). Sphingolipid activator protein deficiency in a 16-week-old atypical Gaucher disease patient and his fetal sibling: biochemical signs of combined sphingolipidoses. *European journal of pediatrics* *149*, 31-39.
- Hassan, A.J., Zeng, J., Ni, X., and Morales, C.R. (2004). The trafficking of prosaposin (SGP-1) and GM2AP to the lysosomes of TM4 Sertoli cells is mediated by sortilin and monomeric adaptor proteins. *Molecular reproduction and development* *68*, 476-483.
- He, Y., Zu, T., Benzow, K.A., Orr, H.T., Clark, H.B., and Koob, M.D. (2006). Targeted deletion of a single Sca8 ataxia locus allele in mice causes abnormal gait, progressive loss of motor coordination, and Purkinje cell dendritic deficits. *J Neurosci* *26*, 9975-9982.
- Henry, K.R., D'Hondt, K., Chang, J., Newpher, T., Huang, K., Hudson, R.T., Riezman, H., and Lemmon, S.K. (2002). Scd5p and clathrin function are important for cortical actin organization, endocytosis, and localization of sla2p in yeast. *Molecular biology of the cell* *13*, 2607-2625.

REFERENCES

- Hentze, M.W., and Kulozik, A.E. (1999). A perfect message: RNA surveillance and nonsense-mediated decay. *Cell* *96*, 307-310.
- Herrup, K. (1983). Role of staggerer gene in determining cell number in cerebellar cortex. I. Granule cell death is an indirect consequence of staggerer gene action. *Brain Res* *313*, 267-274.
- Herrup, K., and Mullen, R.J. (1979a). Regional variation and absence of large neurons in the cerebellum of the staggerer mouse. *Brain Res* *172*, 1-12.
- Herrup, K., and Mullen, R.J. (1979b). Staggerer chimeras: intrinsic nature of Purkinje cell defects and implications for normal cerebellar development. *Brain Res* *178*, 443-457.
- Hineno, T., Sano, A., Kondoh, K., Ueno, S., Kakimoto, Y., and Yoshida, K. (1991). Secretion of sphingolipid hydrolase activator precursor, prosaposin. *Biochemical and biophysical research communications* *176*, 668-674.
- Hiraiwa, M., O'Brien, J.S., Kishimoto, Y., Galdzicka, M., Fluharty, A.L., Ginns, E.I., and Martin, B.M. (1993). Isolation, characterization, and proteolysis of human prosaposin, the precursor of saposins (sphingolipid activator proteins). *Archives of biochemistry and biophysics* *304*, 110-116.
- Hiraiwa, M., Soeda, S., Kishimoto, Y., and O'Brien, J.S. (1992). Binding and transport of gangliosides by prosaposin. *Proceedings of the National Academy of Sciences of the United States of America* *89*, 11254-11258.
- Hiraiwa, M., Taylor, E.M., Campana, W.M., Darin, S.J., and O'Brien, J.S. (1997). Cell death prevention, mitogen-activated protein kinase stimulation, and increased sulfatide concentrations in Schwann cells and oligodendrocytes by prosaposin and prosaptides. *Proceedings of the National Academy of Sciences of the United States of America* *94*, 4778-4781.

REFERENCES

- Holleran, E.A., Karki, S., and Holzbaur, E.L. (1998). The role of the dynactin complex in intracellular motility. *International review of cytology* 182, 69-109.
- Holleran, E.A., Ligon, L.A., Tokito, M., Stankewich, M.C., Morrow, J.S., and Holzbaur, E.L. (2001). beta III spectrin binds to the Arp1 subunit of dynactin. *The Journal of biological chemistry* 276, 36598-36605.
- Holmberg, M., Duyckaerts, C., Durr, A., Cancel, G., Gourfinkel-An, I., Damier, P., Faucheux, B., Trottier, Y., Hirsch, E.C., Agid, Y., and Brice, A. (1998). Spinocerebellar ataxia type 7 (SCA7): a neurodegenerative disorder with neuronal intranuclear inclusions. *Human molecular genetics* 7, 913-918.
- Holmes, G. 1939. The cerebellum of man. The Hughlings Jackson memorial lecture. *Brain* 62: 1-30.
- Holmes, S.E., O'Hearn, E.E., McInnis, M.G., Gorelick-Feldman, D.A., Kleiderlein, J.J., Callahan, C., Kwak, N.G., Ingersoll-Ashworth, R.G., Sherr, M., Sumner, A.J., *et al.* (1999). Expansion of a novel CAG trinucleotide repeat in the 5' region of PPP2R2B is associated with SCA12. *Nature genetics* 23, 391-392.
- Houlden, H., Johnson, J., Gardner-Thorpe, C., Lashley, T., Hernandez, D., Worth, P., Singleton, A.B., Hilton, D.A., Holton, J., Revesz, T., *et al.* (2007). Mutations in TTBK2, encoding a kinase implicated in tau phosphorylation, segregate with spinocerebellar ataxia type 11. *Nature genetics* 39, 1434-1436.
- Howland, D.S., Liu, J., She, Y., Goad, B., Maragakis, N.J., Kim, B., Erickson, J., Kulik, J., DeVito, L., Psaltis, G., *et al.* (2002). Focal loss of the glutamate transporter EAAT2 in a transgenic rat model of SOD1 mutant-mediated amyotrophic lateral sclerosis (ALS). *Proceedings of the National Academy of Sciences of the United States of America* 99, 1604-1609.

REFERENCES

- Hu, C.D., Chinenov, Y., and Kerppola, T.K. (2002). Visualization of interactions among bZIP and Rel family proteins in living cells using bimolecular fluorescence complementation. *Molecular cell* 9, 789-798.
- Huang, K.M., Gullberg, L., Nelson, K.K., Stefan, C.J., Blumer, K., and Lemmon, S.K. (1997). Novel functions of clathrin light chains: clathrin heavy chain trimerization is defective in light chain-deficient yeast. *Journal of cell science* 110 (Pt 7), 899-910.
- Huang, Y.H., Dykes-Hoberg, M., Tanaka, K., Rothstein, J.D., and Bergles, D.E. (2004). Climbing fiber activation of EAAT4 transporters and kainate receptors in cerebellar Purkinje cells. *J Neurosci* 24, 103-111.
- Hulkova, H., Cervenkova, M., Ledvinova, J., Tochackova, M., Hrebicek, M., Poupetova, H., Befekadu, A., Berna, L., Paton, B.C., Harzer, K., *et al.* (2001). A novel mutation in the coding region of the prosaposin gene leads to a complete deficiency of prosaposin and saposins, and is associated with a complex sphingolipidosis dominated by lactosylceramide accumulation. *Human molecular genetics* 10, 927-940.
- Igase, K., Tanaka, J., Kumon, Y., Zhang, B., Sadamoto, Y., Maeda, N., Sakaki, S., and Sakanaka, M. (1999). An 18-mer peptide fragment of prosaposin ameliorates place navigation disability, cortical infarction, and retrograde thalamic degeneration in rats with focal cerebral ischemia. *J Cereb Blood Flow Metab* 19, 298-306.
- Igdoura, S.A., Rasky, A., and Morales, C.R. (1996). Trafficking of sulfated glycoprotein-1 (prosaposin) to lysosomes or to the extracellular space in rat Sertoli cells. *Cell and tissue research* 283, 385-394.

REFERENCES

- Ikeda, H., Yamaguchi, M., Sugai, S., Aze, Y., Narumiya, S., and Kakizuka, A. (1996). Expanded polyglutamine in the Machado-Joseph disease protein induces cell death in vitro and in vivo. *Nature genetics* *13*, 196-202.
- Ikeda, Y., Dick, K.A., Weatherspoon, M.R., Gincel, D., Armbrust, K.R., Dalton, J.C., Stevanin, G., Durr, A., Zuhlke, C., Burk, K., *et al.* (2006). Spectrin mutations cause spinocerebellar ataxia type 5. *Nature genetics* *38*, 184-190.
- Imbert, G., Saudou, F., Yvert, G., Devys, D., Trottier, Y., Garnier, J.M., Weber, C., Mandel, J.L., Cancel, G., Abbas, N., *et al.* (1996). Cloning of the gene for spinocerebellar ataxia 2 reveals a locus with high sensitivity to expanded CAG/glutamine repeats. *Nature genetics* *14*, 285-291.
- Irizarry, M.C., McNamara, M., Fedorchak, K., Hsiao, K., and Hyman, B.T. (1997). APPSw transgenic mice develop age-related A beta deposits and neuropil abnormalities, but no neuronal loss in CA1. *Journal of neuropathology and experimental neurology* *56*, 965-973.
- Ishikawa, K., Toru, S., Tsunemi, T., Li, M., Kobayashi, K., Yokota, T., Amino, T., Owada, K., Fujigasaki, H., Sakamoto, M., *et al.* (2005). An autosomal dominant cerebellar ataxia linked to chromosome 16q22.1 is associated with a single-nucleotide substitution in the 5' untranslated region of the gene encoding a protein with spectrin repeat and Rho guanine-nucleotide exchange-factor domains. *American journal of human genetics* *77*, 280-296.
- Ito, M., Sakurai, M., and Tongroach, P. (1982). Climbing fibre induced depression of both mossy fibre responsiveness and glutamate sensitivity of cerebellar Purkinje cells. *The Journal of physiology* *324*, 113-134.
- Iwaki, A., Kawano, Y., Miura, S., Shibata, H., Matsuse, D., Li, W., Furuya, H., Ohyagi, Y., Taniwaki, T., Kira, J., and Fukumaki, Y. (2008). Heterozygous deletion of ITPR1,

REFERENCES

- but not SUMF1, in spinocerebellar ataxia type 16. *Journal of medical genetics* 45, 32-35.
- Jackson, M., Song, W., Liu, M.Y., Jin, L., Dykes-Hoberg, M., Lin, C.I., Bowers, W.J., Federoff, H.J., Sternweis, P.C., and Rothstein, J.D. (2001). Modulation of the neuronal glutamate transporter EAAT4 by two interacting proteins. *Nature* 410, 89-93.
- Jen, J.C., Wan, J., Palos, T.P., Howard, B.D., and Baloh, R.W. (2005). Mutation in the glutamate transporter EAAT1 causes episodic ataxia, hemiplegia, and seizures. *Neurology* 65, 529-534.
- Jenkins, S.M., and Bennett, V. (2001). Ankyrin-G coordinates assembly of the spectrin-based membrane skeleton, voltage-gated sodium channels, and L1 CAMs at Purkinje neuron initial segments. *The Journal of cell biology* 155, 739-746.
- Kaksonen, M., Sun, Y., and Drubin, D.G. (2003). A pathway for association of receptors, adaptors, and actin during endocytic internalization. *Cell* 115, 475-487.
- Kalume, F., Yu, F.H., Westenbroek, R.E., Scheuer, T., and Catterall, W.A. (2007). Reduced sodium current in Purkinje neurons from Nav1.1 mutant mice: implications for ataxia in severe myoclonic epilepsy in infancy. *J Neurosci* 27, 11065-11074.
- Kanaseki, T., and Kadota, K. (1969). The "vesicle in a basket". A morphological study of the coated vesicle isolated from the nerve endings of the guinea pig brain, with special reference to the mechanism of membrane movements. *The Journal of cell biology* 42, 202-220.
- Kane, S.A., Goodkin, H.P., Keating, J.G., Thach, W.T. 1989. Incoordination in attempted reaching and pinching after inactivation of cerebellar dentate nucleus. *Abstr. Soc. Neurosci.* 15:52.

REFERENCES

- Kane, S.A., Mink, J.W., Thach, W.T. 1988. Fastigial, interposed, and dentate cerebellar nuclei: Somatotopic organization and the movements differentially controlled by each. *Soc. Neurosci. Abstr.* 14:954.
- Kano, M., and Kato, M. (1987). Quisqualate receptors are specifically involved in cerebellar synaptic plasticity. *Nature* 325, 276-279.
- Kapitein, L.C., Schlager, M.A., Kuijpers, M., Wulf, P.S., van Spronsen, M., MacKintosh, F.C., and Hoogenraad, C.C. (2010). Mixed microtubules steer dynein-driven cargo transport into dendrites. *Curr Biol* 20, 290-299.
- Karki, S., and Holzbaaur, E.L. (1995). Affinity chromatography demonstrates a direct binding between cytoplasmic dynein and the dynactin complex. *The Journal of biological chemistry* 270, 28806-28811.
- Karki, S., LaMonte, B., and Holzbaaur, E.L. (1998). Characterization of the p22 subunit of dynactin reveals the localization of cytoplasmic dynein and dynactin to the midbody of dividing cells. *The Journal of cell biology* 142, 1023-1034.
- Kashiwabuchi, N., Ikeda, K., Araki, K., Hirano, T., Shibuki, K., Takayama, C., Inoue, Y., Kutsuwada, T., Yagi, T., Kang, Y., and et al. (1995). Impairment of motor coordination, Purkinje cell synapse formation, and cerebellar long-term depression in GluR delta 2 mutant mice. *Cell* 81, 245-252.
- Kawaguchi, Y., Okamoto, T., Taniwaki, M., Aizawa, M., Inoue, M., Katayama, S., Kawakami, H., Nakamura, S., Nishimura, M., Akiguchi, I., and et al. (1994). CAG expansions in a novel gene for Machado-Joseph disease at chromosome 14q32.1. *Nature genetics* 8, 221-228.

REFERENCES

- Kennedy, S.P., Warren, S.L., Forget, B.G., and Morrow, J.S. (1991). Ankyrin binds to the 15th repetitive unit of erythroid and nonerythroid beta-spectrin. *The Journal of cell biology* *115*, 267-277.
- Kihara, A., Kabeya, Y., Ohsumi, Y., and Yoshimori, T. (2001). Beclin-phosphatidylinositol 3-kinase complex functions at the trans-Golgi network. *EMBO reports* *2*, 330-335.
- Kim, S.J., Zhang, Z., Hitomi, E., Lee, Y.C., and Mukherjee, A.B. (2006). Endoplasmic reticulum stress-induced caspase-4 activation mediates apoptosis and neurodegeneration in INCL. *Human molecular genetics* *15*, 1826-1834.
- Kirchhausen, T. (2000). Clathrin. *Annual review of biochemistry* *69*, 699-727.
- Kirchhausen, T., and Harrison, S.C. (1981). Protein organization in clathrin trimers. *Cell* *23*, 755-761.
- Kishimoto, Y., Hiraiwa, M., and O'Brien, J.S. (1992). Saposins: structure, function, distribution, and molecular genetics. *Journal of lipid research* *33*, 1255-1267.
- Klement, I.A., Skinner, P.J., Kaytor, M.D., Yi, H., Hersch, S.M., Clark, H.B., Zoghbi, H.Y., and Orr, H.T. (1998). Ataxin-1 nuclear localization and aggregation: role in polyglutamine-induced disease in SCA1 transgenic mice. *Cell* *95*, 41-53.
- Knight, M.A., Gardner, R.J., Bahlo, M., Matsuura, T., Dixon, J.A., Forrest, S.M., and Storey, E. (2004). Dominantly inherited ataxia and dysphonia with dentate calcification: spinocerebellar ataxia type 20. *Brain* *127*, 1172-1181.
- Knight, M.A., Kennerson, M.L., Anney, R.J., Matsuura, T., Nicholson, G.A., Salimi-Tari, P., Gardner, R.J., Storey, E., and Forrest, S.M. (2003). Spinocerebellar ataxia type 15 (sca15) maps to 3p24.2-3pter: exclusion of the ITPR1 gene, the human orthologue of an ataxic mouse mutant. *Neurobiology of disease* *13*, 147-157.

REFERENCES

- Kolter, T., and Sandhoff, K. (2005). Principles of lysosomal membrane digestion: stimulation of sphingolipid degradation by sphingolipid activator proteins and anionic lysosomal lipids. *Annual review of cell and developmental biology* *21*, 81-103.
- Komada, M., and Soriano, P. (2002). [Beta]IV-spectrin regulates sodium channel clustering through ankyrin-G at axon initial segments and nodes of Ranvier. *The Journal of cell biology* *156*, 337-348.
- Kondoh, K., Hineno, T., Sano, A., and Kakimoto, Y. (1991). Isolation and characterization of prosaposin from human milk. *Biochemical and biophysical research communications* *181*, 286-292.
- Koob, M.D., Moseley, M.L., Schut, L.J., Benzow, K.A., Bird, T.D., Day, J.W., and Ranum, L.P. (1999). An untranslated CTG expansion causes a novel form of spinocerebellar ataxia (SCA8). *Nature genetics* *21*, 379-384.
- Kordasiewicz, H.B., Thompson, R.M., Clark, H.B., and Gomez, C.M. (2006). C-termini of P/Q-type Ca²⁺ channel alpha1A subunits translocate to nuclei and promote polyglutamine-mediated toxicity. *Human molecular genetics* *15*, 1587-1599.
- Kotani, Y., Matsuda, S., Sakanaka, M., Kondoh, K., Ueno, S., and Sano, A. (1996a). Prosaposin facilitates sciatic nerve regeneration in vivo. *Journal of neurochemistry* *66*, 2019-2025.
- Kotani, Y., Matsuda, S., Wen, T.C., Sakanaka, M., Tanaka, J., Maeda, N., Kondoh, K., Ueno, S., and Sano, A. (1996b). A hydrophilic peptide comprising 18 amino acid residues of the prosaposin sequence has neurotrophic activity in vitro and in vivo. *Journal of neurochemistry* *66*, 2197-2200.

REFERENCES

- Koyano, S., Uchihara, T., Fujigasaki, H., Nakamura, A., Yagishita, S., and Iwabuchi, K. (2000). Neuronal intranuclear inclusions in spinocerebellar ataxia type 2. *Annals of neurology* 47, 550.
- Kraemer, B.C., Burgess, J.K., Chen, J.H., Thomas, J.H., and Schellenberg, G.D. (2006). Molecular pathways that influence human tau-induced pathology in *Caenorhabditis elegans*. *Human molecular genetics* 15, 1483-1496.
- Kreda, S.M., Fujita, N., and Suzuki, K. (1994). Expression of sphingolipid activator protein gene in brain and systemic organs of developing mice. *Developmental neuroscience* 16, 90-99.
- Kubodera, T., Yokota, T., Ohwada, K., Ishikawa, K., Miura, H., Matsuoka, T., and Mizusawa, H. (2003). Proteolytic cleavage and cellular toxicity of the human alpha1A calcium channel in spinocerebellar ataxia type 6. *Neuroscience letters* 341, 74-78.
- Kurihara, H., Hashimoto, K., Kano, M., Takayama, C., Sakimura, K., Mishina, M., Inoue, Y., and Watanabe, M. (1997). Impaired parallel fiber-->Purkinje cell synapse stabilization during cerebellar development of mutant mice lacking the glutamate receptor delta2 subunit. *J Neurosci* 17, 9613-9623.
- Kyuhou, S., Kato, N., and Gemba, H. (2006). Emergence of endoplasmic reticulum stress and activated microglia in Purkinje cell degeneration mice. *Neuroscience letters* 396, 91-96.
- Laezza, F., Gerber, B.R., Lou, J.Y., Kozel, M.A., Hartman, H., Craig, A.M., Ornitz, D.M., and Nerbonne, J.M. (2007). The FGF14(F145S) mutation disrupts the interaction of FGF14 with voltage-gated Na⁺ channels and impairs neuronal excitability. *J Neurosci* 27, 12033-12044.

REFERENCES

- Lambert, S., and Bennett, V. (1993). Postmitotic expression of ankyrinR and beta R-spectrin in discrete neuronal populations of the rat brain. *J Neurosci* *13*, 3725-3735.
- LaMonte, B.H., Wallace, K.E., Holloway, B.A., Shelly, S.S., Ascano, J., Tokito, M., Van Winkle, T., Howland, D.S., and Holzbaur, E.L. (2002). Disruption of dynein/dynactin inhibits axonal transport in motor neurons causing late-onset progressive degeneration. *Neuron* *34*, 715-727.
- Landis, S.C., and Mullen, R.J. (1978). The development and degeneration of Purkinje cells in pcd mutant mice. *The Journal of comparative neurology* *177*, 125-143.
- Leavitt, B.R., Guttman, J.A., Hodgson, J.G., Kimel, G.H., Singaraja, R., Vogl, A.W., and Hayden, M.R. (2001). Wild-type huntingtin reduces the cellular toxicity of mutant huntingtin in vivo. *American journal of human genetics* *68*, 313-324.
- Lee, W.C., Yoshihara, M., and Littleton, J.T. (2004). Cytoplasmic aggregates trap polyglutamine-containing proteins and block axonal transport in a *Drosophila* model of Huntington's disease. *Proceedings of the National Academy of Sciences of the United States of America* *101*, 3224-3229.
- Legendre-Guillemain, V., Metzler, M., Charbonneau, M., Gan, L., Chopra, V., Philie, J., Hayden, M.R., and McPherson, P.S. (2002). HIP1 and HIP12 display differential binding to F-actin, AP2, and clathrin. Identification of a novel interaction with clathrin light chain. *The Journal of biological chemistry* *277*, 19897-19904.
- Leshchyn'ska, I., Sytnyk, V., Morrow, J.S., and Schachner, M. (2003). Neural cell adhesion molecule (NCAM) association with PKCbeta2 via betaI spectrin is implicated in NCAM-mediated neurite outgrowth. *The Journal of cell biology* *161*, 625-639.

REFERENCES

- Levin, S.I., Khaliq, Z.M., Aman, T.K., Grieco, T.M., Kearney, J.A., Raman, I.M., and Meisler, M.H. (2006). Impaired motor function in mice with cell-specific knockout of sodium channel *Scn8a* (NaV1.6) in cerebellar purkinje neurons and granule cells. *Journal of neurophysiology* 96, 785-793.
- Li, A., and Harris, D.A. (2005). Mammalian prion protein suppresses Bax-induced cell death in yeast. *The Journal of biological chemistry* 280, 17430-17434.
- Li, H., Li, S.H., Johnston, H., Shelbourne, P.F., and Li, X.J. (2000). Amino-terminal fragments of mutant huntingtin show selective accumulation in striatal neurons and synaptic toxicity. *Nature genetics* 25, 385-389.
- Li, H., Li, S.H., Yu, Z.X., Shelbourne, P., and Li, X.J. (2001). Huntingtin aggregate-associated axonal degeneration is an early pathological event in Huntington's disease mice. *J Neurosci* 21, 8473-8481.
- Liang, X.H., Jackson, S., Seaman, M., Brown, K., Kempkes, B., Hibshoosh, H., and Levine, B. (1999). Induction of autophagy and inhibition of tumorigenesis by beclin 1. *Nature* 402, 672-676.
- Ligon, L.A., LaMonte, B.H., Wallace, K.E., Weber, N., Kalb, R.G., and Holzbaur, E.L. (2005). Mutant superoxide dismutase disrupts cytoplasmic dynein in motor neurons. *Neuroreport* 16, 533-536.
- Lim, J., Crespo-Barreto, J., Jafar-Nejad, P., Bowman, A.B., Richman, R., Hill, D.E., Orr, H.T., and Zoghbi, H.Y. (2008). Opposing effects of polyglutamine expansion on native protein complexes contribute to SCA1. *Nature* 452, 713-718.
- Lin, C.L., Bristol, L.A., Jin, L., Dykes-Hoberg, M., Crawford, T., Clawson, L., and Rothstein, J.D. (1998). Aberrant RNA processing in a neurodegenerative disease: the

REFERENCES

- cause for absent EAAT2, a glutamate transporter, in amyotrophic lateral sclerosis. *Neuron* 20, 589-602.
- Lin, D.T., Makino, Y., Sharma, K., Hayashi, T., Neve, R., Takamiya, K., and Huganir, R.L. (2009). Regulation of AMPA receptor extrasynaptic insertion by 4.1N, phosphorylation and palmitoylation. *Nature neuroscience* 12, 879-887.
- Lin, X., Antalffy, B., Kang, D., Orr, H.T., and Zoghbi, H.Y. (2000). Polyglutamine expansion down-regulates specific neuronal genes before pathologic changes in SCA1. *Nature neuroscience* 3, 157-163.
- Liu, C.J., Dib-Hajj, S.D., Renganathan, M., Cummins, T.R., and Waxman, S.G. (2003). Modulation of the cardiac sodium channel Nav1.5 by fibroblast growth factor homologous factor 1B. *The Journal of biological chemistry* 278, 1029-1036.
- Liu, C., Dib-Hajj, S.D., Waxman, S.G. Fibroblast growth factor homologous factor 1B binds to the C terminus of the tetrodotoxin-resistant sodium channel rNav1.9a (NaN). *J Biol Chem.* 2001; 276: 18925-18933.
- Liu, S.C., Palek, J., and Prchal, J.T. (1982). Defective spectrin dimer-dimer association with hereditary elliptocytosis. *Proceedings of the National Academy of Sciences of the United States of America* 79, 2072-2076.
- Liu, S.C., Zhai, S., Palek, J., Golan, D.E., Amato, D., Hassan, K., Nurse, G.T., Babona, D., Coetzer, T., Jarolim, P., and et al. (1990). Molecular defect of the band 3 protein in southeast Asian ovalocytosis. *The New England journal of medicine* 323, 1530-1538.
- Lomeli, H., Sprengel, R., Laurie, D.J., Kohr, G., Herb, A., Seeburg, P.H., and Wisden, W. (1993). The rat delta-1 and delta-2 subunits extend the excitatory amino acid receptor family. *FEBS letters* 315, 318-322.

REFERENCES

- Lorenzo, D.N., Li, M.G., Mische, S.E., Armbrust, K.R., Ranum, L.P., and Hays, T.S. 2010. Spectrin mutations that cause spinocerebellar ataxia type 5 impair axonal transport and induce neurodegeneration in *Drosophila*. *The Journal of Cell Biology* 189, 143-158.
- Lou, J.Y., Laezza, F., Gerber, B.R., Xiao, M., Yamada, K.A., Hartmann, H., Craig, A.M., Nerbonne, J.M., and Ornitz, D.M. (2005). Fibroblast growth factor 14 is an intracellular modulator of voltage-gated sodium channels. *The Journal of physiology* 569, 179-193.
- Lux, S.E., Pease, B., Tomaselli, M.B., John, K.M., and Bernstein, S.E. (1979). Hemolytic anemias associated with deficient or dysfunctional spectrin. *Progress in clinical and biological research* 30, 463-469.
- MacAndrew, A. (2003). Comparison of mouse and human coding genes. <http://www.evolutionpages.com/Mouse%20genome%20genes.htm#Homologues>.
- Madar-Shapiro, L., Pasmanik-Chor, M., Vaccaro, A.M., Dinur, T., Dagan, A., Gatt, S., and Horowitz, M. (1999). Importance of splicing for prosaposin sorting. *The Biochemical journal* 337 (Pt 3), 433-443.
- Maltecca, F., Aghaie, A., Schroeder, D.G., Cassina, L., Taylor, B.A., Phillips, S.J., Malaguti, M., Previtali, S., Guenet, J.L., Quattrini, A., *et al.* (2008). The mitochondrial protease AFG3L2 is essential for axonal development. *J Neurosci* 28, 2827-2836.
- Maltecca, F., Magnoni, R., Cerri, F., Cox, G.A., Quattrini, A., and Casari, G. (2009). Haploinsufficiency of AFG3L2, the gene responsible for spinocerebellar ataxia type 28, causes mitochondria-mediated Purkinje cell dark degeneration. *J Neurosci* 29, 9244-9254.

REFERENCES

- Manto, M.U. and Pandolfo, M. (2002). *The cerebellum and its disorders*. Cambridge University Press.
- Marr, D. (1969). A theory of cerebellar cortex. *J Physiol (Lond)* 202:437-70.
- Matsuda, J., Kido, M., Tadano-Aritomi, K., Ishizuka, I., Tominaga, K., Toida, K., Takeda, E., Suzuki, K., and Kuroda, Y. (2004). Mutation in saposin D domain of sphingolipid activator protein gene causes urinary system defects and cerebellar Purkinje cell degeneration with accumulation of hydroxy fatty acid-containing ceramide in mouse. *Human molecular genetics* 13, 2709-2723.
- Matsuda, J., Vanier, M.T., Saito, Y., Tohyama, J., Suzuki, K., and Suzuki, K. (2001). A mutation in the saposin A domain of the sphingolipid activator protein (prosaposin) gene results in a late-onset, chronic form of globoid cell leukodystrophy in the mouse. *Human molecular genetics* 10, 1191-1199.
- Matsumoto, M., and Nagata, E. (1999). Type 1 inositol 1,4,5-trisphosphate receptor knock-out mice: their phenotypes and their meaning in neuroscience and clinical practice. *Journal of molecular medicine (Berlin, Germany)* 77, 406-411.
- Matsumoto, M., Nakagawa, T., Inoue, T., Nagata, E., Tanaka, K., Takano, H., Minowa, O., Kuno, J., Sakakibara, S., Yamada, M., *et al.* (1996). Ataxia and epileptic seizures in mice lacking type 1 inositol 1,4,5-trisphosphate receptor. *Nature* 379, 168-171.
- Matsuura, T., Yamagata, T., Burgess, D.L., Rasmussen, A., Grewal, R.P., Watase, K., Khajavi, M., McCall, A.E., Davis, C.F., Zu, L., *et al.* (2000). Large expansion of the ATTCT pentanucleotide repeat in spinocerebellar ataxia type 10. *Nature genetics* 26, 191-194.

REFERENCES

- Matsuyama, Z., Wakamori, M., Mori, Y., Kawakami, H., Nakamura, S., and Imoto, K. (1999). Direct alteration of the P/Q-type Ca²⁺ channel property by polyglutamine expansion in spinocerebellar ataxia 6. *J Neurosci* *19*, RC14.
- Mayat, E., Petralia, R.S., Wang, Y.X., and Wenthold, R.J. (1995). Immunoprecipitation, immunoblotting, and immunocytochemistry studies suggest that glutamate receptor delta subunits form novel postsynaptic receptor complexes. *J Neurosci* *15*, 2533-2546.
- McCabe, B.D., Marques, G., Haghghi, A.P., Fetter, R.D., Crotty, M.L., Haerry, T.E., Goodman, C.S., and O'Connor, M.B. (2003). The BMP homolog Gbb provides a retrograde signal that regulates synaptic growth at the *Drosophila* neuromuscular junction. *Neuron* *39*, 241-254.
- McCormick, D.A., Lavond, D.G., Clark, G.A., Kettner, R.E., Rising, C.E. and Thompson, R.F. (1981). The engram found? Role of the cerebellum in classical conditioning of nictitating membrane and eyelid responses. *Bull Psychon Soc* *18*: 103-5.
- McCormick, D.A., and Thompson, R.F. (1984). Cerebellum: essential involvement in the classically conditioned eyelid response. *Science (New York, N.Y)* *223*, 296-299.
- Metzler, M., Li, B., Gan, L., Georgiou, J., Gutekunst, C.A., Wang, Y., Torre, E., Devon, R.S., Oh, R., Legendre-Guillemin, V., *et al.* (2003). Disruption of the endocytic protein HIP1 results in neurological deficits and decreased AMPA receptor trafficking. *The EMBO journal* *22*, 3254-3266.
- Michaely, P., Kamal, A., Anderson, R.G., and Bennett, V. (1999). A requirement for ankyrin binding to clathrin during coated pit budding. *The Journal of biological chemistry* *274*, 35908-35913.

REFERENCES

- Mikoshiha, K. (1993). Inositol 1,4,5-trisphosphate receptor. *Trends in pharmacological sciences* 14, 86-89.
- Miura, S., Shibata, H., Furuya, H., Ohyagi, Y., Osoegawa, M., Miyoshi, Y., Matsunaga, H., Shibata, A., Matsumoto, N., Iwaki, A., *et al.* (2006). The contactin 4 gene locus at 3p26 is a candidate gene of SCA16. *Neurology* 67, 1236-1241.
- Miyoshi, Y., Yamada, T., Tanimura, M., Taniwaki, T., Arakawa, K., Ohyagi, Y., Furuya, H., Yamamoto, K., Sakai, K., Sasazuki, T., and Kira, J. (2001). A novel autosomal dominant spinocerebellar ataxia (SCA16) linked to chromosome 8q22.1-24.1. *Neurology* 57, 96-100.
- Moorthy, S., Chen, L., and Bennett, V. (2000). *Caenorhabditis elegans* beta-G spectrin is dispensable for establishment of epithelial polarity, but essential for muscular and neuronal function. *The Journal of cell biology* 149, 915-930.
- Morimoto, S., Martin, B.M., Kishimoto, Y., and O'Brien, J.S. (1988). Saposin D: a sphingomyelinase activator. *Biochemical and biophysical research communications* 156, 403-410.
- Moseley, M.L., Zu, T., Ikeda, Y., Gao, W., Mosemiller, A.K., Daughters, R.S., Chen, G., Weatherspoon, M.R., Clark, H.B., Ebner, T.J., *et al.* (2006). Bidirectional expression of CUG and CAG expansion transcripts and intranuclear polyglutamine inclusions in spinocerebellar ataxia type 8. *Nature genetics* 38, 758-769.
- Mullen, R.J., Eicher, E.M., and Sidman, R.L. (1976). Purkinje cell degeneration, a new neurological mutation in the mouse. *Proceedings of the National Academy of Sciences of the United States of America* 73, 208-212.

REFERENCES

- Munch, C., Sedlmeier, R., Meyer, T., Homberg, V., Sperfeld, A.D., Kurt, A., Prudlo, J., Peraus, G., Hanemann, C.O., Stumm, G., and Ludolph, A.C. (2004). Point mutations of the p150 subunit of dynactin (DCTN1) gene in ALS. *Neurology* 63, 724-726.
- Muresan, V., Stankewich, M.C., Steffen, W., Morrow, J.S., Holzbaur, E.L., and Schnapp, B.J. (2001). Dynactin-dependent, dynein-driven vesicle transport in the absence of membrane proteins: a role for spectrin and acidic phospholipids. *Molecular cell* 7, 173-183.
- Nagaoka, U., Takashima, M., Ishikawa, K., Yoshizawa, K., Yoshizawa, T., Ishikawa, M., Yamawaki, T., Shoji, S., and Mizusawa, H. (2000). A gene on SCA4 locus causes dominantly inherited pure cerebellar ataxia. *Neurology* 54, 1971-1975.
- Nagata, T., Ilieva, H., Murakami, T., Shiote, M., Narai, H., Ohta, Y., Hayashi, T., Shoji, M., and Abe, K. (2007). Increased ER stress during motor neuron degeneration in a transgenic mouse model of amyotrophic lateral sclerosis. *Neurological research* 29, 767-771.
- Nakamura, K., Jeong, S.Y., Uchihara, T., Anno, M., Nagashima, K., Nagashima, T., Ikeda, S., Tsuji, S., and Kanazawa, I. (2001). SCA17, a novel autosomal dominant cerebellar ataxia caused by an expanded polyglutamine in TATA-binding protein. *Human molecular genetics* 10, 1441-1448.
- Nakatsu, F., and Ohno, H. (2003). Adaptor protein complexes as the key regulators of protein sorting in the post-Golgi network. *Cell structure and function* 28, 419-429.
- Nallani, K.C., and Sullivan, W.J., Jr. (2005). Identification of proteins interacting with *Toxoplasma* SRCAP by yeast two-hybrid screening. *Parasitology research* 95, 236-242.

REFERENCES

- O'Brien, J.S., Carson, G.S., Seo, H.C., Hiraiwa, M., and Kishimoto, Y. (1994). Identification of prosaposin as a neurotrophic factor. *Proceedings of the National Academy of Sciences of the United States of America* *91*, 9593-9596.
- O'Brien, J.S., Carson, G.S., Seo, H.C., Hiraiwa, M., Weiler, S., Tomich, J.M., Barranger, J.A., Kahn, M., Azuma, N., and Kishimoto, Y. (1995). Identification of the neurotrophic factor sequence of prosaposin. *Faseb J* *9*, 681-685.
- O'Brien, J.S., and Kishimoto, Y. (1991). Saposin proteins: structure, function, and role in human lysosomal storage disorders. *Faseb J* *5*, 301-308.
- Ochiai, T., Takenaka, Y., Kuramoto, Y., Kasuya, M., Fukuda, K., Kimura, M., Shimeno, H., Misasi, R., Hiraiwa, M., and Soeda, S. (2008). Molecular mechanism for neuroprotective effect of prosaposin against oxidative stress: its regulation of dimeric transcription factor formation. *Biochimica et biophysica acta* *1780*, 1441-1447.
- Ohanian, V., Evans, J.P., and Gratzer, W.B. (1985). A case of elliptocytosis associated with a truncated spectrin chain. *British journal of haematology* *61*, 31-39.
- Ohara, O., Ohara, R., Yamakawa, H., Nakajima, D., and Nakayama, M. (1998). Characterization of a new beta-spectrin gene which is predominantly expressed in brain. *Brain Res Mol Brain Res* *57*, 181-192.
- Ojakangas, C.L., and Ebner, T.J. (1994). Purkinje cell complex spike activity during voluntary motor learning: relationship to kinematics. *Journal of neurophysiology* *72*, 2617-2630.
- Okura, T., Gong, L., Kamitani, T., Wada, T., Okura, I., Wei, C.F., Chang, H.M., and Yeh, E.T. (1996). Protection against Fas/APO-1- and tumor necrosis factor-mediated cell death by a novel protein, sentrin. *J Immunol* *157*, 4277-4281.

REFERENCES

- Ophoff, R.A., Terwindt, G.M., Vergouwe, M.N., van Eijk, R., Oefner, P.J., Hoffman, S.M., Lamerdin, J.E., Mohrenweiser, H.W., Bulman, D.E., Ferrari, M., *et al.* (1996). Familial hemiplegic migraine and episodic ataxia type-2 are caused by mutations in the Ca²⁺ channel gene CACNL1A4. *Cell* 87, 543-552.
- Orioli, P.J., and Strick, P.L. (1989). Cerebellar connections with the motor cortex and the arcuate premotor area: an analysis employing retrograde transneuronal transport of WGA-HRP. *The Journal of comparative neurology* 288, 612-626.
- Orr, H.T., Chung, M.Y., Banfi, S., Kwiatkowski, T.J., Jr., Servadio, A., Beaudet, A.L., McCall, A.E., Duvick, L.A., Ranum, L.P., and Zoghbi, H.Y. (1993). Expansion of an unstable trinucleotide CAG repeat in spinocerebellar ataxia type 1. *Nature genetics* 4, 221-226.
- Oscarsson, O. (1965). Functional Organization of the Spino- and Cuneocerebellar Tracts. *Physiological reviews* 45, 495-522.
- Otis, T.S., Kavanaugh, M.P., and Jahr, C.E. (1997). Postsynaptic glutamate transport at the climbing fiber-Purkinje cell synapse. *Science (New York, N.Y)* 277, 1515-1518.
- Owen, D.J., Collins, B.M., and Evans, P.R. (2004). Adaptors for clathrin coats: structure and function. *Annual review of cell and developmental biology* 20, 153-191.
- Oyadomari, S., and Mori, M. (2004). Roles of CHOP/GADD153 in endoplasmic reticulum stress. *Cell death and differentiation* 11, 381-389.
- Palek, J., and Lambert, S. (1990). Genetics of the red cell membrane skeleton. *Seminars in hematology* 27, 290-332.
- Palay, S.L. and Chan-Palay, V. (1974) *Cerebellar Cortex: Cytology and Organization* (Springer, Berlin).

REFERENCES

- Park, S.J., Lee, B.H., and Kim, D.J. (2009). Identification of proteins that interact with podocin using the yeast 2-hybrid system. *Yonsei medical journal* 50, 273-279.
- Parkinson, N.J., Olsson, C.L., Hallows, J.L., McKee-Johnson, J., Keogh, B.P., Noben-Trauth, K., Kujawa, S.G., and Tempel, B.L. (2001). Mutant beta-spectrin 4 causes auditory and motor neuropathies in quivering mice. *Nature genetics* 29, 61-65.
- Pascual, J., Pfuhl, M., Rivas, G., Pastore, A., and Saraste, M. (1996). The spectrin repeat folds into a three-helix bundle in solution. *FEBS letters* 383, 201-207.
- Paulson, H.L., Perez, M.K., Trotter, Y., Trojanowski, J.Q., Subramony, S.H., Das, S.S., Vig, P., Mandel, J.L., Fischbeck, K.H., and Pittman, R.N. (1997). Intranuclear inclusions of expanded polyglutamine protein in spinocerebellar ataxia type 3. *Neuron* 19, 333-344.
- Payne, A.S., Kelly, E.J., and Gitlin, J.D. (1998). Functional expression of the Wilson disease protein reveals mislocalization and impaired copper-dependent trafficking of the common H1069Q mutation. *Proceedings of the National Academy of Sciences of the United States of America* 95, 10854-10859.
- Perkins, E.M., Clarkson, Y.L., Sabatier, N., Longhurst, D.M., Millward, C.P., Jack, J., Toraiwa, J., Watanabe, M., Rothstein, J.D., Lyndon, A.R., Wyllie, D.J., Dutia, M.B., and Jackson, M. 2010. Loss of β -III spectrin leads to Purkinje cell dysfunction recapitulating the behaviour and neuropathology of spinocerebellar ataxia type 5 in humans. *J Neurosci* 30, 4857-4867.

REFERENCES

- Persson, A.S., Klement, G., Almgren, M., Sahlholm, K., Nilsson, J., Petersson, S., Arhem, P., Schalling, M., and Lavebratt, C. (2005). A truncated Kv1.1 protein in the brain of the megencephaly mouse: expression and interaction. *BMC neuroscience* 6, 65.
- Petersson, S., Persson, A.S., Johansen, J.E., Ingvar, M., Nilsson, J., Klement, G., Arhem, P., Schalling, M., and Lavebratt, C. (2003). Truncation of the Shaker-like voltage-gated potassium channel, Kv1.1, causes megencephaly. *The European journal of neuroscience* 18, 3231-3240.
- Philips, R.J.S. (1960). 'Lurcher', a new gene in linkage group XI of the house mouse. *J Genet* 57: 35-42.
- Piccioni, F., Simeoni, S., Andriola, I., Armatura, E., Bassanini, S., Pozzi, P., and Poletti, A. (2001). Polyglutamine tract expansion of the androgen receptor in a motoneuronal model of spinal and bulbar muscular atrophy. *Brain research bulletin* 56, 215-220.
- Piedras-Renteria, E.S., Watase, K., Harata, N., Zhuchenko, O., Zoghbi, H.Y., Lee, C.C., and Tsien, R.W. (2001). Increased expression of alpha 1A Ca²⁺ channel currents arising from expanded trinucleotide repeats in spinocerebellar ataxia type 6. *J Neurosci* 21, 9185-9193.
- Pielage, J., Fetter, R.D., and Davis, G.W. (2005). Presynaptic spectrin is essential for synapse stabilization. *Curr Biol* 15, 918-928.
- Pielage, J., Fetter, R.D., and Davis, G.W. (2006). A postsynaptic spectrin scaffold defines active zone size, spacing, and efficacy at the *Drosophila* neuromuscular junction. *The Journal of cell biology* 175, 491-503.
- Pietrobon, D. (2002). Calcium channels and channelopathies of the central nervous system. *Molecular neurobiology* 25, 31-50.

REFERENCES

- Pothier, B., Morle, L., Alloisio, N., Ducluzeau, M.T., Caldani, C., Feo, C., Garbarz, M., Chaverroche, I., Dhermy, D., Lecomte, M.C., and et al. (1987). Spectrin Nice (beta 220/216): a shortened beta-chain variant associated with an increase of the alpha I/74 fragment in a case of elliptocytosis. *Blood* 69, 1759-1765.
- Poupon, V., Girard, M., Legendre-Guillemain, V., Thomas, S., Bourbonniere, L., Philie, J., Bright, N.A., and McPherson, P.S. (2008). Clathrin light chains function in mannose phosphate receptor trafficking via regulation of actin assembly. *Proceedings of the National Academy of Sciences of the United States of America* 105, 168-173.
- Pradhan, D., and Morrow, J. (2002). The spectrin-ankyrin skeleton controls CD45 surface display and interleukin-2 production. *Immunity* 17, 303-315.
- Presley, J.F., Cole, N.B., Schroer, T.A., Hirschberg, K., Zaal, K.J., and Lippincott-Schwartz, J. (1997). ER-to-Golgi transport visualized in living cells. *Nature* 389, 81-85.
- Pujol, A., Ferrer, I., Camps, C., Metzger, E., Hindelang, C., Callizot, N., Ruiz, M., Pampols, T., Giros, M., and Mandel, J.L. (2004). Functional overlap between ABCD1 (ALD) and ABCD2 (ALDR) transporters: a therapeutic target for X-adrenoleukodystrophy. *Human molecular genetics* 13, 2997-3006.
- Puls, I., Jonnakuty, C., LaMonte, B.H., Holzbaaur, E.L., Tokito, M., Mann, E., Floeter, M.K., Bidus, K., Drayna, D., Oh, S.J., et al. (2003). Mutant dynactin in motor neuron disease. *Nature genetics* 33, 455-456.
- Pulst, S.M., Nechiporuk, A., Nechiporuk, T., Gispert, S., Chen, X.N., Lopes-Cendes, I., Pearlman, S., Starkman, S., Orozco-Diaz, G., Lunkes, A., et al. (1996). Moderate expansion of a normally biallelic trinucleotide repeat in spinocerebellar ataxia type 2. *Nature genetics* 14, 269-276.

REFERENCES

- Qi, X., Kondoh, K., Krusling, D., Kelso, G.J., Leonova, T., and Grabowski, G.A. (1999). Conformational and amino acid residue requirements for the saposin C neuritogenic effect. *Biochemistry* 38, 6284-6291.
- Qi, X., Qin, W., Sun, Y., Kondoh, K., and Grabowski, G.A. (1996). Functional organization of saposin C. Definition of the neurotrophic and acid beta-glucosidase activation regions. *The Journal of biological chemistry* 271, 6874-6880.
- Raman, I.M., and Bean, B.P. (1999). Ionic currents underlying spontaneous action potentials in isolated cerebellar Purkinje neurons. *J Neurosci* 19, 1663-1674.
- Ranum, L.P., and Cooper, T.A. (2006). RNA-mediated neuromuscular disorders. *Annual review of neuroscience* 29, 259-277.
- Ranum, L.P., Schut, L.J., Lundgren, J.K., Orr, H.T., and Livingston, D.M. (1994). Spinocerebellar ataxia type 5 in a family descended from the grandparents of President Lincoln maps to chromosome 11. *Nature genetics* 8, 280-284.
- Rennolds, J., Boyaka, P.N., Bellis, S.L., and Cormet-Boyaka, E. (2008). Low temperature induces the delivery of mature and immature CFTR to the plasma membrane. *Biochemical and biophysical research communications* 366, 1025-1029.
- Resibois, A., Cuvelier, L., and Goffinet, A.M. (1997). Abnormalities in the cerebellum and brainstem in homozygous lurcher mice. *Neuroscience* 80, 175-190.
- Restituto, S., Thompson, R.M., Eliet, J., Raike, R.S., Riedl, M., Charnet, P., and Gomez, C.M. (2000). The polyglutamine expansion in spinocerebellar ataxia type 6 causes a beta subunit-specific enhanced activation of P/Q-type calcium channels in *Xenopus* oocytes. *J Neurosci* 20, 6394-6403.

REFERENCES

- Rettig, J., Sheng, Z.H., Kim, D.K., Hodson, C.D., Snutch, T.P., and Catterall, W.A. (1996). Isoform-specific interaction of the alpha1A subunits of brain Ca²⁺ channels with the presynaptic proteins syntaxin and SNAP-25. *Proceedings of the National Academy of Sciences of the United States of America* *93*, 7363-7368.
- Rijnboutt, S., Aerts, H.M., Geuze, H.J., Tager, J.M., and Strous, G.J. (1991). Mannose 6-phosphate-independent membrane association of cathepsin D, glucocerebrosidase, and sphingolipid-activating protein in HepG2 cells. *The Journal of biological chemistry* *266*, 4862-4868.
- Robinson, D.A. (1976). Adaptive gain control of vestibuloocular reflex by the cerebellum. *Journal of neurophysiology* *39*, 954-969.
- Robinson, D.N., and Cooley, L. (1997). *Drosophila* kelch is an oligomeric ring canal actin organizer. *The Journal of cell biology* *138*, 799-810.
- Robinson, M.S. (2004). Adaptable adaptors for coated vesicles. *Trends in cell biology* *14*, 167-174.
- Rothstein, J.D., Dykes-Hoberg, M., Pardo, C.A., Bristol, L.A., Jin, L., Kuncl, R.W., Kanai, Y., Hediger, M.A., Wang, Y., Schielke, J.P., and Welty, D.F. (1996). Knockout of glutamate transporters reveals a major role for astroglial transport in excitotoxicity and clearance of glutamate. *Neuron* *16*, 675-686.
- Rothstein, J.D., Martin, L.J., and Kuncl, R.W. (1992). Decreased glutamate transport by the brain and spinal cord in amyotrophic lateral sclerosis. *The New England journal of medicine* *326*, 1464-1468.
- Rothstein, J.D., Van Kammen, M., Levey, A.I., Martin, L.J., and Kuncl, R.W. (1995). Selective loss of glial glutamate transporter GLT-1 in amyotrophic lateral sclerosis. *Annals of neurology* *38*, 73-84.

REFERENCES

- Royle, S.J., Bright, N.A., and Lagnado, L. (2005). Clathrin is required for the function of the mitotic spindle. *Nature* 434, 1152-1157.
- Rusconi, R., Scalmani, P., Cassulini, R.R., Giunti, G., Gambardella, A., Franceschetti, S., Annesi, G., Wanke, E., and Mantegazza, M. (2007). Modulatory proteins can rescue a trafficking defective epileptogenic Nav1.1 Na⁺ channel mutant. *J Neurosci* 27, 11037-11046.
- Sacco, T., De Luca, A., and Tempia, F. (2006). Properties and expression of Kv3 channels in cerebellar Purkinje cells. *Molecular and cellular neurosciences* 33, 170-179.
- Sachs, A.J., David, S.A., Haider, N.B., and Nystuen, A.M. (2009). Patterned neuroprotection in the *Inpp4a(wbl)* mutant mouse cerebellum correlates with the expression of *Eaat4*. *PloS one* 4, e8270.
- Saito, H., Okada, M., Miki, T., Wakamori, M., Futatsugi, A., Mori, Y., Mikoshiba, K., and Suzuki, N. (2009). Knockdown of Cav2.1 calcium channels is sufficient to induce neurological disorders observed in natural occurring *Cacna1a* mutants in mice. *Biochemical and biophysical research communications* 390, 1029-1033.
- Sakaguchi, G., Orita, S., Naito, A., Maeda, M., Igarashi, H., Sasaki, T., and Takai, Y. (1998). A novel brain-specific isoform of beta spectrin: isolation and its interaction with Munc13. *Biochemical and biophysical research communications* 248, 846-851.
- Salminen, A., Kauppinen, A., Suuronen, T., Kaarniranta, K., and Ojala, J. (2009). ER stress in Alzheimer's disease: a novel neuronal trigger for inflammation and Alzheimer's pathology. *Journal of neuroinflammation* 6, 41.

REFERENCES

- Sano, A., Hineno, T., Mizuno, T., Kondoh, K., Ueno, S., Kakimoto, Y., and Inui, K. (1989). Sphingolipid hydrolase activator proteins and their precursors. *Biochemical and biophysical research communications* *165*, 1191-1197.
- Sano, A., Matsuda, S., Wen, T.C., Kotani, Y., Kondoh, K., Ueno, S., Kakimoto, Y., Yoshimura, H., and Sakanaka, M. (1994). Protection by prosaposin against ischemia-induced learning disability and neuronal loss. *Biochemical and biophysical research communications* *204*, 994-1000.
- Sano, A., Mizuno, T., Kondoh, K., Hineno, T., Ueno, S., Kakimoto, Y., and Morita, N. (1992). Saposin-C from bovine spleen; complete amino acid sequence and relation between the structure and its biological activity. *Biochimica et biophysica acta* *1120*, 75-80.
- Sano, A., Radin, N.S., Johnson, L.L., and Tarr, G.E. (1988). The activator protein for glucosylceramide beta-glucosidase from guinea pig liver. Improved isolation method and complete amino acid sequence. *The Journal of biological chemistry* *263*, 19597-19601.
- Sanpei, K., Takano, H., Igarashi, S., Sato, T., Oyake, M., Sasaki, H., Wakisaka, A., Tashiro, K., Ishida, Y., Ikeuchi, T., *et al.* (1996). Identification of the spinocerebellar ataxia type 2 gene using a direct identification of repeat expansion and cloning technique, DIRECT. *Nature genetics* *14*, 277-284.
- Santarosa, M., and Ashworth, A. (2004). Haploinsufficiency for tumour suppressor genes: when you don't need to go all the way. *Biochimica et biophysica acta* *1654*, 105-122.
- Sapp, E., Penney, J., Young, A., Aronin, N., Vonsattel, J.P., and DiFiglia, M. (1999). Axonal transport of N-terminal huntingtin suggests early pathology of corticostriatal

REFERENCES

- projections in Huntington disease. *Journal of neuropathology and experimental neurology* 58, 165-173.
- Sarna, J.R., and Hawkes, R. (2003). Patterned Purkinje cell death in the cerebellum. *Progress in neurobiology* 70, 473-507.
- Sato, N., Amino, T., Kobayashi, K., Asakawa, S., Ishiguro, T., Tsunemi, T., Takahashi, M., Matsuura, T., Flanigan, K.M., Iwasaki, S., *et al.* (2009). Spinocerebellar ataxia type 31 is associated with "inserted" penta-nucleotide repeats containing (TGGAA)_n. *American journal of human genetics* 85, 544-557.
- Saura, C.A., Choi, S.Y., Beglopoulos, V., Malkani, S., Zhang, D., Shankaranarayana Rao, B.S., Chattarji, S., Kelleher, R.J., 3rd, Kandel, E.R., Duff, K., *et al.* (2004). Loss of presenilin function causes impairments of memory and synaptic plasticity followed by age-dependent neurodegeneration. *Neuron* 42, 23-36.
- Sausbier, M., Hu, H., Arntz, C., Feil, S., Kamm, S., Adelsberger, H., Sausbier, U., Sailer, C.A., Feil, R., Hofmann, F., *et al.* (2004). Cerebellar ataxia and Purkinje cell dysfunction caused by Ca²⁺-activated K⁺ channel deficiency. *Proceedings of the National Academy of Sciences of the United States of America* 101, 9474-9478.
- Schengrund, C.L. (1990). The role(s) of gangliosides in neural differentiation and repair: a perspective. *Brain research bulletin* 24, 131-141.
- Schmidt, T., Landwehrmeyer, G.B., Schmitt, I., Trottier, Y., Auburger, G., Laccone, F., Klockgether, T., Volpel, M., Epplen, J.T., Schols, L., and Riess, O. (1998). An isoform of ataxin-3 accumulates in the nucleus of neuronal cells in affected brain regions of SCA3 patients. *Brain pathology (Zurich, Switzerland)* 8, 669-679.

REFERENCES

- Sepkuty, J.P., Cohen, A.S., Eccles, C., Rafiq, A., Behar, K., Ganel, R., Coulter, D.A., and Rothstein, J.D. (2002). A neuronal glutamate transporter contributes to neurotransmitter GABA synthesis and epilepsy. *J Neurosci* 22, 6372-6379.
- Shaw, P.J., Forrest, V., Ince, P.G., Richardson, J.P., and Wastell, H.J. (1995). CSF and plasma amino acid levels in motor neuron disease: elevation of CSF glutamate in a subset of patients. *Neurodegeneration* 4, 209-216.
- Shen, J., and Kelleher, R.J., 3rd (2007). The presenilin hypothesis of Alzheimer's disease: evidence for a loss-of-function pathogenic mechanism. *Proceedings of the National Academy of Sciences of the United States of America* 104, 403-409.
- Shen, Z., Pardington-Purtymun, P.E., Comeaux, J.C., Moyzis, R.K., and Chen, D.J. (1996). Associations of UBE2I with RAD52, UBL1, p53, and RAD51 proteins in a yeast two-hybrid system. *Genomics* 37, 183-186.
- Sheng, Z.H., Rettig, J., Takahashi, M., and Catterall, W.A. (1994). Identification of a syntaxin-binding site on N-type calcium channels. *Neuron* 13, 1303-1313.
- Shotton, D.M., Burke, B.E., and Branton, D. (1979). The molecular structure of human erythrocyte spectrin. Biophysical and electron microscopic studies. *Journal of molecular biology* 131, 303-329.
- Siddhanta, A., Radulescu, A., Stankewich, M.C., Morrow, J.S., and Shields, D. (2003). Fragmentation of the Golgi apparatus. A role for beta III spectrin and synthesis of phosphatidylinositol 4,5-bisphosphate. *The Journal of biological chemistry* 278, 1957-1965.
- Sidman, M., Rauzin, R., Lazar, R., Cunningham, S., Tailby, W., and Carrigan, P. (1982). A search for symmetry in the conditional discriminations of rhesus monkeys, baboons, and children. *Journal of the experimental analysis of behavior* 37, 23-44.

REFERENCES

- Sidman, R.L., Appel, S.H., and Fullier, J.F. (1965). Neurological Mutants of the Mouse. *Science* (New York, N.Y. *150*, 513-516.
- Sidman, R.L., Lane, P.W., and Dickie, M.M. (1962). Staggerer, a new mutation in the mouse affecting the cerebellum. *Science* (New York, N.Y. *137*, 610-612.
- Simpson, J.I., and Alley, K.E. (1974). Visual climbing fiber input to rabbit vestibulo-cerebellum: a source of direction-specific information. *Brain Res* *82*, 302-308.
- Sisson, J.C., Field, C., Ventura, R., Royou, A., and Sullivan, W. (2000). Lava lamp, a novel peripheral golgi protein, is required for *Drosophila melanogaster* cellularization. *The Journal of cell biology* *151*, 905-918.
- Skinner, P.J., Koshy, B.T., Cummings, C.J., Klement, I.A., Helin, K., Servadio, A., Zoghbi, H.Y., and Orr, H.T. (1997). Ataxin-1 with an expanded glutamine tract alters nuclear matrix-associated structures. *Nature* *389*, 971-974.
- Sotelo, C., Alvarado-Mallart, R.M., Gardette, R., and Crepel, F. (1990). Fate of grafted embryonic Purkinje cells in the cerebellum of the adult "Purkinje cell degeneration" mutant mouse. I. Development of reciprocal graft-host interactions. *The Journal of comparative neurology* *295*, 165-187.
- Sotos, J.G. (2009). Abraham Lincoln did not have type 5 spinocerebellar ataxia. *Neurology* *73*, 1328-1332.
- Speicher, D.W., and Marchesi, V.T. (1984). Erythrocyte spectrin is comprised of many homologous triple helical segments. *Nature* *311*, 177-180.
- Speicher, D.W., Morrow, J.S., Knowles, W.J., and Marchesi, V.T. (1982). A structural model of human erythrocyte spectrin. Alignment of chemical and functional domains. *The Journal of biological chemistry* *257*, 9093-9101.

REFERENCES

- Spiegel, R., Bach, G., Sury, V., Mengistu, G., Meidan, B., Shalev, S., Shneur, Y., Mandel, H., and Zeigler, M. (2005). A mutation in the saposin A coding region of the prosaposin gene in an infant presenting as Krabbe disease: first report of saposin A deficiency in humans. *Molecular genetics and metabolism* 84, 160-166.
- Sprague, J.M., Chambers, W.W. 1953. Regulation of posture in intact and decerebrate cat. I. Cerebellum, reticular formation, and vestibular nuclei. *J. Neurophysiol.* 16: 451-63.
- Stankewich, M.C., Gwynn, B., Ardito, T., Ji, L., Kim, J., Robledo, R.F., Lux, S.E., Peters, L.L., and Morrow, J.S. 2010. Targeted deletion of β III spectrin impairs synaptogenesis and generates ataxic and seizure phenotypes. *Proceedings of the National Academy of Sciences of the United States of America* 107, 6022-6027.
- Stankewich, M.C., Tse, W.T., Peters, L.L., Ch'ng, Y., John, K.M., Stabach, P.R., Devarajan, P., Morrow, J.S., and Lux, S.E. (1998). A widely expressed betaIII spectrin associated with Golgi and cytoplasmic vesicles. *Proceedings of the National Academy of Sciences of the United States of America* 95, 14158-14163.
- Stevanin, G., Broussolle, E., Streichenberger, N., Kopp, N., Brice, A., and Durr, A. (2005). Spinocerebellar ataxia with sensory neuropathy (SCA25). *Cerebellum (London, England)* 4, 58-61.
- Stevanin, G., Herman, A., Brice, A., and Durr, A. (1999). Clinical and MRI findings in spinocerebellar ataxia type 5. *Neurology* 53, 1355-1357.
- Stokin, G.B., Lillo, C., Falzone, T.L., Bruschi, R.G., Rockenstein, E., Mount, S.L., Raman, R., Davies, P., Masliah, E., Williams, D.S., and Goldstein, L.S. (2005). Axonopathy and transport deficits early in the pathogenesis of Alzheimer's disease. *Science (New York, N.Y)* 307, 1282-1288.

REFERENCES

- Storey, E., Gardner, R.J., Knight, M.A., Kennerson, M.L., Tuck, R.R., Forrest, S.M., and Nicholson, G.A. (2001). A new autosomal dominant pure cerebellar ataxia. *Neurology* 57, 1913-1915.
- Strahlendorf, J., Box, C., Attridge, J., Diertien, J., Finckbone, V., Henne, W.M., Medina, M.S., Miles, R., Oomman, S., Schneider, M., *et al.* (2003). AMPA-induced dark cell degeneration of cerebellar Purkinje neurons involves activation of caspases and apparent mitochondrial dysfunction. *Brain Res* 994, 146-159.
- Strata, P. (1985). Inferior olive: functional aspects. In *Cerebellar Functions*, ed. J. R. Bloedel, J. Dichgans and W. Precht. Berlin: Springer-Verlag. pp. 231-46.
- Street, V.A., Bosma, M.M., Demas, V.P., Regan, M.R., Lin, D.D., Robinson, L.C., Agnew, W.S., and Tempel, B.L. (1997). The type 1 inositol 1,4,5-trisphosphate receptor gene is altered in the opisthotonos mouse. *J Neurosci* 17, 635-645.
- Sun, Y., Jin, P., Witte, D.P., and Grabowski, G.A. (2000). Prosaposin: promoter analysis and central-nervous-system-preferential elements for expression in vivo. *The Biochemical journal* 352 Pt 2, 549-556.
- Sun, Y., Witte, D.P., and Grabowski, G.A. (1994). Developmental and tissue-specific expression of prosaposin mRNA in murine tissues. *The American journal of pathology* 145, 1390-1398.
- Swisher, D.A., and Wilson, D.B. (1977). Cerebellar histogenesis in the lurcher (Lc) mutant mouse. *The Journal of comparative neurology* 173, 205-218.
- Sylvester, S.R., Morales, C., Oko, R., and Griswold, M.D. (1989). Sulfated glycoprotein-1 (saposin precursor) in the reproductive tract of the male rat. *Biology of reproduction* 41, 941-948.

REFERENCES

- Takahashi, M., Sarantis, M., and Attwell, D. (1996). Postsynaptic glutamate uptake in rat cerebellar Purkinje cells. *The Journal of physiology* 497 (Pt 2), 523-530.
- Tanaka, K., Watase, K., Manabe, T., Yamada, K., Watanabe, M., Takahashi, K., Iwama, H., Nishikawa, T., Ichihara, N., Kikuchi, T., *et al.* (1997). Epilepsy and exacerbation of brain injury in mice lacking the glutamate transporter GLT-1. *Science (New York, N.Y)* 276, 1699-1702.
- Taroni, F., and DiDonato, S. (2004). Pathways to motor incoordination: the inherited ataxias. *Nature reviews* 5, 641-655.
- Terada, N., Banno, Y., Ohno, N., Fujii, Y., Murate, T., Sarna, J.R., Hawkes, R., Zea, Z., Baba, T., and Ohno, S. (2004). Compartmentation of the mouse cerebellar cortex by sphingosine kinase. *The Journal of comparative neurology* 469, 119-127.
- Thach, W.T (1967). Discharge of Purkinje and cerebellar nuclear neurons during rapidly alternating arm movements in the monkey. *J Neurophysiol* 31: 785-96.
- Thach, W.T., Kane, S.A., Mink, J.W., Goodkin, H.P. 1990. Cerebellar nuclear signs: Motor modalities, somatotopy, and incoordination. *Am. Acad. Neurol., Motor Control: Annual Course # 248*: 109-35.
- Thach, W.T., Kane, S.A., Mink, J.W., Goodkin, H.P. 1992. Cerebellar output: Multiple maps and motor modes in movement coordination. In Ramon y Cajal Centenary, ed. R. Llinas, C Sotelo.
- Thomas, D., Kiehn, J., Katus, H.A., and Karle, C.A. (2003). Defective protein trafficking in hERG-associated hereditary long QT syndrome (LQT2): molecular mechanisms and restoration of intracellular protein processing. *Cardiovascular research* 60, 235-241.

REFERENCES

- Thomas, P.S., Jr., Fraley, G.S., Damian, V., Woodke, L.B., Zapata, F., Sopher, B.L., Plymate, S.R., and La Spada, A.R. (2006). Loss of endogenous androgen receptor protein accelerates motor neuron degeneration and accentuates androgen insensitivity in a mouse model of X-linked spinal and bulbar muscular atrophy. *Human molecular genetics* 15, 2225-2238.
- Toru, S., Murakoshi, T., Ishikawa, K., Saegusa, H., Fujigasaki, H., Uchihara, T., Nagayama, S., Osanai, M., Mizusawa, H., and Tanabe, T. (2000). Spinocerebellar ataxia type 6 mutation alters P-type calcium channel function. *The Journal of biological chemistry* 275, 10893-10898.
- Traub, L.M. (2005). Common principles in clathrin-mediated sorting at the Golgi and the plasma membrane. *Biochimica et biophysica acta* 1744, 415-437.
- Trettel, F., Rigamonti, D., Hilditch-Maguire, P., Wheeler, V.C., Sharp, A.H., Persichetti, F., Cattaneo, E., and MacDonald, M.E. (2000). Dominant phenotypes produced by the HD mutation in STHdh(Q111) striatal cells. *Human molecular genetics* 9, 2799-2809.
- Triarhou, L.C. (1998). Rate of neuronal fallout in a transsynaptic cerebellar model. *Brain research bulletin* 47, 219-222.
- Trouillas, P., Takayanagi, T., Hallet, M. et al. (1997). International cooperative ataxia rating scale for pharmacological assessment of the cerebellar syndrome. *J Neuro Sci* 145: 205-11.
- Trudeau, M.M., Dalton, J.C., Day, J.W., Ranum, L.P., and Meisler, M.H. (2006). Heterozygosity for a protein truncation mutation of sodium channel SCN8A in a patient with cerebellar atrophy, ataxia, and mental retardation. *Journal of medical genetics* 43, 527-530.

REFERENCES

- Tsuboi, K., Hiraiwa, M., and O'Brien, J.S. (1998). Prosaposin prevents programmed cell death of rat cerebellar granule neurons in culture. *Brain research* 110, 249-255.
- Tsuji, S., Arita, M., and Nagai, Y. (1983). GQ1b, a bioactive ganglioside that exhibits novel nerve growth factor (NGF)-like activities in the two neuroblastoma cell lines. *Journal of biochemistry* 94, 303-306.
- Ungewickell, E., and Branton, D. (1981). Assembly units of clathrin coats. *Nature* 289, 420-422.
- Ungewickell, E., and Gratzner, W. (1978). Self-association of human spectrin. A thermodynamic and kinetic study. *European journal of biochemistry / FEBS* 88, 379-385.
- Vaccaro, A.M., Ciaffoni, F., Tatti, M., Salvioli, R., Barca, A., Tognozzi, D., and Scerch, C. (1995). pH-dependent conformational properties of saposins and their interactions with phospholipid membranes. *The Journal of biological chemistry* 270, 30576-30580.
- van de Leemput, J., Chandran, J., Knight, M.A., Holtzclaw, L.A., Scholz, S., Cookson, M.R., Houlden, H., Gwinn-Hardy, K., Fung, H.C., Lin, X., *et al.* (2007). Deletion at ITPR1 underlies ataxia in mice and spinocerebellar ataxia 15 in humans. *PLoS genetics* 3, e108.
- van de Warrenburg, B.P., Sinke, R.J., Verschuuren-Bemelmans, C.C., Scheffer, H., Brunt, E.R., Ippel, P.F., Maat-Kievit, J.A., Dooijes, D., Notermans, N.C., Lindhout, D., *et al.* (2002). Spinocerebellar ataxias in the Netherlands: prevalence and age at onset variance analysis. *Neurology* 58, 702-708.
- Van Raamsdonk, J.M., Pearson, J., Rogers, D.A., Bissada, N., Vogl, A.W., Hayden, M.R., and Leavitt, B.R. (2005). Loss of wild-type huntingtin influences motor dysfunction

REFERENCES

- and survival in the YAC128 mouse model of Huntington disease. *Human molecular genetics* 14, 1379-1392.
- van Swieten, J.C., Brusse, E., de Graaf, B.M., Krieger, E., van de Graaf, R., de Koning, I., Maat-Kievit, A., Leegwater, P., Dooijes, D., Oostra, B.A., and Heutink, P. (2003). A mutation in the fibroblast growth factor 14 gene is associated with autosomal dominant cerebellar ataxia [corrected]. *American journal of human genetics* 72, 191-199.
- Vaughan, K.T., and Vallee, R.B. (1995). Cytoplasmic dynein binds dynactin through a direct interaction between the intermediate chains and p150Glued. *The Journal of cell biology* 131, 1507-1516.
- Veitia, R.A., and Birchler, J.A. (2010). Dominance and gene dosage balance in health and disease: why levels matter! *The Journal of pathology*. 220, 174-185.
- Verbeek, D.S., Schelhaas, J.H., Ippel, E.F., Beemer, F.A., Pearson, P.L., and Sinke, R.J. (2002). Identification of a novel SCA locus (SCA19) in a Dutch autosomal dominant cerebellar ataxia family on chromosome region 1p21-q21. *Human genetics* 111, 388-393.
- Verbeek, D.S., van de Warrenburg, B.P., Wesseling, P., Pearson, P.L., Kremer, H.P., and Sinke, R.J. (2004). Mapping of the SCA23 locus involved in autosomal dominant cerebellar ataxia to chromosome region 20p13-12.3. *Brain* 127, 2551-2557.
- Vielhaber, G., Hurwitz, R., and Sandhoff, K. (1996). Biosynthesis, processing, and targeting of sphingolipid activator protein (SAP) precursor in cultured human fibroblasts.

REFERENCES

- Mannose 6-phosphate receptor-independent endocytosis of SAP precursor. *The Journal of biological chemistry* 271, 32438-32446.
- Vogel, M.W., Caston, J., Yuzaki, M., and Mariani, J. (2007). The Lurcher mouse: fresh insights from an old mutant. *Brain Res* 1140, 4-18.
- Vogel, M.W., Fan, H., Sydnor, J., and Guidetti, P. (2001). Cytochrome oxidase activity is increased in +/-Lc Purkinje cells destined to die. *Neuroreport* 12, 3039-3043.
- Vuillaume, I., Devos, D., Schraen-Maschke, S., Dina, C., Lemainque, A., Vasseur, F., Bocquillon, G., Devos, P., Kocinski, C., Marzys, C., *et al.* (2002). A new locus for spinocerebellar ataxia (SCA21) maps to chromosome 7p21.3-p15.1. *Annals of neurology* 52, 666-670.
- Wallace, V.A. (1999). Purkinje-cell-derived Sonic hedgehog regulates granule neuron precursor cell proliferation in the developing mouse cerebellum. *Curr Biol* 9, 445-448.
- Walter, J.T., Alvina, K., Womack, M.D., Chevez, C., and Khodakhah, K. (2006). Decreases in the precision of Purkinje cell pacemaking cause cerebellar dysfunction and ataxia. *Nature neuroscience* 9, 389-397.
- Watase, K., Barrett, C.F., Miyazaki, T., Ishiguro, T., Ishikawa, K., Hu, Y., Unno, T., Sun, Y., Kasai, S., Watanabe, M., *et al.* (2008). Spinocerebellar ataxia type 6 knockin mice develop a progressive neuronal dysfunction with age-dependent accumulation of mutant CaV2.1 channels. *Proceedings of the National Academy of Sciences of the United States of America* 105, 11987-11992.
- Watase, K., Hashimoto, K., Kano, M., Yamada, K., Watanabe, M., Inoue, Y., Okuyama, S., Sakagawa, T., Ogawa, S., Kawashima, N., *et al.* (1998). Motor discoordination and

REFERENCES

increased susceptibility to cerebellar injury in GLAST mutant mice. *The European journal of neuroscience* 10, 976-988.

Watase, K., Weeber, E.J., Xu, B., Antalffy, B., Yuva-Paylor, L., Hashimoto, K., Kano, M., Atkinson, R., Sun, Y., Armstrong, D.L., *et al.* (2002). A long CAG repeat in the mouse *Sca1* locus replicates SCA1 features and reveals the impact of protein solubility on selective neurodegeneration. *Neuron* 34, 905-919.

Waters, M.F., Minassian, N.A., Stevanin, G., Figueroa, K.P., Bannister, J.P., Nolte, D., Mock, A.F., Evidente, V.G., Fee, D.B., Muller, U., *et al.* (2006). Mutations in voltage-gated potassium channel *KCNC3* cause degenerative and developmental central nervous system phenotypes. *Nature genetics* 38, 447-451.

Wechsler-Reya, R.J., and Scott, M.P. (1999). Control of neuronal precursor proliferation in the cerebellum by Sonic Hedgehog. *Neuron* 22, 103-114.

Welsh, J.P., Yuen, G., Placantonakis, D.G., Vu, T.Q., Haiss, F., O'Hearn, E., Molliver, M.E., and Aicher, S.A. (2002). Why do Purkinje cells die so easily after global brain ischemia? Aldolase C, EAAT4, and the cerebellar contribution to posthypoxic myoclonus. *Advances in neurology* 89, 331-359.

Williamson, T.L., and Cleveland, D.W. (1999). Slowing of axonal transport is a very early event in the toxicity of ALS-linked SOD1 mutants to motor neurons. *Nature neuroscience* 2, 50-56.

Wilson, D.B. (1975). Brain abnormalities in the *lurcher* (*Lc*) mutant mouse. *Experientia* 31, 220-221.

REFERENCES

- Wilson, D.B. (1976). Histological defects in the cerebellum of adult lurcher (Lc) mice. *Journal of neuropathology and experimental neurology* 35, 40-45.
- Wittmack, E.K., Rush, A.M., Craner, M.J., Goldfarb, M., Waxman, S.G., and Dib-Hajj, S.D. (2004). Fibroblast growth factor homologous factor 2B: association with Nav1.6 and selective colocalization at nodes of Ranvier of dorsal root axons. *J Neurosci* 24, 6765-6775.
- Worth, P.F., Giunti, P., Gardner-Thorpe, C., Dixon, P.H., Davis, M.B., and Wood, N.W. (1999). Autosomal dominant cerebellar ataxia type III: linkage in a large British family to a 7.6-cM region on chromosome 15q14-21.3. *American journal of human genetics* 65, 420-426.
- Xu, C., Bailly-Maitre, B., and Reed, J.C. (2005). Endoplasmic reticulum stress: cell life and death decisions. *The Journal of clinical investigation* 115, 2656-2664.
- Yagishita, S., and Inoue, M. (1997). Clinicopathology of spinocerebellar degeneration: its correlation to the unstable CAG repeat of the affected gene. *Pathology international* 47, 1-15.
- Yamada, K.M., Wang, Y., and Yuzaki, M. (2003a). Characterization of autophagy pathways following d2 glutamate activation. Program No. 747.9 203 Abstract Viewer/Itinerary Planner. Washington, DC: Society for Neuroscience.
- Yamada, N., Wang, Y., and Yuzaki, M. (2003b). Characterization of autophagy pathways following 2 glutamate receptor activation. Program No. 747.9 2003 Abstract Viewer/Itinerary Planner. Washington, DC: Society for Neuroscience. Online.

REFERENCES

- Yan, Y., Winograd, E., Viel, A., Cronin, T., Harrison, S.C., and Branton, D. (1993). Crystal structure of the repetitive segments of spectrin. *Science (New York, N.Y)* 262, 2027-2030.
- Yeo, C.H., Hardiman, M.J., and Glickstein, M. (1984). Discrete lesions of the cerebellar cortex abolish the classically conditioned nictitating membrane response of the rabbit. *Behavioural brain research* 13, 261-266.
- Yoon, S.H., Yu, H., Eber, S., and Prchal, J.T. (1991). Molecular defect of truncated beta-spectrin associated with hereditary elliptocytosis. *Beta-spectrin Gottingen. The Journal of biological chemistry* 266, 8490-8494.
- Yu, G.Y., Howell, M.J., Roller, M.J., Xie, T.D., and Gomez, C.M. (2005). Spinocerebellar ataxia type 26 maps to chromosome 19p13.3 adjacent to SCA6. *Annals of neurology* 57, 349-354.
- Yuzaki, M. (2004). The delta2 glutamate receptor: a key molecule controlling synaptic plasticity and structure in Purkinje cells. *Cerebellum (London, England)* 3, 89-93.
- Zagha, E., Lang, E.J., and Rudy, B. (2008). Kv3.3 channels at the Purkinje cell soma are necessary for generation of the classical complex spike waveform. *J Neurosci* 28, 1291-1300.
- Zecevic, N., Milosevic, A., and Ehrlich, B.E. (1999). Calcium signaling molecules in human cerebellum at midgestation and in ataxia. *Early human development* 54, 103-116.
- Zephir, H., Stojkovic, T., Latour, P., Hurtevent, J.F., Blankaert, F., and Vermersch, P. (2005). A family with a novel frameshift mutation in the PMP22 gene (c.433_434insC) causing a phenotype of hereditary neuropathy with liability to pressure palsies. *Neuromuscul Disord* 15, 493-497.

REFERENCES

- Zhang, B., Tu, P., Abtahian, F., Trojanowski, J.Q., and Lee, V.M. (1997). Neurofilaments and orthograde transport are reduced in ventral root axons of transgenic mice that express human SOD1 with a G93A mutation. *The Journal of cell biology* *139*, 1307-1315.
- Zhou, D., Lambert, S., Malen, P.L., Carpenter, S., Boland, L.M., and Bennett, V. (1998). AnkyrinG is required for clustering of voltage-gated Na channels at axon initial segments and for normal action potential firing. *The Journal of cell biology* *143*, 1295-1304.
- Zhuchenko, O., Bailey, J., Bonnen, P., Ashizawa, T., Stockton, D.W., Amos, C., Dobyns, W.B., Subramony, S.H., Zoghbi, H.Y., and Lee, C.C. (1997). Autosomal dominant cerebellar ataxia (SCA6) associated with small polyglutamine expansions in the alpha 1A-voltage-dependent calcium channel. *Nature genetics* *15*, 62-69.
- Zoghbi, H.Y. (1991). The spinocerebellar degenerations. *Curr Neurol* *11*: 121-144.
- Zoghbi, H.Y., and Ballabio, A. (1995). Spinocerebellar ataxia type 1. In *The Metabolic and Molecular Basis of Inherited Disease, Seventh Edition*, C.R. Scriver, A.L. Beaudet, W.S. Sly, and D. Valle, eds (New York: McGraw Hill), pp. 4559-4568.
- Zoghbi, H.Y., and Orr, H.T. (1995). Spinocerebellar ataxia type 1. *Seminars in cell biology* *6*, 29-35.
- Zoghbi, H.Y., and Orr, H.T. (2000). Glutamine repeats and neurodegeneration. *Annual review of neuroscience* *23*, 217-247.

REFERENCES

- Zuccato, C., Belyaev, N., Conforti, P., Ooi, L., Tartari, M., Papadimou, E., MacDonald, M., Fossale, E., Zeitlin, S., Buckley, N., and Cattaneo, E. (2007). Widespread disruption of repressor element-1 silencing transcription factor/neuron-restrictive silencer factor occupancy at its target genes in Huntington's disease. *J Neurosci* 27, 6972-6983.
- Zuccato, C., Ciammola, A., Rigamonti, D., Leavitt, B.R., Goffredo, D., Conti, L., MacDonald, M.E., Friedlander, R.M., Silani, V., Hayden, M.R., *et al.* (2001). Loss of huntingtin-mediated BDNF gene transcription in Huntington's disease. *Science (New York, N.Y)* 293, 493-498.
- Zuccato, C., Tartari, M., Crotti, A., Goffredo, D., Valenza, M., Conti, L., Cataudella, T., Leavitt, B.R., Hayden, M.R., Timmusk, T., *et al.* (2003). Huntingtin interacts with REST/NRSF to modulate the transcription of NRSE-controlled neuronal genes. *Nature genetics* 35, 76-83.
- Zuo, J., De Jager, P.L., Takahashi, K.A., Jiang, W., Linden, D.J., and Heintz, N. (1997). Neurodegeneration in Lurcher mice caused by mutation in delta2 glutamate receptor gene. *Nature* 388, 769-773.

APPENDIX 1 PRIMER SEQUENCE AND PCR CONDITIONS

PCR Product Description	Forward Primer	Reverse Primer	PCR conditions	Figure
β-III spectrin exons 1+7 (Bait in overlapping PCR)	Name - 5'BD Sequence – TCA TCG GAA GAG AGT AGT AAC	Name - Revexon7 Sequence - GCC AAT TCT TTT GCC TTC CAC AGC	Annealing temp, 54°C Extension temp, 72°C for 30 seconds	3.2
β-III spectrin exon 7 – 1108 aa (Bait in overlapping PCR)	Name – Forexon7 Sequence – TTA CTA CCA CTA CTT CTC CAA GAT G	Name - reverse3413 Sequence - GGA TCA GCC TGG TCT CTG GTC A	Annealing temp, 65°C Extension temp, 72°C for 3 minutes	3.2
β-III spectrin exon 1+7 – 1108 aa (Product of overlapping PCR)	Name – ForExon1 Sequence – ATG AGC AGC ACT CTG TCA CCC ACT	Name – reverse3360 Sequence - CTC GCT CTG GGC TCT CTC CAC	Annealing temp, 65°C Extension temp, 72°C for 3 minutes	3.2
L253P β-III spectrin in pRK5 vector	Name – for_german Sequence – GGC CTG ACG AAG CCC CTG GAT CCT GAA G	Name – rev_german Sequence – CTT CAG GAT CCA GGG GCT TCG TCA GGC C	Annealing temp, 70°C Extension temp, 68°C for 7.5 minutes	6.2, 6.3, 6.4, 6.7, 6.8, 6.9, 6.10, 6.11, 6.12, 6.14

APPENDIX 1 PRIMER SEQUENCE AND PCR CONDITIONS

PCR Product Description	Forward Primer	Reverse Primer	PCR conditions	Figure
A486T β -III spectrin in pRK5 vector	Name - for_ala486_thr Sequence - CTG CAA GCG GTG GAC ACC GTA GCC GCA GAA CTG	Name - rev_ala486_thr Sequence - CAG TTC TGC GGC TAC GGT GTC CAC CGC TTG CAC	Annealing temp, 55°C Extension temp, 68°C for 20 mins	6.2, 6.6
R634W β -III spectrin in pRK5 vector	Name - for_arg634_trp Sequence - GCA GCA ACT CGA TGG GCC CGA CTG GAA GAG	Name - rev_arg634_trp Sequence - CTC TTC CAG TCG GGC CCA TCG AGT TGC TGC	Annealing temp, 55°C Extension temp, 68°C for 20 mins	6.2, 6.6
R658W β -III spectrin in pRK5 vector	Name - for_arg658_trp Sequence - GCC GAG GCC TGG GTT TGG GAG CAG CAG CAC CTC	Name - rev_arg658_trp Sequence - GAG GTG CTG CTG CTC CCA AAC CCA GGC CTC GGC	Annealing temp, 55°C Extension temp, 68°C for 20 mins	6.2, 6.6
R1278Q β -III spectrin in pRK5 vector	Name - for_arg1278_gln Sequence - CGC CTT CGG GAC AAC CAA GAG CAG CAG CAC TTC	Name - rev_arg1278_gln Sequence - GAA GTG CTG CTG CTC TTG GTT GTC CCG AAG GCG	Annealing temp, 55°C Extension temp, 68°C for 20 mins	6.2, 6.6
Full length β -III spectrin - YC (BiFC assay)	Name - for_beta_venus2 Sequence - ATT TGC GGC CGC ATG AGC AGC ACC CTG TCA CCC A	Name - rev_betafull_v2 Sequence - CCA TCG ATT TTG TTC TTC TTA AAG AAG CTG AAT C	Annealing temp, 65°C Extension temp, 68°C for 7.5 mins	6.9, 7.6

APPENDIX 1 PRIMER SEQUENCE AND PCR CONDITIONS

PCR Product Description	Forward Primer	Reverse Primer	PCR conditions	Figure
β-III spectrin (exons 1-7)-YC (BiFC assay)	Name - for_beta_venus2 Sequence - ATT TGC GGC CGC ATG AGC AGC ACC CTG TCA CCC A	Name - rev_betamino_v2 Sequence - CCA TCG ATG CCA ATT CTT TTG CCT TCC ACA GC	Annealing temp, 65°C Extension temp, 72°C for 2 mins	7.5, 7.8, 7.16
Arp-YN (BiFC assay)	Name - for_arp_venus Sequence - ATT TGC GGC CGC ATG GAG TCC TAC GAT GTG ATC GC	Name - rev_arp_venus Sequence - CCA TCG ATG AAG GTT TTC CTG TGG ATG GAT CG	Annealing temp, 65°C Extension temp, 72°C for 2 mins	7.8
β-III spectrin (β-IIIInt295) with introduced EcoRI restriction sites for introduction into pGBKT7	Name - ForEcoRIexon1 Sequence - GGA ATT CAT GAG CAG CAC TCT GTC ACC CAC T	Name - RevEcoRIexon7 Sequence - GGA ATT CCT AGC CAA TTC TTT TGC CTT CCA CAG C	Annealing temp, 70°C Extension temp, 72°C for 1 min	7.1, 7.3, 7.14
Arp1a with introduced EcoRI and XhoI restriction sites for introduction into pACT2	Name – ForEcoRIARP1A Sequence – GGA ATT CGC ATG GAG TCC TAC GAT GTG ATC GC	Name – RevXhoIARP1A Sequence – CCG CTC GAG TTA GAA GGT TTT CCT GTG GAT GGA	Annealing temp, 65°C Extension temp, 72°C for 2 mins	7.2
β-III spectrin (β-IIIInt851) with introduced EcoRI and XhoI restriction sites for introduction into pGBKT7	Name - ForEcoRIexon1 Sequence - GGA ATT CAT GAG CAG CAC TCT GTC ACC CAC T	Name – RevXhoIbIII851 Sequence – CCG CTC GAG CTA GGC TGC TTC CAG GGC TCG TGC	Annealing temp, 70°C Extension temp, 72°C for 3 mins	7.3, 7.14

APPENDIX 1 PRIMER SEQUENCE AND PCR CONDITIONS

PCR Product Description	Forward Primer	Reverse Primer	PCR conditions	Figure
β-III spectrin (βIII220-851) with introduced EcoRI and XhoI restriction sites for introduction into pGBKT7	Name – ForEcoRIβIIIexon (6) Sequence – GGA ATT CGC CGG CCA GAC CTG TTG GAT TTT GAG	Name – RevXhoIβIII851 Sequence – CCG CTC GAG CTA GGC TGC TTC CAG GGC TCG TGC	Annealing temp, 70°C Extension temp, 72°C for 2 mins	7.3, 7.14
β-III spectrin (βIII259-851) with introduced EcoRI and XhoI restriction sites for introduction into pGBKT7	Name – ForEcoRIβIIIexon (7) Sequence – GGA ATT CGC GAT GTG AAC GTA GAC CAA CCC GAT	Name – RevXhoIβIII851 Sequence – CCG CTC GAG CTA GGC TGC TTC CAG GGC TCG TGC	Annealing temp, 70°C Extension temp, 72°C for 2 mins	7.3, 7.14
Full length prosaposin	Name - for_prosp_full Sequence - ATG TAT GCT CTC GCT CTC CTC GC	Name - rev_prosp_full Sequence - CTA GTT CCA CAC ATG GCG TTT GC	Annealing temp, 65°C Extension temp, 72°C for 2 mins	
Prosaposin with introduced NotI restriction sites	Name - for_prosp_prk5 Sequence - ATT TGC GGC CGC CAT GTA TGC TCT CGC TCT CCT CGC	Name - rev_prosp_prk5 Sequence - TAA AGC GGC CGC CTA GTT CCA CAC ATG GCG TTT GC	Annealing temp, 65°C Extension temp, 72°C for 2 mins	

APPENDIX 1 PRIMER SEQUENCE AND PCR CONDITIONS

PCR Product Description	Forward Primer	Reverse Primer	PCR conditions	Figure
Prosaposin-YN (BiFC assay)	Name - for_prosp_venus1 Sequence - ATT TGC GGC CGC ATG TAT GCT CTC GCT CTC CTC GC	Name - rev_prosp_venus1 Sequence - CCA TCG ATG TTC CAC ACA TGG CGT TTG CAA TG	Annealing temp, 65°C Extension temp, 72°C for 2 mins	7.5
YN-Prosaposin (BiFC assay)	Name - for_venus1_prosp Sequence - CCT CCG GAA TGT ATG CTC TCG CTC TCC TCG C	Name - rev_venus1_prosp Sequence - GCT CTA GAC TAG TTC CAC ACA TGG CGT TTG C	Annealing temp, 65°C Extension temp, 72°C for 2 mins	7.5
YC - β -III spectrin (exons 1-7)(BiFC assay)	Name - for_venus2_beta Sequence - CCT CCG GAA TGA GCA GCA CCC TGT CAC CCA	Name - rev_v2_betaamino Sequence - GCT CTA GAC TAG CCA ATT CTT TTG CCT TCC AC	Annealing temp, 65°C Extension temp, 72°C for 2 mins	6.13 7.5, 7.7, 7.16, 7.17
YC-Full length β -III spectrin (BiFC assay)	Name - for_venus2_beta Sequence - CCT CCG GAA TGA GCA GCA CCC TGT CAC CCA	Name - rev_v2_betafull Sequence - GCT CTA GAC TAC TTG TTC TTC TTA AAG AAG CTG A	Annealing temp, 65°C Extension temp, 68°C for 7.5 mins	7.6
YC- β -III spectrin (exons 1-6) (BiFC assay)	Name - for_venus2_beta Sequence - CCT CCG GAA TGA GCA GCA CCC TGT CAC CCA	Name - Rev_exon_6 Sequence - GCT CTA GAC TAC TTC AGG ATC CAG GAG CTT CGT C	Annealing temp, 65°C Extension temp, 72°C for 2 mins	7.7, 7.9, 7.17
YC- β -III spectrin (exons 1-5) (BiFC assay)	Name - for_venus2_beta Sequence - CCT CCG GAA TGA GCA GCA CCC TGT CAC CCA	Name - Rev_exon_5 Sequence - GCT CTA GAC TAG TGT TTG TGC ACA ATG GCA TTA AAG	Annealing temp, 65°C Extension temp, 72°C for 2 mins	7.7, 7.9, 7.17

APPENDIX 1 PRIMER SEQUENCE AND PCR CONDITIONS

PCR Product Description	Forward Primer	Reverse Primer	PCR conditions	Figure
YC – L253P β-III spectrin (exons 1-7)(BiFC assay)	Name - for_venus2_beta Sequence - CCT CCG GAA TGA GCA GCA CCC TGT CAC CCA	Name - rev_v2_betaamino Sequence - GCT CTA GAC TAG CCA ATT CTT TTG CCT TCC AC	Annealing temp, 65°C Extension temp, 72°C for 2 mins	6.13 7.7, 7.17
YN-Arp (BiFC assay)	Name - for_venus_arp Sequence - CCT CCG GAA TGG AGT CCT ACG ATG TGA TCG C	Name - rev_venus_arp Sequence - GCT CTA GAT TAG AAG GTT TTC CTG TGG ATG GAT	Annealing temp, 65°C Extension temp, 72°C for 2 mins	6.13, 7.8, 7.9
Clathrin light chain (CLC374) with introduced EcoRI and XhoI restriction sites for introduction into pACT2	Name – ForEcoRIclathrin Sequence – GGA ATT CGC ATG GCT GAG TTG GAT CCA TTT GGC	Name – RevXhoIclathmid Sequence - CCG CTC GAG TCA ATC GAG GGC TTC CAG GCG CTC	Annealing temp, 65°C Extension temp, 72°C for 30 secs	7.15
Clathrin light chain (CLC375- 746) with introduced EcoRI and XhoI restriction sites for introduction into pACT2	Name – ForEcoRIClathmid Sequence - GGA ATT CGC GCC AAT TCT CGG AAG CAG GAA GC	Name – RevXhoIclathrin Sequence – CCG CTC GAG TCA ATG CAC CAG GGG CGC CTG	Annealing temp, 65°C Extension temp, 72°C for 30 secs	7.15

APPENDIX 1 PRIMER SEQUENCE AND PCR CONDITIONS

PCR Product Description	Forward Primer	Reverse Primer	PCR conditions	Figure
Clathrin light chain (CLC246-500) with introduced EcoRI and XhoI restriction sites for introduction into pACT2	Name – ForEcoRIClathend Sequence - GGA ATT CGC TAC TAC CAG GAG AGC AAT GGT CCA	Name – RevXhoIClathbeg Sequence - CCG CTC GAG TCA AGC TTC ATC TGC CAC CCT GTT GC	Annealing temp, 65°C Extension temp, 72°C for 30 secs	7.15
Clathrin-YN (BiFC assay)	Name - for_clath_ven1 Sequence - ATT TGC GGC CGC ATG GCT GAG TTG GAT CCA TTT GGC	Name - rev_clath_ven1 Sequence - CCA TCG ATA TGC ACC AGG GGC GCC TGC TT	Annealing temp, 65°C Extension temp, 72°C for 1 min	7.16
YN-Clathrin (BiFC assay)	Name - for_ven1_clath Sequence - CCT CCG GAA TGG CTG AGT TGG ATC CAT TTG GC	Name - rev_ven1_clath Sequence - GCT CTA GAC TAA TGC ACC AGG GGC GCC TGC TT	Annealing temp, 65°C Extension temp, 72°C for 1 min	7.16. 7.17

APPENDIX 2 PREDICTED MOLECULAR WEIGHTS OF FUSION PROTEINS

Protein Name	Size (kDa)
F.L β -III spectrin	270
Δ 2-6 β -III spectrin	250
Calbindin	28
EAAT4	~60
p38	38
GLAST	~60
GLT1	~60
Actin	43
L253P β -III spectrin	270
L253P β -III spectrin (rat) cleaved products	22 and 26
L253P β -III spectrin (human) cleaved products	22 and 26
A486T β -III spectrin	270
R634W β -III spectrin	270
R658W β -III spectrin	270
R1278Q β -III spectrin	270
CHOP	27
GAL4 (BD)- β -IIIInt295	57
GAL4 (AD)-FL-Arp	57
GAL4 (BD)- β -IIIInt219	47
GAL4 (BD)- β -IIIInt258	52
GAL4 (BD)- β -IIIInt851	127
GAL4 (BD)- β -IIIInt220-851	95
GAL4 (BD)- β -IIIInt259-851	90
GAL4 (AD)-COOH prosaposin	26
YN-prosaposin	93
Prosaposin-YN	93
YC- β III295	48
β III295-YC	48
YC- F.L β -III spectrin	314
F.L β -III spectrin-YC	314
YC- β -IIIInt258	43
YC- β -IIIInt219	38
L253P YC- β -III spectrin295	48
YN-Arp	63
Arp-YN	63

APPENDIX 2 PREDICTED MOLECULAR WEIGHTS OF FUSION PROTEINS

Protein Name	Size (kDa)
Prosaposin	72
Saposin D	10
GAL4 (AD)-CLC1	47
GAL4 (AD)-CLC374	31
GAL4 (AD)-375-746	30
GAL4 (AD)-246-500	26
YN-CLC	52
CLC-YN	52

APPENDIX 3 DVD

APPENDIX 4 LIST OF PUBLICATIONS

Clarkson, Y.L., Gillespie, T., Perkins, E.M., Lyndon, A.R., and Jackson, M. 2010. β -III spectrin mutations L253P associated with spinocerebellar ataxia type 5 interferes with binding to Arp1 and protein trafficking from the Golgi. *Human molecular genetics*. 19. 1-8.

Perkins, E.M., Clarkson, Y.L., Sabatier, N., Longhurst, D.M., Millward, C.P., Jack, J., Toraiwa, J., Watanabe, M., Rothstein, J.D., Lyndon, A.R., Wyllie, D.J., Dutia, M.B., and Jackson, M. 2010. Loss of β -III spectrin leads to Purkinje cell dysfunction recapitulating the behaviour and neuropathology of spinocerebellar ataxia type 5 in humans. *J Neurosci* 30, 4857-4867.

Abstracts

Society For Neuroscience. 2009.

Clarkson, Y.L., Perkins, E.M., and Jackson, M. Human SCA5 mutations may have a dominant-negative effect on wild type beta-III spectrin.

Society For Neuroscience. 2008.

Clarkson, Y., Cheng, Y., Perkins, E., and Jackson, M. Newly identified interactors of β -III spectrin and their role in Spinocerebellar Ataxia type 5.

Posters

Y. L. Clarkson, E. M. Perkins, D. Longhurst and M. Jackson. β -III spectrin deficient mice provide a new animal model for cerebellar ataxia. Presented at Edinburgh neuroscience, 2009. Award winning poster.

β -III spectrin mutation L253P associated with spinocerebellar ataxia type 5 interferes with binding to Arp1 and protein trafficking from the Golgi

Yvonne L. Clarkson^{1,2}, Trudi Gillespie³, Emma M. Perkins^{1,2}, Alastair R. Lyndon⁴
and Mandy Jackson^{1,2,*}

¹The Centre for Integrative Physiology, ²Euan MacDonald Centre for Motor Neuron Disease Research and ³IMPACT Imaging facility, The University of Edinburgh, Hugh Robson Building, George Square, Edinburgh EH8 9XD, UK and ⁴School of Life Sciences, Heriot-Watt University, John Muir Building, Riccarton, Edinburgh EH14 4AS, UK

Received June 9, 2010; Revised June 9, 2010; Accepted June 30, 2010

Spinocerebellar ataxia type 5 (SCA5) is an autosomal dominant neurodegenerative disorder caused by mutations in β -III spectrin. A mouse lacking full-length β -III spectrin has a phenotype closely mirroring symptoms of SCA5 patients. Here we report the analysis of heterozygous animals, which show no signs of ataxia or cerebellar degeneration up to 2 years of age. This argues against haploinsufficiency as a disease mechanism and points towards human mutations having a dominant-negative effect on wild-type (WT) β -III spectrin function. Cell culture studies using β -III spectrin with a mutation associated with SCA5 (L253P) reveal that mutant protein, instead of being found at the cell membrane, appears trapped in the cytoplasm associated with the Golgi apparatus. Furthermore, L253P β -III spectrin prevents correct localization of WT β -III spectrin and prevents EAAT4, a protein known to interact with β -III spectrin, from reaching the plasma membrane. Interaction of β -III spectrin with Arp1, a subunit of the dynactin–dynein complex, is also lost with the L253P substitution. Despite intracellular accumulation of proteins, this cellular stress does not induce the unfolded protein response, implying the importance of membrane protein loss in disease pathogenesis. Incubation at lower temperature (25°C) rescues L253P β -III spectrin interaction with Arp1 and normal protein trafficking to the membrane. These data provide evidence for a dominant-negative effect of an SCA5 mutation and show for the first time that trafficking of both β -III spectrin and EAAT4 from the Golgi is disrupted through failure of the L253P mutation to interact with Arp1.

INTRODUCTION

Spinocerebellar ataxia type 5 (SCA5) is an autosomal dominant neurodegenerative disease. It is characterized by gait and limb ataxia, dysarthria and uncoordinated eye movements, and arises from dysfunction and degeneration of the cerebellum (1–3). Different mutations in the gene encoding β -III spectrin (*SPTBN2*) were identified as the genetic cause of SCA5 in three independent families (3).

Spectrins are heterotetramers comprising two α - and two β -subunits. The α - and β -subunits associate laterally, forming anti-parallel heterodimers which interact head-to-head to form the functional heterotetramer (4,5). Short actin filaments then link the spectrin tetramers together

forming a flexible spectrin network attached to the inner leaf of the membrane bilayer. They were originally discovered in erythrocytes and shown to be critical for mechanical support and maintenance of structural membrane integrity, with defects resulting in hereditary elliptocytosis and spherocytosis (6–9). Spectrins also play important roles in stabilizing cell–cell contacts and localizing ion channels and cell adhesion molecules within specific subdomains of the plasma membrane (10–12).

Vertebrates have two α -subunits ($\alpha I/\alpha II$), four β -subunits ($\beta I-\beta IV$) and a β -H subunit creating diversity and specialization of function (13). The mammalian erythrocyte spectrin ($\alpha I/\beta I$) is found in striated muscle and a subset of neurons, whereas $\alpha II/\beta II$, $\alpha II/\beta III$ and $\alpha II/\beta IV$ are the major forms in

*To whom correspondence should be addressed. Tel: +44 1316507518; Email: mandy.jackson@ed.ac.uk

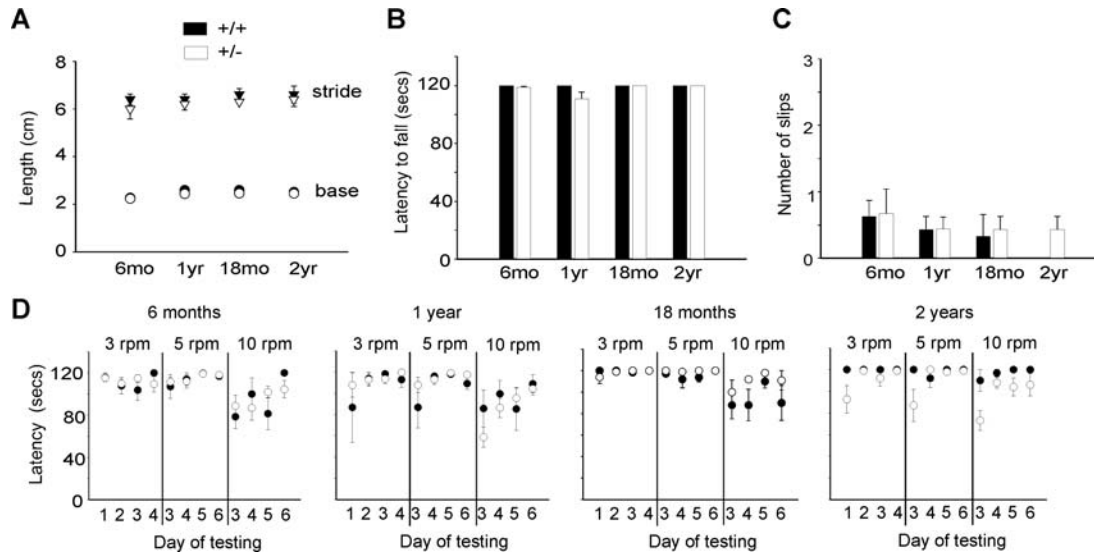


Figure 1. Progressive motor deficits not seen in heterozygous β -III^{+/-} mice. (A) Footprint analysis, base width and stride length of 6-month to 2-year old mice. (B) Ability to remain on stationary rod. Mice were given four consecutive trials, with maximum time of 60 s. (C) Number of hind-limb slips age-matched WT and β -III^{+/-} mice made when crossing narrow, elevated beam. (D) Latency of WT and β -III^{+/-} animals to fall from rotarod at 3, 5 and 10 rpm. Mice were given four trials per day and allowed a maximum retention time of 120 s per trial. All data are means \pm SEM (WT $n = 3-7$, β -III^{+/-} $n = 7-9$).

non-erythroid vertebrate tissues. β -III spectrin is primarily expressed in the nervous system, with the highest levels of expression in the cerebellum, where it is found in Purkinje cell soma and dendrites (14,15). Originally, it was shown to associate with the Golgi apparatus (16), but this staining is now thought to have arisen from antibody cross-reactivity (17). We have previously shown β -III spectrin to stabilize EAAT4, the glutamate transporter predominantly expressed in Purkinje cells, at the cell surface (15). Other investigators have found the N-terminal actin-binding region of β -III spectrin interacts with Arp1, a subunit of the dynactin–dynein complex (18). A role for β -III spectrin in dynein-mediated vesicular transport is implied by observation of axonal transport defects in *Drosophila* expressing mutant forms of β spectrin, which are exacerbated by the expression of mutant dynein and dynactin (19).

We recently generated a functional β -III spectrin knockout mouse (β -III^{-/-}) and found that from a young age it showed characteristic features of cerebellar ataxia, suggesting a loss of β -III spectrin function underlies SCA5 pathogenesis (20). Since the human disease is autosomal dominant, this finding indicates that either the mutant forms of β -III spectrin are simply inactive and the disease arises from haploinsufficiency or, in addition to being non-functional, the mutant subunits also have a dominant-negative effect and suppress the function of wild-type (WT) spectrin. In order to investigate these two possibilities, we analysed heterozygous animals for signs of motor deficits and cerebellar degeneration. We show here that even at 2 years of age, heterozygous animals show no signs of ataxia or cerebellar pathology. Instead, using cell culture studies, we provide evidence that β -III spectrin containing a mutation associated with SCA5 (L253P) has a dominant-negative effect on WT protein function and interferes with membrane protein trafficking.

RESULTS

Heterozygous β -III^{+/-} spectrin mice show no signs of ataxia or cerebellar degeneration

We previously reported that homozygous β -III spectrin-deficient mice (β -III^{-/-}) develop characteristics of ataxia including a wider hind-limb gait, progressive motor incoordination, cerebellar atrophy and Purkinje cell loss (20). To determine whether heterozygous (β -III^{+/-}) mice eventually show signs of ataxia, we carried out behavioural tests and histological analysis on mice aged 6 months to 2 years of age. Analysis of footprint patterns showed no significant difference in base width or stride length between β -III^{+/-} and WT littermates (Fig. 1A). There was also no significant difference in motor performance between the genotypes, heterozygous animals performing as well as WT controls on a stationary rod (Fig. 1B), an elevated beam (Fig. 1C) and a rotating rod task (Fig. 1D).

Cerebellar sections stained for Nissl demonstrated that the size and morphology of the cerebellum appeared normal in 2-year old β -III^{+/-} mice, apart from slight differences in folia I and II (Fig. 2A1 and B1). Immunostaining for calbindin showed no changes to Purkinje cell morphology in β -III^{+/-} mice (Fig. 2A2 and A3, and B2 and B3), whereas quantification of Purkinje cell density and molecular layer thickness revealed no cell loss or cerebellar atrophy (WT, 39.6 ± 3.4 ; β -III^{+/-}, 37 ± 8.6 cell/mm; $P = 0.73$ and WT, 181.7 ± 7.1 ; β -III^{+/-}, 197.7 ± 11.4 μ m; $P = 0.37$; $n = 3$ of each genotype). We also saw no significant reduction in glutamate transporter levels in β -III^{+/-} mice (Fig. 2C), providing additional evidence that the loss of EAAT4 and GLAST in β -III^{-/-} mice (20) may be important aspects of disease pathogenesis. Therefore, β -III^{+/-} mice display none of the characteristics of cerebellar ataxia, arguing against haploinsufficiency as a disease mechanism in the mouse, and hence arguing for a

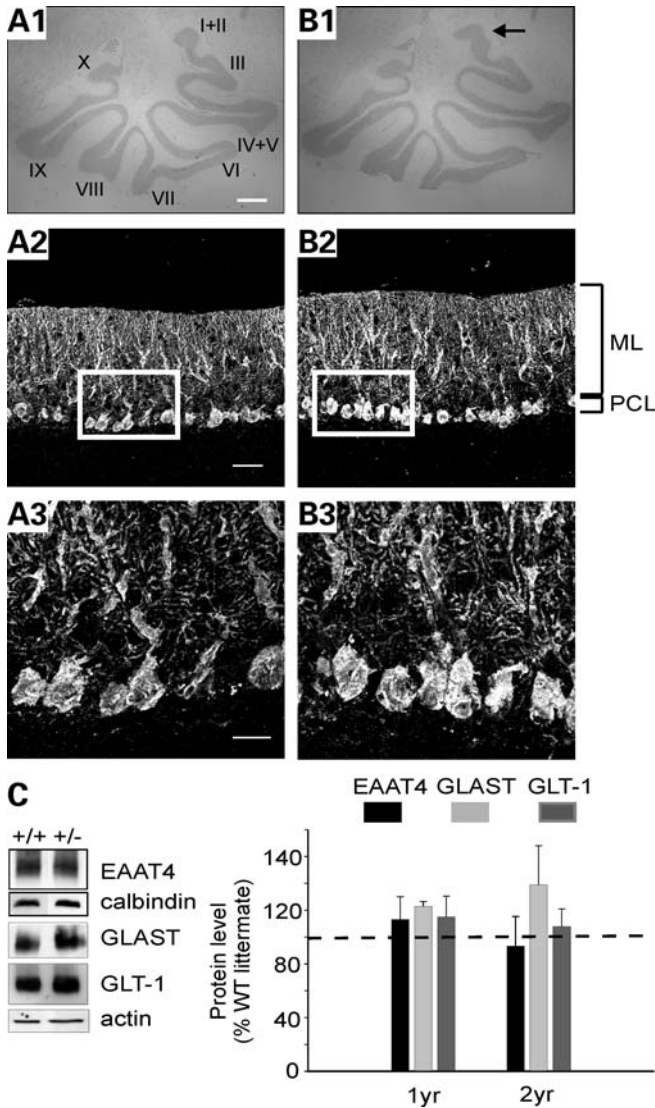


Figure 2. No cerebellar pathology in β -III^{+/-} mice. Histological analysis of cerebellum from 2-year old WT (A) and β -III^{+/-} (B) mice. (A1, B1) Cresyl violet stain shows whole cerebellar morphology. (A2–B3) Calbindin immunostaining reveals Purkinje cell morphology (ML, molecular layer; PCL, Purkinje cell layer; scale bars: A1 and B1, 500 μ m; A2 and B2, 50 μ m; A3 and B3, 20 μ m). (C) Representative western blot and densitometry data quantifying levels of plasma membrane glutamate transporters in 2-year-old β -III^{+/-} and WT animals. EAAT4 levels normalized with calbindin, a Purkinje cell specific marker. GLAST and GLT1 normalized with actin. All data are means \pm SEM ($n = 3$ of each genotype).

dominant-negative effect of mutant β -III spectrin on WT β -III spectrin function associated with SCA5.

β -III spectrin associates with the Golgi apparatus when Leu253 is substituted by proline

To investigate potential dominant-negative effects, we transfected Neuro2a and human embryonic kidney (HEK) 293T cells with constructs encoding either myc-tagged WT β -III spectrin or β -III spectrin containing a mutation associated with SCA5. The missense mutation (L253P) found in one family with SCA5 was introduced by site-directed

mutagenesis into rat β -III spectrin cDNA. The leucine 253 residue and the N-terminus of β -III spectrin are highly conserved from fly to human (3). Immunostaining with an anti-c-myc antibody revealed that, unlike WT, L253P β -III spectrin appears to accumulate in a discrete intracellular location and is no longer found at the plasma membrane (Fig. 3A). No difference in the cellular distribution was seen between the two cell lines examined. We therefore used Neuro2a cells, unless otherwise stated, for all subsequent experiments since β -III spectrin is predominantly a neuronal protein (14–16). To elucidate the intracellular distribution, we co-expressed β -III spectrin constructs with either a Golgi or an endoplasmic reticulum (ER) marker. This revealed that L253P β -III spectrin appears to associate with the Golgi apparatus (Fig. 3B).

To determine the effect of L253P β -III spectrin on WT protein, we co-expressed yellow fluorescent protein (YFP)-tagged WT β -III spectrin with myc-tagged L253P β -III spectrin. We found that the presence of L253P β -III spectrin resulted in WT β -III spectrin–YFP being trapped in the same intracellular location as L253P (Fig. 3C). In contrast, WT β -III spectrin–YFP was found at the plasma membrane when myc-tagged WT β -III spectrin was co-expressed. This finding suggests that the presence of the L253P missense mutation confers a dominant-negative effect on WT β -III spectrin protein.

L253P β -III spectrin interferes with protein trafficking and fails to interact with Arp1

EAAT4 is known to interact directly with and be stabilized at the cell membrane by β -III spectrin (15). Moreover, a decrease in EAAT4 protein is seen in young β -III^{-/-} mice (20) and dramatic changes in EAAT4 distribution are seen in SCA5 autopsy tissue (3). Taken together, these findings suggest that EAAT4 may play an important role in disease pathogenesis. We therefore examined what effect the expression of L253P β -III spectrin had on EAAT4 cellular distribution. Immunofluorescence microscopy revealed accumulation of EAAT4 at the Golgi apparatus when L253P was co-expressed compared with WT β -III spectrin, suggesting a disruption to protein trafficking (Fig. 4A). To test whether a lower temperature could rescue the defect, we incubated transfected cells at 25°C for an additional 12 h before immunostaining. We found that the permissive temperature resulted in L253P β -III spectrin reaching the plasma membrane (Fig. 4B). Western blot analysis confirmed protein levels were not altered by the temperature shift but did show that the expression of L253P β -III spectrin was less than WT protein (Fig. 4B). In addition EAAT4 was no longer trapped intra-cellularly in cells expressing L253P β -III spectrin when incubated at the lower temperature (Fig. 4C).

A role for β -III spectrin in vesicular trafficking has been proposed given its ability to interact with Arp1 and copurify with dynein and dynactin on intracellular vesicles from rat brain (18). We used a biomolecular fluorescence complementation (BiFC) assay to investigate whether the L253P mutation interfered with the ability of the N-terminus of β -III spectrin to interact with Arp1. The BiFC technique is based on the generation of a fluorescent signal when

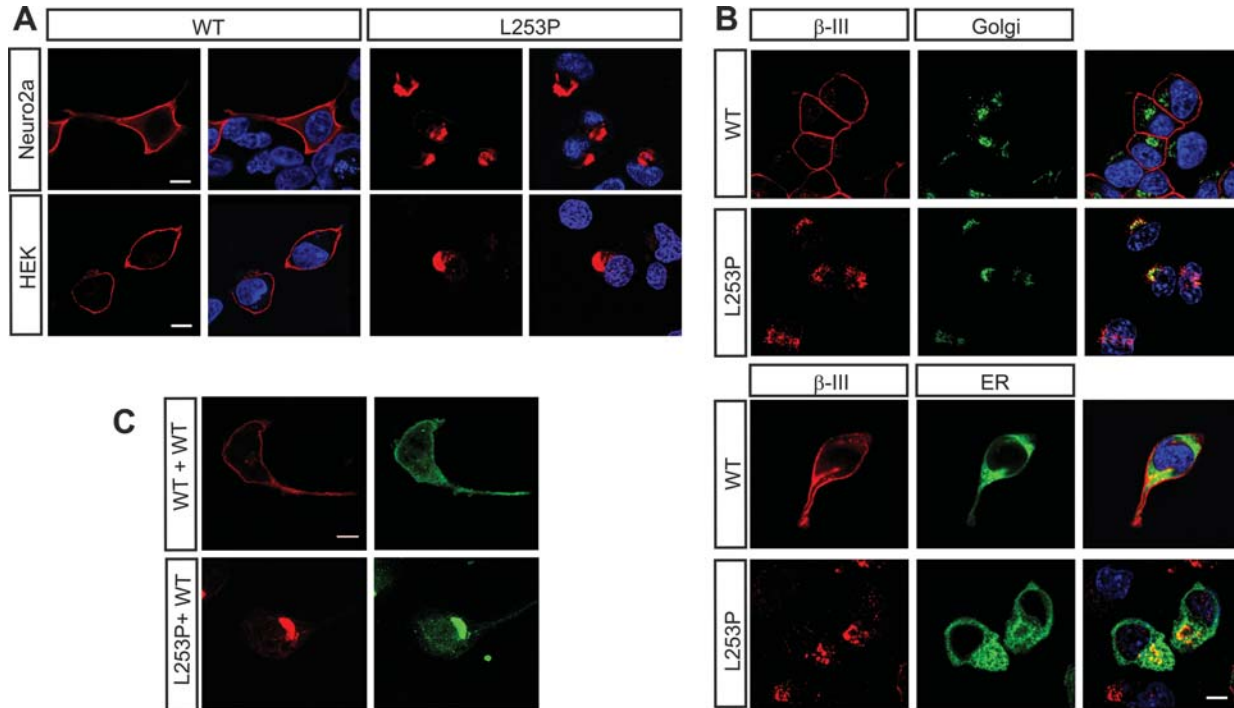


Figure 3. Cellular localization of full-length L253P β -III spectrin overlaps with Golgi marker. (A) Neuro2a and HEK293 cells transfected with either myc-tagged WT or L253P β -III spectrin, fixed and stained using anti-c-myc antibody. Nucleus stained with DAPI (blue). (B) Neuro2a cells cotransfected with either a Golgi (green) or ER (green) marker and myc-tagged WT or L253P β -III spectrin (red). Nucleus stained with DAPI (blue). (C) Neuro2a cells cotransfected with YFP-tagged WT β -III spectrin and either myc-tagged WT or L253P β -III spectrin. Cells immunostained using anti-c-myc antibody (red) and anti-GFP antibody (green). All images are representative of three independent experiments (scale bar, 10 μ m).

the two halves of enhanced YFP are brought together, mediated by the association of two interacting partners fused to the YFP fragments (21,22). We cloned full-length Arp1 and the N-terminus of β -III spectrin (amino acids 1–294) downstream of the N-terminal (YN) and C-terminal fragments (YC) of YFP, respectively, and transfected HEK 293T cells with the expression vectors. Co-expression of YN–Arp1 and WT YC– β -III spectrin yielded fluorescence, but no fluorescence was observed when L253P YC– β -III spectrin was co-expressed with YN–Arp1 (Fig. 4D), indicating that the mutation does indeed eliminate the interaction between β -III spectrin and Arp1. However, incubation at 25°C for an additional 12 h produced a fluorescence signal (Fig. 4D), suggesting that a conformational change underlies the observed lack of interaction at 37°C. Western blot analysis confirmed that all proteins were expressed at 37°C.

Unfolded protein response not induced by L253P expression

A number of neurodegenerative diseases have been shown to be associated with the accumulation of abnormal protein, impaired ER homeostasis and activation of the unfolded protein/endoplasmic stress response (UPR) (23–26). The UPR can be triggered by a block in trafficking at the ER and Golgi, as well as the accumulation of unfolded or misfolded proteins in the ER. Therefore, since L253P appears to

accumulate intra-cellularly and disrupt the trafficking of proteins through the Golgi, we investigated whether the UPR was induced by the expression of L253P.

We looked at increased expression levels and nuclear translocation of the transcription factor growth arrest and DNA damage/C/EBP-homologous protein (GADD153/CHOP), a commonly used indicator of ER stress and thought to be a downstream effector of all three UPR pathways (27,28). Western blot analysis revealed no difference in the level of CHOP protein when L253P β -III spectrin was expressed compared with WT β -III spectrin (Fig. 5A and B). CHOP levels were normalized to those obtained when GFP was overexpressed, and the pharmacological induction of ER stress using tunicamycin, a blocker of N-linked glycosylation, confirmed the ability to induce CHOP expression in the cell culture system. Immunofluorescence microscopy confirmed the absence of CHOP activation in cells transfected with L253P as no nuclear staining was observed, in comparison with high levels observed in tunicamycin-treated cells (Fig. 5C). Finally, we only saw a small increase in the expression of CHOP in symptomatic β -III^{-/-} mice compared with litter mate controls ($116 \pm 7.8\%$ of WT; $n = 4$ of each genotype; $P = 0.11$). These data suggest that UPR is not a major consequence of β -III spectrin loss and is unlikely to underlie the Purkinje cell degeneration observed in the β -III^{-/-} mouse model of ataxia. Furthermore, UPR appears not to be a downstream effect of a β -III spectrin mutation associated with SCA5.

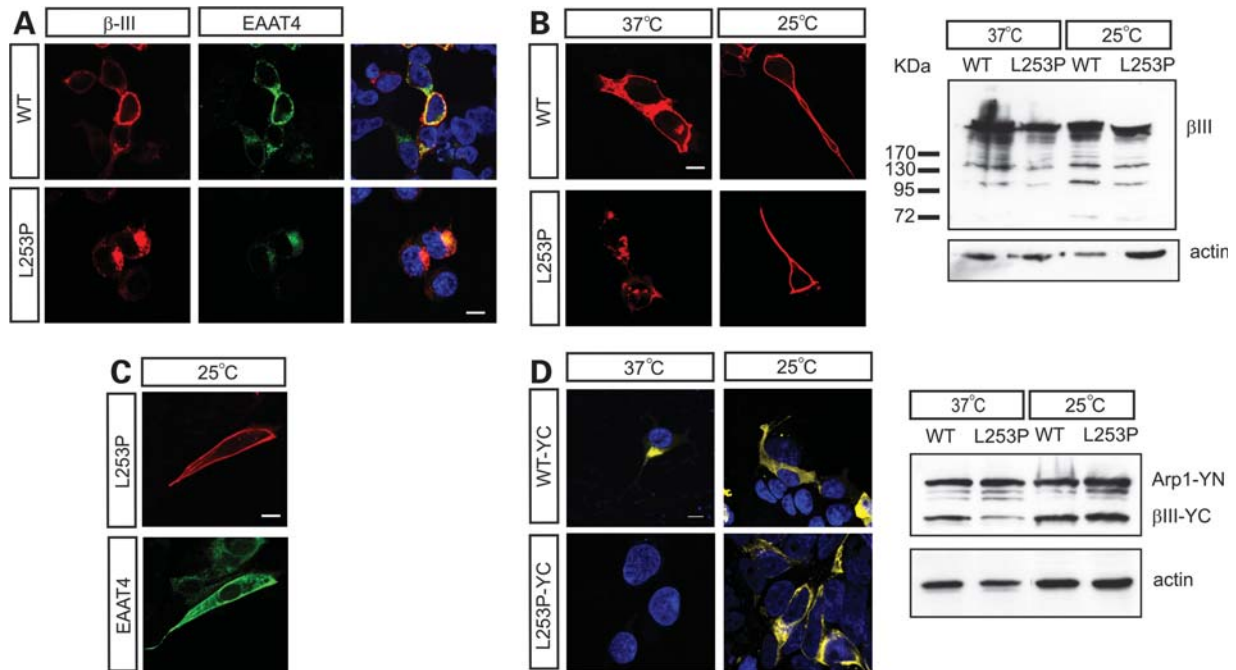


Figure 4. L253P β -III spectrin does not interact with Arp1 and interferes with protein trafficking. (A) Neuro2a cells cotransfected with EAAT4 and either myc-tagged WT or L253P β -III spectrin. Cells immunostained using anti-c-myc antibody (red), anti-EAAT4 antibody (green) and nucleus stained with DAPI (blue). (B) Cells transfected with either myc-tagged WT or L253P β -III spectrin and 24 h after transfection incubated at 37 or 25°C for a further 12 h. Cells immunostained using anti-c-myc antibody (red). Western blot analysis of cell homogenates probed with anti-c-myc antibody. (C) Cells expressing myc-tagged L253P β -III spectrin and EAAT4 incubated at 25°C for a further 12 h. Cells immunostained using anti-c-myc antibody (red) and anti-EAAT4 antibody (green). (D) BiFC assay using cells transfected with Arp1 fused to the N-terminal half of YFP (YN-Arp1) and the actin-binding region of β -III spectrin, with or without the L253P substitution, fused to the C-terminal half of YFP (YC- β -III). Twenty-four hours after transfection cells were incubated at 37 or 25°C for a further 12 h. Western blot analysis of cell homogenates probed with anti-GFP antibody. All images are representative of three independent experiments (scale bar, 10 μ m).

DISCUSSION

A number of dominantly inherited human diseases have recently been shown to arise from haploinsufficiency (29–31). Often in these cases, the genes involved encode proteins where a correct stoichiometry is vital for function and a single WT gene copy is insufficient. Examples are transcription factors or proteins that form macromolecular complexes. Since spectrin functions as a heterotetramer and assembly appears to be rate limited by the β subunit (32), one possibility is that SCA5 arises from β -III spectrin haploinsufficiency due to the mutant β polypeptides failing to associate with other subunits. Here we provide strong evidence that haploinsufficiency is unlikely to be the disease mechanism, as we see no signs of motor deficits or cerebellar degeneration in heterozygous β -III^{+/-} mice even at 2 years of age. This indicates that the loss of β -III spectrin function, thought to be important in disease pathogenesis (20), must arise from mutations associated with SCA5 having a dominant-negative effect on WT β -III spectrin function. It is possible that the heterozygous animals do not live long enough for a phenotype to be detected or the motor tasks used are not sensitive enough to detect minor motor deficits. However, our cell culture studies do indicate that the proline substitution found in one SCA5 family (L253P) appears to have a dominant-negative effect on WT β -III spectrin, preventing protein trafficking from the Golgi apparatus.

Previously, β -III spectrin was shown to stabilize EAAT4 at the plasma membrane (15) and, using total internal reflection fluorescence microscopy, Ranum and co-authors (3) revealed that the in-frame deletion found in the Lincoln SCA5 pedigree fails to stabilize EAAT4 at the cell surface to the same extent as WT β -III spectrin. Here we now show that β -III spectrin also has a role in the vesicular trafficking of EAAT4 from the Golgi to the plasma membrane and the L253P mutation disrupts this process. The observation that a large number of vesicles are found surrounding Golgi cisternae in β -III^{-/-} mice (20) supports this cellular function. Further we have shown that the L253P substitution prevents the normal interaction between Arp1 and the N-terminus of β -III spectrin. Based on their work in *Drosophila*, a link between defects in the dynein–dynactin complex and SCA5 pathogenesis is suggested by Lorenzo *et al.* (19). When flies overexpressing mutant human β -III spectrin (the Lincoln mutation) were crossed with either a hypomorphic dynein heavy chain allele or a dominant mutation in the p150^{Glued} subunit of dynactin, the larvae displayed exacerbated posterior paralysis and slowing of vesicle transport, inferring a synergistic effect between spectrin and dynein–dynactin. Similarly, the rough eye phenotype in flies overexpressing either the Lincoln or the L253P mutation was enhanced by the dynein–dynactin mutants. Here we provide the first direct evidence that a SCA5 mutation interferes with the ability of spectrin to interact with a component of the dynactin complex, highlighting

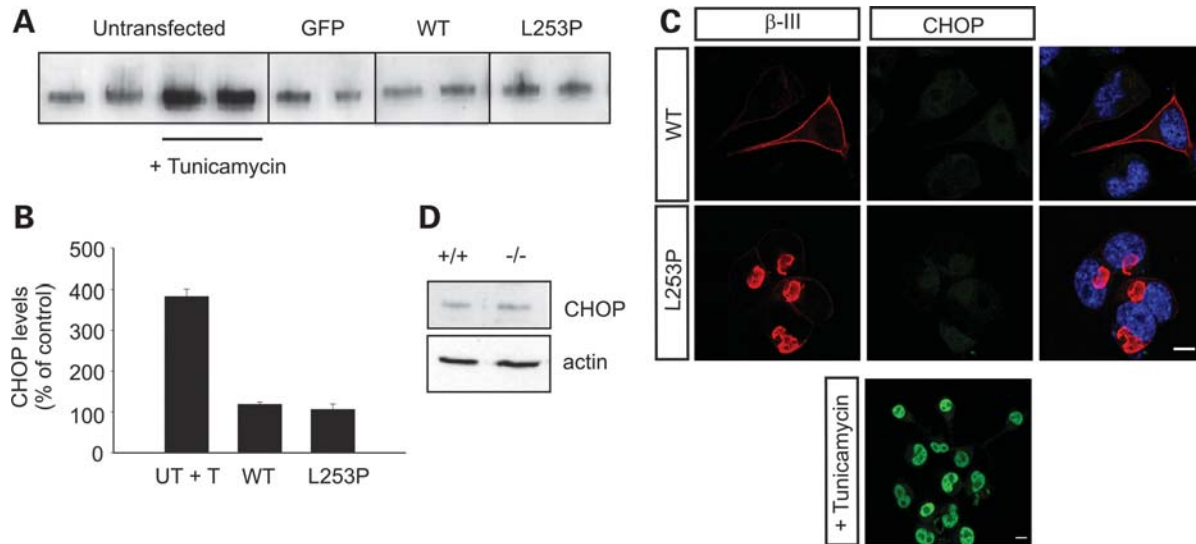


Figure 5. No induction of unfolded protein response by L253P β -III spectrin compared with WT β -III spectrin. (A) Total cellular homogenates of Neuro2a cells transfected with constructs encoding GFP, WT β -III spectrin, L253P β -III spectrin or untransfected cells treated with tunicamycin for 12 h resolved by SDS-PAGE, and immunoblotted using anti-GADD153 antibody. (B) Data quantified by densitometry (means \pm SEM). (C) Representative confocal images of cells immunostained for CHOP (green) and nucleus stained with DAPI (blue). Scale bar, 10 μ m. (D) Total cerebellar homogenates of symptomatic β -III^{-/-} and age-matched WT mice resolved by SDS-PAGE, immunoblotted using anti-GADD153 antibody.

how normal trafficking can be disrupted in SCA5. The fact both the interaction with Arp1 and protein trafficking defects were rescued by incubating at a lower temperature suggests that the L253P substitution results in a protein conformation defect. Ongoing work by Ranum and colleagues supports temperature sensitivity of conformation of the mutant human protein (K.A. Dick Krueger and L.P.W. Ranum personal communication). Importantly, a direct role for dynein in the transport of proteins into dendrites has recently been shown (33), supporting the possibility that interfering with Arp1 binding will result in defects to protein trafficking within the Purkinje cell dendritic tree of SCA5 patients.

Irrespective of the mechanism, the intracellular accumulation of proteins can lead to ER stress, the induction of UPR, and apoptotic cell death. However, we see no major induction of GADD153/CHOP, a downstream effector of UPR in transfected cells or in symptomatic β -III^{-/-} mice. Taken together, these results suggest that unlike other neurodegenerative disorders, the disease mechanism in SCA5 does not involve the induction of UPR. Instead, the actual loss of membrane proteins and their cellular functions appears to be more critical for disease pathogenesis. The expression of mutant forms of β -III spectrin in Purkinje cells and identification of other membrane proteins that are altered will be fundamental to fully understanding the mechanisms of Purkinje cell dysfunction and degeneration. The N-terminus of β spectrin is known to bind actin and 4.1, forming a spectrin/4.1/actin junction. Protein 4.1 has been shown to bind several membrane proteins and be required for their stable cell-surface expression (34–36). Incorporation of a mutant β subunit could alter the conformation of the whole tetramer preventing normal function and interaction with proteins including protein 4.1. Future research should investigate whether different mutations associated with SCA5 alter the ability of β -III

spectrin to interact with components of the dynein–dynactin complex or with protein 4.1.

In summary, the present work has shown that mutant β -III spectrin disrupts protein trafficking from the Golgi apparatus through elimination of normal interaction between β -III spectrin and the dynactin component Arp1. This helps explain the mislocalization of membrane proteins seen in SCA5. Furthermore, haploinsufficiency is not supported as a disease mechanism as indicated by a lack of disease phenotype in mice heterozygous for loss of β -III spectrin.

MATERIALS AND METHODS

Analysis of β -III^{+/-} mice

All genotyping, motor tasks, histology and western blotting analysis were carried out as previously described (20). Seven days prior to the behavioural tests, old mice were habituated to the test environment by handling (10 min each day).

Antibodies

Sagittal cerebellar sections were immunostained using mouse anti-calbindin D (1:50) and cyanine 3 (Cy3)-conjugated goat anti-mouse IgG (Jackson Laboratories). Mouse anti-c-myc (Ab-1, Calbiochem) and either Cy3- or Cy2-conjugated goat anti-mouse IgG (Jackson Laboratories) were used to detect pRK5-myc-tagged constructs. YFP-tagged β -III spectrin was detected with rabbit anti-GFP (Molecular Probes, Invitrogen) and fluorescein isothiocyanate-conjugated goat anti-rabbit IgG (Cappel). Polyclonal antibodies against EAAT4, GLAST and GLT1 were a kind gift of Jeffrey Rothstein, and mouse anti-actin, -calbindin and rabbit anti-GADD153 obtained from Sigma and Santa Cruz, respectively.

Plasmids

The missense mutation L253P was introduced using the QuickChange site-directed mutagenesis kit (Stratagene) according to the manufacturer's instructions using pRK5-myc-tagged β -III spectrin as template and 5'-GGCCTGACGAAGC CCCTGGATCCTGAAG-3' and 5'-CTTCAGGATCCAGG GGCTTCGTCAGGCC-3' as primers. Full-length WT β -III spectrin and the first 294 amino acids of WT and L253P β -III spectrin were amplified by PCR using primers that introduced either *NotI* and *ClaI* (5'-ATTGCGGCCGCATGAGCA GCACCCTGTCACCCA-3' and 5'-CCATCGATTTTGTCTT CTAAAGAAGCTGAAT-3') or *BspEI* and *XbaI* (5'-CCTC CGGAATGAGCAGCACCCGTGTACCCA-3' and 5'-GCTC TAGACTAGCCAATTCTTTGCCTTCCAC-3') restriction sites, respectively, and the products cloned into pcDNA3.1(zeo)-YC vector (kind gift of Stephen Michnick). Full-length Arp 1 was amplified using Quickclone cDNA (Clontech) as template and cloned into the *BspEI* and *XbaI* sites of pcDNA3.1(zeo)-YN. Other plasmids were pcDNA3.1 rat EAAT4 (15) and Golgi (pECFP-golgi) and ER (pDsRed2-ER) markers from Clontech.

Cell culture and transfections

HEK 293T cells were grown in minimum essential medium (MEM, Sigma) containing 10% fetal bovine serum, 10 mM glutamine, 1 \times non-essential amino acids and antibiotics (penicillin and streptomycin). Mouse neuronal 2a (N2a) cells were grown in Dulbecco's modified Eagle's medium (DMEM, Gibco) containing the aforementioned components and supplemented with 4.5 g/l glucose and 0.11 g/l sodium pyruvate (Gibco). For cell homogenates, cells were plated onto 35 mm dishes and for microscopic observation cells were plated onto poly-L-lysine-coated coverslips in 35 mm dishes. A total of 2 μ g of DNA was used to transfect cells with Fugene HD at a ratio of 3:2 according to the manufacturer's instructions (Roche). Twenty-four hours post-transfection cells were either harvested for western blot analysis, fixed with 4% paraformaldehyde for immunostaining, maintained at 37 or 25°C for an additional 12 h (to test for temperature sensitivity shown by K.A. Dick Krueger *et al.*, manuscript submitted) or treated with 2 μ g/ml tunicamycin (Calbiochem) for 12 h. All coverslips were mounted using hard set vectashield containing DAPI unless Cy2-conjugated goat anti-mouse IgG was used. In this instance, vectashield was used as mounting agent (Vector Laboratories, Burlingame, CA, USA).

Microscopy

Images were captured with an Olympus BX51 microscope or using a Zeiss Axiovert confocal laser scanning microscope. All acquisition settings were kept constant between samples, and colours were applied using Image J.

Statistics

Statistical analysis was performed using Student's *t*-test, two sample assuming unequal variance, apart from densitometry

analysis of western blots where one sample *t*-test was used with a predicted value of 100% for the WT.

ACKNOWLEDGEMENTS

We thank Jeffrey Rothstein, Laura Ranum and Paul Skehel for help and useful discussions.

Conflict of Interest statement. The authors have no conflicts of interest to declare.

FUNDING

This work was supported by grants from The Wellcome Trust (077946), the National Institutes of Health (NS056158) and a MRC PhD studentship (to Y.L.C.).

REFERENCES

1. Stevanin, G., Herman, A., Brice, A. and Durr, A. (1999) Clinical and MRI findings in spinocerebellar ataxia type 5. *Neurology*, **53**, 1355–1357.
2. Burk, K., Zuhlke, C., Konig, I.R., Ziegler, A., Schwinger, E., Globas, C., Dichgans, J. and Hellenbroich, Y. (2004) Spinocerebellar ataxia type 5: clinical and molecular genetic features of a German kindred. *Neurology*, **62**, 327–329.
3. Ikeda, Y., Dick, K.A., Weatherspoon, M.R., Gincel, D., Armbrust, K.R., Dalton, J.C., Stevanin, G., Durr, A., Zuhlke, C., Burk, K. *et al.* (2006) Spectrin mutations cause spinocerebellar ataxia type 5. *Nat. Genet.*, **38**, 184–190.
4. Shotton, D.M., Burke, B.E. and Branton, D. (1979) The molecular structure of human erythrocyte spectrin: biophysical and electron microscopic studies. *J. Mol. Biol.*, **131**, 303–329.
5. Ungewickell, E. and Gratzer, W. (1978) Self-association of human spectrin: a thermodynamic and kinetic study. *Eur. J. Biochem.*, **88**, 379–385.
6. Bodine, D.M.I.V., Birkenmeier, C.S. and Barker, J.E. (1984) Spectrin deficient inherited haemolytic anemias in the mouse: characterization by spectrin synthesis and mRNA activity in reticulocytes. *Cell*, **37**, 721–729.
7. Tse, W.T., Lecomte, M.C., Costa, F.F., Garbarz, M., Feo, C., Boivin, P., Dhery, D. and Forget, B.G. (1990) Point mutation in the beta-spectrin gene associated with alpha I/74 hereditary elliptocytosis. Implications for the mechanism of spectrin dimer self-association. *J. Clin. Invest.*, **86**, 909–916.
8. Gallagher, P.G., Tse, W.T., Coetzer, T., Lecomte, M.C., Garbarz, M., Zarkowsky, H.S., Baruchel, A., Ballas, S.K., Dhery, D. and Palek, J. (1992) A common type of the spectrin alpha I 46-50a-kD peptide abnormality in hereditary elliptocytosis and pyropoikilocytosis is associated with a mutation distant from the proteolytic cleavage site. Evidence for the functional importance of the triple helical model of spectrin. *J. Clin. Invest.*, **89**, 892–898.
9. Becker, P.S., Tse, W.T., Lux, S.E. and Forget, B.G. (1993) β spectrin kissimmee: a spectrin variant associated with autosomal dominant hereditary spherocytosis and defective binding to protein 4.1. *J. Clin. Invest.*, **92**, 612–616.
10. Komada, M. and Soriano, P. (2002) β IV-spectrin regulates sodium channel clustering through ankyrin-G at axon initial segments and nodes of Ranvier. *J. Cell. Biol.*, **156**, 337–348.
11. Nishimura, K., Akiyama, H., Komada, M. and Kamiguchi, H. (2007) betaIV-spectrin forms a diffusion barrier against L1CAM at the axon initial segment. *Mol. Cell. Neurosci.*, **34**, 422–430.
12. Wechsler, A. and Teichberg, V.I. (1998) Brain spectrin binding to the NMDA receptor is regulated by phosphorylation, calcium and calmodulin. *EMBO J.*, **17**, 3931–3939.
13. Bennett, V. and Baines, A.J. (2001) Spectrin and ankyrin-based pathways: metazoan inventions for integrating cells into tissues. *Physiol. Rev.*, **81**, 1353–1392.
14. Sakaguchi, G., Orita, S., Naito, A., Maeda, M., Igarashi, H., Sasaki, T. and Takai, Y. (1998) A novel brain-specific isoform of β spectrin: isolation

- and its interaction with Munc13. *Biochem. Biophys. Res. Commun.*, **248**, 846–851.
15. Jackson, M., Song, W., Liu, M.-Y., Jin, L., Dykes-Hoberg, M., Lin, C.-L.G., Bowers, W.B., Federoff, H.J., Sternweis, P.C. and Rothstein, J.D. (2001) Modulation of the neuronal glutamate transporter EAAT4 by two interacting proteins. *Nature*, **410**, 89–93.
 16. Stankewich, M.C., Tse, W.T., Peters, L.L., Ch'ng, Y., John, K.M., Stabach, P.R., Devarajan, P., Morrow, J.S. and Lux, S.E. (1998) A widely expressed β III spectrin associated with Golgi and cytoplasmic vesicles. *Proc. Natl Acad. Sci. USA*, **95**, 14158–14163.
 17. Gough, L.L., Fan, J., Chu, S., Winnick, S. and Beck, K.A. (2003) Golgi localization of Syne-1. *Mol. Biol. Cell.*, **14**, 2410–2424.
 18. Holleran, E.A., Ligon, L.A., Tokito, M., Stankewich, M.C., Morrow, J.S. and Holzbaur, L.F. (2001) β III spectrin binds to the Arp1 subunit of dynactin. *J. Biol. Chem.*, **276**, 36598–36605.
 19. Lorenzo, D.N., Li, M.-G., Mische, S.E., Armbrust, K.R., Ranum, L.P.W. and Hays, T.S. (2010) Spectrin mutations that cause spinocerebellar ataxia type 5 impair axonal transport and induce neurodegeneration in *Drosophila*. *J. Cell. Biol.*, **189**, 143–158.
 20. Perkins, E.M., Clarkson, Y.L., Sabatier, N., Longhurst, D.M., Millward, C.P., Jack, J., Toraiwa, J., Watanabe, M., Rothstein, J.D., Lyndon, A.R. *et al.* (2010) Loss of β -III spectrin leads to Purkinje cell dysfunction recapitulating the behaviour and neuropathology of spinocerebellar ataxia type 5 in humans. *J. Neurosci.*, **30**, 4857–4867.
 21. Hu, C.D., Chinenov, Y. and Kerppola, T.K. (2002) Visualization of interactions among bZIP and Rel family proteins in living cells using bimolecular fluorescence complementation. *Mol. Cell*, **9**, 789–798.
 22. Hu, C.D. and Kerppola, T.K. (2003) Simultaneous visualization of multiple protein interactions in living cells using multicolour fluorescence complementation analysis. *Nat. Biotechnol.*, **21**, 539–545.
 23. Atkin, J.D., Farg, M.A., Turner, B.J., Tomas, D., Lysaght, J.A., Nunan, J., Rembach, A., Nagley, P., Beart, P.M., Cheema, S.S. and Horne, M.K. (2006) Induction of the unfolded protein response in familial amyotrophic lateral sclerosis and association of protein-disulfide isomerase with superoxide dismutase 1. *J. Biol. Chem.*, **281**, 30152–30165.
 24. Nagata, T., Ilieva, H., Murakami, T., Shiote, M., Narai, H., Ohta, Y., Hayashi, T., Shoji, M. and Abe, K. (2007) Increased ER stress during motor neuron degeneration in a transgenic mouse model of amyotrophic lateral sclerosis. *Neurol. Res.*, **29**, 767–771.
 25. Kim, S.J., Zhang, Z., Hitomi, E., Lee, Y.C. and Mukherjee, A.B. (2006) Endoplasmic reticulum stress-induced caspase-4 activation mediates apoptosis and neurodegeneration in INCL. *Hum. Mol. Genet.*, **15**, 1826–1834.
 26. Salminen, A., Kauppinen, A., Suuronen, T., Kaarniranta, K. and Ojala, J. (2009) ER stress in Alzheimer's disease: a novel neuronal trigger for inflammation and Alzheimer's pathology. *J. Neuroinflammation*, **6**, 41–53.
 27. Oyadomari, S. and Mori, M. (2004) Roles of CHOP/GADD153 in endoplasmic reticulum stress. *Cell Death Differ.*, **11**, 381–389.
 28. Xu, C., Bailly-Maitre, B. and Reed, J.C. (2005) Endoplasmic reticulum stress: cell life and death decisions. *J. Clin. Invest.*, **115**, 2656–2664.
 29. Veitita, R.A. and Birchler, J.A. (2010) Dominance and gene dosage balance in health and disease: why levels matter! *J. Pathol.*, **220**, 174–185.
 30. Dang, V.T., Kassahn, K.S., Marcos, A.E. and Ragan, M.A. (2008) Identification of human haploinsufficient genes and their genomic proximity to segmental duplications. *Eur. J. Hum. Genet.*, **16**, 1350–1357.
 31. Iwaki, A., Kawano, Y., Miura, S., Shibata, H., Matsuse, D., Li, W., Furuya, H., Ohyagi, Y., Taniwaki, T., Kira, J. and Fukumaki, Y. (2008) Heterozygous deletion of ITPR1, but not SUMF1, in spinocerebellar ataxia type 16. *J. Med. Genet.*, **45**, 32–35.
 32. Hanspal, M. and Palek, J. (1987) Synthesis and assembly of membrane skeletal proteins in mammalian red cell precursors. *J. Cell. Biol.*, **105**, 1417–1424.
 33. Kapitein, L.C., Schlager, M.A., Kuijpers, M., Wulf, P.S., van Spronsen, M., MacKintosh, F.C. and Hoogenraad, C.C. (2010) Mixed microtubules steer dynein-driven cargo transport into dendrites. *Curr. Biol.*, **20**, 290–299.
 34. Anderson, R.A. and Lovrien, R.E. (1984) Glycophorin is linked by band 4.1 protein to the human erythrocyte membrane skeleton. *Nature*, **307**, 655–658.
 35. Coleman, S.K., Cai, C., Mottershead, D.G., Haapalahti, J.-P. and Keinänen, K. (2003) Surface expression of GluR-D AMPA receptor is dependent on an interaction between its C-terminal domain and a 4.1 protein. *J. Neurosci.*, **23**, 798–806.
 36. Lin, D.-T., Makino, Y., Sharma, K., Hayashi, T., Neve, R., Takamiya, K. and Huganir, R.L. (2009) Regulation of AMPA receptor extrasynaptic insertion by 4.1N, phosphorylation and palmitoylation. *Nat. Neurosci.*, **12**, 879–887.

Loss of β -III Spectrin Leads to Purkinje Cell Dysfunction Recapitulating the Behavior and Neuropathology of Spinocerebellar Ataxia Type 5 in Humans

Emma M. Perkins,¹ Yvonne L. Clarkson,¹ Nancy Sabatier,¹ David M. Longhurst,¹ Christopher P. Millward,¹ Jennifer Jack,¹ Junko Toraiwa,¹ Mitsunori Watanabe,² Jeffrey D. Rothstein,³ Alastair R. Lyndon,⁴ David J. A. Wyllie,¹ Mayank B. Dutia,¹ and Mandy Jackson¹

¹The Centre for Integrative Physiology, The University of Edinburgh, George Square, Edinburgh EH8 9XD, United Kingdom, ²Department of Neurology, Hirosaki University Graduate School of Medicine, Hirosaki 036-8562, Japan, ³Department of Neurology and Neuroscience, Johns Hopkins University, Baltimore, Maryland 21287, and ⁴School of Life Sciences, Heriot-Watt University, Riccarton, Edinburgh EH14 4AS, United Kingdom

Mutations in *SPTBN2*, the gene encoding β -III spectrin, cause spinocerebellar ataxia type 5 in humans (SCA5), a neurodegenerative disorder resulting in loss of motor coordination. How these mutations give rise to progressive ataxia and what the precise role β -III spectrin plays in normal cerebellar physiology are unknown. We developed a mouse lacking full-length β -III spectrin and found that homozygous mice reproduced features of SCA5 including gait abnormalities, tremor, deteriorating motor coordination, Purkinje cell loss, and cerebellar atrophy (molecular layer thinning). *In vivo* analysis reveals an age-related reduction in simple spike firing rate in surviving β -III^{-/-} Purkinje cells, whereas *in vitro* studies show these neurons to have reduced spontaneous firing, smaller sodium currents, and dysregulation of glutamatergic neurotransmission. Our data suggest an early loss of EAAT4- (protein interactor of β -III spectrin) and a subsequent loss of GLAST-mediated uptake may play a role in neuronal pathology. These findings implicate a loss of β -III spectrin function in SCA5 pathogenesis and indicate that there are at least two physiological effects of β -III spectrin loss that underpin a progressive loss of inhibitory cerebellar output, namely an intrinsic Purkinje cell membrane defect due to reduced sodium currents and alterations in glutamate signaling.

Introduction

Dominant spinocerebellar ataxias (SCAs) are a heterogeneous group of inherited neurodegenerative disorders characterized by postural abnormalities, progressive motor incoordination, and cerebellar degeneration (Dueñas et al., 2006; Soong and Paulson, 2007). Recently, using a large kindred descended from the grandparents of President Abraham Lincoln, mutations in *SPTBN2*, the gene encoding β -III spectrin, were found to cause spinocerebellar ataxia type 5 (Ikeda et al., 2006). However, the mechanism through which the in-frame deletions and missense mutations cause disease is still unknown, with toxic gain-of-function, loss-of-function with a dominant-negative effect on wild-type protein, or haploinsufficiency all being possibilities.

Spectrins, heterotetramers consisting of two α and two β subunits, are important structural components of the plasma mem-

brane skeleton and are thought to play a significant role in restricting and stabilizing membrane-spanning proteins within specific subdomains of the plasma membrane. β -III spectrin is primarily expressed in the nervous system with the highest levels of expression in the cerebellum, where it is found in Purkinje cell soma and dendrites (Sakaguchi et al., 1998; Jackson et al., 2001). However, transcripts are also found in a number of different organs (Stankewich et al., 1998), and low levels of β -III spectrin protein are detected in kidney and liver (our unpublished observation). We have shown that β -III spectrin interacts with EAAT4, the glutamate transporter predominately expressed in Purkinje cells, and stabilizes it at the plasma membrane (Jackson et al., 2001). This implicates β -III spectrin in clearance of glutamate from the synaptic cleft, and consequently both modulation of glutamatergic neurotransmission and prevention of glutamate-mediated neurotoxicity. Other investigators have shown β -III spectrin interacts with ARP1 and is found in a complex with dynactin (Holleran et al., 2001). Since dynactin is the accessory protein that mediates the association of dynein with cytoplasmic vesicles, another suggested function of β -III spectrin is to facilitate protein trafficking by linking the microtubule motor to vesicle-bound cargo. An earlier study also suggested that β -III spectrin associates with Golgi and cytoplasmic vesicles (Stankewich et al., 1998). In the case of *Drosophila* and *Caenorhabditis elegans*, which have only one form of β -spectrin, loss of β -spectrin results in destabilization of the neuromuscular junc-

Received Dec. 8, 2009; revised Jan. 19, 2010; accepted Feb. 6, 2010.

This work was supported by grants from The Wellcome Trust (077946), the National Institutes of Health (NS056158), and Research Councils UK (T27983). We thank Vladimir Buchman and Natalia Ninkina for the gift of ES cells and advice on their culturing, Peter Brophy and Diane Sherman for advice and assistance with blastocyst injections, Seth Grant for the mouse BAC library, Stephen Mitchell for assistance with electron microscopy, Trudi Gillespie from the IMPACT Imaging facility at the University of Edinburgh for technical assistance with microscopy, and Paul Skehel, Matt Nolan, and Laura Ranum for help and useful discussions.

Correspondence should be addressed to Dr. Mandy Jackson, The Centre for Integrative Physiology, The University of Edinburgh, Hugh Robson Building, George Square, Edinburgh EH8 9XD, UK. E-mail: Mandy.Jackson@ed.ac.uk.

DOI:10.1523/JNEUROSCI.6065-09.2010

Copyright © 2010 the authors 0270-6474/10/304857-11\$15.00/0

tion through loss of synaptic cell-adhesion molecules (Pielage et al., 2005) and axonal breakage (Hammarlund et al., 2007), respectively.

To further investigate the role of β -III spectrin in normal cerebellar development and SCA5 disease pathogenesis, we generated a mouse model in which β -III spectrin expression is disrupted. Here, we show that a functional β -III spectrin knock-out mouse (β -III^{-/-}) develops characteristic features of cerebellar ataxia including progressive motor incoordination, a wider hind-limb gait, tremor, cerebellar atrophy, and Purkinje cell loss, thus resembling clinical cases. Therefore, the β -III^{-/-} mouse is a new model of cerebellar ataxia and, furthermore, our results implicate several physiological defects arising from loss of β -III spectrin in disease pathogenesis.

Materials and Methods

Creation of β -III spectrin-deficient mice. Mouse β -III spectrin gene was cloned from a 129Sv mouse BAC library (ResGen). To construct the targeting vector, two gene fragments were subcloned into the vector pPNT: a 2.0 kb KpnI fragment containing intron 6 was cloned in between the *PGK-neo* selection cassette and the *PGK-tk* cassette to form the 3' homology region; and a 7.0 kb XhoI-Sse I fragment containing exons 1 and 2 was cloned upstream of the *PGK-neo* cassette forming the 5' region of homology. The targeting vector was linearized with NotI and electroporated into 129/Ola embryonic stem (ES) cells (clone E14Tg2a). Stably transfected ES cell clones were isolated after double selection with G418 and ganciclovir, and homologously recombined ES cell clones identified by Southern blotting. Genomic DNA from 700 G418- and ganciclovir-resistant ES clones was digested with SphI and transferred to Hybond-N membrane (GE Healthcare). A 208 bp and a 160 bp intronic fragment, external to vector, were used as 5' and 3' probes, respectively. Correctly targeted ES clones were karyotyped and used for blastocyst injections. The resulting chimeric males were bred with C57Bl6J females to identify germ-line transmission by agouti coat color. Heterozygous F₁ mice were then backcrossed with C57Bl6J for at least six further generations. All procedures involved in generation and analysis of mutant mice were performed according to the United Kingdom Animals (Scientific Procedures) Act (1986) and other Home Office regulations under specific pathogen-free conditions.

Genotyping. Animals were genotyped by PCR analysis on genomic DNA extracted from ear notch biopsies using ChargeSwitch gDNA tissue kit (Invitrogen). A common upstream primer (5'-gagcagaagcctgctgagaag-3') and primers specific for the wild-type allele (5'-aggatgatgtccacactagcc-3') and the *PGK-neo* cassette in the mutant allele (5'-ctaccggtggatgtggaag-3') were used for amplification. The 710 bp (from wild-type allele) and 562 bp (from targeted allele) PCR products were resolved by electrophoresis on a 1% agarose gel. β -III spectrin-deficient mice were fully viable and generally born at a ratio consistent with Mendelian inheritance (1:2:1). Litters composed of 41 wild-type (WT), 79 β -III^{+/-}, and 44 β -III^{-/-} animals.

Immunoblotting. Whole cerebella were homogenized in 400 μ l of ice-cold homogenization buffer [20 mM HEPES, pH 7.4, 1 mM EDTA, 1 mM phenylmethylsulfonyl fluoride, and Protease Inhibitor Cocktail Set III (Calbiochem)] with a Teflon-glass homogenizer. Protein concentrations were determined using Coomassie-Plus Reagent and bovine serum albumin as standard (Pierce). Protein samples were resolved by denaturing SDS-PAGE and transferred to nitrocellulose membranes (GE Healthcare, Pharmacia). The membranes were blocked for 1 h at room temperature with 5% w/v nonfat dry milk in Tris-buffered saline/Tween 20 (TBS/T) (20 mM Tris, 17 mM NaCl, pH 7.6, with 0.1% v/v Tween 20). Blots were incubated overnight at 4°C with either rabbit anti- β III spectrin, -EAAT4, -GLAST (1:200), -GLT1 (1:4000), -GluR1 (1:1000; AbCam), or mouse anti-actin, -calbindin (1:1600; Sigma) in blocking buffer. After washing with TBS/T, the blots were incubated for 1 h at room temperature with either HRP-conjugated donkey anti-rabbit IgG, or HRP-conjugated sheep anti-mouse IgG (1:4000; GE Healthcare, Pharmacia). Immunoreactive proteins were visualized with ECL (Insight Biotechnology).

Immunohistochemistry. Brains were removed and immersion fixed with 4% paraformaldehyde in 0.1 M sodium phosphate buffer, pH 7.4, overnight at 4°C and cryoprotected by immersion in 0.1 M sodium phosphate buffer, pH 7.4, containing 30% sucrose. Tissue was quick-frozen on dry ice, then 15- μ m-thick cerebellar sections were cut and fixed onto microscope slides coated with poly-L-lysine. After air drying for 30 min, sections either were stained for Nissl with cresyl violet (0.25%) or immunostained. All quantification was performed in a blinded manner on Nissl-stained sections by counting the number of Purkinje cells along a 1 mm linear length in folia II, III, IV, VI, and VIII (these folia were found to be the most consistent in shape between animals) and the counts averaged for each animal. The thickness of the molecular layer was measured in each animal at the same three points within each of the five chosen folia and the 15 measurements averaged. For deep cerebellar nuclei (DCN) counts, four areas (150 μ m² each) were measured and the counts averaged for each animal. For immunostaining, sections were incubated for 1 h with blocking solution (5% normal goat serum with 0.4% Triton X-100 in PBS). Rabbit anti- β -III spectrin, anti-EAAT4 or mouse anti-calbindin primary antibody (1:50) (2% normal goat serum/0.1% Triton X-100 in PBS) was applied for 1 h at room temperature. Sections were washed three times in PBS before applying goat anti-rabbit FITC-conjugated secondary antibody (Cappel) or goat anti-mouse Cy-3-conjugated secondary antibody (Jackson ImmunoResearch) for 1 h at room temperature followed by three rinses in PBS and coverslipping with Vectashield (Vector Laboratories). Mouse anti-calbindin primary antibody (1:50) and anti-Neu-N antibody (1:100; Millipore Bioscience Research Reagents) was applied overnight at 4°C and biotinylated universal horse anti-mouse/rabbit IgG, diluted at 1:200 in PBS, was applied for 1 h at room temperature. Detection of biotinylated secondary antibody was performed using ABC method with DAB and H₂O₂ used as peroxidase substrate (Vector Laboratories). Images were captured with an Olympus IX70 fluorescence microscope using Openlab software (Improvision) or a Zeiss inverted LSM510 confocal laser scanning microscope.

Electron microscopy. Brains were dissected out and immersion fixed overnight (4°C) with a mixture of 2% paraformaldehyde and 2% glutaraldehyde in 0.1 M sodium cacodylate buffer, pH 7.3. Specimens were postfixated in 1% osmium tetroxide in 0.1 M sodium cacodylate for 45 min, washed three times in 0.1 M sodium cacodylate buffer, and dehydrated in 50%, 70%, 90%, and 100% normal grade acetones for 10 min each, followed by two 10 min changes in analar acetone. Samples were embedded in Araldite resin, and 1- μ m-thick sections cut, stained with toluidine blue, and viewed in a light microscope to select suitable areas for investigation. Ultrathin 60-nm-thick sections were cut from selected areas, stained with uranyl acetate and lead citrate, and viewed in a Phillips CM120 transmission electron microscope (FEI). Morphological criteria used were irregular cell body, dark cytoplasm, and shrinkage. Images were taken on a Gatan Orius CCD camera.

Semiquantitative reverse transcriptase-PCR. Total RNA was extracted from mouse cerebellum using RNeasy Mini kit (Qiagen), and reverse transcriptase (RT)-PCRs were performed using One-Step RT-PCR kit (Qiagen) according to manufacturer's instructions. Primers for RT-PCRs located in exon 1, 7, 34, and 36 of β -III spectrin were: F1 5'-atgagcagcactctgtcaccact-3'; R7 5'-gccattctttgctccacagc-3'; F34 5'-ggccagggaagtgtggcctt-3'; and R36 5'-cttaagaagctgaatctgttctgc-3'. Amplification of the ubiquitously expressed elongation factor α was used to control for RNA levels (Stratagene).

Cell culture and transfection. β -III spectrin cDNA lacking exons 2–6 was subcloned into the NotI site of pCDNA3.1 (Invitrogen) and a Myc-tagged pRK5 vector. For microscopic observation, HEK293 and Neuro2A cells were plated onto coverslips coated with poly-L-lysine in 35 mm dishes and transfected with 1 μ g of each DNA construct using FuGene reagent (Roche) in accordance with the manufacturer's instructions. Anti-c-myc (Ab-1; Calbiochem) and tetramethylrhodamine isothiocyanate-conjugated goat anti-mouse IgG (SouthernBiotech) were used for immunofluorescence. For cell homogenates and biotinylation assays, HEK and HEK-rEAAT4 cells, respectively, were plated onto 35 mm dishes and transfected with 4 μ g of each DNA using Lipofectamine 2000 (Invitrogen) according to manufacturer's instructions.

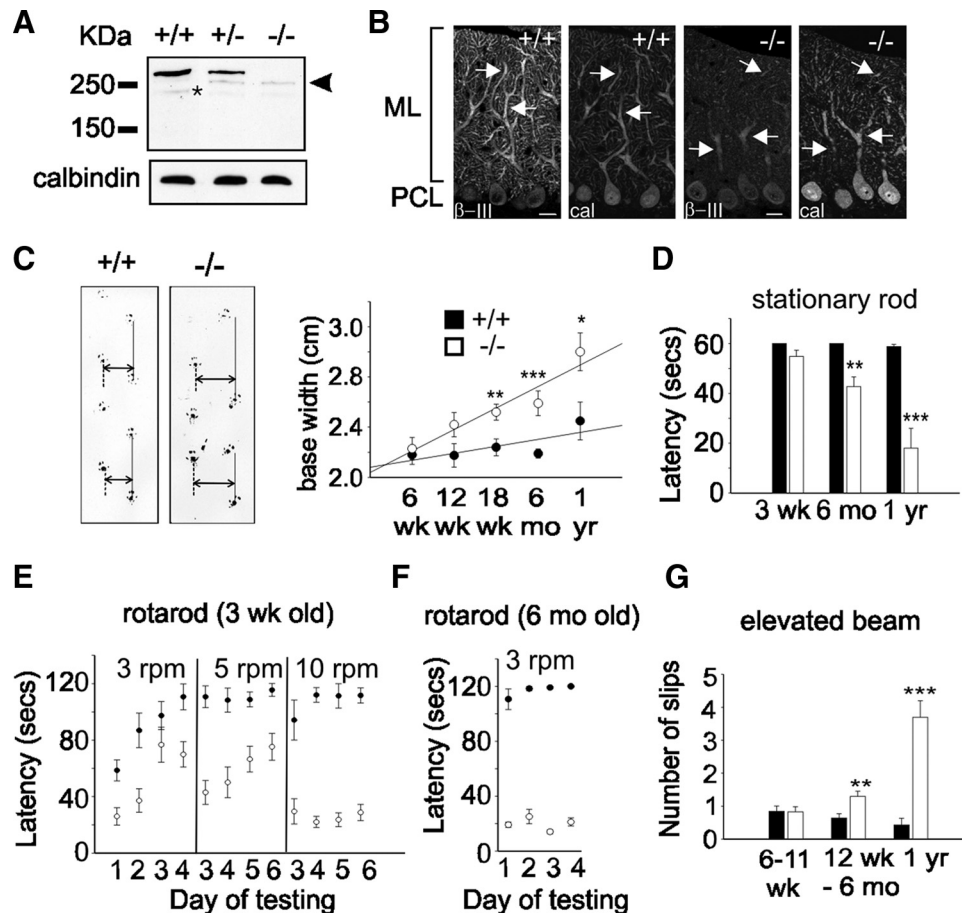


Figure 1. Progressive motor impairment in β -III^{-/-} mice. **A**, Western blot analysis of whole cerebellar homogenates (10 μ g) confirms full-length β -III spectrin (270 kDa) is absent in β -III^{-/-} mice, but a smaller molecular weight protein (~250 kDa; arrowhead) is expressed at low levels in β -III^{+/-} and β -III^{-/-} animals. Degradation product is identified by an asterisk. Calbindin levels confirm equal protein loading. **B**, Cerebellar sections, from 3-week-old mice, immunostained with anti- β -III spectrin and anti-calbindin antibody show intense β -III labeling (arrow) of WT (+/+) dendritic tree but faint staining in β -III^{-/-} mice, although still present in proximal and distal dendrites. ML, Molecular layer; PCL, Purkinje cell layer. Scale bar, 50 μ m. **C**, Left, Representative footprints of 18-week-old WT and β -III^{-/-} littermates. Base width shown by double arrow and stride length by solid line. Right, Summary data showing significant increase in β -III^{-/-} base width compared with WT at 18 weeks ($p = 0.0078$), 6 months ($p = 2.82 \times 10^{-6}$), and 1 year ($p = 0.02$) of age. **D**, Time mice remained on stationary rod before falling reveals 6-month-old and 1-year-old β -III^{-/-} mice are impaired ($p = 0.004$ and 0.0007). Mice were given four consecutive trials, with maximum time of 60 s. **E**, Latency of 3-week-old animals to fall from rotarod at 3, 5, and 10 rpm. Mice were given four trials per day and allowed a maximum retention time of 120 s per trial. Both genotypes improved performance during consecutive days at 3 and 5 rpm, but difference in latency to fall remained significant in all comparisons, except on day 3 at 3 rpm ($p = 0.218$). **F**, 6-month-old β -III^{-/-} mice failed to stay on rotarod at 3 rpm and showed no improvement. **G**, Number of hindlimb slips β -III^{-/-} mice made when crossing narrow, elevated beam increased from 12 weeks of age ($p = 0.001$ and 0.0006). All data are means \pm SEM (WT, $N = 5$ –12; β -III^{-/-}, $N = 4$ –15). * $p < 0.05$; ** $p < 0.01$; *** $p < 0.001$.

Motor coordination tests. Footprint patterns were analyzed using a runway (80 cm by 10.5 cm wide) with white paper at the bottom. Hindpaws of animals were dipped in nontoxic, water-soluble black ink (Indian Ink, Winsor & Newton). Three consecutive strides were measured for each animal. Stride length measurements were taken from the base of two consecutive paw prints on the same side, and the base width was measured as the distance between the center of one paw print to the center of the next print on the opposite side. The elevated beam test was performed using a narrow horizontal beam (2 cm wide, 80 cm long, held at a height of 30 cm from the table). The number of hindpaw slips the animal made while traversing the beam were counted. For the hanging wire test, mice were placed on a wire cage lid, which was turned upside down, and the latency to fall measured. A 60 s cutoff time was used. In the rotarod test, the ability of mice to maintain balance on a stationary (maximum time, 60 s) or rotating (3, 5, and 10 rpm) 3-cm-diameter cylinder was assessed (TSE Rotarod) and the time a mouse remained on the accelerating cylinder recorded (maximum, 120 s).

Glutamate uptake assays. Each cerebellum was homogenized in 800 μ l of tissue buffer (5 mM Tris/320 mM sucrose, pH 7.4) with Protease Inhibitor Cocktail Set III (Calbiochem), using Teflon-glass homogenizer. Each sample was split and pellets washed twice in ice-cold Tissue Buffer, before

being resuspended in either Na⁺-containing Krebs buffer (120 mM NaCl, 25 mM NaHCO₃, 5 mM KCl, 2 mM CaCl₂, 1 mM KH₂PO₄, 1 mM MgSO₄, 10% glucose) or Na⁺-free Krebs (120 mM choline-Cl and 25 mM Tris-HCl, pH 7.4, substituted for NaCl and NaHCO₃, respectively). Samples were then incubated with 5 μ M ³H-glutamate for 10 min at 37°C and uptake stopped by placing back on ice. Pellets were washed twice with Wash Buffer (5 mM Tris/160 mM NaCl, pH 7.4) and radioactivity measured using a scintillation counter. Na⁺-dependent uptake was determined by subtracting Na⁺-free counts.

In vivo electrophysiology. Extracellular recordings were obtained from Purkinje cells in the vermis of the posterior lobe (lobules V and VI) in WT and β -III^{-/-} mice anesthetized with intraperitoneal injection of 1.5 g/kg urethane (solution at 12.5%). The head of the animal was immobilized in a stereotaxic frame and the cerebellum exposed by a craniotomy extending from the obex to the lambdoid ridge. The dura was opened along the midline, and the brain covered with a mixture of paraffin oil and vaseline to prevent dessication. Glass microelectrodes filled with 0.9% NaCl were placed \pm 1 mm on either side of the midline then lowered into the vermis using a hydraulic micromanipulator (Narishige). Recordings of the spontaneous firing activity were made to a depth of 2 mm. Purkinje cells were identified by their characteristic firing of complex spikes followed

by a pause in simple spike firing (see Fig. 5). Spike activity was digitized at 10 kHz for a minimum of 3 min for each cell of interest, using Spike2 software (CED). The mean firing rates of complex and simple spikes were quantified using analysis functions in the Spike2 software.

Slice electrophysiology. Cerebella were dissected out into ice-cold modified artificial CSF (ACSF) containing the following (in mM): 60 NaCl, 118 sucrose, 26 NaHCO_3 , 2.5 KCl, 11 glucose, 1.3 MgCl_2 , and 1 NaH_2PO_4 at pH 7.4 when bubbled with 95% O_2 :5% CO_2 . The cerebellar vermis was glued to the vibratome cutting platform (Dosaka EM Co) with cyanoacrylate adhesive. Two-hundred-micrometer-thick sagittal slices were cut and incubated for 30 min at 30°C in standard ACSF composed of the following (in mM): 119 NaCl, 2.5 CaCl_2 , 26 NaHCO_3 , 2.5 KCl, 11 glucose, 1.3 MgCl_2 , and 1 NaH_2PO_4 at pH 7.4 when bubbled with 95% O_2 :5% CO_2 . Slices were stored at room temperature until required for recording. Slices were transferred to a submerged recording chamber and superfused with standard ACSF (3–5 ml min^{-1}) at room temperature for voltage-clamp experiments and at $32 \pm 2^\circ\text{C}$ for recording spontaneous action potentials. Purkinje cells were visualized with 40 \times immersion objective and Normarski differential interference contrast optics. Whole-cell recordings were obtained from Purkinje cells using thick-walled borosilicate glass pipettes pulled to 5–8 M Ω . For recording action potentials, the internal solution contained the following (in mM): 125 K-gluconate, 15 KCl, 10 HEPES, 5 EGTA, 2 MgCl_2 , 0.4 NaGTP, 2 NaATP, and 10 Naphosphocreatine, adjusted to pH 7.4 with KOH. For parallel fiber (PF)-mediated EPSC (PF-EPSC) measurements, the internal solution contained the following (in mM): 108 Cs-methanesulfonate, 9 NaCl, 9 HEPES, 1.8 EGTA, 1.8 MgCl_2 , 0.4 NaGTP, 2 MgATP, 63 sucrose, and 5 QX-314, adjusted to pH 7.4 with CsOH. Picrotoxin (50 μM) was added to the ACSF. PF-EPSCs were evoked by placing a patch pipette filled with standard ACSF at the same position in the molecular layer and applying a range of stimuli (1.5–5.0 V, 200 μs duration). Pairs of PF-EPSCs (100 ms apart) were evoked at 0.033 Hz, and a minimum of three PF-EPSCs were averaged under each condition. Series resistances were $<15 \text{ M}\Omega$ and were compensated for by 40–60%. Membrane currents and voltages were filtered at 5 kHz and sampled at 10 and 200 kHz, respectively, for voltage-clamp and current-clamp experiments. Data were acquired using pClamp 9 (Molecular Devices) and analyzed using IGOR Pro (WaveMetrics). The amplitudes and decay time constants of PF-evoked EPSCs were measured using the ChanneLab analysis program (Synaptosoft Inc).

Dissociated Purkinje cell electrophysiology. Purkinje cells were isolated from P16–P20 mice using dissociation techniques modified from Raman and Bean (1997). Isolated Purkinje cells were visually identified by their large, pear-shaped soma (due to the stump of the apical dendrite). The control extracellular recording solution contained the following (in mM): 110 TEA-Cl, 25 NaCl, 2 BaCl_2 , 0.3 CdCl_2 , 10 HEPES, and 10 glucose, buffered to pH 7.4 with NaOH. Recordings were made at room temperature with borosilicate pipettes (3–5 M Ω) containing the following (in mM): 117 CsCl, 9 EGTA, 9 HEPES, 1.8 MgCl_2 , 14 Na-phosphocreatine, 4 MgATP, and 0.3 NaGTP, adjusted to pH 7.4 with CsOH. To isolate the TTX-sensitive Na^+ current voltage protocols were repeated in the presence of 300 nM TTX and subtracted from the control recordings.

Statistics. Statistical analysis was performed using Student's *t* test, two samples assuming unequal variance, apart from densitometry analysis of

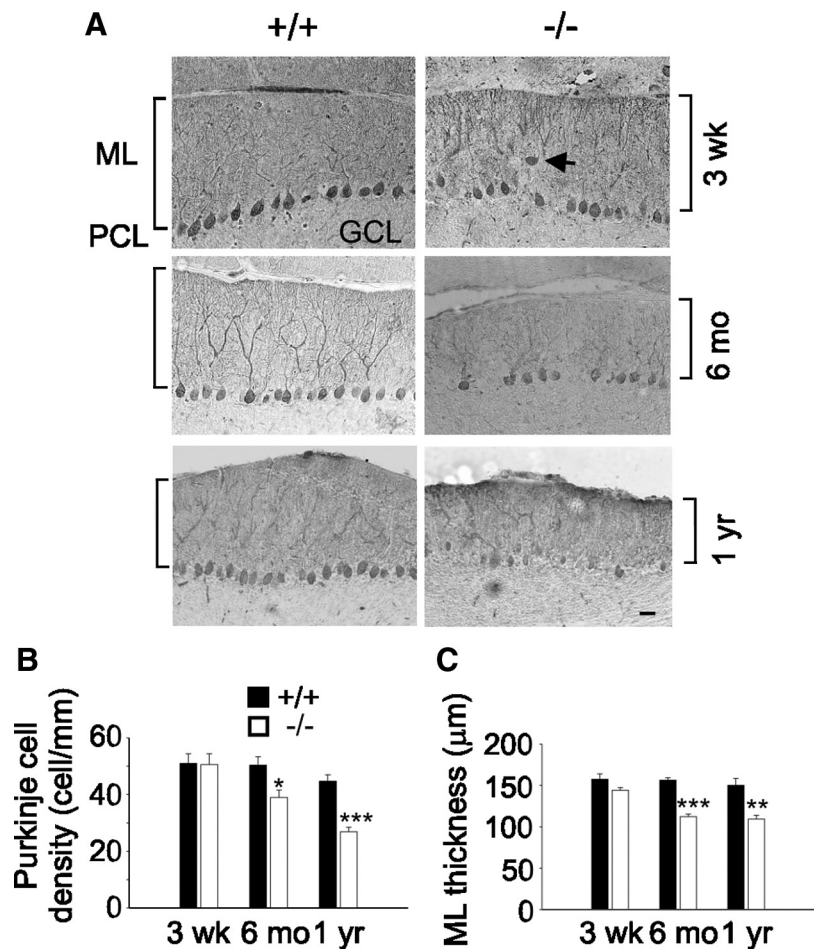


Figure 2. Cerebellar degeneration in old β -III $^{-/-}$ spectrin mice. **A**, Cerebellar sections immunostained with anti-calbindin D antibody reveal some ectopically expressed Purkinje cells (arrow) in 3-week-old β -III $^{-/-}$ mice and shrunken Purkinje cell soma in 6-month-old and 1-year-old β -III $^{-/-}$ mice. ML, Molecular layer; GCL, granule cell layer; PCL, Purkinje cell layer. Scale bar, 50 μm . **B**, Mean Purkinje cell density measured from cerebellar folia II–IV, VI, and VIII shows Purkinje cell loss in 6-month-old and 1-year-old but not 3-week-old β -III $^{-/-}$ mice. **C**, Mean molecular layer thickness shows thinning of molecular layer in old β -III $^{-/-}$ mice. All data are means \pm SEM. * $p < 0.05$; ** $p < 0.01$; *** $p < 0.001$.

Western blots where one sample *t* test was used with a predicted value of 100% for WT and proportion data were arcsine transformed before *t* test.

Results

Generation of β -III spectrin-deficient mice

We used targeted recombination to knock out expression of β -III spectrin, and our targeting strategy involved replacing exons 3–6 with the neomycin-resistance gene (see Materials and Methods). In the recombinant allele, when exon 2 is spliced onto exon 7 this will disrupt the open reading frame, introducing a premature stop codon at the beginning of exon 7. WT (+/+), heterozygous (β -III $^{+/-}$; +/+), and homozygous (β -III $^{-/-}$; -/-) progeny were identified by PCR analysis (see Materials and Methods).

To determine whether we had successfully abolished β -III spectrin expression, we analyzed, using a previously characterized polyclonal antibody raised against a C-terminal epitope of β -III spectrin (Jackson et al., 2001), whole cerebellar homogenates by Western blot analysis. This revealed that full-length β -III spectrin (270 kDa) was absent in β -III $^{-/-}$ mice and its quantity approximately halved ($58.4 \pm 7.4\%$ of WT) in β -III $^{+/-}$ animals (Fig. 1A). However, a smaller molecular weight protein was detected, at low levels, in β -III $^{-/-}$ mice ($18.8 \pm 2.2\%$ of full-length β -III spectrin in WT) (Fig. 1A) and β -III $^{+/-}$ mice but not WT

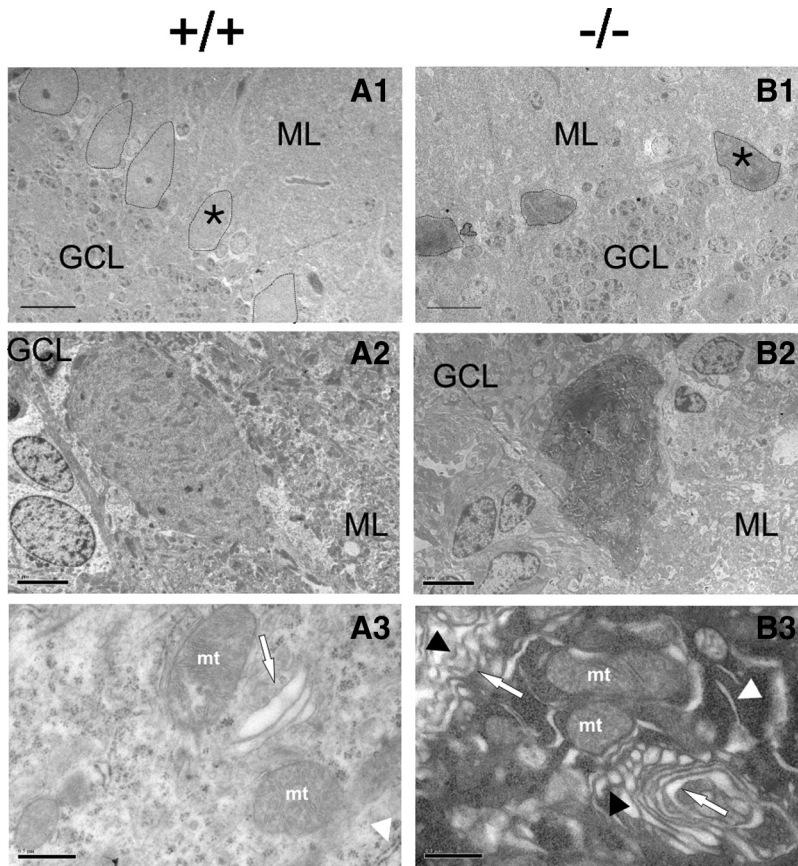


Figure 3. Signs of glutamate-mediated excitotoxicity in β -III^{-/-} Purkinje cells. **A1–B2**, Ultrastructural analysis of cerebellar sections from 6-month-old mice shows normal cell bodies in WT (**A1**, **A2**) but shrunken and electron dense soma in β -III^{-/-} (**B1**, **B2**). **A1**, **B1**, 170 \times magnification; scale bar, 20 μ m. **A2**, **B2**, 750 \times magnification; scale bar, 5 μ m. **A3**, **B3**, Electron micrographs (8400 \times magnification; scale bars, 0.5 μ m) show dilated smooth endoplasmic reticulum (ER) (**B3**, white arrowhead), and fragmented Golgi cisternae (arrow) with increased number of vesicles, some of which are invaginated (black arrowhead) in β -III^{-/-} Purkinje cell somas compared with abundant rough ER (**A3**, white arrowhead) and normal Golgi apparatus (arrow) in WT. ML, Molecular layer; GCL, granule cell layer; mt, mitochondria; all Purkinje cell bodies outlined. *Denotes from which cell high-magnification images were obtained. Note different cell orientation in **A2** and **B2** compared with **A1** and **B1**.

animals. Confocal immunofluorescence microscopy revealed that this protein was still located throughout the β -III^{-/-} Purkinje cell dendritic tree but, consistent with results from Western blot analysis, at a substantially reduced level when compared with WT β -III spectrin (Fig. 1B).

We determined that the smaller molecular weight protein arises from exon 1, not exon 2, being spliced onto exon 7 in the targeted but not WT allele (supplemental Fig. 1A, available at www.jneurosci.org as supplemental material). This retains the reading frame, and so no premature stop codon is introduced. Therefore, the mutant mice lack full-length β -III spectrin but express, at a low level, a form of β -III spectrin (~250 kDa) that lacks most of the actin-binding domain encoded by exons 2–6 (supplemental Fig. 1B, available at www.jneurosci.org as supplemental material). *In vitro* studies demonstrate that Δ 2–6 β III protein has no obvious gain-of-function or adverse property but, if anything, appears to be less functional than WT (supplemental Fig. 1C–F, available at www.jneurosci.org as supplemental material), providing persuasive evidence that the β -III^{-/-} mouse is a functional knock-out (hypomorph).

β -III spectrin deficiency causes cerebellar ataxia

To test whether β -III^{-/-} mice show signs of ataxia, we first analyzed the footprint patterns of 6-week-old to 1-year-old animals

for differences in base width and stride length (Fig. 1C). Hindlimb gait of β -III^{-/-} mice became progressively wider than that of littermate WT mice, but there was no significant alteration in step length at any age. However, variation in walking speed down the runway introduced heterogeneity in stride length that may have masked genotype-dependent differences.

To quantify motor performance and coordination, we used three behavioral tests: stationary rod, rotarod, and elevated beam. We found no significant difference at 3 weeks of age between β -III^{-/-} and WT mice in maintaining balance on a stationary rod, whereas 6-month-old and 1-year-old β -III^{-/-} mice struggled to maintain balance (Fig. 1D). Performance of young β -III^{-/-} mice on a rotating rod (3 rpm) was initially significantly below that of WT animals (Fig. 1E). However, the performance improved on days 3 and 4, demonstrating that β -III^{-/-} mice are able to learn motor tasks and can perform well when the task is relatively easy. When the speed was increased to 5 rpm, again β -III^{-/-} mice fell off more rapidly than WT controls, and at 10 rpm they showed no improvement during consecutive days of testing (Fig. 1E). In contrast, by 6 months of age β -III^{-/-} mice performed much worse and showed no improvement even at 3 rpm (Fig. 1F; see supplemental video, available at www.jneurosci.org as supplemental material). To test whether weakness contributed to poorer rotarod performance, we evaluated muscle strength with a hanging wire test. There was no significant difference between the performance of β -III^{-/-} mice and WT animals at any age, suggesting no muscle weakness (supplemental Fig. 2A, available at www.jneurosci.org as supplemental material). Defects in motor performance were also not due to body size variation as there was no significant difference in body weight (supplemental Fig. 2B, available at www.jneurosci.org as supplemental material). Finally, an elevated beam test was used to evaluate motor coordination and balance. The beam width was 2 cm, so that impaired coordination and balance would result in hindlimb errors. The β -III^{-/-} mice were generally more hesitant to cross the beam compared with WT animals (see supplemental video, available at www.jneurosci.org as supplemental material) and when turning sometimes fell off the beam, which WT mice never did. Counting the number of slips made by each animal while traversing the beam showed that β -III^{-/-} mice made more, and generally bigger, slips than WT littermates from 12 weeks of age (Fig. 1G). However, β -III^{-/-} mice remain ambulatory and do not fall when walking, resembling a mild form of ataxia that is observed in SCA5 patients, in contrast to SCA1 transgenic mice, which display a more severe form of ataxia (Burrigh et al., 1995). Finally, a tremor, a characteristic of some forms of cerebellar ataxia, was observed in β -III^{-/-} mice (see supplemental video, available at www.jneurosci.org as supplemental material).

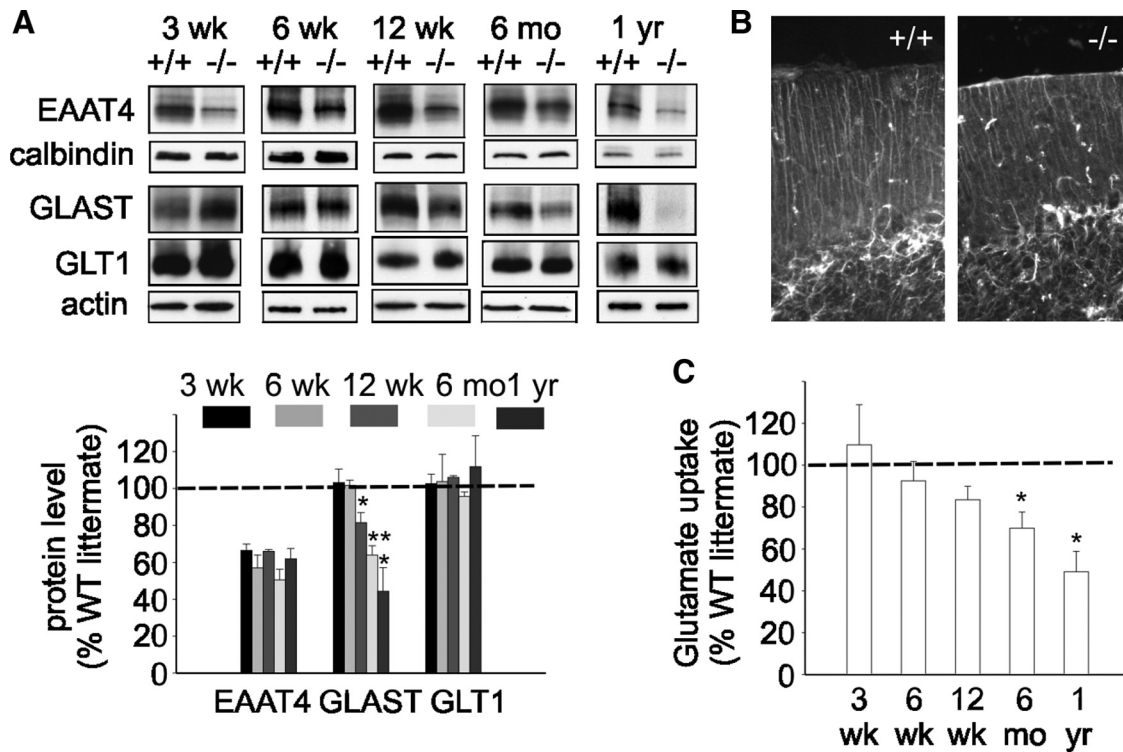


Figure 4. Loss of neuronal and astroglial glutamate transporters in β -III^{-/-} mice. **A**, Top, Representative Western blots illustrating loss of EAAT4 protein in β -III^{-/-} mice from 3 weeks of age. Loss of astroglial glutamate transporter GLAST observed in β -III^{-/-} mice from 12 weeks of age. No loss of GLT1 seen at any age. Bottom, Densitometry data quantifying levels. EAAT4 levels normalized with calbindin, a Purkinje cell-specific marker ($p < 0.02$ for all ages). GLAST and GLT1 normalized with actin. **B**, Cerebellar sections immunostained with anti-GFAP antibody show no astrogliosis in 1-year-old β -III^{-/-} mice. **C**, Glutamate uptake assays on whole cerebellar homogenates show reduced uptake in β -III^{-/-} mice from 12 weeks of age. All data are means \pm SEM ($N = 3-6$). * $p < 0.05$; ** $p < 0.01$.

Thinning of molecular layer and Purkinje cell loss in β -III^{-/-} mice

We then looked for cerebellar atrophy and Purkinje cell loss, other features of patients with ataxia, in β -III^{-/-} mice. Staining and quantification of cerebellar sections (see Materials and Methods) revealed a thinning of the molecular layer, generally correlated with degeneration of dendrites (He et al., 2006), and a progressive loss of Purkinje cells at 6 months (WT, 50.4 ± 3 cells/mm; β -III^{-/-}, 39 ± 1.9 cells/mm; $N = 4$ and 3 , respectively; $p = 0.035$; and WT, 156.2 ± 3 μ m; β -III^{-/-}, 112.2 ± 3.1 μ m; $73 \pm 2.5\%$ of WT; $p = 1.71 \times 10^{-5}$) and 1 year of age (WT, 44.7 ± 2.3 cells/mm; β -III^{-/-}, 26.9 ± 1.5 cells/mm; $N = 4$; $p = 0.001$; and WT, 150 ± 8.5 μ m; β -III^{-/-}, 109.3 ± 4.7 μ m; $73 \pm 3.1\%$ of WT; $p = 0.005$). This is not observed in young (3-week-old) β -III^{-/-} animals (WT, 51 ± 3.4 cells/mm; β -III^{-/-}, 50.6 ± 3.8 cells/mm; $N = 10$ and 9 , respectively; $p = 0.94$; and WT, 157.5 ± 6.4 μ m; β -III^{-/-}, 144.1 ± 3.4 μ m; $p = 0.097$) (Fig. 2). There was no obvious variation in the pathology of the lobules examined, with the same degree of neuronal loss and atrophy being detected in all five examined. Immunostaining also highlighted that the remaining Purkinje cell somas in old β -III^{-/-} animals were generally smaller (WT, 14.5 ± 0.13 μ m; β -III^{-/-}, 11.6 ± 0.27 μ m; $N = 3$, $n = 100$ /animal; $p = 0.0025$) and more irregularly shaped compared with WT littermates. It also revealed that in young β -III^{-/-} mice more Purkinje cells were found to lie outside the Purkinje cell layer (WT, $0.28 \pm 0.17\%$; β -III^{-/-}, $3 \pm 0.34\%$; $N = 3$, $n = 350-520$ /animal; $p = 0.006$) (Fig. 2A), a finding also observed in SCA1 mutant mice (Burrigh et al., 1995), whereas, we saw no differences in the densities of DCN among genotypes at any age (supplemental Fig. 3, available at www.jneurosci.org as supplemental material).

Also, no gross morphological change (cell layer thickness) or neuronal loss was observed in hippocampus (CA1 or CA3), cortex, or dentate gyrus (supplemental Table 1, available at www.jneurosci.org as supplemental material).

Subsequent ultrastructural analysis using transmission electron microscopy of Purkinje cells confirmed somal shrinkage and revealed an age-dependent accumulation of cells undergoing "dark cell degeneration" (Fig. 3), a process linked to AMPA receptor-elicited delayed excitotoxicity (Garthwaite and Garthwaite, 1991; Turmaine et al., 2000), in β -III^{-/-} mice. In 8-month-old β -III^{-/-} animals, the percentage of Purkinje cells with normal morphology, relative to WT, was $29 \pm 2.1\%$ compared with $94.5 \pm 1.9\%$ at 8 weeks of age (8 weeks: $N = 4$, $n = 18-35$ /animal; 8 months: $N = 5$, $n = 7-18$ /animal; *** $p = 7.2 \times 10^{-6}$). These cells showed irregular somal morphology, increased electron density, dilated cisternae of endoplasmic reticulum denuded of ribosomes, and changes to Golgi apparatus (numerous vesicles, some of which were invaginated, a sign of Golgi fragmentation (Siddhanta et al., 2003)).

Loss of glutamate transporter expression in β -III^{-/-} mice

We therefore examined levels of EAAT4, the Purkinje cell-specific glutamate transporter, in β -III^{-/-} mice, since our previous work showed EAAT4 interacts with and is stabilized by β -III spectrin (Jackson et al., 2001). Moreover, dramatic changes in EAAT4 distribution were seen in SCA5 autopsy tissue (Ikeda et al., 2006). Even at 3 weeks of age, a decrease in EAAT4 protein was obvious in β -III^{-/-} mice compared with WT littermate controls ($66.5 \pm 3.5\%$ of WT; $N = 6$ each; $p = 0.0002$) (Fig. 4A). Values were normalized to calbindin, a Purkinje cell-specific marker.

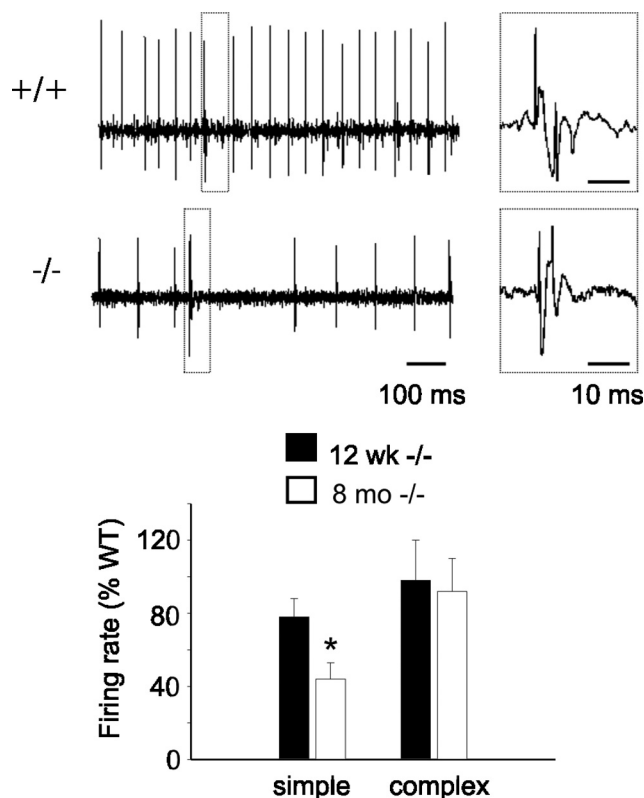


Figure 5. Reduced *in vivo* simple spike firing rate in old β -III^{-/-} mice compared with young β -III^{-/-} mice. Top, Representative trace of *in vivo* Purkinje cell output from 8-month-old WT and β -III^{-/-} animals. Complex spike (dashed box) enlarged on right of trace. Bottom, Firing rates of 12-week-old and 8-month-old β -III^{-/-} mice expressed as percentage of wild-type frequency show reduction in simple but not complex spikes with age. All data are means \pm SEM (12 weeks: WT, $N = 3$, $n = 11$; β -III^{-/-}, $N = 3$, $n = 12$; 8 months: WT, $N = 3$, $n = 8$; β -III^{-/-}, $N = 3$, $n = 10$; $p = 0.02$).

Immunofluorescence microscopy reveals that in β -III^{-/-} mice the remaining EAAT4 is still located throughout the dendritic tree (supplemental Fig. 4, available at www.jneurosci.org as supplemental material). In contrast, no loss of the astroglial glutamate transporters GLAST ($103.2 \pm 7.4\%$ of WT; $p = 0.687$) and GLT1 ($102.7 \pm 5.1\%$ of WT; $p = 0.62$) was observed at this early stage.

Western blot analysis and densitometry (Fig. 4A) did reveal a progressive reduction in GLAST protein compared with littermate controls in 12-week-, 6-month-, and 1-year-old animals ($81.5 \pm 5.5\%$ of WT, $p = 0.0206$; $64 \pm 5\%$ of WT, $p = 0.0055$; $44.3 \pm 13\%$ of WT; $p = 0.05$; $N = 3$ each) in addition to the fairly consistent loss of EAAT4 ($67.3 \pm 6.2\%$ of WT, $p = 0.0033$; $50.5 \pm 5.9\%$ of WT, $p = 0.0035$; $62 \pm 5.5\%$ of WT, $p = 0.02$). In contrast, no reduction in GLT1 levels was observed at any age ($108.3 \pm 2.4\%$; $95.8 \pm 2.4\%$; $111.7 \pm 16.9\%$, respectively). The fact that there was no difference in GFAP expression in old β -III^{-/-} animals (Fig. 4B) suggests that the progressive loss of GLAST was not a consequence of global defects in Bergmann glial integrity.

To investigate whether a loss of transporter protein corresponded to a loss in cerebellar glutamate uptake, we measured uptake of radioactively labeled glutamate into crude cerebellar membrane preparations. We found a slight reduction in 12-week-old β -III^{-/-} animals ($83.5 \pm 6.4\%$ of WT; $N = 3$ and 4 ; $p = 0.08$) when the ataxic phenotype starts to become obvious, and further losses in 6-month-old and 1-year-old animals when the motor deficits are more pronounced ($70 \pm 7.6\%$ of WT, $p = 0.047$,

and $49.2 \pm 9.7\%$ of WT, $p = 0.034$, respectively; $N = 3$ each) (Fig. 4C). Together, these results suggest that impaired glutamate uptake, resulting from loss of EAAT4 and GLAST, correlates with neuronal degeneration and plays a role in disease progression.

Reduced *in vivo* Purkinje cell simple spike firing rate in β -III^{-/-} mice

Purkinje neurons provide the sole output from the cerebellar cortex, in the form of inhibitory inputs to the DCN, and so it is their firing rate that encodes the timing signals essential for motor planning, execution, and coordination. They are one of a few neuronal populations that fire regularly in the absence of synaptic input, but integration of excitatory and inhibitory inputs modulates their output (Häusser and Clark, 1997). We therefore recorded the *in vivo* firing pattern of Purkinje cells in 12-week-old and 8-month-old β -III^{-/-} and WT mice (Fig. 5). We found that the simple spike firing rate was much less at 8 months than 12 weeks in β -III^{-/-} mice compared with WT animals, indicating an age-related decrease in output from surviving Purkinje cells. There was no difference in the firing rate of complex spikes, but some Purkinje cells from 8-month-old animals appeared to fire only complex spikes, with the number of such cells being greater in β -III^{-/-} mice (WT, 1 of 9 cells; β -III^{-/-}, 5 of 15 cells). These cells were not included in the calculation of the mean simple spike firing rate.

Reduced spontaneous activity in β -III^{-/-} mice

To identify a possible cellular basis for the impaired Purkinje cell output in β -III^{-/-} mice, we first measured spontaneous activity *in vitro* (Fig. 6A). We found an approximately twofold reduction in cells from 3-week-old β -III^{-/-} animals (18.3 ± 2.6 Hz; $N = 2$, $n = 7$) compared with WT cells (43.4 ± 3.5 Hz; $N = 3$, $n = 9$; $p = 5.22 \times 10^{-5}$). The difference in the firing rate was not abolished in the presence of bicuculline, an inhibitor of GABAergic neurotransmission, demonstrating that the observed reduction is not due to increased inhibition. There was also very little effect on firing rate when excitatory inputs were blocked with NBQX, revealing very little tonic excitatory input within the *in vitro* slice, similar to published data (Häusser and Clark, 1997). Therefore, the observed reduction is due to an intrinsic membrane defect (i.e., altered ion channel activity) in β -III^{-/-} Purkinje cells. There was no further reduction in firing frequency observed in cells from 6-month-old β -III^{-/-} animals (20.8 ± 1.2 Hz; $N = 2$, $n = 16$; $p = 0.432$), suggesting that the intrinsic defect does not underlie the progressive nature of the disease phenotype. No significant difference in cell input resistance, indicating no change in “leak” conductance, or zero current potential was detected between the two genotypes in either 3-week-old (WT, 74 ± 12 M Ω ; β -III^{-/-}, 78 ± 8 M Ω ; and WT, -55 ± 1 mV; β -III^{-/-}, -54 ± 3 mV) or 6-month-old animals (WT, 78 ± 6 M Ω ; β -III^{-/-}, 76 ± 6 M Ω ; and WT, -56 ± 0.3 mV; β -III^{-/-}, -57 ± 0.8 mV).

It is known that voltage-gated potassium and sodium channels play important roles in sustaining the high-frequency tonic firing in Purkinje cells (Raman and Bean, 1999; Sacco et al., 2006; Zaghera et al., 2008). There was no difference in action potential properties from WT and β -III^{-/-} Purkinje cells (half-width: WT, 0.24 ± 0.05 ms; β -III^{-/-}, 0.23 ± 0.009 ms, $p = 0.287$; peak: WT, 10.9 ± 1.6 mV; β -III^{-/-}, 11.9 ± 2.1 mV, $p = 0.483$; hyperpolarization peak: WT, -60.6 ± 1.9 mV; β -III^{-/-}, -60.3 ± 0.9 mV, $p = 0.337$; $n = 7$ – 10 for all analyses), suggesting that the intrinsic firing defect was not due to a potassium channel; whereas, when we recorded whole-cell sodium currents from acutely

dissociated P16–20 Purkinje neurons, they were found to be significantly smaller in β -III^{-/-} Purkinje cells compared with WT cells (Fig. 6B). The current–voltage relationships were similar for both genotypes, indicating no difference in voltage dependence of channel activation, and there was no difference in cell capacitance (WT, 10.1 ± 0.5 pF; β -III^{-/-}, 10.0 ± 0.4 pF; $p = 0.92$), suggesting that the growth and morphology of mutant Purkinje cells was the same as wild-type Purkinje cells. In addition, the resurgent sodium current amplitude, which is an important aspect of the fast repetitive Purkinje cell firing, accelerating depolarization between action potentials, was also found to be smaller in β -III^{-/-} cells (Fig. 6C). These results suggest that it is a sodium channel defect that underlies the changes in the intrinsic membrane properties of β -III^{-/-} Purkinje cells and that β -III spectrin may play a role in maintaining a high density of sodium channels within the soma and dendrites, similar to β -IV spectrin in axons (Komada and Soriano, 2002).

Altered glutamatergic transmission in β -III^{-/-} mice

Next, since the tonic simple spike firing rate is increased by PF inputs, we examined, in cerebellar slices, PF-EPSCs. We found that PF-EPSC amplitudes, at various stimuli, were considerably larger in 6-week-old β -III^{-/-} mice compared with WT (Fig. 7A,B). However, no enhancement in PF-EPSC peak amplitude was seen in cells from 6-month-old β -III^{-/-} animals, and recordings from 1-year-old β -III^{-/-} animals reveal a decrease compared with WT cells (Fig. 7A,B). This indicates Purkinje cell excitation is initially enhanced, which would partly offset some of the intrinsic Purkinje cell defect, but then progressively declines in β -III^{-/-} mice, compounding such deficits.

Western blot analysis of cerebellar tissue from these mice shows no difference between genotypes in the level of GluR1, an AMPA receptor subunit, to account for the enhancement ($97.7 \pm 1.8\%$ of littermate controls; $N = 3$ and 4; $p = 0.3$) (Fig. 7C). There is also no difference in paired-pulse facilitation between young β -III^{-/-} and WT mice (1.25 ± 0.14 and 1.25 ± 0.02 , respectively; $p = 0.92$) at 100 ms intervals, suggesting that a difference in release probability does not underlie the larger EPSCs. Instead, we found, similar to other published data (Takayasu et al., 2004), that application of TBOA, a global glutamate transporter antagonist, enhanced EPSC amplitude in young WT cells such that there was no longer a significant difference in amplitude between genotypes ($p = 0.162$). In contrast, a loss of AMPA receptors ($64.5 \pm 10\%$ of WT; $p = 0.038$) (Fig. 7C) and a slight difference in paired-pulse facilitation (WT 1.4 ± 0.03 ; β -III^{-/-} 1.29 ± 0.03 ; $p = 0.02$) is observed in 1-year-old β -III^{-/-} animals.

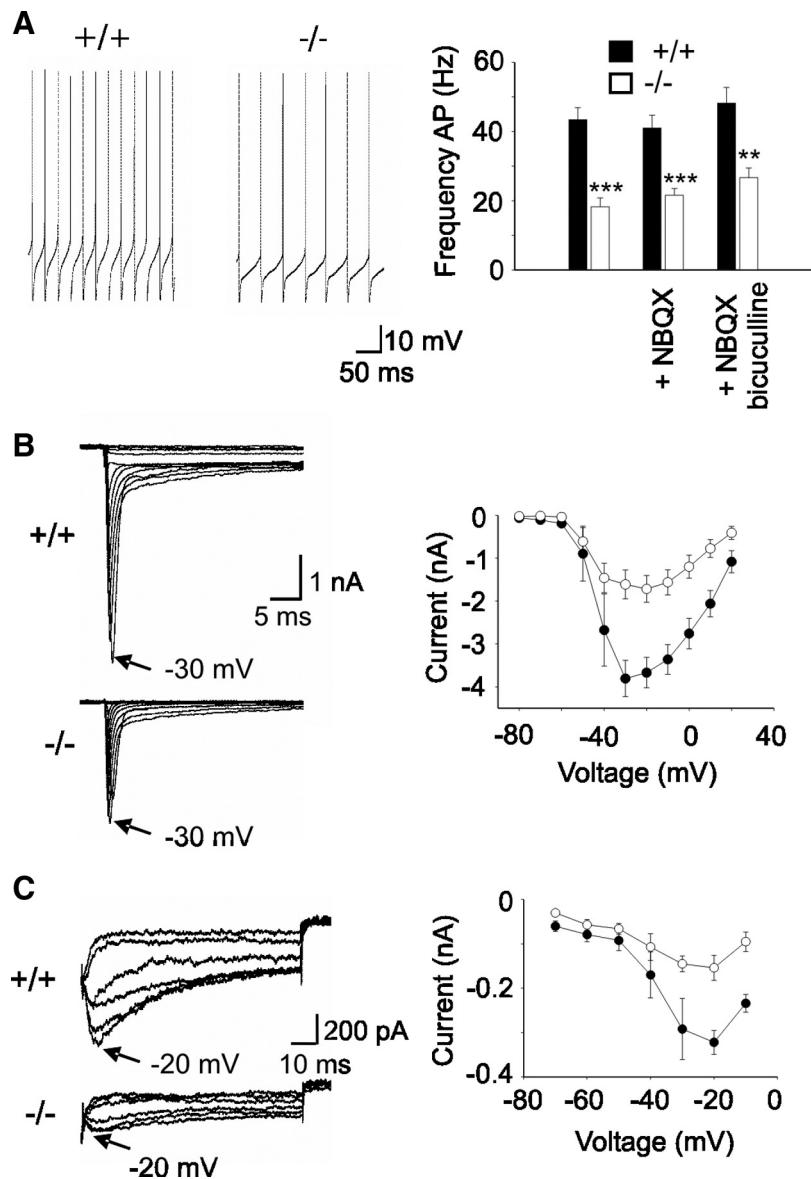


Figure 6. Reduced spontaneous firing due to smaller sodium currents in Purkinje cells from β -III^{-/-} mice. **A**, Left, Representative traces of Purkinje cell spontaneous firing measured from 3-week-old WT and β -III^{-/-} littermates. Right, Quantification of mean firing frequency shows a reduction in spike frequency in Purkinje cells from 3-week-old β -III^{-/-} mice compared with WT mice. Presence of NBQX or bicuculline does not abolish genotype difference in firing rate. **B**, Left, Sodium current traces from representative cells evoked with a series of 50 ms depolarizations from a holding potential of -90 mV to potentials ranging from -80 to $+20$ mV in 10 mV increments. Right, Current–voltage relationship shows reduced whole-cell current in β -III^{-/-} mice. **C**, Left, Representative traces of resurgent sodium currents in WT and β -III^{-/-} mice. Currents evoked using a 20 ms step to $+30$ mV, followed by repolarizations from -20 to -70 mV. Right, Mean peak resurgent sodium current versus voltage shows reduced resurgent current in β -III^{-/-} mice. All data are means \pm SEM. ** $p < 0.01$; *** $p < 0.001$.

Together, the results indicate that the decreased spontaneous firing rate arising from loss of β -III spectrin is, in young animals, partly offset by greater excitation. However, this declines in older animals, likely due to dendritic degeneration, and compounds the intrinsic defect. Ultimately, the combination of Purkinje cell death and reduced output from the surviving neurons leads to less inhibition onto the DCN and a progressive ataxic phenotype.

Discussion

Loss of function in disease pathogenesis

In this study, we show that loss of β -III spectrin produces a phenotype that resembles that of SCA5 patients with gait abnormalities, progressive motor coordination deficits, thinning of the

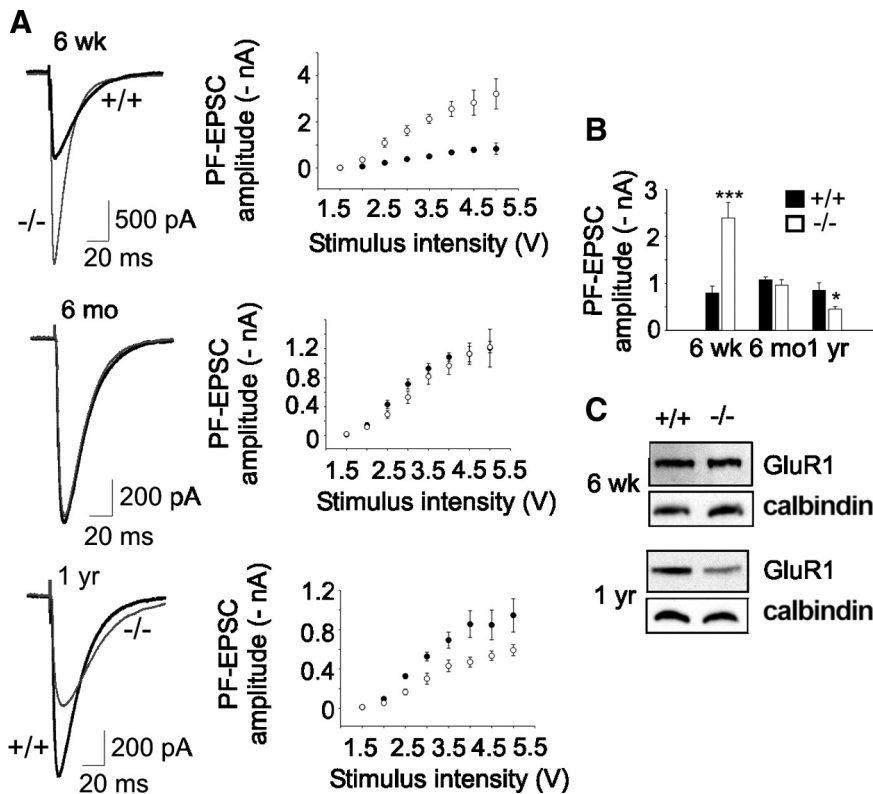


Figure 7. Altered PF-EPSCs in β -III^{-/-} mice. **A**, Left, Representative EPSC waveforms (4 V stimulus) from 6-week-old, 6-month-old, and 1-year-old WT and β -III^{-/-} littermates. Right, Mean PF-EPSC amplitudes versus stimulus intensity shows consistent differences between WT and β -III^{-/-} cells at different stimuli. **B**, Mean peak amplitude of EPSCs at 4 V stimulus shows changes in PF-evoked currents with age in β -III^{-/-} cells (6 weeks: $N = 3$, $n = 10$, $p = 0.001$; 6 months: WT, $N = 2$, $n = 10$; β -III^{-/-}, $N = 2$, $n = 9$, $p = 0.44$; 1 year: WT, $N = 1$, $n = 6$; β -III^{-/-}, $N = 2$, $n = 11$, $p = 0.05$). **C**, Western blot analysis shows loss of GluR1 in 1-year-old but no change in 6-week-old β -III^{-/-} mice.

molecular layer, and Purkinje cell loss (Stevanin et al., 1999; Bürk et al., 2004; Ikeda et al., 2006). Therefore, these results suggest that loss of β -III spectrin function underlies SCA5 pathogenesis, providing mechanistic insights into this autosomal-dominant disease. Although autosomal-dominant diseases were originally thought to result from toxic gain-of-function properties, recently several studies have implicated loss-of-function in the pathogenesis of other dominant neurodegenerative diseases (Van Raamsdonk et al., 2005; Thomas et al., 2006; Lim et al., 2008).

To date, heterozygous animals have displayed no obvious ataxic phenotype (our unpublished observation), arguing against haploinsufficiency as a disease mechanism and pointing toward the human mutations possessing dominant-negative effects on wild-type β -III spectrin function. Additional models in which β -III spectrin with a known SCA5 mutation is expressed should address this issue.

Sodium channel dysfunction may play a role in SCA5

Results from our *in vitro* current-clamp experiments revealed a substantial reduction in spontaneous Purkinje neuron activity in β -III^{-/-} mice. It is known that several ion channels are essential for the sustained high-frequency tonic firing of Purkinje cells (Raman and Bean, 1999; Sacco et al., 2006; Zagha et al., 2008). Moreover, their loss in mice has been shown to cause ataxia (Sausbier et al., 2004; Akemann and Knopfel, 2006; Levin et al., 2006; Walter et al., 2006), and, more importantly, loss of ion channel function has been identified as a genetic defect in several SCA subtypes (Browne et al., 1994; Ophoff et al., 1996; Zhuchenko et al., 1997; Waters et al., 2006).

Here, we report that there are reduced sodium currents in acutely dissociated Purkinje neurons from β -III^{-/-} mice. Of note, a mutation in the gene that encodes Na_v1.6 has been found in a patient with cerebellar atrophy and ataxia (Trudeau et al., 2006), and β IV-spectrin has been shown to be required for correct localization and stabilization of voltage-gated sodium and potassium channels within axons and its loss results in progressive ataxia (Parkinson et al., 2001; Komada and Soriano, 2002). Together, these findings suggest that sodium channel dysfunction is a factor in the pathogenesis of some forms of SCA.

Spectrin is known to be a key factor in forming specialized membrane domains by linking transmembrane proteins such as ion channels and cell-adhesion molecules to membrane phospholipids and the actin cytoskeleton (Baines, 2009). Future analysis of β -III^{-/-} mice will delineate the role β -III spectrin plays in assembling such domains as in its absence, or that of associated proteins (Jenkins and Bennett, 2001), sodium channels may no longer be maintained within specific subdomains, potentially contributing to Purkinje cell dysfunction. Alternatively, given β -III spectrin's putative role in facilitating protein transport (Holleran et al., 2001) sodium channels may be incorrectly trafficked.

Role for GLAST dysfunction in Purkinje cell degeneration

We found that in older β -III^{-/-} mice, when motor deficits are more pronounced, there is, in addition to the loss of EAAT4 seen in young β -III^{-/-} mice, a loss of the astroglial transporter GLAST and corresponding reductions in glutamate uptake. These results and the evidence of glutamate-mediated excitotoxicity in Purkinje cells of β -III^{-/-} mice from 6 months onward suggest that it may be the delayed and progressive loss of GLAST activity that leads to Purkinje cell degeneration and the worsening ataxic phenotype. Therefore, a non-cell-autonomous mechanism involving GLAST dysfunction might be a pathogenic mechanism common to several SCAs. A complete loss-of-function mutation in EAAT1 (GLAST), with a dominant-negative effect on wild-type protein, was recently identified in a child with episodic and progressive ataxia (Jen et al., 2005), and this is in accordance with the finding that a GLAST knock-out mouse possesses motor deficits (Watase et al., 1998). Furthermore, Purkinje cell degeneration is also seen when expanded ataxin-7 is expressed solely in Bergmann glia, resulting in impaired glutamate uptake and loss of GLAST (Custer et al., 2006). Therefore, glutamate-mediated excitotoxicity, involving GLAST dysfunction, appears to play a critical role in Purkinje cell degeneration. Exactly how loss of β -III spectrin gives rise to this is not yet determined as β -III spectrin does not appear to be expressed in Bergmann glia (our unpublished observation). One possibility is that β -III spectrin, by orchestrating specialized microdomains in Purkinje cells, assembles a multiprotein transmembrane complex that maintains cell-to-cell contact with Bergmann glia and

retains GLAST at the glial membrane. Alternatively, given the role of spectrin in vesicular transport, it may be that β -III spectrin is involved in the trafficking and secretion of trophic factors from Purkinje cells that modulate GLAST protein levels.

Cumulative effects of different insults important for disease progression

It is known that enhanced DCN hyperexcitability is sufficient to induce ataxia (Shakkottai et al., 2004), and so any reduction in GABAergic Purkinje cell output will contribute to motor deficits by reducing inhibition onto the DCN. However, although we identified a reduction in Purkinje cell intrinsic spontaneous firing rate in β -III^{-/-} mice, this loss in output could not account for the increasing disease severity as the same degree of reduction was seen in 3-week-old and 6-month-old animals, which show mild and more severe motor deficits, respectively.

Therefore, it is apparent that additional factors are involved in modifying Purkinje cell output and affecting disease severity. Furthermore, these findings highlight the cellular complexity of cerebellar degeneration and ataxia. From the present study one contributing factor would appear to be altered excitatory inputs. Although previous work suggests EAAT4 to affect current decay (Takayasu et al., 2005), our results show that in young β -III^{-/-} mice, loss of EAAT4, and not GLAST (Fig. 4A) corresponds with increased EPSCs (Fig. 7A,B). One possibility for the discrepancy is that there is less compensation from the other transporter subtypes in β -III^{-/-} mice compared with EAAT4 knock-out mice. It may also be that GLAST is not in close opposition with dendritic spines, reducing rapid removal of glutamate. In contrast, prolonged EPSCs in 1-year-old β -III^{-/-} animals correlate with a loss of GLAST protein, similar to published data (Marcaggi et al., 2003; Stoffel et al., 2004; Takayasu et al., 2005; Takatsuru et al., 2006). These recordings also confirm that the removal of synaptically released glutamate is retarded in old β -III^{-/-} mice and raises the possibility that accumulation of glutamate results in AMPA receptor desensitization. Unexpectedly, given the loss of EAAT4, PF-EPSCs appear to decay faster in cells from young β -III^{-/-} mice. Although both astroglial transporters are slightly elevated in young β -III^{-/-} mice this is unlikely to be the sole reason for the faster decay, due to the small extent of protein increase and lack of increased glutamate uptake. Previous work has shown the sodium channel inhibitor QX-314 may not block all channel subtypes equally (Yeh, 1978). We saw no difference in decay constants between young WT and β -III^{-/-} mice when recordings were performed in the absence of sodium channel blockers. It is possible, therefore, that in β -III^{-/-} mice, due to the loss of sodium currents (Fig. 6B,C) there may be less of a contaminating current, precluding detection of slowing of the EPSC decay. A similar finding of briefer PF-EPSC decay times was observed in Na_v1.6 knock-out animals (Levin et al., 2006).

Therefore, loss of EAAT4 may coincidentally have a biphasic effect on Purkinje cell physiology: initially, the loss is compensatory, maintaining Purkinje cell output and downstream DCN inhibition, resulting in only a mild ataxic phenotype. However, with time it elicits AMPA receptor-elicited excitotoxicity, resulting in dendritic degeneration and eventual cell death, both leading to progressively less Purkinje cell output and hyperexcitability of DCN. Although there are no reports that EAAT4 knock-out mice develop ataxia, a downregulation of EAAT4 is seen before any behavioral phenotype in two other models of ataxia, SCA1 transgenic mouse (Lin et al., 2000; Serra et al., 2004) and *staggerer* (Gold et al., 2003). Together, the results from these three different mouse ataxia models suggest that EAAT4 may indeed be a com-

mon factor in early disease pathogenesis. It appears that for normal glutamatergic neurotransmission a loss of EAAT4 is not deleterious, as GLAST is able to fully compensate, but when GLAST is lost (as here), the cumulative effect becomes pathogenic. A similar concerted role of EAAT4 and GLAST is apparent in brain ischemia where Purkinje cells with low EAAT4 levels are selectively lost in GLAST knock-out mice (Yamashita et al., 2006).

In conclusion, the β -III^{-/-} mouse described here represents a new model of cerebellar ataxia, showing not only progressive behavioral abnormalities but also Purkinje cell degeneration. This is similar to clinical cases, therefore making it a valuable disease model for future study. The data also reveal that at least two separate disease pathways are involved in the loss of inhibitory cerebellar output underlying the ataxic phenotype. The first is a decrease in the tonic firing rate of Purkinje cells due to altered intrinsic membrane properties arising from reduced sodium currents. The second is a reduction in excitatory inputs and Purkinje cell death, possibly a consequence of glutamate-mediated excitotoxicity, arising from loss of EAAT4- and GLAST-mediated glutamate uptake. Therefore, β -III spectrin appears to play an important part in the prevention of glutamate-mediated neurotoxicity and to have a critical role in maintaining Purkinje cell tonic firing. Future analysis of this model will provide a greater understanding of what may be convergent disease mechanisms for various SCAs (i.e., ion channel dysfunction, glutamate-mediated excitotoxicity, and protein-trafficking defects). Insights into the human disease will be obtained by addressing whether known SCA5 mutations have similar detrimental effects to the present mouse model on either or both of the sodium channels or the astroglial glutamate transporter GLAST.

References

- Akemann W, Knöpfel T (2006) Interaction of Kv3 potassium channels and resurgent sodium current influences the rate of spontaneous firing of Purkinje neurons. *J Neurosci* 26:4602–4612.
- Baines AJ (2009) Evolution of spectrin function in cytoskeletal and membrane networks. *Biochem Soc Trans* 37:796–803.
- Browne DL, Gancher ST, Nutt JG, Brunt ER, Smith EA, Kramer P, Litt M (1994) Episodic ataxia/myokymia syndrome is associated with point mutations in the human potassium channel gene, KCNA1. *Nat Genet* 8:136–140.
- Bürk K, Zühlke C, König IR, Ziegler A, Schwinger E, Globas C, Dichgans J, Hellenbroich Y (2004) Spinocerebellar ataxia type 5: clinical and molecular genetic features of a German kindred. *Neurology* 62:327–329.
- Burright EN, Clark HB, Servadio A, Matilla T, Feddersen RM, Yunis WS, Duvick LA, Zoghbi HY, Orr HT (1995) SCA1 transgenic mice: a model for neurodegeneration caused by an expanded CAG trinucleotide repeat. *Cell* 82:937–948.
- Custer SK, Garden GA, Gill N, Rueb U, Libby RT, Schultz C, Guyenet SJ, Deller T, Westrum LE, Sopher BL, La Spada AR (2006) Bergmann glia expression of polyglutamine-expanded ataxin-7 produces neurodegeneration by impairing glutamate transport. *Nat Neurosci* 9:1302–1311.
- Dueñas AM, Goold R, Giunti P (2006) Molecular pathogenesis of spinocerebellar ataxias. *Brain* 129:1357–1370.
- Garthwaite G, Garthwaite J (1991) Mechanisms of AMPA neurotoxicity in cerebellar and hippocampal slices. *Eur J Neurosci* 3:729–736.
- Gold DA, Baek SH, Schork NJ, Rose DW, Larsen DD, Sachs BD, Rosenfeld MG, Hamilton BA (2003) ROR α coordinates reciprocal signaling in cerebellar development through sonic hedgehog and calcium-dependent pathways. *Neuron* 40:1119–1131.
- Hammarlund M, Jorgensen EM, Bastiani MJ (2007) Axons break in animals lacking beta-spectrin. *J Cell Biol* 176:269–275.
- Häusser M, Clark BA (1997) Tonic synaptic inhibition modulates neuronal output pattern and spatiotemporal synaptic integration. *Neuron* 19:665–678.
- He Y, Zu T, Benzow KA, Orr HT, Clark HB, Koob MD (2006) Targeted deletion of a single Sca8 ataxia locus allele in mice causes abnormal gait,

- progressive loss of motor coordination, and Purkinje cell dendritic deficits. *J Neurosci* 26:9975–9982.
- Holleran EA, Ligon LA, Tokito M, Stankewich MC, Morrow JS, Holzbaier EL (2001) β III spectrin binds to the Arp1 subunit of dynactin. *J Biol Chem* 276:36598–36605.
- Ikeda Y, Dick KA, Weatherspoon MR, Gincel D, Armbrust KR, Dalton JC, Stevanin G, Dürr A, Zühlke C, Bürk K, Clark HB, Brice A, Rothstein JD, Schut LJ, Day JW, Ranum LP (2006) Spectrin mutations cause spinocerebellar ataxia type 5. *Nat Genet* 38:184–190.
- Jackson M, Song W, Liu MY, Jin L, Dykes-Hoberg M, Lin CI, Bowers WJ, Federoff HJ, Sternweis PC, Rothstein JD (2001) Modulation of the neuronal glutamate transporter EAAT4 by two interacting proteins. *Nature* 410:89–93.
- Jen JC, Wan J, Palos TP, Howard BD, Baloh RW (2005) Mutation in the glutamate transporter EAAT1 causes episodic ataxia, hemiplegia and seizures. *Neurology* 65:529–534.
- Jenkins SM, Bennett V (2001) Ankyrin-G coordinates assembly of the spectrin-based membrane skeleton, voltage-gated sodium channels, and L1 CAMs at Purkinje neuron initial segments. *J Cell Biol* 155:739–746.
- Komada M, Soriano P (2002) β IV-spectrin regulates sodium channel clustering through ankyrin-G at axon initial segments and nodes of Ranvier. *J Cell Biol* 156:337–348.
- Levin SI, Khaliq ZM, Aman TK, Grieco TM, Kearney JA, Raman IM, Meisler MH (2006) Impaired motor function in mice with cell-specific knockout of sodium channel Scn8a (Nav1.6) in cerebellar Purkinje neurons and granule cells. *J Neurophysiol* 96:785–793.
- Lim J, Crespo-Barreto J, Jafar-Nejad P, Bowman AB, Richman R, Hill DE, Orr HT, Zoghbi HY (2008) Opposing effects of polyglutamine expansion on native protein complexes contribute to SCA1. *Nature* 452:713–718.
- Lin X, Antalffy B, Kang D, Orr HT, Zoghbi HY (2000) Polyglutamine expansion downregulates specific neuronal genes before pathologic changes in SCA1. *Nat Neurosci* 3:157–163.
- Marcaggi P, Billups D, Attwell D (2003) The role of glial glutamate transporters in maintaining the independent operation of juvenile mouse cerebellar parallel fibre synapses. *J Physiol* 552:89–107.
- Ophoff RA, Terwindt GM, Vergouwe MN, van Eijk R, Oefner PJ, Hoffman SM, Lamerdin JE, Mohrenweiser HW, Bulman DE, Ferrari M, Haan J, Lindhout D, van Ommen GJ, Hofker MH, Ferrari MD, Frants RR (1996) Familial hemiplegic migraine and episodic ataxia type-2 are caused by mutations in the Ca²⁺ channel gene CACNL1A4. *Cell* 87:543–552.
- Parkinson NJ, Olsson CL, Hallows JL, McKee-Johnson J, Keogh BP, Noben-Trauth K, Kujawa SG, Tempel BL (2001) Mutant β -spectrin 4 causes auditory and motor neuropathies in quivering mice. *Nat Genet* 29:61–65.
- Pielage J, Fetter RD, Davis GW (2005) Presynaptic spectrin is essential for synapse stabilization. *Curr Biol* 15:918–928.
- Raman IM, Bean BP (1997) Resurgent sodium current and action potential formation in dissociated cerebellar Purkinje neurons. *J Neurosci* 17:4517–4526.
- Raman IM, Bean BP (1999) Ionic currents underlying spontaneous action potentials in isolated cerebellar Purkinje neurons. *J Neurosci* 19:1663–1674.
- Sacco T, De Luca A, Tempia F (2006) Properties and expression of Kv3 channels in cerebellar Purkinje cells. *Mol Cell Neurosci* 33:170–179.
- Sakaguchi G, Orita S, Naito A, Maeda M, Igarashi H, Sasaki T, Takai Y (1998) A novel brain-specific isoform of β spectrin: isolation and its interaction with Munc13. *Biochem Biophys Res Commun* 248:846–851.
- Sausbier M, Hu H, Arntz C, Feil S, Kamm S, Adelsberger H, Sausbier U, Sailer CA, Feil R, Hofmann F, Korth M, Shipston MJ, Knaus HG, Wolfner DP, Pedroarena CM, Storm JF, Ruth P (2004) Cerebellar ataxia and Purkinje cell dysfunction caused by Ca²⁺-activated K⁺ channel deficiency. *Proc Natl Acad Sci U S A* 101:9474–9478.
- Serra HG, Byam CE, Lande JD, Tousey SK, Zoghbi HY, Orr HT (2004) Gene profiling links SCA1 pathophysiology to glutamate signaling in Purkinje cells of transgenic mice. *Hum Mol Genet* 13:2535–2543.
- Shakkottai VG, Chou CH, Oddo S, Sailer CA, Knaus HG, Gutman GA, Barish ME, LaFerla FM, Chandy KG (2004) Enhanced neuronal excitability in the absence of neurodegeneration induces cerebellar ataxia. *J Clin Invest* 113:582–590.
- Siddhanta A, Radulescu A, Stankewich MC, Morrow JS, Shields D (2003) Fragmentation of the golgi apparatus: a role for β III spectrin and synthesis of phosphatidylinositol 4,5-bisphosphate. *J Biol Chem* 278:1957–1965.
- Soong BW, Paulson HL (2007) Spinocerebellar ataxias: an update. *Curr Opin Neurol* 20:438–446.
- Stankewich MC, Tse WT, Peters LL, Ch'ng Y, John KM, Stabach PR, Devarajan P, Morrow JS, Lux SE (1998) A widely expressed β III spectrin associated with Golgi and cytoplasmic vesicles. *Proc Natl Acad Sci U S A* 95:14158–14163.
- Stevanin G, Herman A, Brice A, Dürr A (1999) Clinical and MRI findings in spinocerebellar ataxia type 5. *Neurology* 53:1355–1357.
- Stoffel W, Körner R, Wachtmann D, Keller BU (2004) Functional analysis of glutamate transporters in excitatory synaptic transmission of GLAST1 and GLAST1/EAAC1 deficient mice. *Mol Brain Res* 128:170–181.
- Takatsuru Y, Takayasu Y, Iino M, Nikkuni O, Ueda Y, Tanaka K, Ozawa S (2006) Roles of glial glutamate transporters in shaping EPSCs at the climbing fiber-Purkinje cell synapses. *Neurosci Res* 54:140–148.
- Takayasu Y, Iino M, Ozawa S (2004) Roles of glutamate transporters in shaping excitatory synaptic currents in cerebellar Purkinje cells. *Eur J Neurosci* 19:1285–1295.
- Takayasu Y, Iino M, Kakegawa W, Maeno H, Watase K, Wada K, Yanagihara D, Miyazaki T, Komine O, Watanabe M, Tanaka K, Ozawa S (2005) Differential roles of glial and neuronal glutamate transporters in Purkinje cell synapses. *J Neurosci* 25:8788–8793.
- Thomas PS Jr, Fraley GS, Damian V, Woodke LB, Zapata F, Sopher BL, Plymate SR, La Spada AR (2006) Loss of endogenous androgen receptor protein accelerates motor neuron degeneration and accentuates androgen insensitivity in a mouse model of X-linked spinal and bulbar muscular atrophy. *Hum Mol Genet* 15:2225–2238.
- Trudeau MM, Dalton JC, Day JW, Ranum LP, Meisler MH (2006) Heterozygosity for a protein truncation mutation of sodium channel SCN8A in a patient with cerebellar atrophy, ataxia and mental retardation. *J Med Genet* 43:527–530.
- Turmaine M, Raza A, Mahal A, Mangiarini L, Bates GP, Davies SW (2000) Nonapoptotic neurodegeneration in a transgenic mouse model of Huntington's disease (2000). *Proc Natl Acad Sci U S A* 97:8093–8097.
- Van Raamsdonk JM, Pearson J, Rogers DA, Bissada N, Vogl AW, Hayden MR, Leavitt BR (2005) Loss of wild-type huntingtin influences motor dysfunction and survival in the YAC128 mouse model of Huntington disease. *Hum Mol Genet* 14:1379–1392.
- Walter JT, Alviña K, Womack MD, Chevez C, Khodakhah K (2006) Decreases in the precision of Purkinje cell pacemaking cause cerebellar dysfunction and ataxia. *Nat Neurosci* 9:389–397.
- Watase K, Hashimoto K, Kano M, Yamada K, Watanabe M, Inoue Y, Okuyama S, Sakagawa T, Ogawa S, Kawashima N, Hori S, Takimoto M, Wada K, Tanaka K (1998) Motor discoordination and increased susceptibility to cerebellar injury in GLAST mutant mice. *Eur J Neurosci* 10:976–988.
- Waters MF, Minassian NA, Stevanin G, Figueroa KP, Bannister JP, Nolte D, Mock AF, Evidente VG, Fee DB, Müller U, Dürr A, Brice A, Papazian DM, Pulst SM (2006) Mutations in voltage-gated potassium channel KCNC3 cause degenerative and developmental central nervous system phenotypes. *Nat Genet* 38:447–451.
- Yamashita A, Makita K, Kuroiwa T, Tanaka K (2006) Glutamate transporters GLAST and EAAT4 regulate postischemic Purkinje cell death: an in vivo study using a cardiac arrest model in mice lacking GLAST or EAAT4. *Neurosci Res* 55:264–270.
- Yeh JZ (1978) Sodium inactivation mechanism modulates QX-314 block of sodium channels in squid axons. *Biophys J* 24:569–574.
- Zagha E, Lang EJ, Rudy B (2008) Kv3.3 channels at the Purkinje cell soma are necessary for generation of the classical complex spike waveform. *J Neurosci* 28:1291–1300.
- Zhuchenko O, Bailey J, Bonnen P, Ashizawa T, Stockton DW, Amos C, Dobyns WB, Subramony SH, Zoghbi HY, Lee CC (1997) Autosomal-dominant cerebellar ataxia (SCA6) associated with small polyglutamine expansions in the alpha 1A-voltage-dependent calcium channel. *Nat Genet* 15:62–69.